NONLINEAR MODELLING AND BIFURCATIONS IN THE RECTIFIED DC VOLTAGE FED DC-DC BOOST CONVERTER

A

Thesis

submitted for the Degree of

Doctor of Philosophy (Engineering)

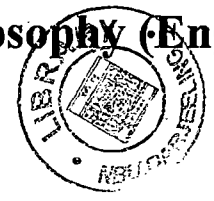

by

PRADIP KUMAR SAHA

Department of Electrical Engineering

Jalpaiguri Government Engineering College

Jalpaiguri, India

UNIVERSITY OF NORTH BENGAL

Rajarammohanpur, Dist- Darjeeling

West Bengal, INDIA

www.nbu.org

STOCK TAKING - 2011

Ref.
530.155
S 131 n.

198546
29 AUG 2007

CERTIFICATE

This is to certify that the thesis entitled "NONLINEAR MODELLING AND BIFURCATIONS IN THE RECTIFIED DC VOLTAGE FED DC-DC BOOST CONVERTER" submitted by Sri Pradip Kumar Saha who got his name registered on 07.10.2002 for the award of PhD (Engineering) degree of the University of North Bengal , absolutely based upon his own work under my supervision and that neither the thesis nor any part of it has been submitted for any degree or diploma or any other academic award anywhere before.

(Dr. Jyotirmoy Jhampati)
Professor and Head,
Department of Electrical Engineering
Jalpaiguri Government Engineering College
Jalpaiguri- 725102 ,
West Bengal, India

Prof. & Head
Department of Electrical Engineering
Jalpaiguri Govt. Engg. College

ACKNOWLEDGEMENTS

With great pleasure I express my deep gratitude and indebtedness to and everyone, who cooperated me and helped me with their valuable advice.

I am greatly indebted to my project supervisor and head of the department, Dr. J. Jhampati for his inspiring guidance, affection and care for me.

I express my sincere thanks and gratitude to my colleage and philosopher cum friend Prof. G.K.Panda, for his continuous encouragement and to provide the courage to admire the research area.

I express my sincere thanks and gratitude to my colleage and former head of the department Dr. S. Mal for his encouragement and providing all the facilities in the department.

I express my thanks to all of my colleages in the department as well as the institution for helping me to carry out the work.

I express my sincere thanks to the Principal of this college for providing me the infrastructure of this college to carry out the work.

Acknowledgements is not completed if I do not mention the name of my family members for their mental support and encouragement.

Last but not the least, I acknowledge the help of all the persons who directly or indirectly encourage me for the completion of the work

(Pradip Kumar Saha)

Assistant Professor

Department of Electrical Engineering

Jalpaiguri Government Engineering College

Jalpaiguri- 725102 , West Bengal, India

ABSTRACT

NONLINEAR MODELLING AND BIFURCATIONS IN THE RECTIFIED DC VOLTAGE FED DC-DC BOOST CONVERTER

As the power converters exhibit a wealth of nonlinear phenomena due to the presence of switching element , many researchers and investigators reported about the occurance of nonlinear phenomena like chaos and subharmonics in power electronics circuits. These phenomena are investigated in current mode control of converter to conform the practical closed loop control of converter. All of those investigations are carried out taking the pure DC voltage as input . But in most of the cases rectified DC voltage is fed to the current mode controlled DC-DC boost converter. So considering the wider applications and to conform the very practical situation, the current mode controlled rectified voltage fed DC-DC boost converter with all the parasitic effects is taken for our study and investigations. For realistic study , a nonlinear model of the same may be developed to study the nonlinear phenomena and bifurcation in details . Routes of chaos may be investigated and proper methods may be developed to control bifurcations / chaos in these systems to stabilize it.

The present investigation will make an endeavour to explore a piecewise solution of the overall chaotic response of current mode controlled rectified voltage fed DC-DC boost converter. This result will be compared with the result obtained for a purely DC fed DC-DC boost converter.

****

PREFACE

This work deals with a dynamical systems which are piecewise linear, with an overall nonlinear behaviour contributed by discrete switching of the devices. All the circuits used in power electronics are in this category due to switching on and off operation of the power electronic devices like Thyristors, Power BJTs , Power MOSFETs, IGBTs, GTOs etc. The system equations are formed with linear differential equations and the switching from one set to another is controlled by feedback process.

The current mode controlled rectified voltage fed DC-DC boost converter with all the parasitic effects is taken for our study and investigations to conform the very practical situation.

The occurance of an unusually high amount of noise and erratic behaviour in power electronic circuits is a universal experience of practicing engineers for a long time. Such phenomena is diagnosed as chaos. The detailed study and investigation of nonlinear phenomena and chaos in the current mode controlled rectified voltage fed DC-DC boost converter circuits are necessary.

Since the power electronic circuits with the current mode controlled rectified voltage fed DC-DC boost converters have wider applications, it is important to study and investigation of nonlinear phenomena, bifurcation and chaos in the current mode controlled rectified voltage fed DC-DC boost converter which may help to develop methods to control chaos in the system. The control of bifurcations / chaos has justified implications. It offer way to stabilize those circuits which tend to develop chaotic behaviour. It has also the wide variety of unstable periodic orbits available in chaotic attractor those can be utilized by stabilizing the system in the most desirable orbit. It helps in the current mode controlled rectified voltage fed DC-DC boost converter for desired output characteristics.

This thesis is presented in the following fashion.

Chapter 1 introduces the basic ideas of power electronic circuits, devices, components, control methods, nonlinear phenomenas, modelings, mappings, bifurcations, bifurcation controls, chaos controls.

Chapter 2 introduces the basic concepts of nonlinear dynamics , bifurcations and chaos. We are familiarized and get the ideas of characterizing the chaos through various dimensions, lyapunov exponent, poincare section, eigen values, attractors etc.

Chapter 3 introduces the non linear phenomena in boost converter. We get the idea of modeling, mapping of boost converter. We are familiarized and get the ideas of characterizing the chaos of boost converter through various dimensions, lyapunov exponent, poincare section, eigen values, attractors etc.

Chapter 4 introduces the practical boost converter i.e. with all parasitic effects. We make the model of i. Pure dc fed current mode controlled DC-DC boost converter ii. Rectified dc fed current mode controlled DC-DC boost converter. We present the modeling and mapping of the circuits and study the bifurcation, chaos.

Chapter 5 introduces the development of the 1-D modeling for both the pure dc fed current controlled dc-dc boost converter & single phase full wave rectified dc fed current controlled dc-dc boost converter with parasitic effect for the application of the theory of bifurcations in 1-D piecewise smooth piecewise monotonic maps for both the circuits. The different Bifurcation diagrams are presented for the developed 1-D modeling which are useful in analyzing, identifying and describing the nonlinear phenomena in such circuits

Chaper 6 introduces the theory of bifurcations in 1-D discontinuous piecewise smooth piecewise monotonic maps to develop the 1-D discontinuous modeling of the current controlled boost converter with parasitic effect for two types of source voltage one for pure DC & another

for Rectified DC. The different Bifurcation diagrams are presented for the developed 1-D discontinuous modeling which are useful in analyzing, identifying and describing the nonlinear phenomena in such circuits

Chapter 7 introduces the methods for bifurcation control and chaos, as they are twins. It gives the idea of various bifurcations control circuits. We apply variable ramp compensation technique for control.

Chapter 8 gives us the conclusions and future expansions of the work.

****

CONTENTS

.....

Chapter 1

INTRODUCTION

1.1 Aim of power electronics:

Power electronics is the most important and fast growing sphere of electronics with huge practical application [18]-[22],[81],[82]. It deals with the processing of electrical energy of the power level from a of fraction of watts to kilowatts. Power electronics is a green technology with the following aims:

- To convert electrical energy from one form to another with its good regulation and control
- To achieve high conversion efficiency and less heat generation
- To minimize the mass to power ratio

1.2 Classification of power electronics circuits:

Power electronics circuits are classified on the basis of input voltage (dc or ac), output voltage (dc or ac) and operation as:

- AC-DC uncontrolled rectifiers
- AC-DC controlled rectifiers or converters
- DC-DC converters or choppers
- DC-AC converters or inverters
- AC-AC converters or cyclo converters
- AC-AC converters or AC voltage controllers

Among the above circuits DC-DC choppers are very useful to study for non linear modeling , bifurcation and chaos.

1.3 Causes of nonlinearities in power electronics:

Power electronics converters (DC-DC choppers) is a wealth of nonlinear phenomena for study and investigation. The prime source of nonlinearity in Power electronics converters (DC-DC choppers)

- The switching elements present
  - Thyristor, BJT, MOSFET, IGBT, Power diode etc.
- Nonlinear components
  - Inductor: Choke, transformer, magnetic amplifier, saturable reactor etc.
  - Capacitor
- The control circuits and methods.
  - Sliding mode control
  - Hysteresis control
    - Digital control
    - Pulse width modulation control
    - Phase locked loop
    - Monostable
    - Geometric control
    - Hamiltonian control
    - Tolerance band control
    - Ripple-based control
    - Energy-based control
    - Passivity-based control
    - Multipliers in the loop
    - Boundary control etc.

1.4 Classification of chopper :

DC-DC converters (chopper) are classified as:

- Buck converter
- Boost converter
  - Pure DC fed Current control
  - Rectified DC fed Current control
  - Pure DC fed voltage control
  - Rectified DC fed Current control

Practical boost converter defines boost converter with parasitic effect, like loss component of inductor, capacitor etc and rectified DC as input.

1.5 Different non-linear phenomena in boost converter:

DC-DC converters were first studied in depth for nonlinear phenomena. The important characteristics to be studied for nonlinear phenomena are:

- Sudden change in operating modes (bifurcations)
- Alternative stable operating modes (coexisting attractors)
- Apparently random behaviour (chaos)
- Sub-harmonics (periodicity)
- Basins of attractors

1.6 Modeling of boost converters:

Dynamic modeling methods of power electronics converters (DC-DC choppers) for analysis ,simulation and control are reported :

- Averaged data model
- Sampled data model
- Map based model

- State variable model

1.7 Mapping of boost converters:

Mappings methods for models of power electronics converters (DC-DC choppers) are presented:

- Poincare map
- Stroboscopic map
- Stroboscopic non-switching map
- Closed loop map
- S-switching map
- A-switching map

1.8 Type of bifurcations in boost converter

Types of bifurcations in power electronics converters (DC-DC choppers) are classified:

- Pitchfork bifurcation
- Saddle-node bifurcation
- Flip bifurcation
- Hopf bifurcation
- Bifurcation in 1-D continuous form (smooth)
- Bifurcation in 1-D discontinuous form
- Bifurcation in 2-D form
- Border collision bifurcation

Knowledge of switching map investigation, to use or avoid those phenomena in converters are vital for reliable design, fabrication and operation.

1.9 Control of bifurcation in boost converters:

Research and intensive studies are going on to Control bifurcation of boost converter and bifurcation can be obtained in the following ways.

- Bifurcation control via state feedback and washout filter-aided dynamic
- feedback controllers
- Bifurcation control via normal forms and invariants
- Bifurcation control via harmonic balance approximations by
- Ramp compensation technique
- Variable ramp compensation technique

1.10 Control of chaos. in boost converter s:

Control of chaos can be achieved by :

- Using feedback to enforce periodic orbit
- Delaying the onset of bifurcations
- OGY method
- Integral control
- State feedback control

1.11 Goal of our study:

Sudden change in operating modes bifurcations), alternative stable operating modes (coexisting attractors) , apparently random behaviour (chaos), sub-harmonics (periodicity) and basins of attractors may be investigated in current mode control of converter to conform the practical closed loop control of converter that is rectified DC voltage is fed to the current mode controlled DC-DC boost converter. So with the wider applications and to conform the very practical situation, the current mode controlled rectified voltage fed DC-DC boost

converter is taken for our study and investigations. A nonlinear model of the same may be developed to study the nonlinear phenomena and bifurcation in details . Bifurcation phenomena can be investigated in piecewise one dimensional smooth map and one dimensional discontinuous map. Routes of chaos may be investigated and methods may be developed to control bifurcation and chaos (as they are twins) in these systems to stabilize it. Investigation are carried out to explore a piecewise solution of the overall chaotic response of current mode controlled rectified voltage fed DC-DC boost converter and the result may be compared with the result obtained for a purely DC fed DC-DC boost converter.

****

Chapter 2

INTRODUCTION TO NONLINEAR DYNAMICS AND CHAOS

2.1 Introduction

Tell me, O Muses who dwell on Olympos, and observe proper order
for each thing as it first came into being.
Chaos was born first and after her came Gaia
the broad-breasted, the firm seat of all
the immortals who hold the peaks of snowy Olympos,...

- *Hesiod*, Theogony, *lines 114-118*

This chapter covers the basic concepts of chaos.

2.2 Dynamic System, State and State-space:

Everything in this world exists in motion. Nothing is static or unchangeable. Some matters of this material world may appear to be static but those are also changing. Ever since this fact is recognized the study of dynamics has been a major topic. At first, all investigations were piecemeal: Newtonian scientists were studying the dynamics of the moving bodies , biologists were studying the changes in living organisms, chemists were studying the chemical properties of the materials etc. Gradually, it has been realized that though the objective of these studies are different, there are common elements in all changes. Therefore, a body of knowledge is gradually emerged which is Dynamical System in general.

A system whose status changes with time is called a ***Dynamical System.*** The status of a Dynamical System at any instant and the change in status of the system with time is uniquely expressed by a minimum number of properly identified variables known as *State Variables*. The aim of study of the dynamics of a dynamical system [49],[106] is essentially an investigation

of how these state variables change with respect to time. Mathematically, this is expressed by the rate of change of these state variables to their current values in terms of a system of first order differential equations. Thus, if state variables are given by $\{x_i, i = 1,2,.....,n\}$ then the state-space model of the system is expressed as in the form of a set of first order differential equations as follows:

$$\dot{x}_1 = \frac{dx_1}{dt} = f(x_1, x_2, ...x_n)$$

$$\dot{x}_2 = \frac{dx_2}{dt} = f(x_1, x_2, ...x_n)$$

.

.

$$\dot{x}_n = \frac{dx_n}{dt} = f(x_1, x_2, ...x_n)$$

In general, $\dot{x}_i = f_i(x_1, x_2, ..., x_n)$ (2.1)

or in vector form, $\dot{\mathbf{X}} = \mathbf{f(X)}$ (2.2)

The ability to express $\dot{\mathbf{X}}$ purely as a function of $\mathbf{X}$ is what identifies x_i as state variables.

Some systems change discretely. Such a situation may arise when a system is actually changing continuously but is observed only at certain intervals. Most power electronic circuits are modeled in this way. There can be inherently discrete systems as in digital electronic systems or populations of various species. In such cases the state variables at the (n+1)-th instant are expressed as a function of those at the n-th instant:

$$\mathbf{x_{n+1}} = f(\mathbf{x_n}) \quad (2.3)$$

The equations of forms 2.2 or 2.3 with a given set of initial conditions can be solved either analytically or numerically and the solutions give the future states of the system as functions of time.

The dynamics of a system can be visualized by constructing a space with the state variables as coordinates. which is called the state space or phase space. The state of the system at any instant is represented by a point in the space. Starting from any given initial condition, the state-point moves in the state space and this movement is completely determined by the state

equations. The path of the state point is called the orbit or the trajectory of the system that starts from the given initial conditions. The trajectories are obtained as the solutions of the differential equations(2.2) or iterates of the map(2.3).

2.3 Autonomous and non-autonomous system:

If the system equations do not have any externally applied time-varying input or other time variations, the system is said to be ***autonomous***. In autonomous such systems the right hand side of (2.2) does not contain any time-dependent term. A typical example is the Lorentz system[10],[15]which is a simplified model of atmospheric convection:

$$\begin{aligned} \dot{x} &= -3(x-y) \\ \dot{y} &= -xz + rx - y \\ \dot{z} &= xy - z \end{aligned} \tag{2.4}$$

where r is a parameter. On the contray systems with external inputs or forcing functions or time variations in their definition, are called ***non-autonomous*** systems. In such systems, right hand side of (2.2) contains time dependent terms. As a typical example one can consider a pendulum with an oscillating support, the equations of which are

$$\begin{aligned} \dot{x} &= y + 5 \\ \dot{y} &= -y - y\sin x + r\sin \omega t \end{aligned} \tag{2.5}$$

Likewise, power electronic circuits with clock-driven control logic are non-autonomous systems.

2.4 Vector fields:

In studying the dynamical behavior of a given system, one has to compute the trajectory starting from a given initial condition which can be done numerically. It is generally not necessary to compute all possible trajectories (which may be a cumbersome exercise) in order to study a given system. It may be noted that the left hand side of (2.2) gives the rate of change of the state variables. This is a vector, which is expressed as a function of the state variables. The equation (2.2) thus defines a vector at every point of the state space. This is called the *vector field.* A solution starting from the given initial condition follows the direction of the vectors, i.e., the vectors are tangent to the solutions. The properties of a system can be studied by studying

this vector field. To give an example, the vector field for the system $\ddot{x} - (1-x^2)\dot{x} + x = 0$ is shown in Fig. 2.1.

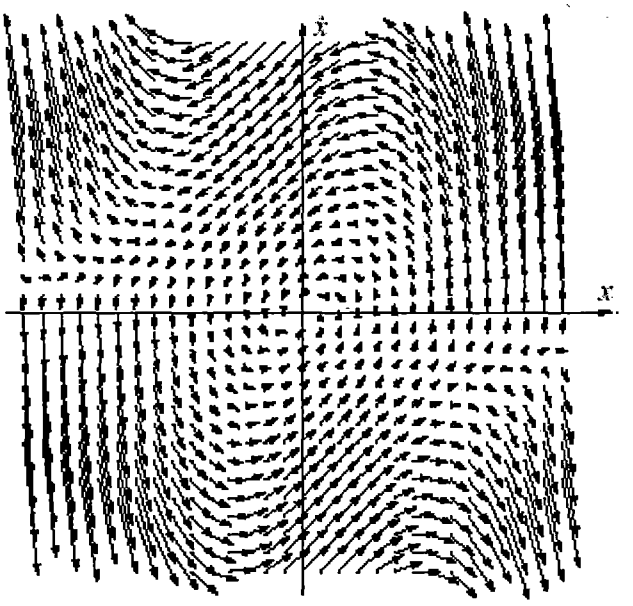

Fig.2.1: vector field for the system $\ddot{x} - (1-x^2)\dot{x} + x = 0$

2.5 *Local Behavior of Vector Fields Around Equilibrium Points:*

The points where the $\dot{x}$ vector has zero magnitude, i.e., where $\dot{x}=f(x)=0$, are called the *equilibrium points*. Since the velocity vector at the equilibrium point has magnitude zero, if an initial condition is placed there, the state-point will forever remain there. However, this does not guarantee that the equilibrium state will be stable, i.e., any deviation from it will die down. It is therefore necessary to study the *local* behavior of the system in the neighborhood of an equilibrium point. As it is straightforward to obtain the solutions of a set of *linear* differential equations, the local properties of the state space in the neighborhood of an equilibrium point can be studied by locally linearizing the differential equations at that point. Most tools for the design and analysis of engineering systems concentrate only on the local behavior — because in general, the nominal operating point of any system is located at an equilibrium point, and if perturbations are small then the linear approximation gives a simple satisfactory and workable model of the dynamical system.

The local linearization is done by using the Jacobian matrix of the functional form at an equilibrium point. As for example, if the state space is two dimensional, given by

$$\begin{aligned} \dot{x} &= f_1(x,y) \\ \dot{y} &= f_2(x,y) \end{aligned} \tag{2.6}$$

then the local linearization at an equilibrium point (x^*, y^*) is given by

$$\begin{bmatrix} \delta\dot{x} \\ \delta\dot{y} \end{bmatrix} = \begin{bmatrix} \frac{\partial f_1}{\partial x} & \frac{\partial f_1}{\partial y} \\ \frac{\partial f_2}{\partial x} & \frac{\partial f_2}{\partial y} \end{bmatrix} \tag{2.7}$$

where $\delta x = x - x^*, \delta y = y - y^*$. The matrix containing the partial derivatives is called the Jacobian matrix and the numerical values of the partial derivatives are calculated at the equilibrium point. This is really just a (multivariate) Taylor series expanded to first order. Notice that in the linearized state space, the state variables are the *deviations* from the equilibrium point (x^*, y^*). To avoid notational complexity, we do not consider the δ and will proceed with the equation

$$\dot{\mathbf{x}} = \mathbf{A}\mathbf{x} \tag{2.8}$$

with the understanding that the origin is shifted to the equilibrium point. If the original system is non-autonomous, there will be time-dependent terms in the Jacobian matrix. In engineering study and analysis it is customary to separate out the time-dependent and time-independent terms in the form

$$\dot{\mathbf{x}} = \mathbf{A}\mathbf{x} + \mathbf{B}\mathbf{u} \tag{2.9}$$

where **A** and **B** are time-independent matrices, and the components of the vector **u** are the externally imposed inputs of the system. From (2.9) it is proved that the term **Bu** has influence on the location of the equilibrium point, while stability of the equilibrium point is given by the matrix . Therefore, while studying the stability of the equilibrium point, one considers the unforced system (2.8).

2.6 Eigenvalues and eigenvectors:

In (2.8), **A** *operates* on the vector **x** to give the vector $\dot{\mathbf{x}}$ which is the basic function of any matrix — mapping one vector into another vector. Generally the derived vector is different from the source vector, both in magnitude and direction. But there may be some special directions in the state space such that if the vector **x** is in that direction, the resultant vector $\dot{\mathbf{x}}$also lies along the same direction. It only gets stretched or squeezed. Any vector along these special directions are called *eigenvectors* and the factor by which any eigenvector expands or contracts when it is operated on by the matrix **A** , is called the *eigenvalue*.

To find the eigenvectors, we need to find their eigenvalues first. When the matrix **A** operates on the vector **x** , and if **x** happens to be an eigenvector, then we can write

$$\mathbf{Ax}=\lambda\mathbf{x}$$

where λ is the eigenvalue. This yields

$$(\mathbf{A}-\lambda\mathbf{I})\mathbf{x}=\mathbf{0}$$

where **I** is the identity matrix of the same dimension as **A** . This condition would be satisfied if the determinant $|\mathbf{A}-\lambda\mathbf{I}|=\mathbf{0}$.Thus

$$\left|\begin{bmatrix} A_{11} & A_{12} \\ A_{21} & A22 \end{bmatrix} \begin{bmatrix} \lambda & 0 \\ 0 & \lambda \end{bmatrix}\right| = 0 \qquad (2.10)$$

$$\Rightarrow \lambda^2 - (A_{11} + A_{22})\lambda + (A_{11}A_{22} - A_{12}A_{21}) = 0$$

This is called the *characteristic equation* and their roots are the eigenvalues. Thus, for a 2x2 matrix, one gets a quadratic equation — which in general yields two eigenvalues. For each eigenvalue there is one *direction* of eigenvector, and any vector in that direction is an eigenvector. The direction of the eigenvector is determinate but the magnitude is indeterminate.

If the eigenvalues are real and negative, the system is stable in the sense that any perturbation from an equilibrium point decays exponentially and the system settles back to the equilibrium point and this stable equilibrium point is called a *node*. If the real parts of the eigenvalues are positive, any deviation from the equilibrium point grows exponentially, and the system is unstable.

If one eigenvalue is real and negative while the other is real and positive, the system is stable along the eigenvector associated with the negative eigenvalue, and is unstable away from this. Such an equilibrium point is called a *saddle*, and a system with a saddle equilibrium point is globally unstable. The vector fields of the three types of systems are shown in Fig. 2.2.

- Complex eigen values always occur as complex conjugate pairs. If $\lambda=\sigma+j\omega$ is an eigen value, $\lambda=\sigma-j\omega$ is also an eigen value. Let **v** be an eigenvector corresponding to the Sudden change in operating modes (bifurcations)
- Alternative stable operating modes (coexisting attractors)
- Apparently random behaviour (chaos)
- Sub-harmonics (periodicity)
- Basins of attractors
- Sudden change in operating modes (bifurcations)
- Alternative stable operating modes (coexisting attractors)
- Apparently random behaviour (chaos)
- Sub-harmonics (periodicity)
- Basins of attractors

eigenvalue $\lambda=\sigma+j\omega$. This is a complex-valued vector. It is easy to check that $\bar{\mathbf{v}}$, the conjugate of the vector **v** , is associated with the eigenvalue, $\lambda=\sigma-j\omega$.

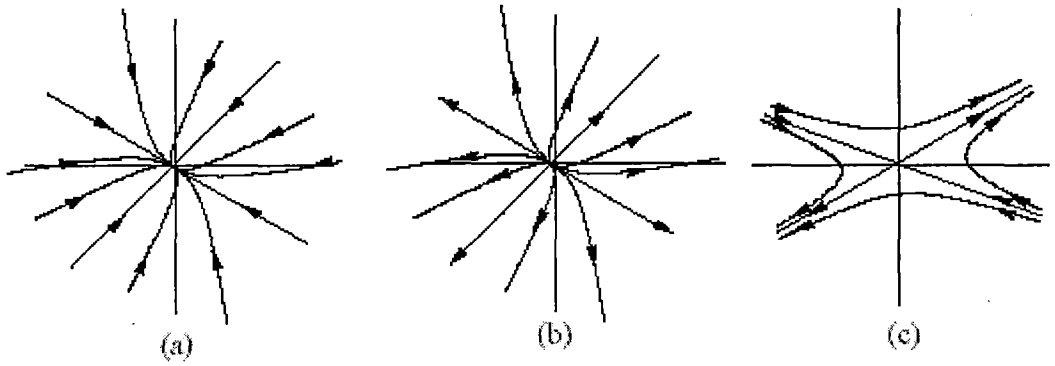

Fig.2.2: vector Field of the Linear Systems with Real Eigenvalues- (a) both eigenvalues negative, (b) both eigenvalues positive, (c) one eigen values negative and other positive.

In general, if the eigenvalues are purely imaginary, the orbits are elliptical. For initial conditions at different distances from the equilibrium point, the orbits form a family of geometrically similar ellipses which are inclined at a constant angle to the axes, but having the same cyclic frequency. When the eigenvalues are complex, with σ nonzero, the sinusoidal variation of the state variables will be multipled by an exponential term $e^{\sigma t}$. If σ is negative, this term will decay as time progesses. Therefore the waveform in time-domain will be a damped sinusoid, and in the state space the state will spiral in towards the equilibrium point. If σ is positive, the term $e^{\sigma t}$ will increase with time, and so in the state space the behavior will be an outgoing spiral as shown in Fig 2.3.

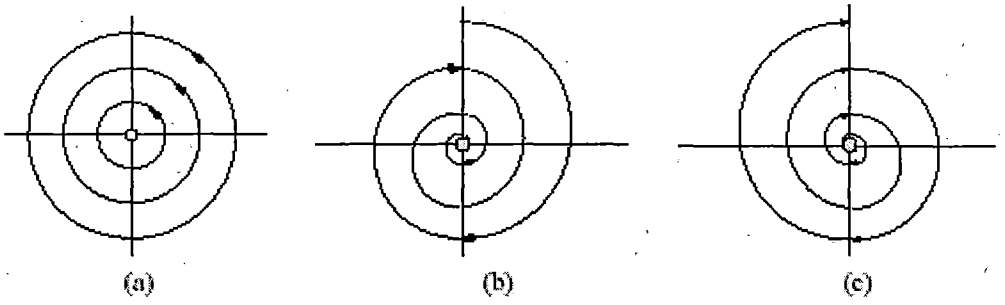

Fig.2.3: The structure of the vector field in the state space for (a) imaginary eigenvalues, (b) complex eigenvalues with negative real part, and (c) complex eigenvalues with positive real part.

2.7 Attractors in nonlinear systems:

To illustrate some typical features of nonlinear systems[24], we take the system given by $\ddot{x} - \mu(1-x^2)\dot{x} + x = 0$ known as the *van der Pol* equation. Fig. 6.13 shows the vector field of this system with state variables x and $y = \dot{x}$. If the parameter μ is varied from a negative value to a positive value, a fundamental change in the property of the vector field occurs. The stable equilibrium point becomes unstable and the field lines spiral outwards. But it does not become globally unstable as the field lines at a distance from the equilibrium point still point inwards. Where the two types of field lines meet,

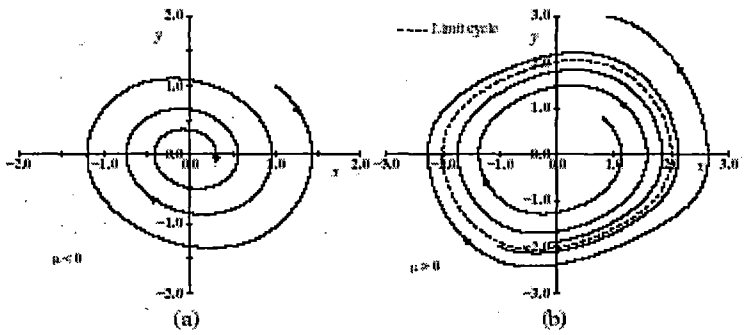

Fig.2.4: The vector fields for $\ddot{x} - \mu(1-x^2)\dot{x} + x = 0$, (a) for $\mu<0$, (b) for $\mu>0$
The dashed line shows the limit cycle.

there develops a stable periodic behavior. This is called a limit cycle. It is a *global* behavior whose existence can never be predicted from linear system theory. One point is to be noted here. There is a fundamental difference between the periodic behaviors in a linear system with purely imaginary eigenvalues and Fig.2.4. In the first case a different periodic orbit (though of constant period) is attained for initial conditions at different radii, while in case of the limit cycle, trajectories starting from different initial conditions converge on to the same periodic behavior. The limit cycle appears to attract points of the state space. This is an example of an *attractor*. Thus in a two-dimensional nonlinear system one can come across periodic attractors as in Fig.2.4. If the state space is of higher dimension, say three, there can be more intricate attractors. To understand this point, suppose a third-order dynamical system is going through oscillations and when we plot one of the variables against time, it has a periodic waveform as shown in Fig.2.5, corresponding to a state-space trajectory that shows a single loop.

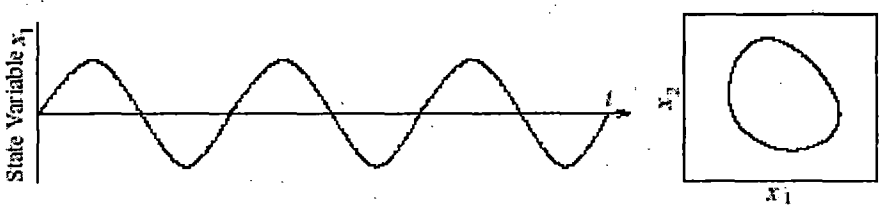

Fig2.5: The time plot (left) and the state space trajectory (right) for a period-1 attractor.

When some parameter is varied, the waveform can change to the type shown in Fig. 2.6, which has twice the period of the earlier periodic waveform. In order for such orbits to exist, the

state must three dimensions. (Note that the figure actually shows a projection of a 3-D state space onto two dimensions — a real state-space orbit cannot cross itself because there is a unique velocity vector $\dot{\mathbf{x}}$ associated with every point in the state space.)

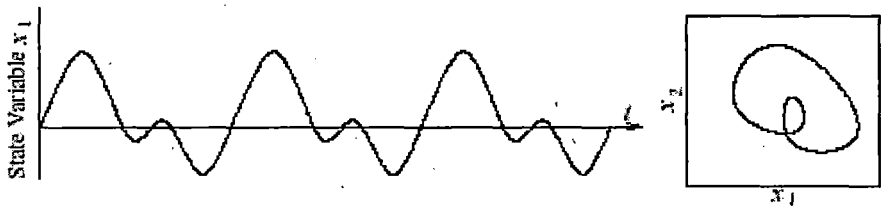

Fig.2.6: The appearance of period-2 waveform in the time domain and in state space.

Sometimes the orbit has one periodicity superimposed on another, and we have a torus-shaped attractor in the state space. This is called a quasiperiodic attractor. Fig.2.7 gives a graphic illustration.

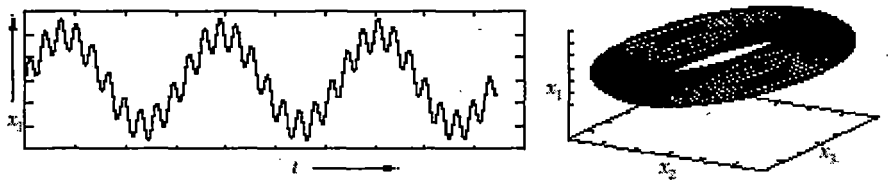

Fig. 2.7: The appearance of a quasiperiodic attractor in time domain and in state space.

One interesting possibility opens up in systems of order 3 or greater : bounded aperiodic orbits, as shown in Fig. 2.7. In such a case the system state remains bounded —within a definite volume in the state space, but the same state never repeats. In every loop through the state space the state traverses a new trajectory. This situation is called *chaos* and the resulting attractor is called a *strange attractor*. When such a situation occurs in an electrical circuit or a mechanical systems, the system undergoes apparently random oscillations.

2.8 Bifurcation:

*A **bifurcation*** is defined as a point where the flow is unstable. A qualitative change in the dynamics which occurs as a system parameter is changed is called *bifurcation*. Conceptually, it is

when there is a change in dynamic behavior, i.e., when a fixed point branches into two fixed points, or when a system changes from a sink to a saddle. This change does not happen over the course of time, but due to a change in parameters. Studying the bifurcations [41],[45],[48],[50]-[54],[56],[58],[98],[99],[103],[105] is helpful in determining whether a system is purely random or an actual chaotic system. Bifurcations happen at regular intervals, which is the determinism inherent in an otherwise random system. There are several kinds of bifurcations[102],[116],[118]: the Hopf bifurcation, pitchfork bifurcation, explosive bifurcation, limit-induced bifurcation, period doubling bifurcation, saddle node bifurcation , border collision bifurcation and fold bifurcation. A pitchfork bifurcation branches from one fixed point into two fixed points and one unstable point. Using μ as the parameter that changes, we see a pitchfork bifurcation in the Fig2.8:

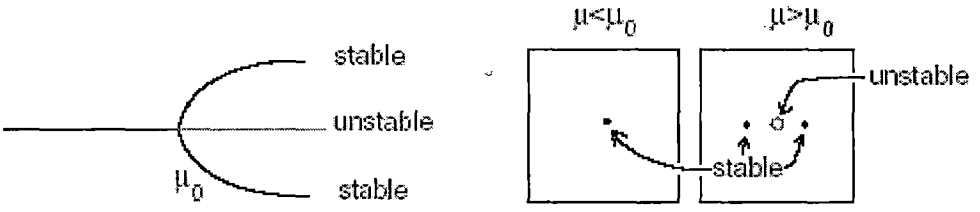

Fig. 2.8: Pitchfork bifurcation.

The phenomenon of a system evolving into a limit cycle from a fixed point is called a Hopf bifurcation, Fig. 2.9. As the system approaches the critical value μ_0, the trajectories take longer and longer to enter the equilibrium of the final state, until it takes an infinite amount of time to the equilibrium state. A secondary Hopf bifurcation when a system branches from a limit cycle to a torus. All other bifurcations transform the system from an $(n-1)$ dimensional torus to an n-dimensional torus.

A Hopf bifurcation breeds a new limit cycle, whereas a flip bifurcation turns one limit cycle into two. Successive bifurcations give birth to more limit cycles.

198546

29 AUG 2007

LIBRARY · SWINBURNE · UNIVERSITY

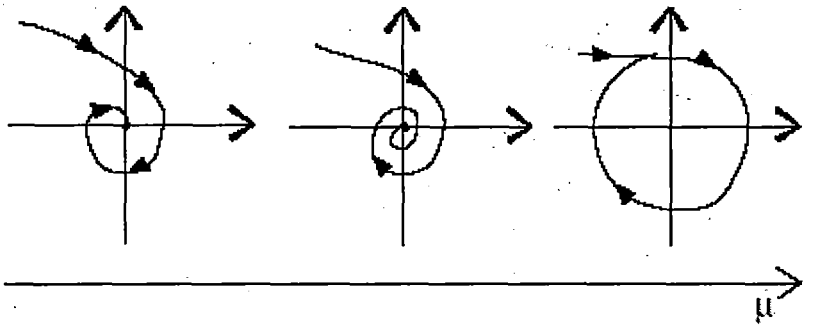

Fig. 2.9: Hopf bifurcation.

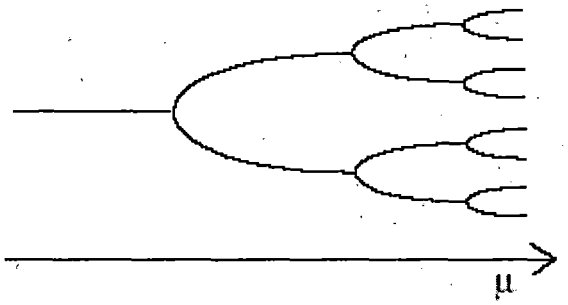

Fig. 2.10: Flip bifurcation.

Bifurcation occurs when a fixed point loses stability. Condition of stability of a fixed point, i.e., Eigen values should remain inside the unit circle. The classification of bifurcations depends on where an eigen value crosses the unit circle. Smooth systems can lose stability in three possible ways.

(a) A period doubling bifurcation: eigen value crosses the unit circle on the negative real line,

(b) A saddle-node or fold bifurcation: an eigenvalue touches the unit circle on the positive real line,

(c) A Hopf or Naimark bifurcation: a complex conjugate pair of eigenvalues cross the unit circle.

Explosive bifurcations are when bifurcations lead to chaotic attractors, like $\mu = 4.0$ in the logistic map, which is an example of period doubling as well. The logistic map is as follows:

$$x_{n+1} = \mu x_n(1 - x_n) \tag{2.10}$$

The system has one fixed point until μ = 2:98, then the system undergoes bifurcation, having two periods, rather than just one. When a system bifurcates and doubles the amount of stable points, the system undergoes ***period doubling***. The system bifurcates again around μ = 3:445. As μ is increased, the intervals between period doubling become shorter and shorter until at $^{\prime}$ = 4:0, when the system becomes completely chaotic. At this point, the system is non-periodic, where it has an infinite amount of periods. This evolution of periodic doubling is a ***route to chaos*** as shown in Fig. 2.8.

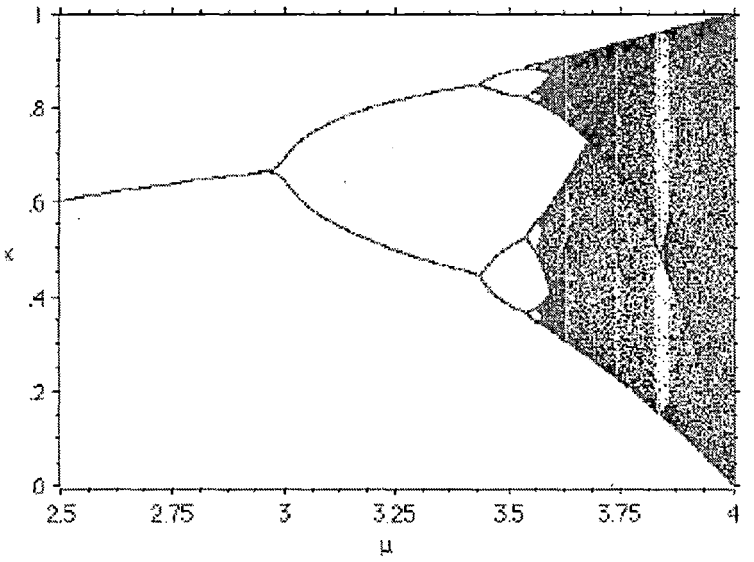

Fig. 2.11: Bifurcation diagram of the logistic mapping.

2.9 Chaos:

The word ***chaos*** is defined three ways. The word originates from the ancient Greek word **χάος**. According to Hesiod's *Theogony*, Chaos was the first god to come into existence. She was Void, what the universe was before order and logic were laid down. The second definition of chaos is the vernacular one: a condition of great disorder or confusion, which implies randomness. Lastly, chaos may be defined as complex behavior that displays randomness, yet

arises deterministically[[25]-[35],[37]-[39],[42],[55]-[58][64],[85],[97],[104]. This contrasts the original Greek meaning of the word. The ancient Greek definition of chaos conveys indescribability and incomprehension. There is no way of knowing or predicting the outcome of behavior, even in a probabilistic sense[107]-[109]. There is no order in this description, it is the antithesis of logic. This is the primary difference between the ancient Greek usage and the vernacular definition. The American Heritage Dictionary defines vernacular chaos as, \a condition or place of great disorder or confusion." This use describes the inability to correctly predict future behavior, which is a half of the definition of scientific chaos. The difference between this definition and the ancient Greek one is that the behavior is somewhat ordered. This means that the behavior is not completely disordered: there are probabilities for future behavior, rather than a complete lack of information. Quantum mechanics is an example of this kind of chaos. There is a finite amount of accuracy in measuring the system due to Heisenberg's Uncertainty Principle, and the wave function deals with probabilities. So statistics make the behavior more logical, but complete determinism of the behavior is impossible. This is where the new definition of chaos is different. The new science of chaos is defined as stochastic behavior occurring in a deterministic system. Picking this definition apart, ***stochastic behavior*** is random behavior due to random external forces. For example, a spinning top that is randomly forced exhibits stochastic behavior. Thus, stochastic behavior is behavior that has random attributes due to *indeterminate* factors. Conversely, chaotic behavior has random attributes due to *determinant* factors. A ***system***, then, is a group of elements that form a complex whole. These elements may take the form of differential equations, or the factors that produce weather patterns. A system is chaotic if it is non-periodic, deterministic and exhibits sensitivity towards initial conditions. ***Non-periodic*** behavior does not follow a set pattern. If there is periodic behavior in a system, then future behavior may be determined. Non-periodicity is an outcome of randomness, a sign of a chaotic system. The second aspect to chaos is sensitivity towards initial conditions. A system is ***sensitive towards initial conditions*** when a slight difference in initial conditions exponentially grows over time. For example, let us drop a ball on a nail head: small differences in initial conditions result in vastly different behavior. To put it more mathematically, a system is chaotic if an initial difference of $\Delta f = x_0$ between two systems exponentially grows in the form of $\Delta f = x_0 e^{\lambda t}$ with time. This basic definition of chaos lead to the discovery of chaos in 1961, by Edward Lorenz. While working on a system of equations that is now called the Lorenz system,

he ran the computer modeling program twice with the same initial conditions, except that one was to accurate to six digits, while the other was accurate to three digits. At first the two behaved identically, but after a short while they acted drastically different. He published his results in a meteorological journal in 1963, but was not recognized for his work for almost ten years until people asked questions about random, deterministic behavior.

2.10 Poincáre Section:

While the phase plotting shows the general behavior of a system, it does not show whether a system is repetitious in a messy way, or truly chaotic. The *Poincáre Section* plot is a way to discern these two phenomena. This is done by taking an n-1 dimensional slice from an n dimensional system. See the fig below for a graphical representation of a Poincáre Section in a three dimensional chaotic system with two periods.

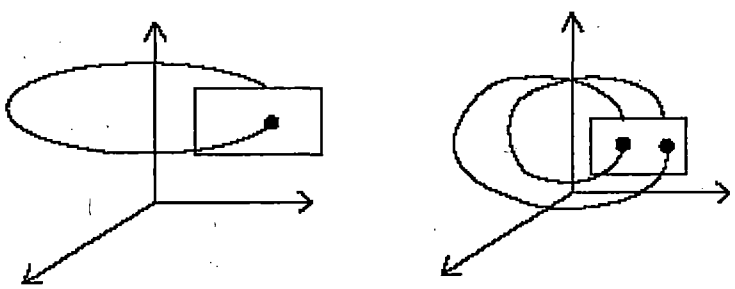

Fig. 2.12: Poincáre Section plot.

2.11 Lyapunov Exponents:

A *Lyapunov exponent* measures the exponential rate of growth (or decay) of one variable in a system. A chaotic system exhibits sensitivity towards initial conditions, where the difference grows exponentially. Thus, if a system has a positive Lyapunov exponent, it is chaotic. The Lyapunov exponent of a function $f(x)$ may be found by taking two trajectories, x and x', where

$x_0' = x_0 + \varepsilon$, and ε is some small amount. Let the difference $d = |x - x'|$. Looking at the rate of expansion over N iterations, we find:

$$d_N = \varepsilon^{N\lambda}$$

where λ is the Lyapunov exponent. , may be found by:

$$\lambda = \underset{N\to\infty}{Lt} \frac{1}{N} \sum_{i=1}^{N-1} \ln \left| \frac{f(x_i) - f(x_{i-1})}{dt} \right| \tag{2.11}$$

In order to determine chaos, all the exponents must be looked at. If one of the Lyapunov exponents is positive, the system is chaotic. In phase space, this represents the system's volume growing over time. It takes more information to determine its original state. If the sum is zero, then the system is stable. There is no loss of information over time. If the sum is less than zero then the system is merely dissipative. Another tool for verifying chaos is to look at the frequency distribution of the data. Determination of Lyapunov exponent has been described in [16],[17],[64],[85].

2.12 Frequency Distribution and Power Spectrum:

The frequency distribution of a system shows whether a system is periodic or not. A finite number of peaks corresponds to a number of periods, so if there are no distinguishable peaks, the system is non-periodic. So a chaotic system will have no distinguishable peaks. To find the frequency distribution, we must use Fourier analysis. Named after Joseph Fourier in the 1820's, Fourier analysis dictates that any signal may be represented by a series of sines and cosines. Given a set of $\{x\} = x_1, x_2, \ldots\ldots, x_{N-1}$, it is possible to take the Fourier transform and get another set of data, $\{X\} = X_1, X_2, \ldots\ldots, X_{N-1}$ where X is the Fourier transform. For any $0 < k <$ N-1,

$$X_k = \sum_{j=0}^{N-1} x_j e^{-2\pi ijk/N} \tag{2.12}$$

which puts {X} on the complex plane. To see all the information, we look at the ***power spectrum*** P, where $P_i = |X_i|^2$. For a simple system of a 1Hz wave, the power spectrum is given in Fig. 2.13.

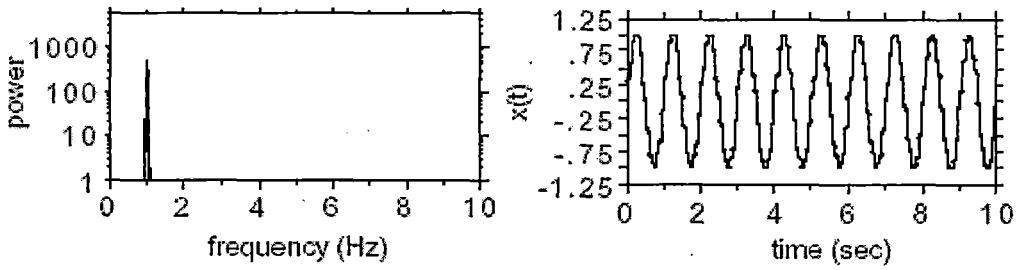

Fig. 2.13: Sinusoidal waveform power spectrum (left), or signal (right).

2.13 Dimensions:

There are three kinds of dimensions: topological, Euclidean and fractal. Topological dimension is the continuity of the points, and Euclidean dimension is the dimension that the system is embedded in. Take the object below for example (Fig. 2.13). It is a disfigured plane, like a sheet of aluminum that has been struck several times with a hammer. A plane is a two dimensional object, giving it a topological dimension of $DT = 2$. However, this is embedded in Three dimensions (x; y; z), thus $DE = 3$. Therefore, the dimension of the object, D, must

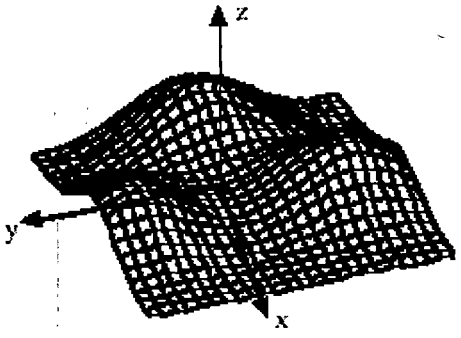

Fig.13: DT = 2 while DE = 3, thus 2 · D · 3

between two and three dimensions, which is the ***fractal dimension***. The conventional method of determining dimension of a set of points is the Hausdorff- Besicovitch method, or ***box counting***. The H-B dimension is found by minimally covering the set of points with hypercubes y of

different size. The difference comes from the dimension having identically sized cubes while the H-B dimension cubes may be differently sized. First we find a hypercube with side length L that encompasses that contains all points in the set. We may choose any length L as long as it binds the system. Numerically, it is better to choose the smallest possible one due to memory restrictions. Next, we fill the hypercube with hypercubes of side length $l = L/2$. $N(l)$ is the count of how many boxes contain a point inside. Doing this for $l_n = L/2^n$ for increasing n gives a dimension defined as follows:

$$D = \lim_{n\to\infty} \frac{\log(N(l_n))}{\log(l_n)} \tag{2.13}$$

Another way of finding dimension is using the Lyapunov exponents.

$$D = j + \sum_{i=1}^{j} \lambda_i / \left|\lambda_{j+1}\right| \tag{2.14}$$

where j is defined by the condition that:

$$\sum_{i=1}^{j} \lambda_i > 0 \text{ and } \sum_{i=1}^{j+1} \lambda_i < 0 \tag{2.15}$$

****

Chapter 3

POWER ELECTRONICS AND MODEL OF B00ST CONVERTER

3.1 Power Electronics:

Power electronics uses the semiconductor devices as switching element which are developing technically rapidly[18]-[21],[120]. It has a variety of nonlinear behavior due to its nonlinear operation and dynamics. It helps to study the modeling strategies ,the chaotic dynamics and to observe the bifurcation scenarios [15],[23],[24]. In the past decades power electronics has gone through intense development in many aspects of technology including power devices, control methods, circuit design, computer-aided analysis, passive components, packaging techniques, etc. Power electronics is mainly motivated by practical applications. However good analytical models allowing better understanding and systematic circuit design were only developed in late 1970's and in-depth analytical and modeling work is still being actively pursued today[25]-[58]. Our aim is to give an account of methods and techniques that can be applied to study the many "strange" phenomena previously observed in power electronics. Simple DC/DC boost converters (fig.3.1) are used to illustrate the modeling approaches that are capable of retaining the essential qualitative properties. Such properties peculiar to switching and non-smooth systems are systematically analyzed in terms of possible bifurcation scenarios and nonlinear phenomena. A circuit of simple dc/dc boost converter is presented for discussion of the modeling methods for characterizing nonlinear phenomena such as bifurcation and chaos in power electronics.

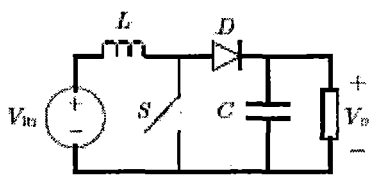

Simple DC-DC boost converter.

3.2 Power Electronics Circuits and the DC-DC Boost converters :

A power electronics circuit operates by toggling its topology among a set of linear or nonlinear circuit topologies under the control of a feedback system. They can be considered as piecewise switched circuits. In the above circuit an inductor is 'switched' between the input and the output through an appropriate switching element (*S*)[121]. The way in which the inductor is switched determines the output voltage level and transient behavior. Semiconductor switches like SCR / IGBT / FET / BJT etc. are used to implement the switching and through the use of a feedback control circuit the relative durations of the various switching intervals can be continuously adjusted. Such feedback action effectively controls the dynamics and steady-state behavior of the circuit. Thus both the circuit topology and the control method determines the dynamical behavior of the circuit.

In a typical period-1 operation the switch *S* and the diode *D* are turned on and off in a cyclic and complementary fashion under the command of a pulse-width modulator. When the switch *S* is closed (diode *D* is open) the inductor current rises up and when the switch *S* is open (diode *D* closed) the inductor current decays. The duty ratio continuously controlled by a feedback circuit , maintain the output voltage at a fixed level even under input and load variations in the mode either *continuous conduction mode* (CCM) or *discontinuous conduction mode* (DCM). In CCM the inductor current is maintained non-zero throughout the entire repetition cycle. This happens when the inductance *L* is relatively large or the load current demand is relatively high. In DCM the inductor current is zero for an interval of time within a cycle. This happens when the inductance *L* is relatively small or the load current demand is low causing the inductor current to fall to zero as the inductor is being discharged. During the interval of zero inductor current both switch *S* and diode *D* are open. For both CCM and DCM the output voltage has a fixed relationship with the input voltage as determined by the duty ratio. A steady-state relationship can be easily found. The expression (equation no. 3.1& 3.2) shows the steady-state output voltage expressions for stable period-1 operation which is preferred for most industrial applications. Here we denote steady-state duty ratio by δs and the repetition period by T. It represents only one particular operating regime. Because of the existence of

many possible operating regimes it would be of practical importance to have a thorough understanding of what determines the behavior of the circuit so as to guarantee a desired operation or to avoid an undesirable one.

3.3 Typical control strategies for DC-DC Boost converters :

The dc-dc Boost converters are designed to deliver a regulated output voltage. The control of it takes on two approaches namely voltage feedback control and current-programmed control also known as *voltage-mode* and *current-mode* control respectively . In voltage-mode control the output voltage is compared with a reference to generate a control signal which drives the pulse-width modulator via some typical feedback compensation configuration. For current-mode control an inner current loop is used in addition to the voltage feedback loop, the aim of which is to force the peak inductor current to follow a reference signal which is derived from the output voltage feedback loop . The result of current-mode control is a faster response. This kind of control is mainly applied to boost and buck-boost converters which suffer from an undesirable non-minimum phase response. The simplified schematics is given below

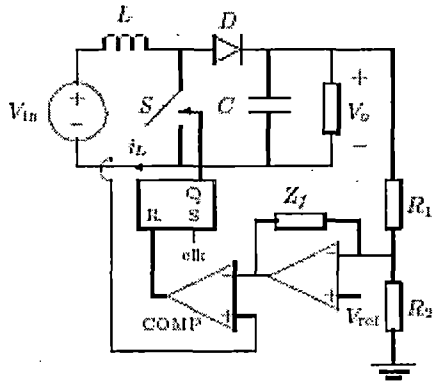

Fig. 3.2 Typical control approaches for DC-DC current-mode control.

$$V_o = \frac{1}{1-\delta} V_i \qquad \text{--------} \quad (3.1)$$

$$V_o = \frac{V_i}{2}\left(1+\sqrt{1+\frac{2\delta^2 L}{RT}}\right) \qquad \text{--------} (3.2)$$

Steady state relationship of input and output (1) for CCM and (2) for DCM for stable period-1 operation. Different control are explained elaborately in [59]-[62], [65],[66],[96].

3.4 Conventional Treatments for the dc/dc Boost converters :

Power electronics circuits are essentially piecewise switched circuits . The number of possible circuit topologies is fixed and the switching is done in a cyclic manner but may not necessarily periodically because of the feedback action. This results in a nonlinear time-varying operating mode demanding the use of nonlinear methods for analysis and design. The methods like state-space averaging, phase-plane trajectory analysis, Lyapunov based control, Volterra series approximation etc. are introduced to study the non linearities. For many practical reasons the design of power electronics systems demands "adequate" simplifying models. As closed-loop stability and transient responses are basic design concerns in practical power electronics systems models that can permit the direct application of conventional frequency-domain approaches will present obvious advantages. Most engineers are trained to use linear methods is also a strong motivation for developing linearized models like the averaging approach [68] .

3.5 Bifurcations and Chaos in dc/dc Boost converters :

Power electronics engineers frequently encounter phenomena such as sub harmonics oscillations , jumps, quasi-periodic operations, sudden broadening of power spectra, bifurcations and chaos. Power supply engineers have experienced bifurcation phenomena and chaos in switching regulators when some parameters like input voltage and feedback gain are varied but usually do not examine the phenomena in detail they avoid these phenomena by adjusting component values and parameters. So the phenomena remain somewhat mysterious and rarely examined in a formal manner. So it immediate needs for investigating such nonlinear phenomena as chaos and bifurcation. The study of nonlinear[45],[48],[119] phenomena offers the opportunity of rationalizing the commonly observed behavior. Thus knowing how and when chaos occurs will certainly help to avoid it or to exploit for useful engineering applications.. That

is why the study of bifurcations and chaos in dc/dc Boost converters has recently attracted much attention from both the power electronics and the circuits and systems communities.

3.6 A Survey of Research Findings:

The occurrence of bifurcations and chaos in power electronics was first reported in the literature in the late eighties by Hamill *et al.* Experimental observations regarding boundedness, chattering and chaos were also made by Krein and Bass back in 1990. These early reports did not contain any rigorous analysis rather they seriously pointed out the importance of studying the complex behavior of power electronics and its likely benefits for practical design. Since then much interest has been taken in the power electronics and circuits research communities in pursuing formal studies of the complex phenomena commonly observed in power electronics. In 1990, Hamill *et al* presented a paper at the IEEE Power Electronics Specialists Conference reporting an attempt to study chaos in a simple buck converter which became a subject of intensive research in the following decade. Using an implicit iterative map the occurrence of period-doublings, sub harmonics and chaos in a simple buck converter was demonstrated by numerical analysis, PSPICE simulation, MATLAB simulation, Multisim simulation and laboratory measurement. The derivation of a closed-form iterative map for the boost converter under a current-mode control scheme was presented later by the same group of researchers . This closed-form iterative map allowed the analysis and classification of bifurcations and structural instabilities of this simple converter. Since then, a number of authors have contributed to the identification of bifurcation patterns and strange attractors in a wider class of circuits and devices of relevance in power electronics. Some key publications are summarized below.

The occurrence of period-doubling for a simple dc/dc converter was reported in 1994 by Tse fig.3.3 . By modeling the dc/dc converter as a first-order iterative map, the period-doubling bifurcations can be located analytically. The idea is based on evaluating the Jacobian of the iterative map about the fixed point corresponding to the solution undergoing the period-doubling

bifurcation . Simulations and laboratory measurements have confirmed the findings. Formal theoretical studies of conditions for the occurrence

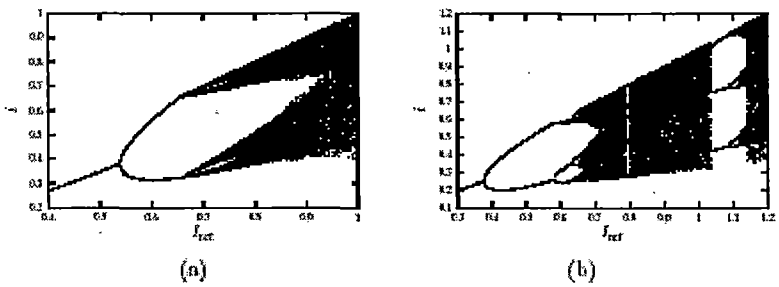

Fig. 3.3 Bifurcation diagrams from a current-mode controlled boost converter with For (a) *T/CR* = 0.125 and for (b) *T/CR* = 0.625.

of period-doubling in dc/dc converter were reported subsequently. Chakrabarty *et al.* who specifically studied the bifurcation behavior under variation of a range of circuit parameters including storage inductance, load resistance, output capacitance, etc. In 1996, Fossas and Olivar presented a detailed analytical description of dc/dc converter dynamics identifying the topology of its chaotic attractor and studying the regions associated with different system evolutions. Various possible types of operation of the converter were also investigated through the so-called stroboscopic map obtained by periodically sampling the system states. The bifurcation behavior of dc/dc Boost converters under current-mode control has been studied by a number of authors. Deane first reported on the route to chaos in a current-mode controlled boost converter. Chan and Tse studied various types of routes to chaos and their dependence upon the choice of bifurcation parameters. Figure two bifurcation diagrams numerically obtained from a current-mode controlled boost converter with output current level being the bifurcation parameter. In 1995, the study of bifurcation phenomena was extended to a fourth-order 'Cuk DC/DC converter under a current-mode control scheme. The four dimensional system is represented by an implicit fourth order iterative map, from which routes to chaos are identified numerically. It can be seen from figures (fig. 3.4) for the case of the boost converter the bifurcation behavior contains transitions where a "sudden jump from periodic solutions to chaos" is observed. These transitions cannot be explained in terms of standard bifurcations such as period-doubling" and "saddle-node".

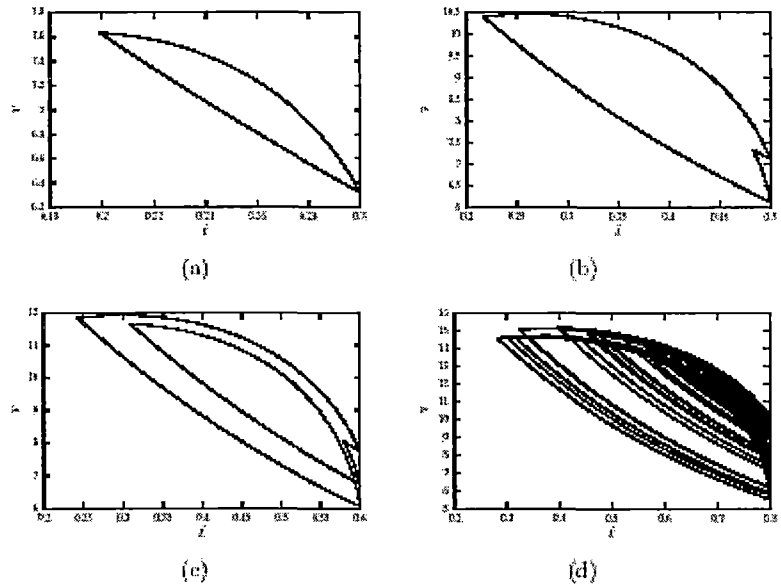

Fig. 3.4 Trajectories from a current-mode controlled boost converter. (a) Stable period-1 operation (b) stable period-2 operation (c) stable period-4 operation and (d) chaotic operation.

In fact,as studied by Banerjee *et al an*d Di Bernardo these transitions are due to a novel class of bifurcation known as "grazing" or "border-collision" bifurcation which is unique to switched dynamical systems. Since most power electronics circuits are non-autonomous systems driven by fixed-period clock signals, the study of the dynamics can be effectively carried out using appropriate discrete-time maps. In addition to the aforementioned stroboscopic maps). Di Bernardo *et al.* studied alternative sampling schemes and their applications to the study of bifurcation and chaos in power electronics. It has been found that non-uniform sampling can be used to derive discrete-time maps (termed A-switching maps) which can be used to effectively characterize the occurrence of bifurcations and chaos in both autonomous and non-autonomous systems. These maps turned out to be particularly useful for the investigation of nonsmooth bifurcation in power electronics circuits and systems. Also, the occurrence of periodic chattering was explained in terms of sliding solutions . When external clocks are absent and the system is "free-running", for example,under a hysteretic control scheme, the system is autonomous and does not have a . fixed switching period. Such free-running converters were indeed extremely common in the old days when fixed-period integrated-circuit controllers were not available. For

this type of autonomous converters, chaos cannot occur if the system order is below three. Power electronics circuits other than dc/dc converters have also been examined in recent years. Dobson *et al.* reported "switching time bifurcation" of diode and thyristor circuits. Such bifurcation manifests as jumps in the switching times. Some attempts have been made to study higher order parallel-connected systems of converters which are becoming popular design choice for high current applications.

3.7 Modeling Strategies:

Different modeling strategies are presented in[36],[40],[52],[53],[67]-[69],[86],[91]. Averaging techniques retains the low-frequency properties while ignoring the detailed dynamics within a switching cycle. Usually, the validity of averaged models is only restricted to the low-frequency range up to an order of magnitude below the switching frequency. Averaging techniques can be useful to analyze those bifurcation phenomena which are confined to the low-frequency range. An effective approach for modeling power electronics circuits with a high degree of exactness is to use appropriate discrete-time maps obtained by uniform or non-uniform sampling of the system states. The aim is to derive an iterative function that expresses the state variables at one sampling instant in terms of those at an earlier sampling instant. The basic concepts of discrete-time maps and how they can be used to explore nonlinear phenomena in power electronics are explained.

3.8 Discrete-time maps

As is often the case in nonlinear dynamical systems, the analysis of complex phenomena that are of relevance to engineering requires "adequate" models. As mentioned previously, discrete-time maps [43],[93] obtained by suitable sampling of the system dynamics can be extremely useful for characterizing the occurrence of bifurcations and chaos in power electronics circuits. We distinguish two different classes of maps, *Poincare maps* and *normal form maps*. *Poincare maps* is useful for describing the global dynamics of the system under investigation from one sampling instant to the next. N*ormal form maps* is valid locally to a bifurcation point, is an invaluable tool for classifying the system behavior of a bifurcation. Several kinds of

Poincar'e maps have been defined for the analysis of nonlinear phenomena in power electronics circuits.

Derivation of the most commonly used maps, the *stroboscopic* map, the *S-switching* (synchronous switching) map, and the *A-switching* (asynchronous switching) map are performed. The boost converter can be described by a piecewise smooth system of the form:

$$\frac{di_L}{dt} = -\frac{1}{L}v_c + \frac{\delta t}{L}V_i \quad \text{.....(3.3)}$$

$$\frac{dv_c}{dt} = \frac{1}{C}i_L - \frac{1}{RC}V_c \quad \text{.....(3.4)}$$

where $i(t)$ is the inductor current, $v(t)$ the capacitor voltage, E a constant input voltage, and $\delta(t)$ a modulated signal. In general, discrete-time maps can be categorized into the following three classes .

- *Stroboscopic map:* obtained by sampling the system states *periodically* at time instants which are multiples of the period of the clock signal (stroboscopic instants). Note that the system states are sampled at each stroboscopic instant irrespectively of whether the system configuration switches or not at that instant.

- *S-switching map (synchronous switching):* obtained by sampling the system states at those stroboscopic time instants when the system commutes from phase 2 to phase 1.

- *A-switching map (asynchronous switching):* obtained by sampling the system states at time instants within each clock cycle when the system commutes from phase 1 to phase 2.

In order to derive the relevant maps, the following two simplifying assumptions are introduced which can be removed later.

i. No more than one commutation takes place during each period of the modulating signal.

ii. The commutation from phase 2 to phase 1 can only take place at time instants which are multiples of the ramp cycle T. It is always true when the converter is under current-mode control.

3.9 Derivation of stroboscopic and S-switching maps

The stroboscopic map is the most widely used type of discrete-time maps for modeling dc/dc boost converters. It is obtained by sampling the system dynamics every T seconds, (at the beginning of each clock cycle).We use suffix k as the counting index for this map. Applying a simple iterative procedure to the solutions of the state equations for phases 1 and 2, the stroboscopic map is obtained.

i. Derivation of A-switching maps

The A-switching map is obtained when the state vector is asynchronously sampled at switching times internal to the modulating period. All the maps introduced above can be used to obtain analytical conditions for the existence of given periodic orbits and standard bifurcations such as period-doubling and saddle-node. Many reports of standard bifurcations, as surveyed earlier, have effectively employed the stroboscopic and S-switching maps . The A-switching maps are particularly useful for the analysis of multi-switching behavior, and can be constructed more conveniently for operations where skipped cycles are frequent such as when the converter is operating in a chaotic regime.

ii. Analysis and Classification of Non-smooth Bifurcations

Focus on the non-smooth bifurcations, which are relevant to power electronics.

iii. System formulation

As discussed earlier, because of their switching nature, power electronics systems

are often modeled by sets of ordinary differential equations (ODEs) or maps which are piecewise-smooth (PWS). Particularly whenever the circuit under investigation switches to a different configuration (from ON to OFF or vice versa), the vector field of the corresponding model changes from one functional form to another. According to the properties of the system along its discontinuity boundaries, we can identify three main classes of PWS dynamical systems:

- Systems with discontinuous states (jumps);
- Systems with a discontinuous vector field, i.e., the first derivative of the system states is discontinuous across the phase-space boundaries;
- Systems with a discontinuous Jacobian, i.e., the second derivative of the system states is discontinuous across the phase-space boundaries.

The discontinuity boundaries between different phase-space regions can themselves be smooth or piecewise smooth.

iv. Bifurcation possibilities

Power electronics systems can exhibit standard bifurcations such as period doubling or saddle-node. Such bifurcations are indeed frequently observed both analytically and experimentally as surveyed earlier. Some of the most common dynamical transitions observed in power electronics circuits, such as the "sudden jump to chaos" mentioned earlier, cannot be explained in terms of standard bifurcations. Power electronics systems, being *switched dynamical systems,* exhibit an interesting class of bifurcations which are not observed in their smooth counterparts. For switched dynamical systems, a dramatic change of the system behavior is observed when a part of the system trajectory hits tangentially one of the boundaries between different regions in phase space. When this occurs, the system is said to undergo a *grazing* bifurcation which is also known as C-bifurcation.

3.10 Derivation of normal-form map near a grazing bifurcation.

When the system undergoes a grazing bifurcation, fixed point of such a normal-form map crosses transversally some boundary in the phase space.). This is also called *border-collision bifurcation* whose occurrence in one-dimensional and two-dimensional maps was first reported in the western literature by Nusse *et al.* It is worth noting that such normal-form maps are not always piecewise linear. It can be shown that the form of the normal-form map at a grazing depends on the discontinuity of the system vector field, and is piecewise linear only if the discontinuity boundary between the ON and OFF zones is itself discontinuous such as in the cases of many power electronics circuits[100],[101],[110],[115]. Knowing the form of the normal-form map associated with a border collision becomes important when the aim is to predict the dynamical behavior of the system following such a bifurcation. i.e., from a fixed point associated with an orbit which does not cross the boundary to one corresponding to a solution which crosses the boundary. Linearizing the system flow about each of these fixed points, it can then be obtained a piecewise linear map. This approximate map is valid if the switching hyper plane which itself non-smooth. An acceptable method for classifying and predicting the dynamical scenarios following a border-collision bifurcation is given in Di Bernardo *et al.* It is worth mentioning that power electronics systems can exhibit a peculiar type of solution, termed *sliding*, which lies within the system discontinuity set. Intuitively, this can be seen as associated with an infinite number of switching between different phase-space regions which keep the trajectory

3.11 Chaos in Power Electronics

Chaos in power electronics are presented and explained in [32]-[35], [37]-44],[87]-[90], [95],[96]. The presence of sliding bifurcation can give rise to the formation of so-called sliding orbits, i.e., periodic solutions characterized by sections of sliding motion (or chattering). These solutions play an important role in organizing the dynamics of a given power electronics circuit . Research is still on-going in identifying a novel class of bifurcations, called *sliding bifurcations,* which involve interactions between the system trajectories and discontinuity sets where sliding motion is possible.

3.12 Current Status and Future Work

Research in nonlinear phenomena of power electronics is heading first most of the work reported so far has focused on identifying the phenomena and explaining them in the language of the nonlinear dynamics literature. The engineers commonly observed "strange" phenomena (e.g., chaos and bifurcation) and its become the topics that can be scientifically approached, rather than just being "bad" laboratory observations not relevant to the main technical interest. The chaos and system theorists published and demonstrated the rich dynamics of power electronics, offering a new area for theoretical study. It seems that identification work will continue to be an important area of investigation to know when and how a certain bifurcation occurs and how to avoid it. Power electronics is an emerging discipline with new circuits and applications creation every day. The lack of general solutions for nonlinear problems makes it necessary for each application to be studied separately and the associated nonlinear phenomena identified independently. Future research will inevitably move toward any profitable exploitation of the nonlinear properties of power electronics. As a start, some applications of chaotic power electronics systems and related theory have been identified, for instance, in the control of electromagnetic interference by "spreading" the noise spectrum , in the application of "targeting" orbits with less iterations (i.e., directing trajectories to certain orbits in as little time as possible)and in the stabilization of periodic operations.

****

Chapter 4

NON LINEAR MODELING OF PRACTICAL BOOST CONVERTER AND STUDY OF BIFURCATION

4.1 Introduction

It has been observed that some power electronic circuits exhibit deterministic chaos [34], [36]-[38] and this may be responsible for unusual noise in some power electronic circuits. It is reported about the bifurcation behaviour of the power electronic converter on variation of circuit parameters. It is also demonstrated that current mode controlled boost converter are prone to subharmonic behaviour and chaos. As it is proved that boost converter has nonlinear behaviour , a nonlinear model of the system is developed and also the detailed studies are performed about the bifurcation behaviour of it on variation of its parameters. The state space averaging technique does not serve the purpose and fails to explain the subharmonic modes and chaos in the boost converter. [34] & [9] used a large signal analysis of the continuous time system while [6] proposed that discrete model should be developed for power electronic circuits as mapping of the form

$$x_{n+1} = f(x_n) \quad \text{----------} \quad (4.1)$$

In the current mode controlled boost converter, the map can be obtained in closed form. Such a map based model was developed in [10] assuming idealized circuit elements. For some practical situation a map based model was developed in [44] considering all parasitic elements and showed that it is still in closed form. They also derived the map when observations are made at every clock instant instead of every switching instant .All of those investigation are carried out with the smooth (pure) dc input for the current mode controlled boost converter. But in most of the practical converter input voltage is nonsmooth dc (dc with ripple) is used for the current mode controlled boost converter. So to conform the very practical situation the nonsmooth dc voltage fed current mode controlled boost converter with all parasitic elements are taken in this paper for study. A nonlinear model of the same with

single phase full wave rectified voltage as input is developed in this chapter to study the nonlinear phenomenon and bifurcation in details.

4.2 Practical Boost Converter

For our study the boost converters fig. 4.1(a) and fig.4.1 (b) consist of control switch (s), an uncontrolled switch (D5), an inductor (L), a capacitor (C), a load resistor (R), an internal resistance of the inductor (r_i), an internal resistance of the capacitor (r_c), The switch is controlled by the feedback path consisting of a comparator, a flip-flop and driver. The supply is given to the converter directly from a pure DC voltage for figure 4.1.(a) and single phase supply through a single phase full wave bridge rectifier (D1,D2,D3 D4) for fig.4.1.(b). The comparator compares the inductor current and reference current (Iref).

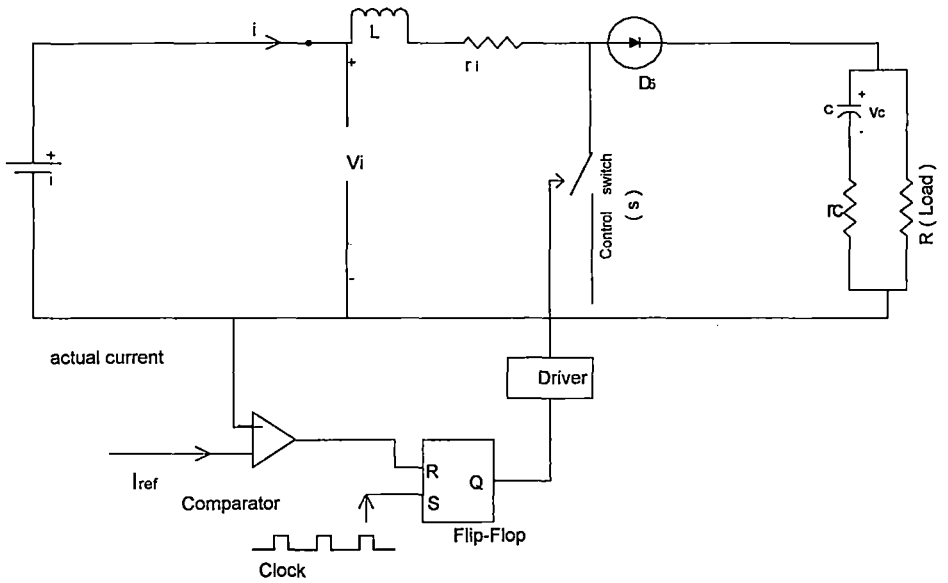

Fig 4.1 (a) pure dc fed current controlled dc/dc boost converter

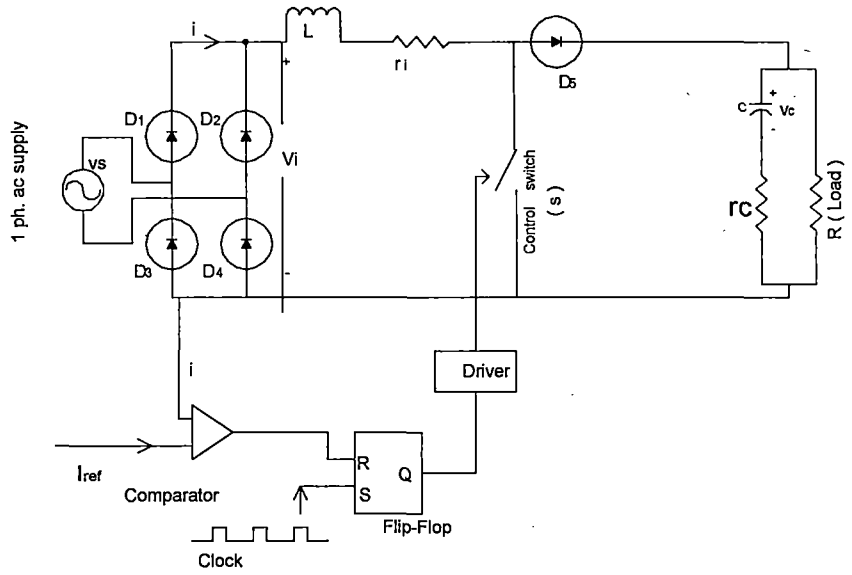

Fig. 4.1 (b) Single phase rectified dc fed current controlled dc/dc boost converter

Boost converter has the higher output voltage than the input voltage. When the control switch is turned on, the inductor stores energy from source and during off time of the control switch, the inductor transfers the stored energy to the connected capacitor across the load. The circuit is operated in continuous current mode (CCM) which means that inductor current never becomes zero.

The circuit has two states depending on whether the control switch is opened or closed. When switch is closed (on period) the state equations are

$$L\frac{di}{dt} = V_i - ir_i \quad \text{---------- (4. 2)}$$

$$C\frac{dv_c}{dt} = -\frac{v_c}{R + r_c} \quad \text{---------- (4. 3)}$$

and the states equations during off period (when switch is off) are

$$L\frac{di}{dt} = V_i - ir_i - i\frac{Rr_c}{R + r_c} - v_c\frac{R}{R + r_c} \quad \text{---------- (4. 4)}$$

$$C\frac{dv_c}{dt} = -\frac{v_c}{R+r_c} + i\frac{R}{R+r_c} \quad \text{---------- (4. 5)}$$

where Vi= Vi a constant (pure) dc voltage

Vi = $|V_m Sin\omega t|$ a rectified dc voltage

Switching logic of the circuit is that when switch is closed the inductor current rises and it continues till the inductor current reaches to Iref , ignoring any arriving clock pulse . As soon as the inductor current reaches to Iref , the inductor current falls. The switch closes again on the arrival of the next clock pulse. This is also explained by the fig.4.2

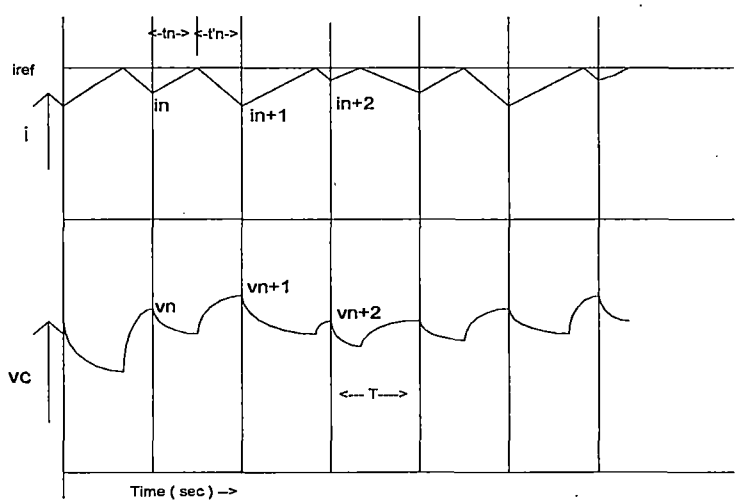

Fig. 4.2 Time plot of capacitor voltage and inductor current of the boost converter with clock pulses

4.3 The Model of Practical Boost Converter

An expression is derived for the mapping from one switching instant to the next considering the continuous conduction of the converter in fig 1(a). Fig.4. 2 shows the behavior of the state variables along with the clock pulses. At the starting of on period or off period, the initial conditions (i.e. at t=0) be $i = i_0$ and $v_c = v_0$. Final conditions of one state are the initial conditions of next other state. The switch turns off when the inductor current reaches reference

current (I_{ref}). Using Laplace equations and considering initial conditions, the expressions of time response for both on time and off time are established.

a. Pure dc fed boost converter:

During on period, the equation of v_c and i are obtained from (4.2) and (4.3) are

$$v_c(t) = V_0 e^{-t/(R+r_c)C} \quad \text{---------- (4.6)}$$

$$i(t) = \frac{V_i}{r_i}[-e^{-r_i t/L} + 1] - i_0 e^{-r_i t/L} \quad \text{----------(4.7)}$$

i_0 and V_0 are the initial current and voltage during this on period.

During off period, the equation of v_c and i are obtained from (4.4) and (4.5) are

$$i(t) = (v_i/M) + \frac{V_0 R}{K(R+r_c)} e^{-t/[(R+r_c)C]} - e^{-Ht/(2G)} \cos(Pt)[\frac{V_i}{M} + \frac{1}{K(R+r_c)C}]$$
$$- e^{-Ht/(2G)} \sin(Pt) \frac{1}{G}[\frac{V_i H}{MP} + \frac{M-1}{KP} + Li_0]$$

----------(4.8)

$$v_c(t) = [v_i R(R+r_c)/M] + e^{-Ht/(2G)} \cos(Pt)[V_0 L(R+r_c)^2 - (v_i R(R+r_c)/M)]$$
$$+ \frac{1}{PG} e^{-Ht/(2G)} \sin(Pt)[V_0 AC(R+r_c)^2 + LR(R+r_c)i_0 - v_i R(R+r_c)\frac{H}{M}]$$

----------(4.9)

Here we consider $H^2 < 16MG$, which is the most important from a practical point of view.

where $A = r_i + \frac{Rr_c}{R+r_c}$, $M = r_i(R+r_c) + Rr_c + R^2$,

$H = (R+r_c)(L + Cr_i(R+r_c) + RCr_c$,

$G = LC(R+r_c)^2$, $P = \sqrt{\frac{M}{G} - \frac{H^2}{4G^2}}$, K=M+E,

i_0 and V_0 are the initial current and voltage during this off period.

If at any instant (t_n) the value of v_c and i are v_n and i_n then for the next value of them at the next instant (t_{n+1}) are v_{n+1} and i_{n+1} taking $v_0 = v_n$ and $i_0 = i_n$.

The on-time (t_{on}) can be calculated from equations (4.6) ans (4.7) and the off-time (t_{off}) can be calculated from equations (4.8) and (4.9)

The map based model can be used to predict the behavior of the system under different parameter combinations. Here the boost converter are represented by two ways, first by locating the peak of the capacitor voltage and second by sampling it in synchronism with the clock.

b. Single phase rectified dc fed boost converter:

During on period, the equation of v_c and i are obtained from (4.2) and (4.3) are

$$v_c(t) = v_0 e^{-t/(R+r_c)C} \quad \text{---------- (4.10)}$$

$$i(t) = \frac{V_m \omega L}{(\omega^2 L^2 + r_i^2)}[e^{-r_i t/L} - \cos\omega t + \frac{r_i}{L}\sin\omega t] - i_0 e^{-r_i t/L} \quad \text{-------- (4.11)}$$

i_0 and V_0 are the initial current and voltage during this on period.

During off period, the equation of v_c and i are obtained from (4.4) and (4.5) are

$$i(t) = \frac{v_i \omega}{GD}[\cos(\omega t) + \frac{(G\omega^2 - M)\sin(\omega t)}{H\omega}] - [\frac{V_0 R}{K(R+r_c)} e^{-t/[(R+r_c)C]}$$

$$- e^{-Ht/(2G)}\cos(Pt)[\frac{v_i \omega}{GD} + \frac{1}{K(R+r_c)C}] - e^{-Ht/(2G)}\sin(Pt)\frac{1}{G}[\frac{v_i \omega B}{GDP} + \frac{M-1}{KP} + Li_0]$$

----------(4.12)

$$v_c(t) = [v_i \omega R(R + r_c)/(GD)][\cos(\omega t) + ((G\omega^2 - M)\sin(\omega t))/(H\omega)]$$

$$+ e^{-Ht/(2G)}\cos(Pt)[V_0 L(R + r_c)^2 - (v_i \omega R(R + r_c)/(GD))]$$

$$+ \frac{1}{PG} e^{-Ht/(2G)}\sin(Pt)[V_0 AC(R + r_c)^2 + LR(R + r_c) i_0 - v_i \omega R(R + r_c)\frac{B}{D}]$$

----------(4.13)

Here we consider $H^2 < 16MG$, which is the most important from a practical point of view.

where $A = r_i + \frac{Rr_c}{R + r_c}$, $M = r_i(R + r_c) + Rr_c + R^2$, $H = (R + r_c)(L + Cr_i(R + r_c) + RCr_c$,

$G = LC(R + r_c)^2$, $P = \sqrt{\frac{M}{G} - \frac{H^2}{4G^2}}$, K=M+E, $D = (H^2\omega^2 - M^2 - \omega^4 G^2)/(GH)$,

$B = (G^2\omega^2 - MG + H^2)/(GH)$,

If at any instant (t_n) the value of v_c and i are v_n and i_n then for the next value of them at the next instant (t_{n+1}) are v_{n+1} and i_{n+1} taking $v_0 = v_n$ and $i_0 = i_n$.

The on-time (t_{on}) can be calculated from equations (4.10) ans (4.11) and the off-time (t_{off}) can be calculated from equations (4.12) and (4.13)

The map based model can be used to predict the behavior of the system under different parameter combinations. Here the boost converter are represented by two ways, first by locating the peak of the capacitor voltage and second by sampling it in synchronism with the clock.

4.4 Bifurcation Phenomena of the Boost Converter

The operation of the boost converter is considered here from clock point of view. As the clock pulse has an externally determined periodicity, we identify the system periodicity as in numbers of clock pulses in a period of waveform. So the sampling is done at each clock pulse. Also we detect the peak capacitor voltage for analysis. The model provides a fast and easy way of obtaining bifurcation diagrams. Some initial readings are eliminated due to initial transient. There are nine parameters in the system, input voltage($V_i = V_m/\sqrt{2}$), load resistance(R), inductance(L), Capacitance (C), reference current(I_{ref}), clock frequency(f_c), input voltage frequency(fs= $\omega/2\pi$), internal resistance of inductor (r_i), internal resistance of capacitor (r_c).

Parameters are set for the converter, if not stated otherwise : I_{ref} =4amps, r_i=1.2 ohms, r_c=0.1 ohms(fs). R=20 ohms. Clock frequency(f_c)=500Hz. Input voltage(rms value)=20V, Input voltage frequency=50Hz, L=27 mH, C=120 μF.

For these set values the phase plots of the two state variables, time plots of the two state variables are determined and different plotting results are reported in this chapter. Bifurcation diagrams of the state variables with the variation of different parameter values are also reported in this chapter. Reading of the state values are taken at clock for non autonomous case and at their peak values for autonomous case.

a. Pure dc fed boost converter:

i. **Input voltage (Vi) as bifurcation parameter**: The bifurcation diagrams of the rectified dc fed boost converter with input voltage (Vi) as variable parameter are shown in figure 4.102, 4.103 and 4.104. Fig.4.102 & 4.104 shows the bifurcation diagram for non autonomous system (i.e inductor current and capacitor voltage are sampled at clock) and fig. 4.103 shows the bifurcation diagram for autonomous system (i.e capacitor voltage are sampled at its peak values). Keeping other parameters at set values, the input voltage (Vi) is varied from 07 to 60 volts in step of 0.1 volt.

The autonomous (fig. 4.103) case of the converter shows period doubling cascade from period- 1 region to chaos as the input voltage is decreased from 60 volts. Period- 1 region exists from 60 volts to 33.8 volts. Period-1 bifurcates to period-2 below 33.8 volts and it continues to 23.7 volts. Period-2 bifurcates to period-4 below 23.7 volts and it continues to 23.4 volts. Then it enters the period-3 region and continues to 22.1 volts. Period-3 bifurcates to period-6 below 22.1 volts and it continues to 20.6 volts. Then it enters the chaos and chaotic window is noticed in the chaotic region. period –2 window appears at 15.1 volts and period –4 window appears at 15.4 volts.

In non autonomous (fig. 4.102 & 4.104) case of the converter, almost same behaviors are observed. Here also the diagram shows period doubling cascade from period- 1 region to chaos as the input voltage is decreased from 60 volts. Period- 1 region exists from 60 volts to 32.9 volts. Period-1 bifurcates to period-2 below 32.9 volts and it continues to 23.0 volts. Period-2 bifurcates to period-4 below 23.0 volts and it continues to 22.5 volts. Then it enters the period-3 region and continues to 21.3 volts.

Period-3 bifurcates to period-6 below 21.3 volts and it continues to 19.1 volts. Then it enters the chaos and chaotic window is noticed in the chaotic region. period –2 window appears at 14.9 volts and period –4 window appears at 14.4 volts.

The fig. 4.104 shows a staircase like structure in the chaotic region. It increases with decrease of input voltage as the attractor size increases. Steps of the staircases changes at 23.0, 14.8, 11.0, 8.9 and 7.8 for 1,2,3,4 and 5 stairs respectively.

ii. **Load resistance (R) as bifurcation parameter**: The bifurcation diagrams of the pure dc fed boost converter with load resistance (R) as variable parameter are shown in figure 4.93, 4.94 and 4.95. Fig.4.93 & 4.94 shows the bifurcation diagram for non autonomous system (i.e inductor current and capacitor voltage are sampled at clock) and fig. 4.95 shows the bifurcation diagram for autonomous system (i.e capacitor voltage are sampled at its peak values). Keeping other parameters at set values, the load resistance (R) is varied from 01 to 100 ohms in step of 0.1 ohm.

Te autonomous (fig. 4.95) case of the converter shows period doubling cascade from period- 1 region to chaos as the load resistance (R) is increased from 01 ohm. Period- 1 region exists from 01 to 08.2 ohms. Period-1 bifurcates to period-2 above 08.2 ohms and it continues to 13.2 ohms. Period-2 bifurcates to period-3 above 13.2 ohms and it continues to 16.8 ohms. Then it goes through period doubling cascade then it enters the chaos and chaotic window is noticed in the chaotic region at 44.4 ohms with multi period window.

In the non autonomous (fig. 4.93 & 4.94) cases of the converter, the same behaviors are observed at the same values of load resistance (R).

iii. **Reference current (Iref) as bifurcation parameter**: The bifurcation diagrams of the pure dc fed boost converter with reference current (Iref) as variable parameter are shown in figure 4.105, 4.106 and 4.107. Fig.4.106 & 4.107 shows the bifurcation diagram for non autonomous system (i.e inductor current and capacitor voltage are

sampled at clock) and fig. 4.105 shows the bifurcation diagram for autonomous system (i.e capacitor voltage are sampled at its peak values). Keeping other parameters at set values, reference current (Iref) is varied from 01 to 07 amps in step of 0.01 amp.

The autonomous (fig. 4.105) case of the converter shows period doubling cascade from period- 1 region to chaos as the reference current (Iref) is increased from 01 amp. Period- 1 region exists from 01 amp. to 2.82 amps. Period-1 bifurcates to period-2 above 2.82 amps and it continues to 3.37 amps. Period-2 bifurcates to period-3 above 3.37 amps and it continues to 3.62 amps. Then it enters the period-5 region and continues to 3.82 amps. Then it enters the chaos and chaotic period window is noticed in the chaotic region from 5.32 amps to 5.63 amps.

In non autonomous (fig. 4.106 & 4.107) case of the converter, the same behaviors are observed at the same values of reference current.

iv. **Capacitance (C) as bifurcation parameter**: The bifurcation diagrams of the pure dc fed boost converter with capacitance (C) as variable parameter are shown in figure 4.81, 4.82 and 4.83. Fig.4.81 & 4.82 shows the bifurcation diagram for non autonomous system (i.e inductor current and capacitor voltage are sampled at clock) and fig. 4.83 shows the bifurcation diagram for autonomous system (i.e capacitor voltage are sampled at its peak values). Keeping other parameters at set values, the capacitance (C) is varied from 01 to 200 microfarads in step of 0.5 microfarad.

Both the autonomous (fig. 4.83) case and the non autonomous (fig.4.81 & 4.82) of the converter show a chaotic operation with a periodic windows in the chaotic region with a clearly visible period doubling cascade. Periodic window appears at 11.5 microfarads and continued to 45.5 microfarads. Period- 3, Period- 6, Period- 12 and other periodic windows are forecasted in the converter.

v. **Inductance (L) as bifurcation parameter**: The bifurcation diagrams of the pure dc fed boost converter with inductance (L) as variable parameter are shown in figure 4.90,

4.91 and 4.92. Fig.4.90 & 4.91 shows the bifurcation diagram for non autonomous system (i.e inductor current and capacitor voltage are sampled at clock) and fig. 4.92 shows the bifurcation diagram for autonomous system (i.e capacitor voltage are sampled at its peak values). Keeping other parameters at set values, the inductance (L) is varied from 01 to 100 milihenries in step of 0.5 milihenries.

The autonomous (fig. 4.92) case of the converter shows period doubling cascade from period- 1 region to chaos as the inductance (L) is increased from 01 to 100 milihenries . Period- 1 region exists from 01 to 3.5 milihenries . Period-1 bifurcates to period-2 above 3.5 milihenries and it continues to 13.0 milihenries . Period-2 bifurcates to period-4 above 13.0 milihenries and it continues to 17.5 milihenries . Then it enters the period-9 region and continues to 24.5 milihenries . Then it enters the chaos and chaotic period window is noticed in the chaotic region from 63.5 milihenries to 71.5 milihenries . Period- 5 and other periodic windows are forecasted in the converter.

In non autonomous (fig. 4.90 & 4.91) case of the converter, the same behaviors are observed at the same values of inductance.

vi. **Frequency of clock (fc) as bifurcation parameter**: The bifurcation diagrams of the pure dc fed boost converter with frequency of clock (fc) as variable parameter are shown in figure 4.87, 4.88 and 4.89. Fig.4.87 & 4.88 shows the bifurcation diagram for non autonomous system (i.e inductor current and capacitor voltage are sampled at clock) and fig. 4.89 shows the bifurcation diagram for autonomous system (i.e capacitor voltage are sampled at its peak values). Keeping other parameters at set values, frequency of clock (fc) is varied from 100 to 20000 hertzs in step of 100 hertzs .

Both the autonomous (fig. 4.89) case and the non autonomous (fig.4.87 & 4.88) of the converter show a chaotic operation throughout without any periodic windows in the chaotic region.

vii. **Series inductor resistance (r_i) as bifurcation parameter:** The bifurcation diagrams of the pure dc fed boost converter with series inductor resistance (r_i) as variable parameter are shown in figure 4.99, 4.100 and 4.101. Fig.4.99 & 4.100 shows the bifurcation diagram for non autonomous system (i.e inductor current and capacitor voltage are sampled at clock) and fig. 4.101 shows the bifurcation diagram for autonomous system (i.e capacitor voltage are sampled at its peak values). Keeping other parameters at set values, series inductor resistance (r_i) is varied from 0.1 to 2.0 ohms in step of 0.01 ohm.

The autonomous (fig. 4.101) case of the converter shows period doubling cascade from period- 4 region to chaos as the series inductor resistance (r_i) is increased from 0.1 ohms. Period- 4 region exists from 0.1 to 0.48 ohms. Period-4 bifurcates to period-8 below 0.48 ohms and it continues to 0.6 ohms. Period-8 bifurcates to period-16 below 0.6 ohms and it continues to 0.74 ohms. Then it enters the chaos with period doubling bifurcations.

In non autonomous (fig. 4.99 & 4.101) case of the converter, the same behaviors are observed at the same values of series inductor resistance (r_i).

viii. **Series capacitor resistance (r_c) as bifurcation parameter:** The bifurcation diagrams of the pure dc fed boost converter with series capacitor resistance (r_c) as variable parameter are shown in figure 4.96, 4.97 and 4.98. Fig.4.96 & 4.97 shows the bifurcation diagram for non autonomous system (i.e inductor current and capacitor voltage are sampled at clock) and fig. 4.98 shows the bifurcation diagram for autonomous system (i.e capacitor voltage are sampled at its peak values). Keeping other parameters at set values, series capacitor resistance (r_c) is varied from 0.1 to 2.0 ohms in step of 0.01 ohm.

Both the autonomous (fig. 4.98) case and the non autonomous (fig.4.96 & 4.97) of the converter show a chaotic operation throughout without any periodic windows in the chaotic region

ix. **Time period of clock (CTP) as bifurcation parameter**: The bifurcation diagrams of the pure dc fed boost converter with time period of clock (CTP) as variable parameter are shown in figure 4.84, 4.85 and 4.86. Fig.4.84 & 4.85 shows the bifurcation diagram for non autonomous system (i.e inductor current and capacitor voltage are sampled at clock) and fig. 4.86 shows the bifurcation diagram for autonomous system (i.e capacitor voltage are sampled at its peak values). Keeping other parameters at set values, time period of clock (CTP) is varied from 1 to 2.5 miliseconds in step of 0.01 milisecond .

Both the autonomous (fig. 4.86) case and the non autonomous (fig.4.84 & 4.85) of the converter show a chaotic operation throughout without any periodic windows in the chaotic region.

b. Single phase full wave rectified dc fed boost converter:

i. **Input voltage (Vi) as bifurcation parameter**: The bifurcation diagrams of the single phase full wave rectified dc fed boost converter with input voltage (Vi) as variable parameter are shown in figure 4.3, 4.4 and 4.5. Fig.4.3 & 4. 4 shows the bifurcation diagram for non autonomous system (i.e inductor current and capacitor voltage are sampled at clock) and fig. 4.5 shows the bifurcation diagram for autonomous system (i.e capacitor voltage are sampled at its peak values). Keeping other parameters at set values, the input voltage (Vi) is varied from 07 to 60 volts in step of 0.1 volt.

The autonomous (fig. 4.5) case of the converter shows period doubling cascade from period- 1 region to chaos as the input voltage is decreased from 60

volts. Period- 1 region exists from 60 volts to 57.5 volts. Period-1 bifurcates to period-2 below 57.5 volts and it continues to 50.1 volts. Period-2 converted to chaos below 50.1 volts and it continues to 44.2 volts. Then it enters the period-4 region and continues to 28.8 volts. Period-4 bifurcates to period-8 below 28.8 volts and it continues to 25.3 volts. Then again it enters the chaos and chaotic window is noticed in the chaotic region. Chaotic window appears at 13.4 volts and continues to 10.1 volts.

In non autonomous (fig. 4.3 & 4. 4) case of the converter, almost same behaviors are observed. Here the diagram shows from chaotic region to chaotic region through period doubling cascade as the input voltage is decreased from 60 volts. Period- 5 region and period-10 region and other periodic regions are forecasted .

The fig. 4.4 shows a staircase like structure in the chaotic region. It increases with decrease of input voltage as the attractor size increases. Steps of the staircases changes at 29.0, 22.1, 17.0, 11.2 and 9.3 for 1,2,3,4 and 5 stairs respectively.

The observations are supported by Phase plot fig. 4.7 (plot between two state variables that is capacitor voltage at clock and inductor current at clock.), Time plot of capacitor voltage at clock fig. 4.6 , time plot of inductor current at clock fig. 4.9 and time plot of peak capacitor voltage at clock fig. 4.8.

ii. **Load resistance (R) as bifurcation parameter**: The bifurcation diagrams of the single phase full wave rectified dc fed boost converter with load resistance (R) as variable parameter are shown in figure 4.66, 4.67 and 4.68. Fig.4.66 & 4.67 shows the bifurcation diagram for non autonomous system (i.e inductor current and

capacitor voltage are sampled at clock) and fig. 4.68 shows the bifurcation diagram for autonomous system (i.e capacitor voltage are sampled at its peak values). Keeping other parameters at set values, the load resistance (R) is varied from 01 to 100 ohms in step of 0.1 ohm.

The autonomous (fig. 4.68) case and the non autonomous (fig.4.66 & 4.67) of the converter show a chaotic operation throughout with two periodic windows in the chaotic region. Chaotic windows appear at 13.4 ohms and 34.3 ohms.

The non autonomous (fig. 4.66 & 4.67) case, the converter shows period doubling cascade from period- 5 region to chaos as the load resistance is increased from 01 ohm. Period- 5 region starts from 3.5 ohms. Period-5 bifurcates to period-10 above 3.5 ohms and it continues to higher period. Then it enters the chaos and shows two chaotic window in the chaotic region. Chaotic window appears at 13.4 ohms and 34.3 ohms.

iii. **Reference current (Iref) as bifurcation parameter**: The bifurcation diagrams of the single phase full wave rectified dc fed boost converter with reference current (Iref) as variable parameter are shown in figure 4.10, 4.11 and 4.12. Fig.4.10 & 4.12 shows the bifurcation diagram for non autonomous system (i.e inductor current and capacitor voltage are sampled at clock) and fig. 4.11 shows the bifurcation diagram for autonomous system (i.e capacitor voltage are sampled at its peak values). Keeping other parameters at set values, reference current (Iref) is varied from 01 to 07 amps in step of 0.01 amp.

In the autonomous (fig. 4.11) case of the converter shows period doubling cascade from period- 1 region to chaos as the reference current (Iref) is increased from 01 amp. Period- 1 region exists from 01 amp. to 1.34 amps. Period-1 bifurcates to period-2 above 1.34 amps and it continues to 1.62 amps. Period-2 enters the chaotic region above 1.62 amps and it continues to 1.69 amps. Then it enters the period-4 region and continues to 2.72 amps. Period-4 bifurcates to period-8 above

2.72 amps and it continues to 3.11 amps. Period-8 bifurcates to period-16 above 3.11 amps and it continues to 3.3 amps Then again it enters the chaotic region and continues to 6.08amps. Again period doubling cascade bifurcation occurs after that.

In non autonomous (fig. 4.10 & 4. 12) case of the converter, almost same behaviors are observed. Here the diagram shows from chaotic region to chaotic region through period doubling cascade as the reference current is increased from 01 amp. Period- 5 region and period-10 region and other periodic regions are forecasted .

The observations are supported by:

- For reference current of 2.5 amps, phase plot fig. 4.13 (plot between two state variables that is capacitor voltage at clock and inductor current at clock.), Time plot of capacitor voltage at clock fig. 4.14 , time plot of inductor current at clock fig. 4.16 and time plot of peak capacitor voltage at clock fig. 4.15.

- For reference current of 3.0 amps, phase plot fig. 4.17 (plot between two state variables that is capacitor voltage at clock and inductor current at clock.), Time plot of capacitor voltage at clock fig. 4.19 , time plot of inductor current at clock fig. 4.18 and time plot of peak capacitor voltage at clock fig. 4.20.

- For reference current of 5.0 amps, phase plot fig. 4.21 (plot between two state variables that is capacitor voltage at clock and inductor current at clock.), Time plot of capacitor voltage at clock fig. 4.23 , time plot of inductor current at clock fig. 4.22 and time plot of peak capacitor voltage at clock fig. 4.24.

iv. **Capacitance (C) as bifurcation parameter**: The bifurcation diagrams of the single phase full wave rectified dc fed boost converter with capacitance (C) as variable parameter are shown in figure 4.25, 4.26 and 4.27 Fig.4.25 & 4.26 shows the

bifurcation diagram for non autonomous system (i.e inductor current and capacitor voltage are sampled at clock) and fig. 4.26 shows the bifurcation diagram for autonomous system (i.e capacitor voltage are sampled at its peak values). Keeping other parameters at set values, the capacitance (C) is varied from 01 to 200 microfarads in step of 0.5 microfarad.

Both the autonomous (fig. 4.27) case and the non autonomous (fig.4.25 & 4.26) of the converter show a chaotic operation with a periodic windows in the chaotic region with a clearly visible period doubling cascade. Periodic window appears at 6.5 microfarads and continued to 158 microfarads. Period-10, Period-20, and other periodic windows are forecasted in the converter.

The observations are supported by:

- For capacitance value of 15 microfarads, phase plot fig. 4.28 (plot between two state variables that is capacitor voltage at clock and inductor current at clock.), Time plot of capacitor voltage at clock fig. 4.30 , time plot of inductor current at clock fig. 4.29 and time plot of peak capacitor voltage at clock fig. 4.31.

- For capacitance value of 200 microfarads, phase plot fig. 4.32 (plot between two state variables that is capacitor voltage at clock and inductor current at clock.), Time plot of capacitor voltage at clock fig. 4.34 , time plot of inductor current at clock fig. 4.33 and time plot of peak capacitor voltage at clock fig. 4.35.

- For capacitance value of 100 microfarads, phase plot fig. 4.36 (plot between two state variables that is capacitor voltage at clock and inductor current at clock.), Time plot of capacitor voltage at clock fig. 4.38 , time plot of inductor current at clock fig. 4.37 and time plot of peak capacitor voltage at clock fig. 4.39.

v. **Inductance (L) as bifurcation parameter:** The bifurcation diagrams of the single phase full wave rectified dc fed boost converter with inductance (L) as variable parameter are shown in figure 4.40, 4.41 and 4.42. Fig.4.40 & 4.41 shows the bifurcation diagram for non autonomous system (i.e inductor current and capacitor voltage are sampled at clock) and fig. 4.42 shows the bifurcation diagram for autonomous system (i.e capacitor voltage are sampled at its peak values). Keeping other parameters at set values, the inductance (L) is varied from 01 to 100 milihenries in step of 0.5 milihenries.

In the autonomous (fig. 4.42) case of the converter shows period doubling cascade from period- 1 region to chaos as the inductance (L) is increased from 01 to 100 milihenries .

In non autonomous (fig. 4.40 & 4.41) case of the converter, show a chaotic operation throughout with a period doubling cascade in the chaotic region.

For inductance value of 5 milihenries , phase plot fig. 4.44 (plot between two state variables that is capacitor voltage at clock and inductor current at clock.), Time plot of capacitor voltage at clock fig. 4.45 , time plot of inductor current at clock fig. 4.43 and time plot of peak capacitor voltage at clock fig. 4.46.

vi. **Frequency of clock (fc) as bifurcation parameter:** The bifurcation diagrams of the single phase full wave rectified dc fed boost converter with frequency of clock (fc) as variable parameter are shown in figure 4.57, 4.58 and 4.59. Fig.4.57 & 4.58 shows the bifurcation diagram for non autonomous system (i.e inductor current and capacitor voltage are sampled at clock) and fig. 4.59 shows the bifurcation diagram for autonomous system (i.e capacitor voltage are sampled at its peak values). Keeping other parameters at set values, frequency of clock (fc) is varied from 100 to 20000 hertzs in step of 100 hertzs .

Both the autonomous (fig. 4.59) case and the non autonomous (fig.4.57 & 4.58) of the converter show a chaotic operation throughout without any periodic windows in the chaotic region.

vii. **Series inductor resistance (r_i) as bifurcation parameter:** The bifurcation diagrams of the single phase full wave rectified dc fed boost converter with series inductor resistance (r_i) as variable parameter are shown in figure 4.47, 4.48 and 4.49. Fig.4.47 & 4.48 shows the bifurcation diagram for non autonomous system (i.e inductor current and capacitor voltage are sampled at clock) and fig. 4.49 shows the bifurcation diagram for autonomous system (i.e capacitor voltage are sampled at its peak values). Keeping other parameters at set values, series inductor resistance (r_i) is varied from 0.1 to 2.0 ohms in step of 0.01 ohm.

Both the autonomous (fig. 4.49) case and the non autonomous (fig.4.47 & 4.48) of the converter show a chaotic operation throughout with one periodic window with period doubling cascade in the chaotic region. Period-16 and period-32 are forecasted in the chaotic window.

For series inductor resistance value of 0.75 ohm., phase plot fig. 4.51 (plot between two state variables that is capacitor voltage at clock and inductor current at clock.), Time plot of capacitor voltage at clock fig. 4.50 , time plot of inductor current at clock fig. 4.53 and time plot of peak capacitor voltage at clock fig. 4.52.

viii. **Series capacitor resistance (r_c) as bifurcation parameter:** The bifurcation diagrams of the single phase full wave rectified dc fed boost converter with series capacitor resistance (r_c) as variable parameter are shown in figure 4.60, 4.61 and 4.62. Fig.4.60 & 4.61 shows the bifurcation diagram for non autonomous system (i.e inductor current and capacitor voltage are sampled at clock) and fig. 4.62 shows the bifurcation diagram for autonomous system (i.e capacitor voltage are sampled at its

peak values). Keeping other parameters at set values, series capacitor resistance (r_c) is varied from 0.1 to 2.0 ohms in step of 0.01 ohm.

Both the autonomous (fig. 4.98) case and the non autonomous (fig.4.96 & 4.97) of the converter show the operation from multi period to the chaotic region.

ix. **Time period of clock (CTP) as bifurcation parameter**: The bifurcation diagrams of the single phase full wave rectified dc fed boost converter with time period of clock (CTP) as variable parameter are shown in figure 4.54, 4.55 and 4.56. Fig.4.54 & 4.55 shows the bifurcation diagram for non autonomous system (i.e inductor current and capacitor voltage are sampled at clock) and 4.56 shows the bifurcation diagram for autonomous system (i.e capacitor voltage are sampled at its peak values). Keeping other parameters at set values, time period of clock (CTP) is varied from 1 to 2.5 miliseconds in step of 0.01 milisecond .

Both the autonomous (fig. 4.56) case and the non autonomous (fig.4.54 & 4.55) of the converter show a chaotic operation throughout without any periodic windows in the chaotic region.

The fig. 4.55 shows a staircase like structure in the chaotic region. It increases with decrease of time period of clock as the attractor size increases

x. **Frequency of supply (fs) as bifurcation parameter**: The bifurcation diagrams of the single phase full wave rectified dc fed boost converter with frequency of supply (fs) as variable parameter are shown in figure 4.63, 4.64 and 4.65. Fig.4.63 & 4.65 shows the bifurcation diagram for non autonomous system (i.e inductor current and capacitor voltage are sampled at clock) and 4.64 shows the bifurcation diagram for autonomous system (i.e capacitor voltage are sampled at its peak values). Keeping other parameters at set values, frequency of supply (fs) is varied from 1 to 200 hertzs in step of 1 hertz .

In the autonomous (fig. 4.64) case of the converter show a chaotic operation throughout with one periodic window in the chaotic region.

In the non autonomous (fig.4.63 & 4.64) of the converter show a chaotic operation throughout with one periodic windows in the chaotic region.

The fig. 4.63 shows a staircase like structure in the chaotic region. It increases with decrease of supply frequency as the attractor size increases. Steps of the staircases changes at 199.0, 62.0, 37.0, 24.0, 16.0 and 10.0 hertzs for 1,2,3,4,5 and 6 stairs respectively.

c. Multi phase half wave rectified dc fed boost converter:

Number of phase as bifurcation parameter: If the number of phase of a multi phase half wave rectified dc fed boost converter is varied we get the bifurcation diagrams. The bifurcation diagrams of the multi phase half wave rectified dc fed boost converter with number of phase as variable parameter are shown in figure 4.69, 4.70 and 4.71. Fig.4.69 & 4.70 shows the bifurcation diagram for non autonomous system (i.e inductor current and capacitor voltage are sampled at clock) and fig. 4.71 shows the bifurcation diagram for autonomous system (i.e capacitor voltage are sampled at its peak values). Keeping other parameters at set values, number of phase is varied from 1 to 36 in step of 1 .

Both the autonomous (fig. 4.71) case and the non autonomous (fig.4.69 & 4.70) of the converter show a period doubling cascade from period –2 to chaos as the number of phase is decreased from 36 to 1. In the autonomous (fig. 4.71) case of the converter period- 2 region continues to 17. Period-2 bifurcates to period-4 , 8,16 etc below 17 then it enters the the chaotic region at 4.

In the non autonomous (fig.4.69 & 4.70) case of the converter period- 2 region continues to 12. Period-2 bifurcates to period-4 , 8,16 etc below 12 then it enters the the chaotic region at 6.

d. Three phase full wave rectified dc fed boost converter:

i. Input voltage (Vi) as bifurcation parameter: The bifurcation diagrams of the three phase full wave rectified dc fed boost converter with input voltage (Vi) as variable parameter are shown in figure 4.75, 4.76 and 4.77. Fig.4.75 & 4.76 shows the bifurcation diagram for non autonomous system (i.e inductor current and capacitor voltage are sampled at clock) and fig. 4.77 shows the bifurcation diagram for autonomous system (i.e capacitor voltage are sampled at its peak values). Keeping other parameters at set values, the input voltage (Vi) is varied from 07 to 60 volts in step of 0.1 volt.

In the autonomous (fig. 4.77) case of the converter shows period doubling cascade from period- 5 region to chaos as the input voltage is decreased from 60 volts. Period- 5 region from 60 volts to 24.3 volts. Period-5 bifurcates to period-10 below 24.3 volts and it continues to 17.2 volts. Then Period-10 to period-20 and finally enters the chaotic region 14.6 volts.

In non autonomous (fig. 4.75 & 4.76) case of the converter, same behaviors are observed.

The fig. 4.76 shows a staircase like structure in the chaotic region. It increases with decrease of input voltage as the attractor size increases. Steps of the staircases changes at 17.0, 10.7 and 8.3 for 1,2 and 3 stairs respectively.

ii. Reference current (Iref) as bifurcation parameter: The bifurcation diagrams of the three phase full wave rectified dc fed boost converter with reference current (Iref) as variable parameter are shown in figure 4.72, 4.73 and 4.74. Fig.4.72 & 4.73 shows the bifurcation diagram for non autonomous system (i.e inductor current and capacitor voltage are sampled at clock) and 4.74 shows the bifurcation diagram for autonomous system (i.e capacitor voltage are sampled at its peak values). Keeping

other parameters at set values, reference current (Iref) is varied from 01 to 07 amps in step of 0.01 amp.

Both in the autonomous (fig. 4.74) case and non autonomous (fig. 4.72 & 4. 73) case of the converter shows period doubling cascade from period- 5 region to chaos as the reference current is decreased from 07 amp. Period-5 region from 01 amp. to 3.31 amps. Period-5 bifurcates to period-10 above 3.31 amps and it continues to 4.62 amps. Period-10 enters the chaotic region above 4.62 amps and it continues..

f. Six phase half wave rectified dc fed boost converter:

Input voltage (Vi) as bifurcation parameter: The bifurcation diagrams of the sixe phase half wave rectified dc fed boost converter with input voltage (Vi) as variable parameter are shown in figure 4.78, 4.79 and 4.80. Fig.4.78 & 4.79 shows the bifurcation diagram for non autonomous system (i.e inductor current and capacitor voltage are sampled at clock) and 4.80 shows the bifurcation diagram for autonomous system (i.e capacitor voltage are sampled at its peak values). Keeping other parameters at set values, the input voltage (Vi) is varied from 07 to 60 volts in step of 0.1 volt.

In the autonomous (fig. 4.80) case of the converter shows period doubling cascade from period- 5 region to chaos as the input voltage is decreased from 60 volts. Period- 5 region from 60 volts to 34.3 volts. Period-5 bifurcates to period-10 below 34.3 volts and it continues to 23.2 volts. Then Period-10 to period-20 and finally enters the chaotic region 21.6 volts.

In non autonomous (fig. 4.78 & 4.79) case of the converter, same behaviors are observed.

The fig. 4.79 shows a staircase like structure in the chaotic region. It increases with decrease of input voltage as the attractor size increases.

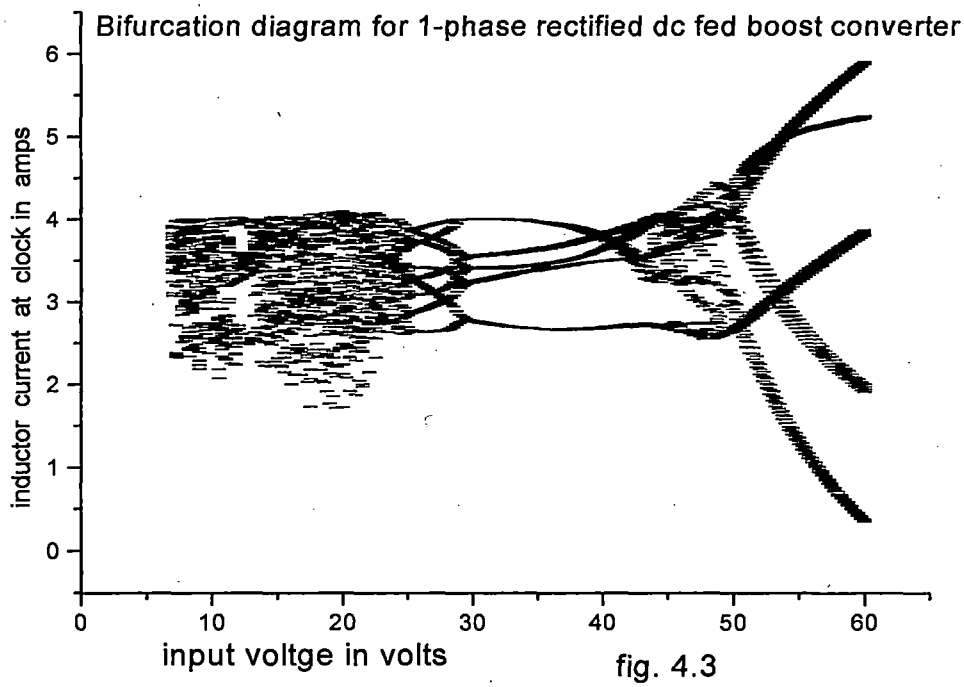
Bifurcation diagram for 1-phase rectified dc fed boost converter
inductor current at clock in amps
0
1
2
3
4
5
6
0
10
20
30
40
50
60
input voltge in volts

fig. 4.3

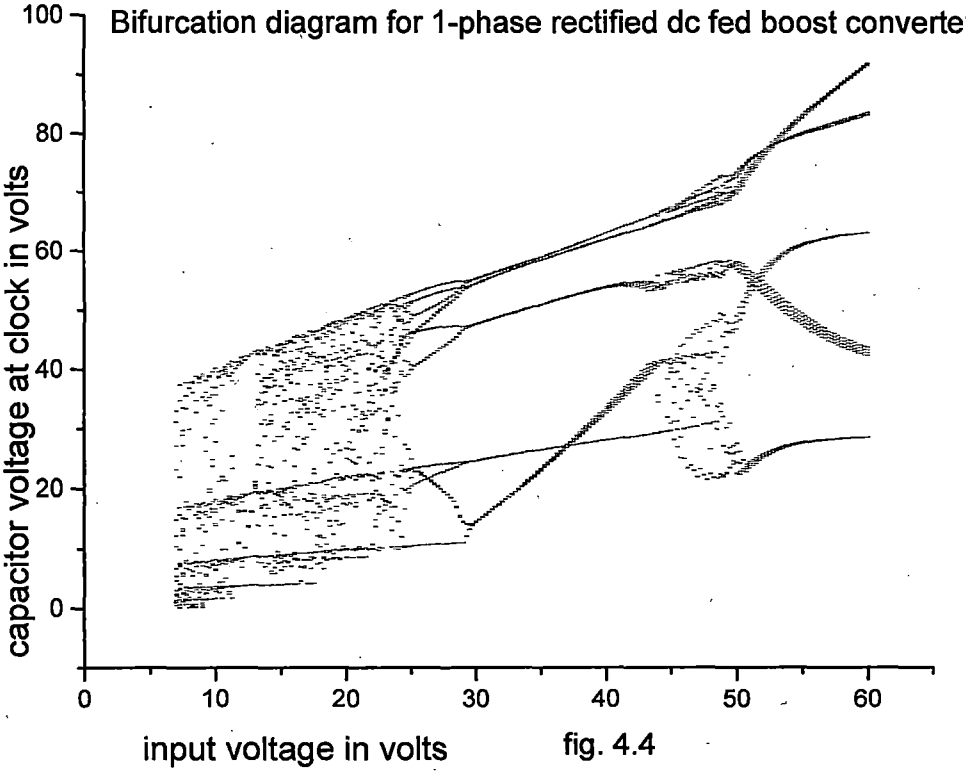
Bifurcation diagram for 1-phase rectified dc fed boost converter
capacitor voltage at clock in volts
0
20
40
60
80
100
0
10
20
30
40
50
60
input voltage in volts

fig. 4.4

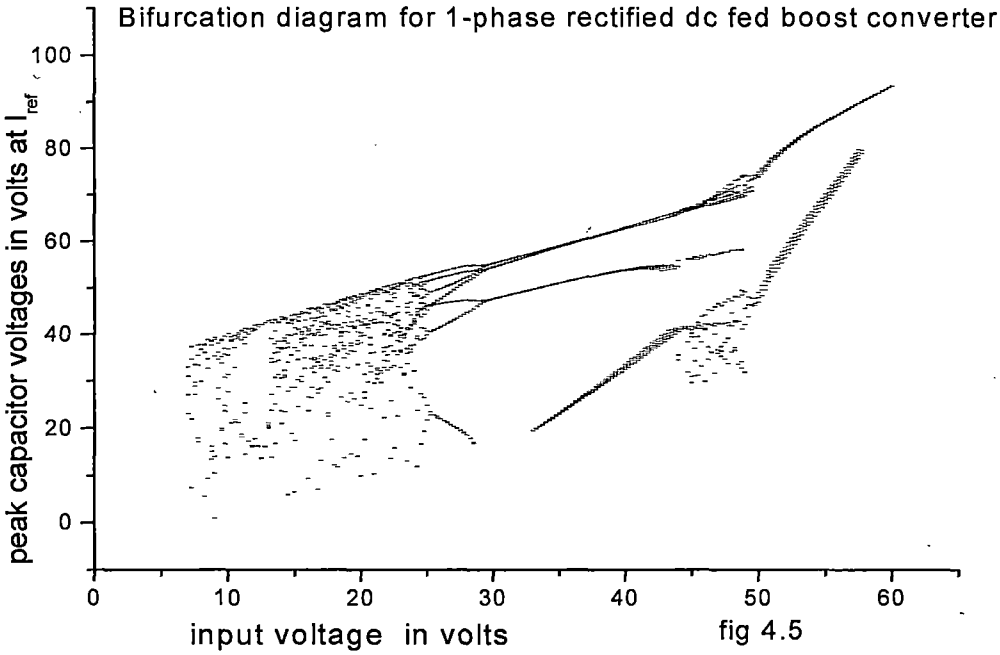
Bifurcation diagram for 1-phase rectified dc fed boost converter
peak capacitor voltages in volts at I_{ref}
100
80
60
40
20
0
0
10
20
30
40
50
60
input voltage in volts

fig 4.5

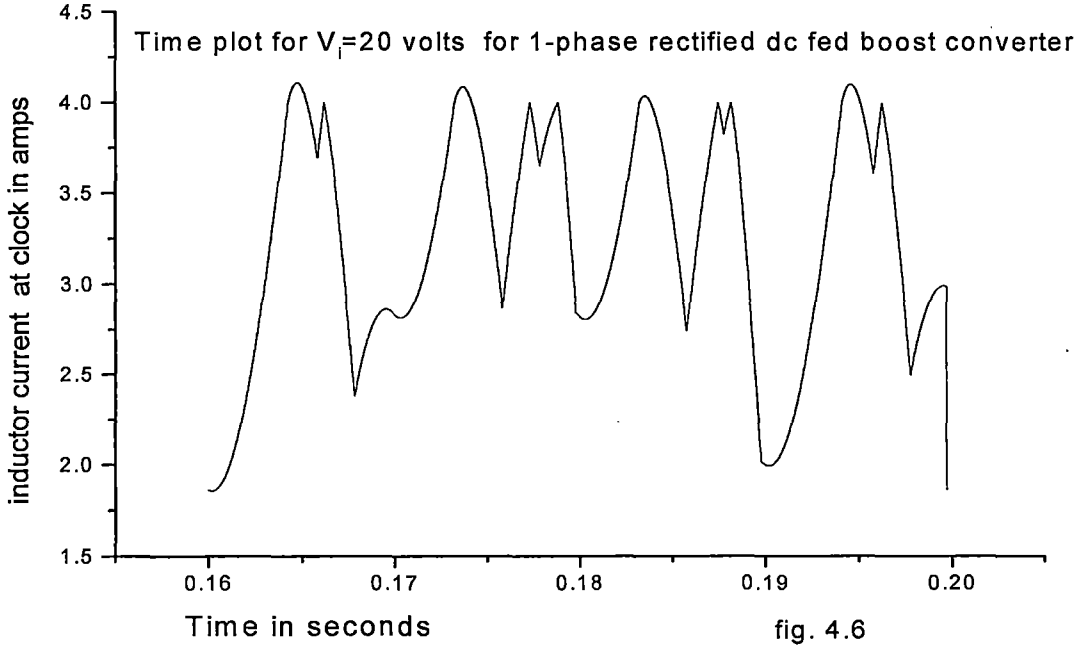
Time plot for V_i=20 volts for 1-phase rectified dc fed boost converter
inductor current at clock in amps
4.5
4.0
3.5
3.0
2.5
2.0
1.5
0.16
0.17
0.18
0.19
0.20
Time in seconds

fig. 4.6

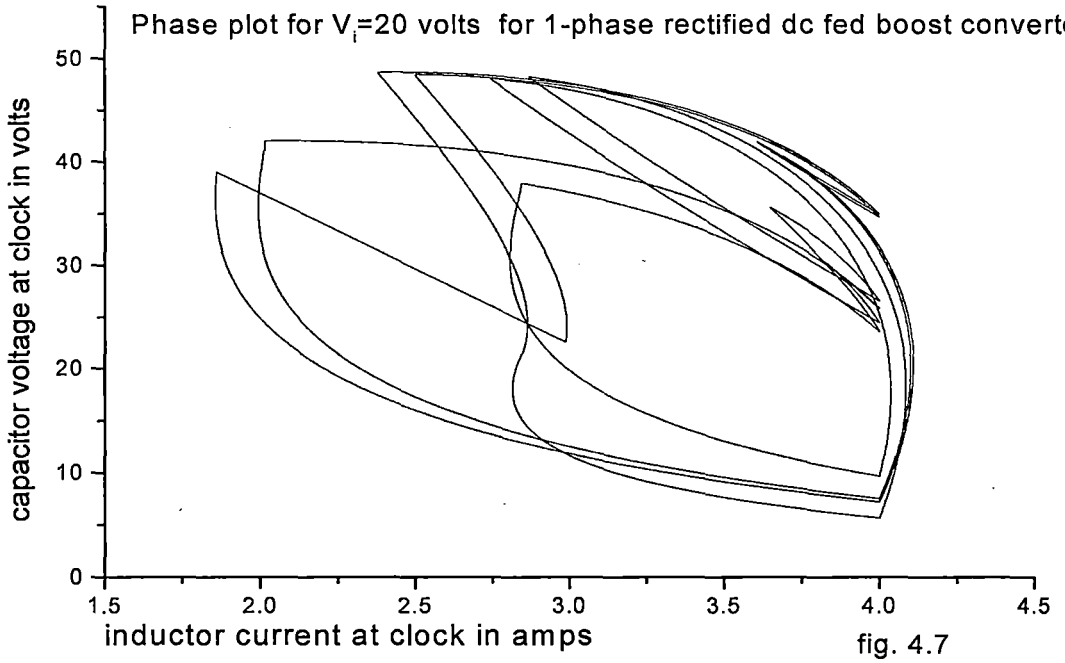
Phase plot for V_i=20 volts for 1-phase rectified dc fed boost converter
capacitor voltage at clock in volts
50
40
30
20
10
0
1.5
2.0
2.5
3.0
3.5
4.0
4.5
inductor current at clock in amps

fig. 4.7

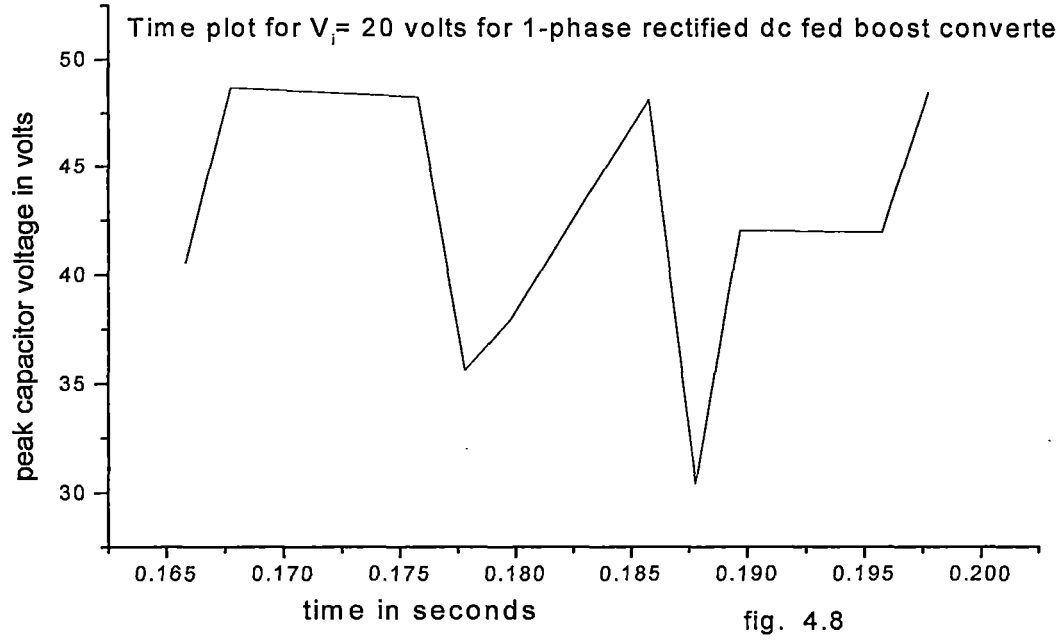
Time plot for V_i= 20 volts for 1-phase rectified dc fed boost converter
peak capacitor voltage in volts
50
45
40
35
30
0.165
0.170
0.175
0.180
0.185
0.190
0.195
0.200
time in seconds

fig. 4.8

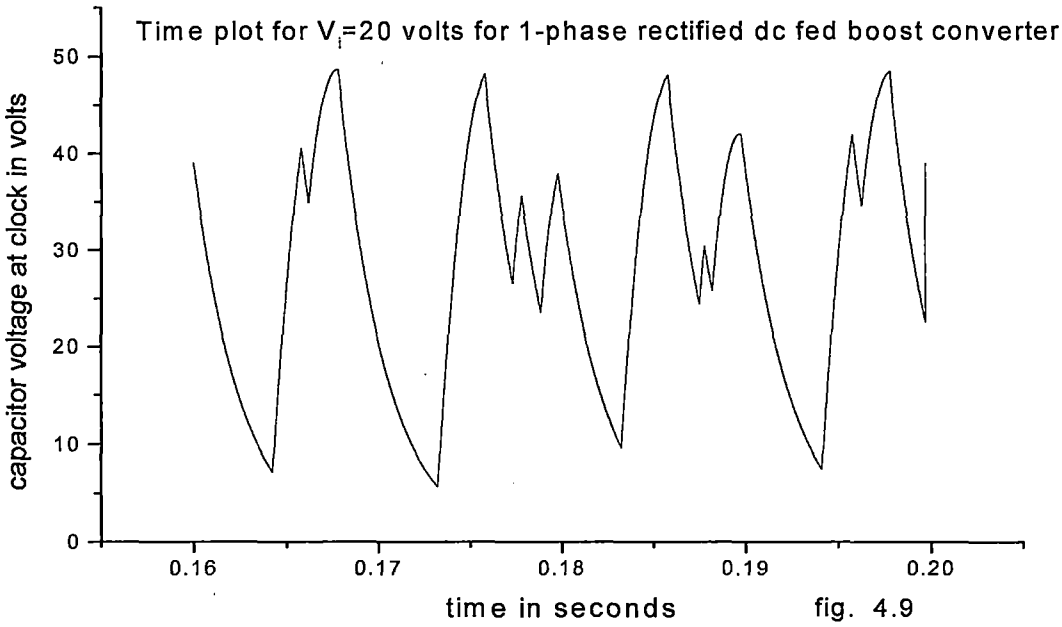

fig. 4.9

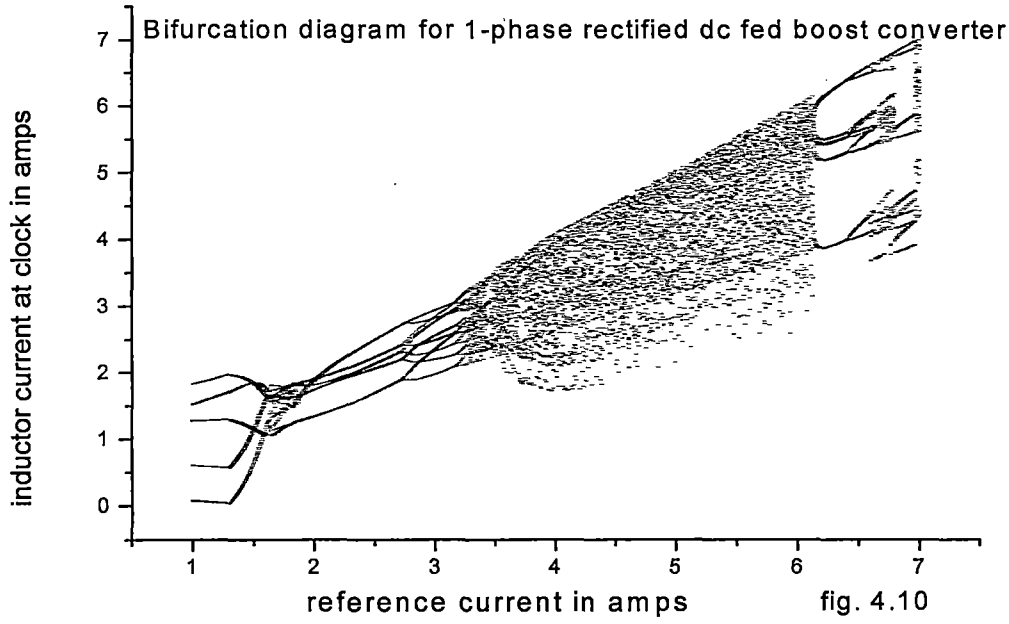

fig. 4.10

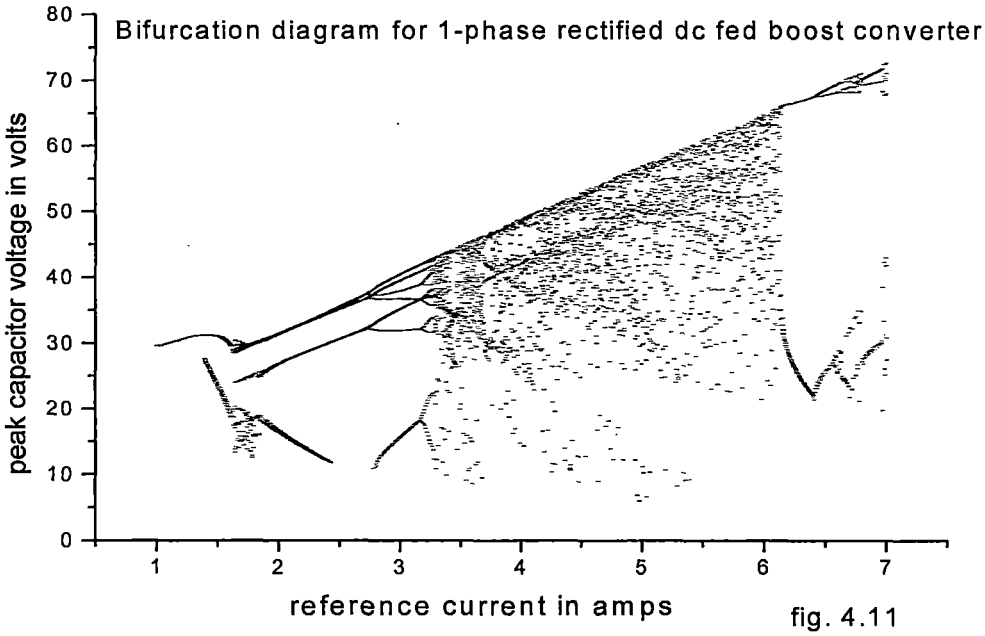

fig. 4.11

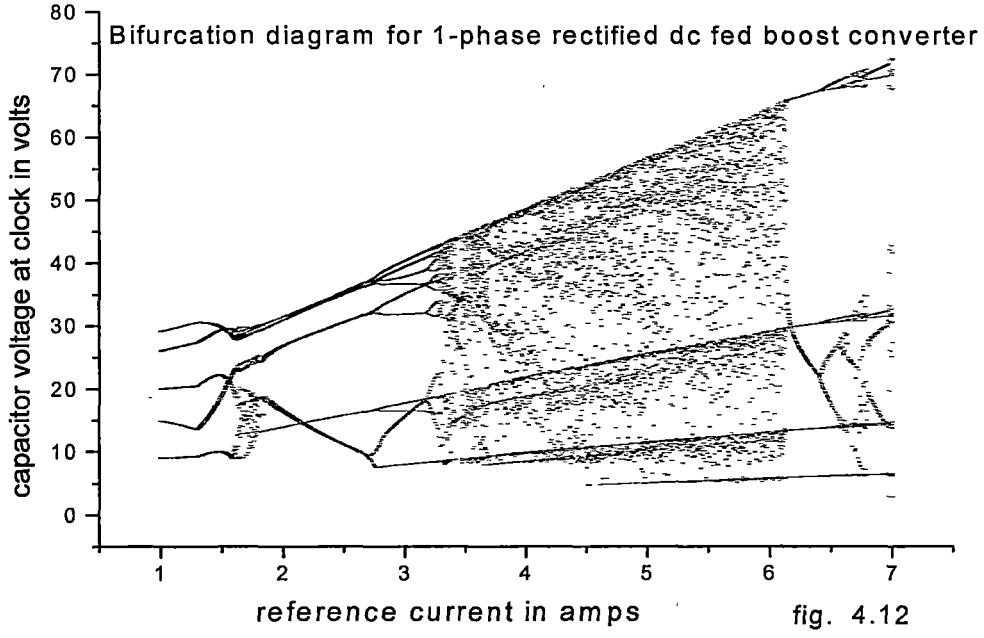

fig. 4.12

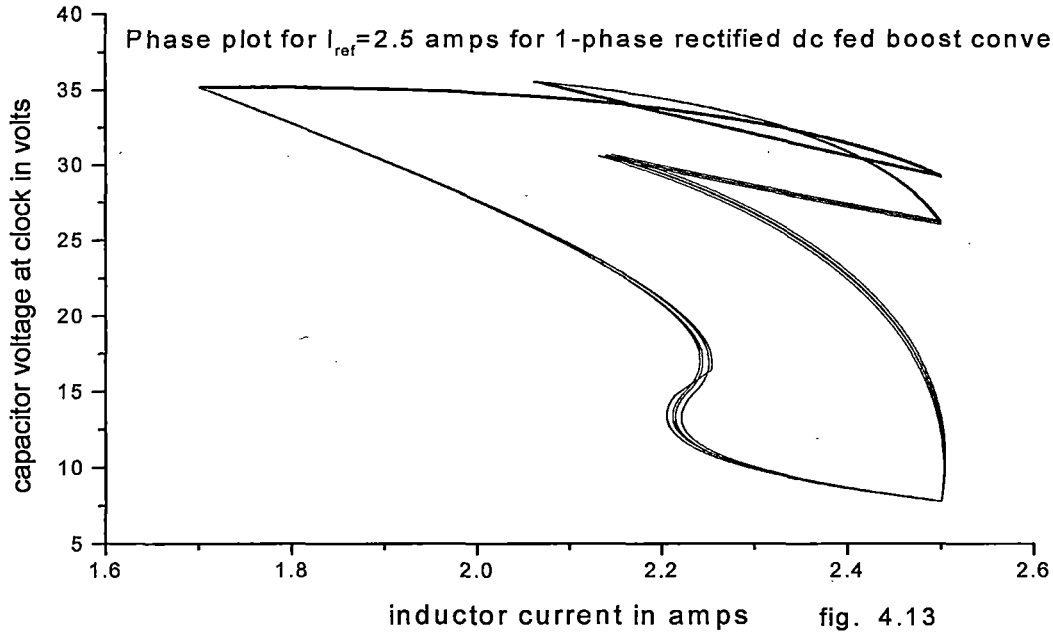

fig. 4.13

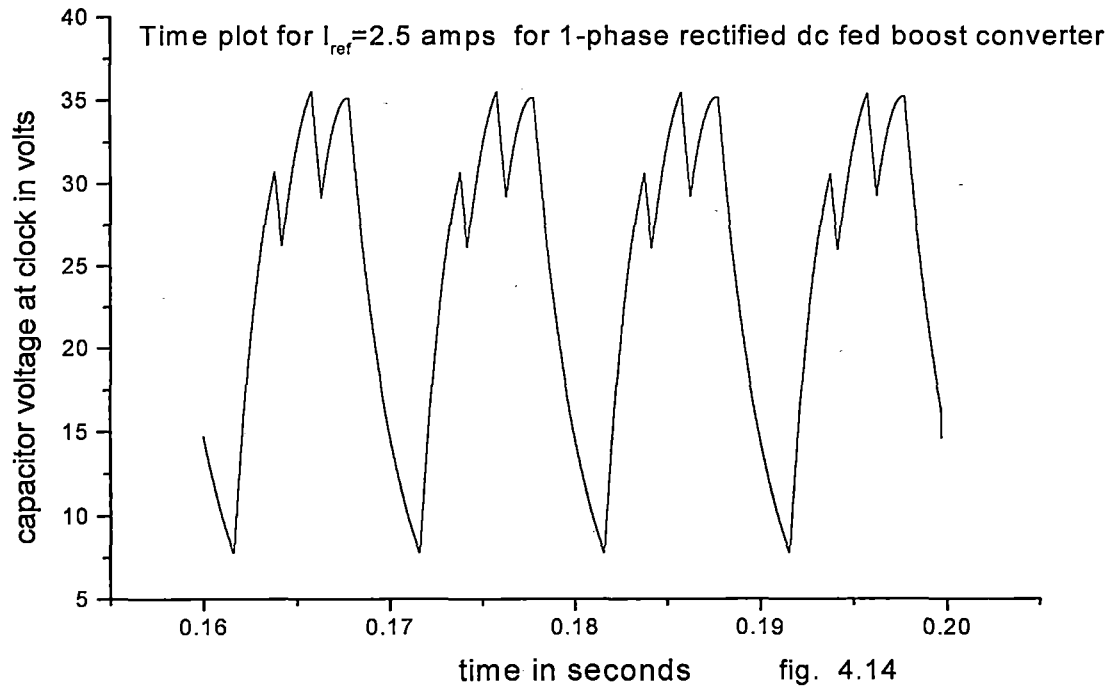

fig. 4.14

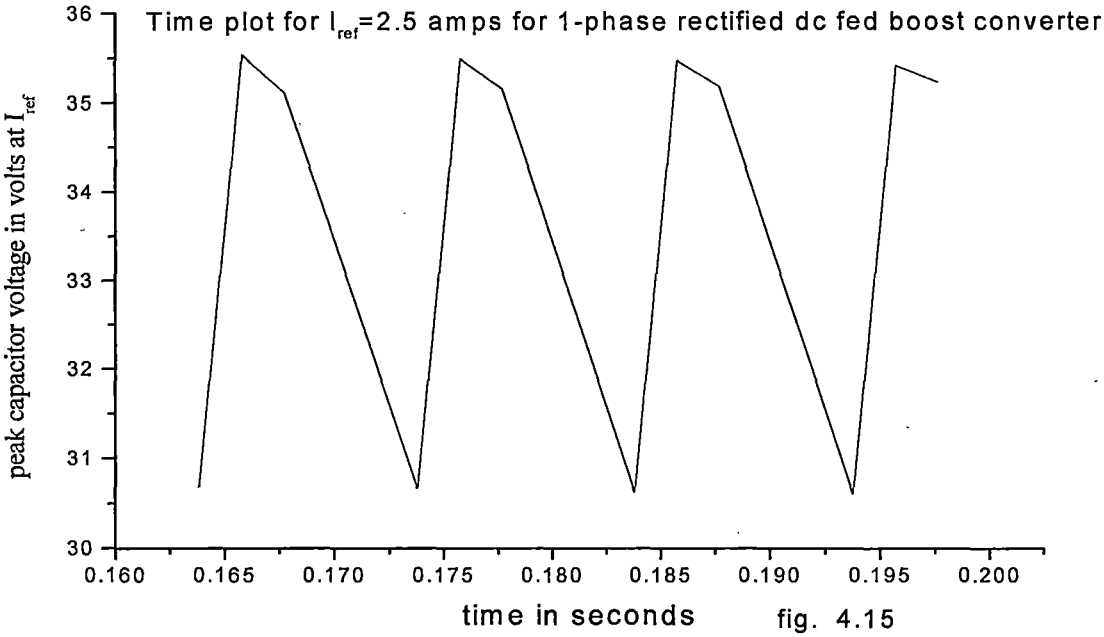

fig. 4.15

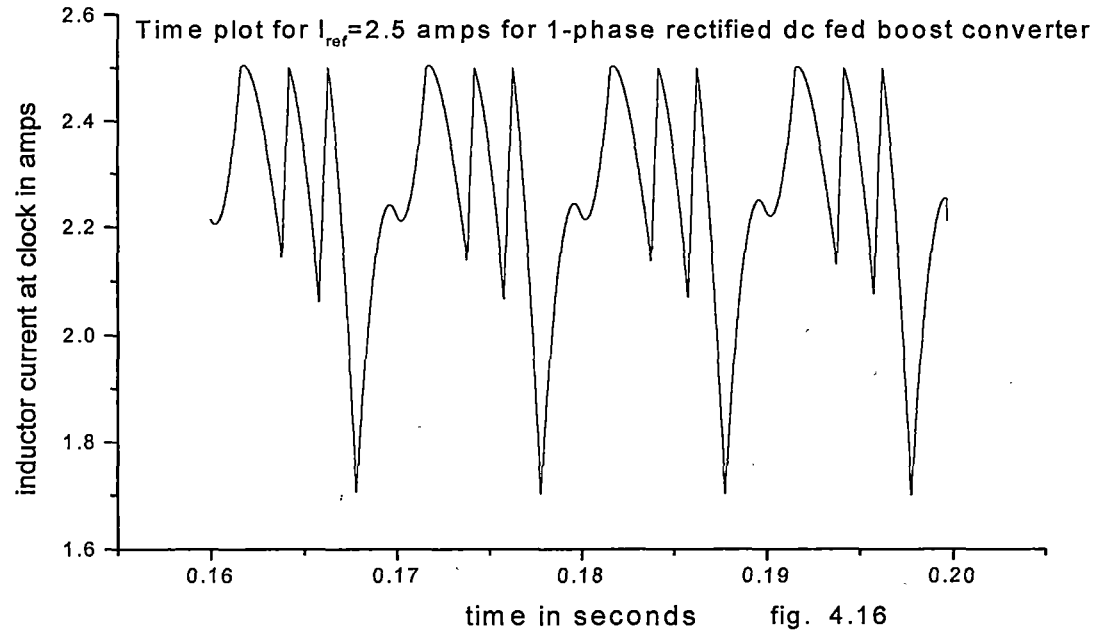

fig. 4.16

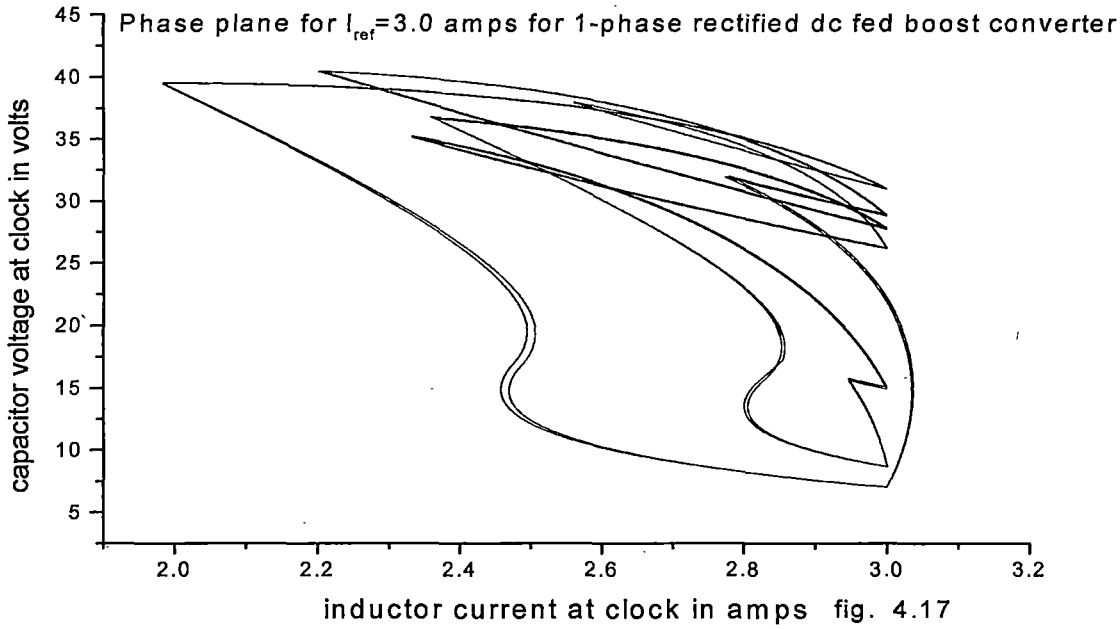

fig. 4.17

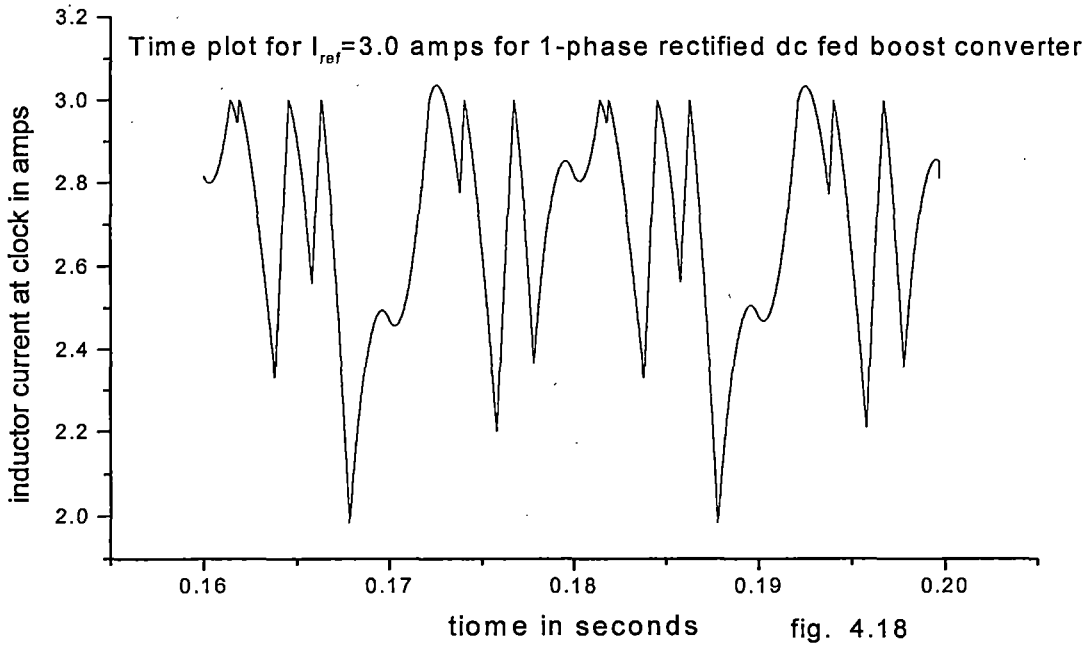

fig. 4.18

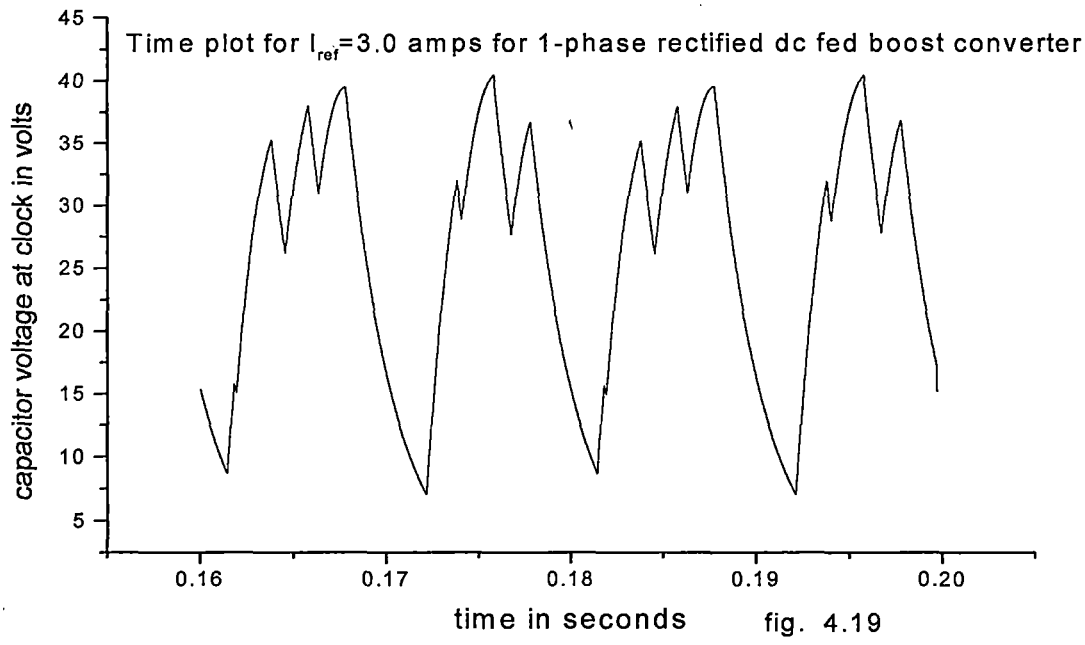

fig. 4.19

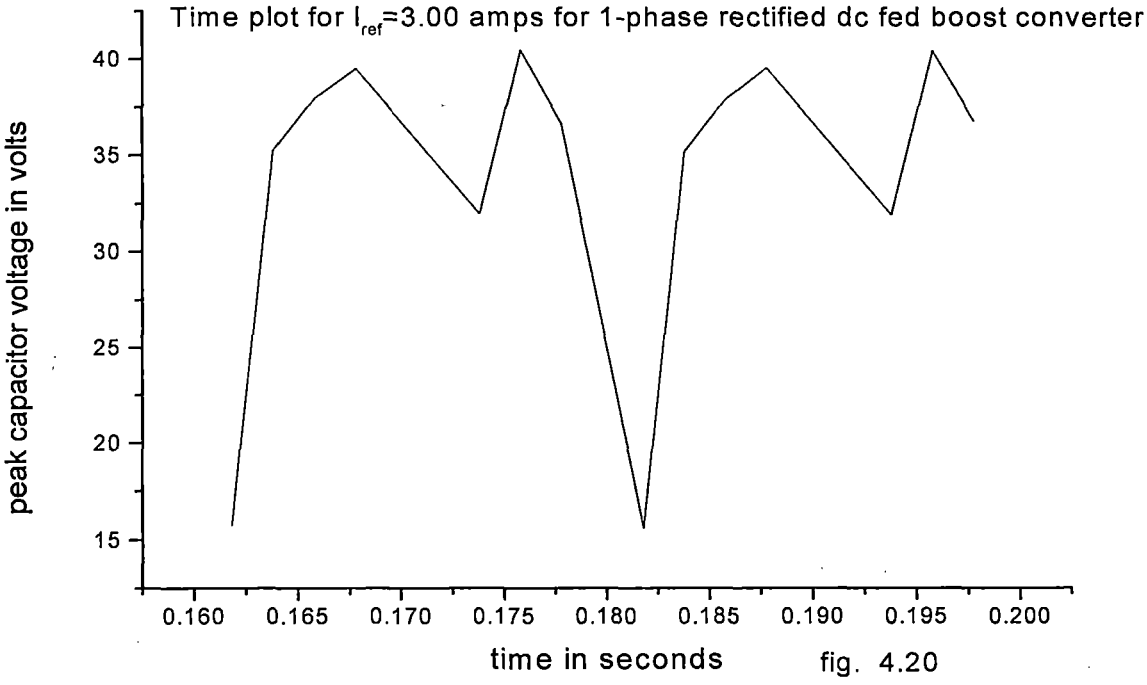

fig. 4.20

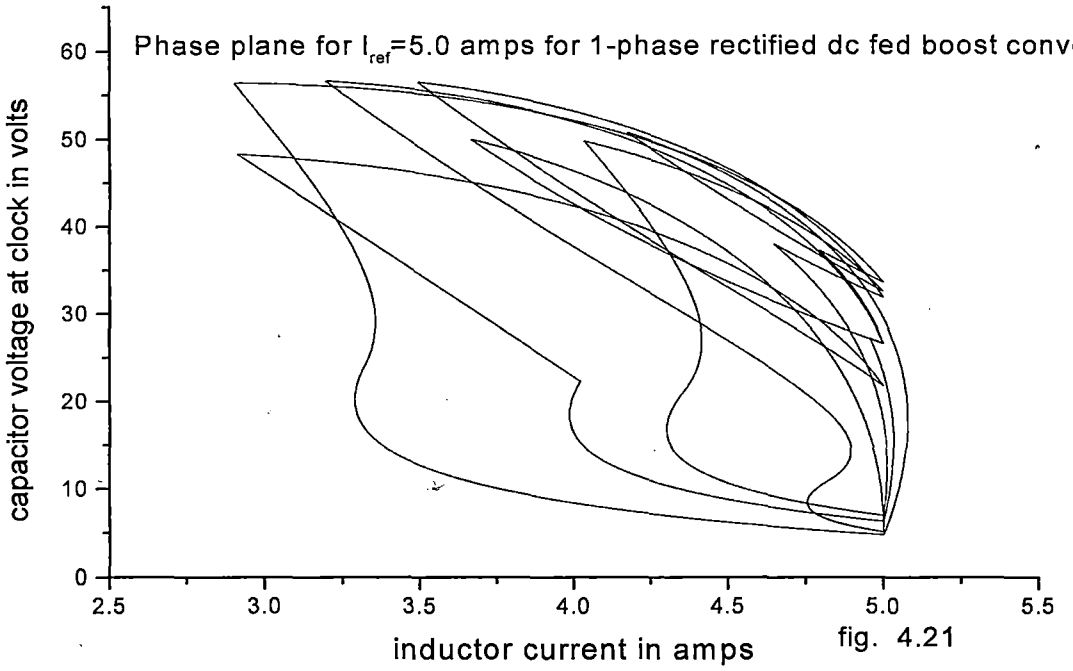

fig. 4.21

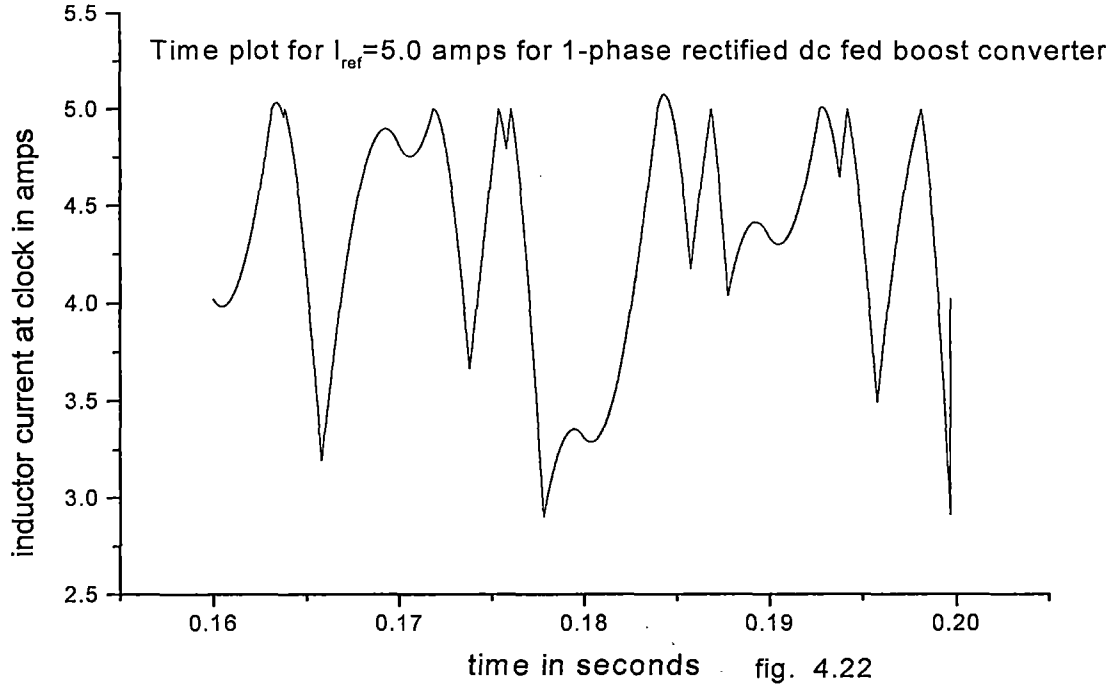

fig. 4.22

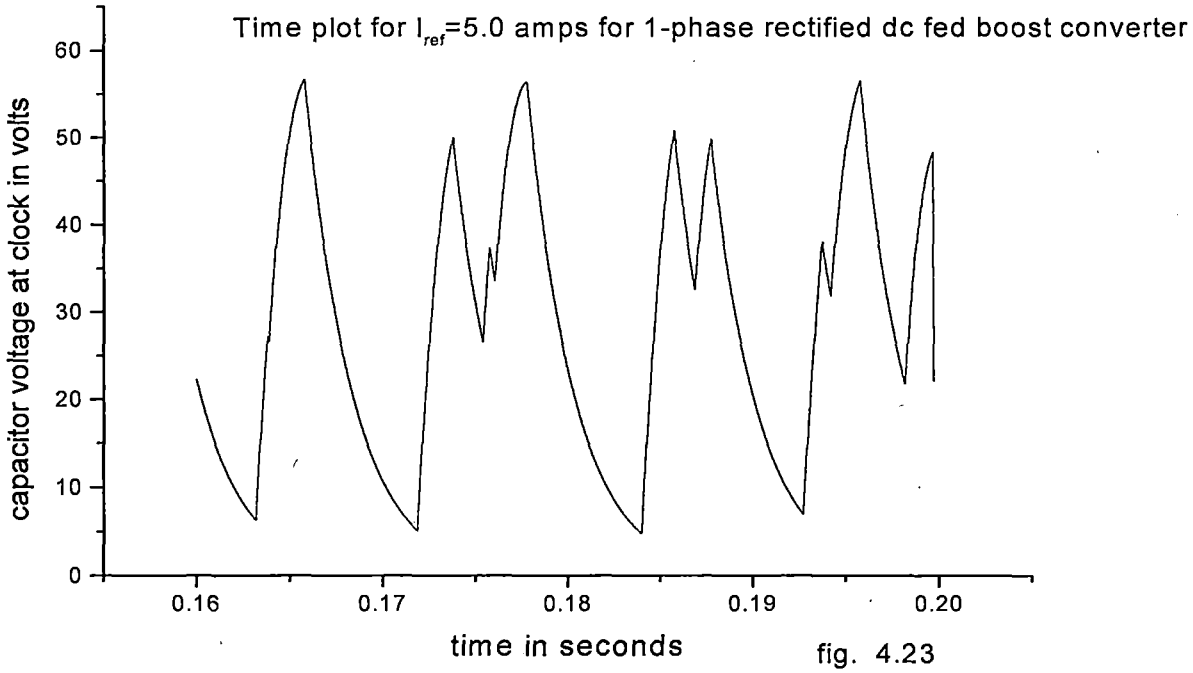

fig. 4.23

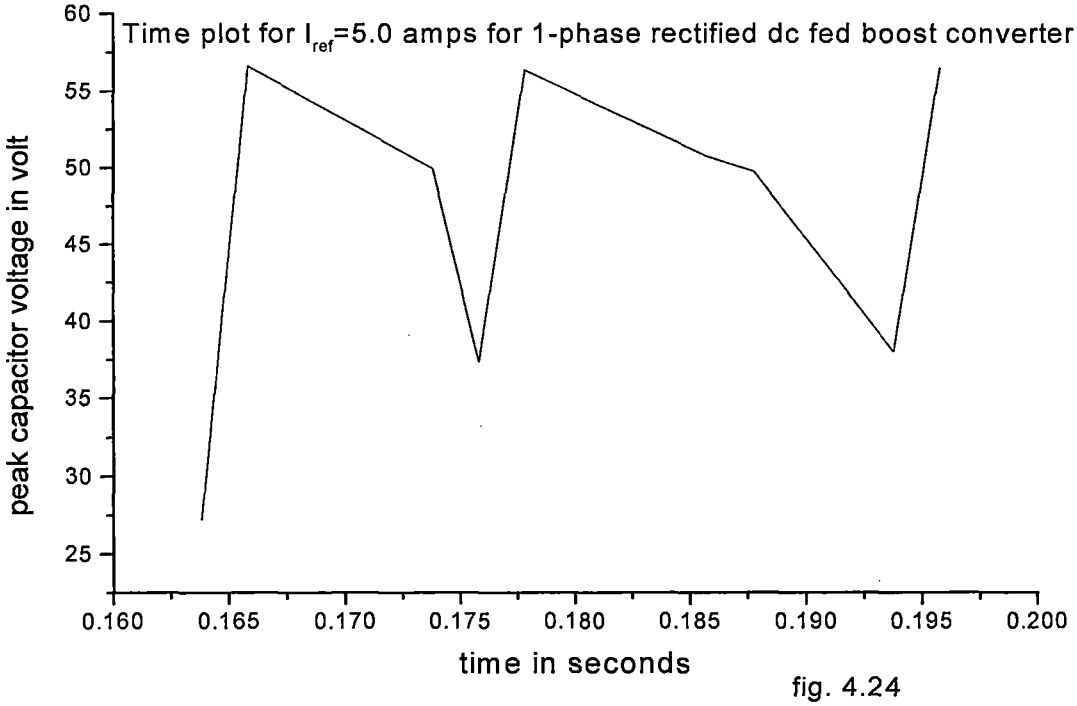

fig. 4.24

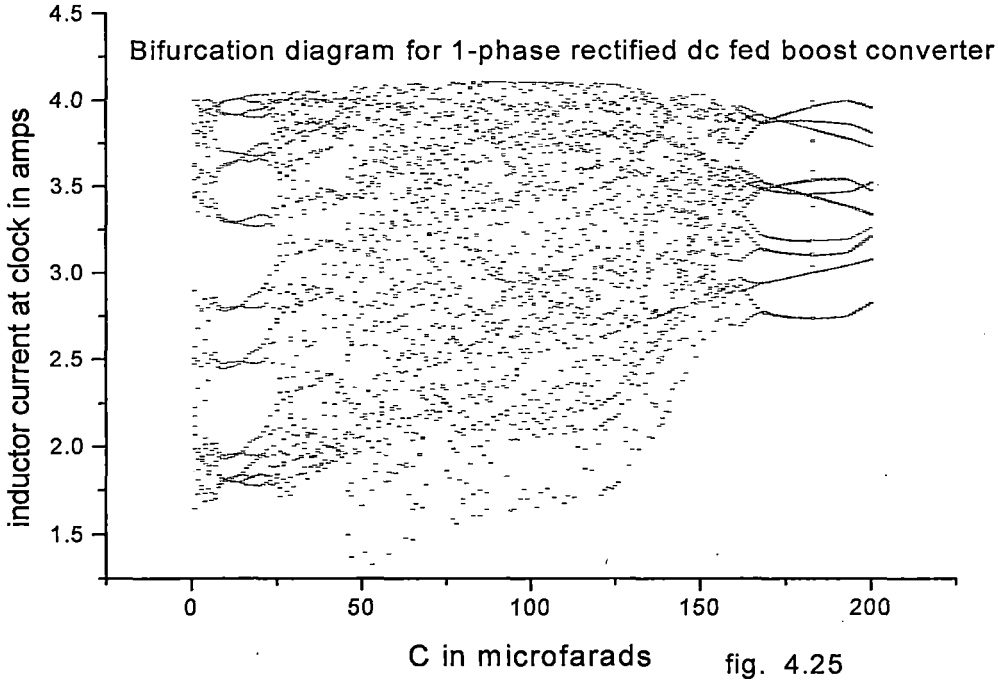

fig. 4.25

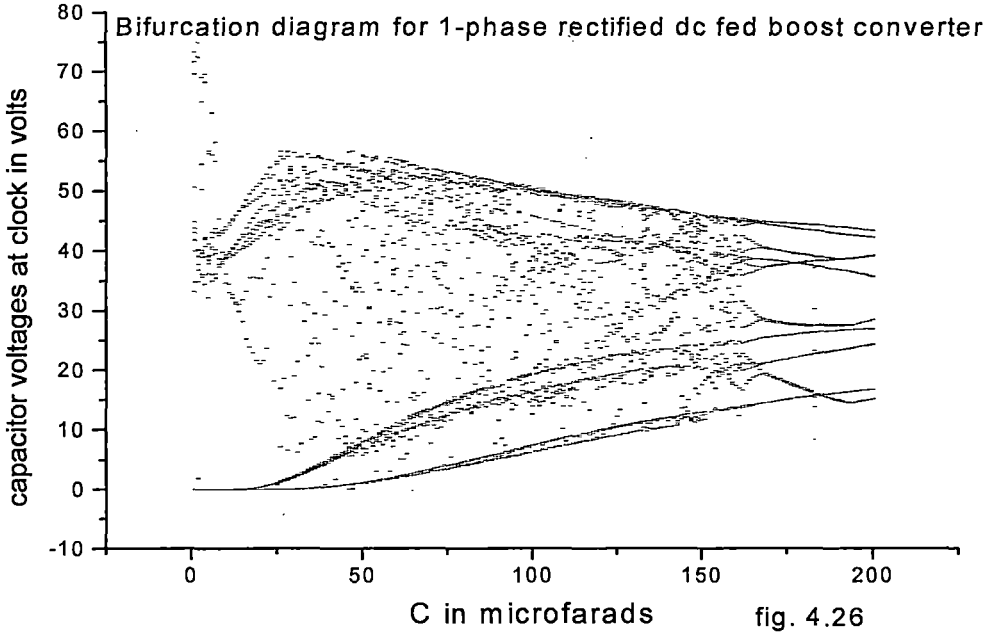

fig. 4.26

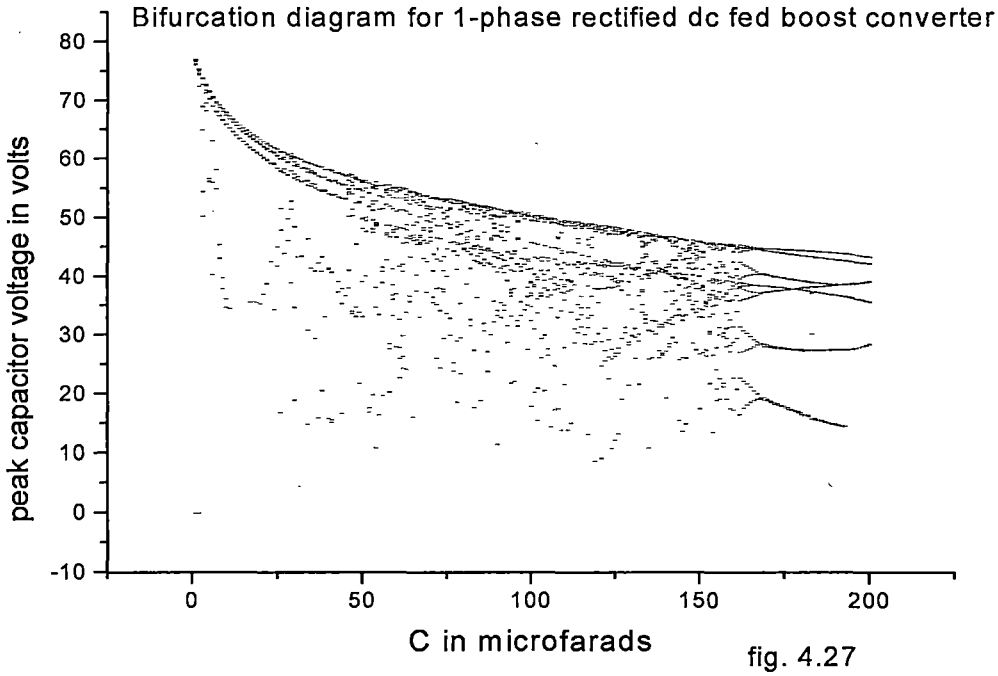

fig. 4.27

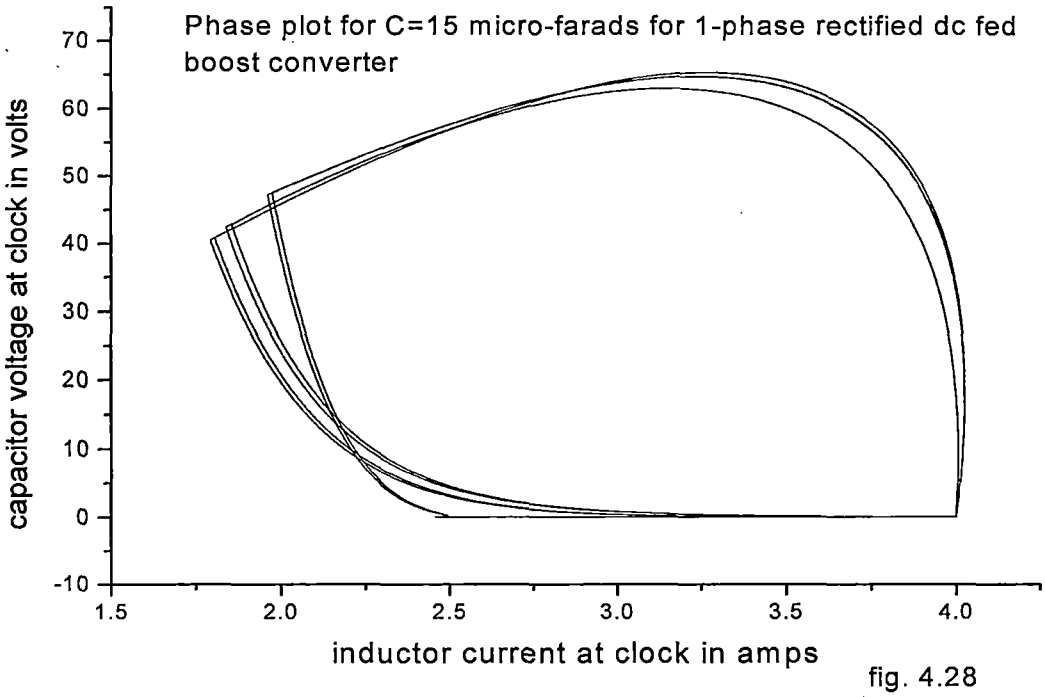

fig. 4.28

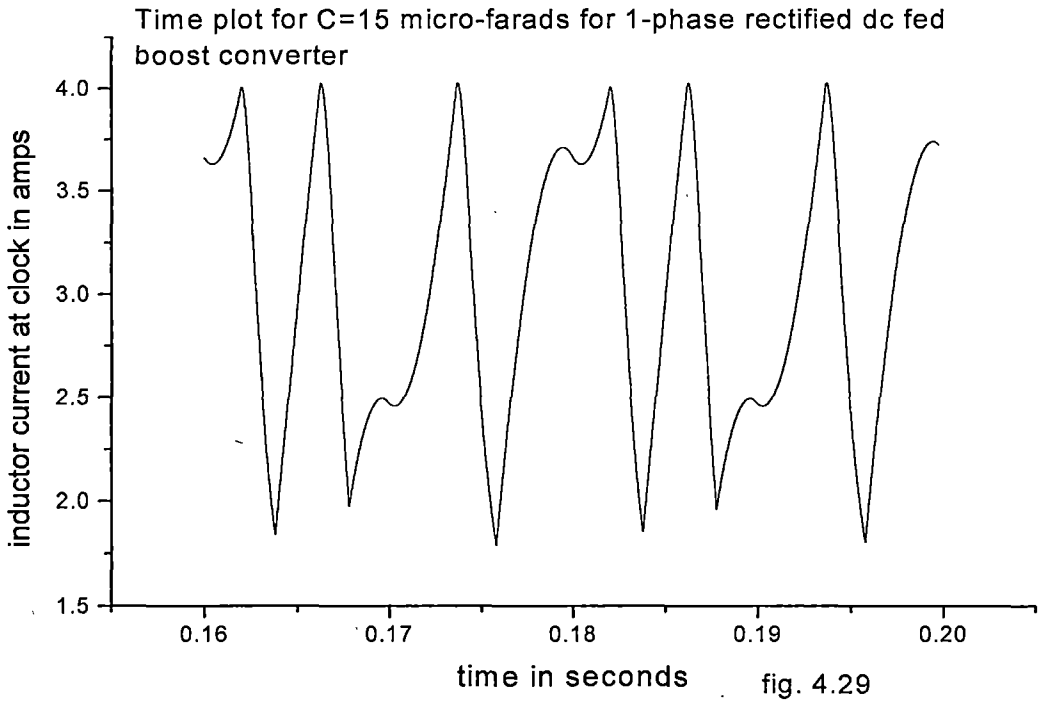

fig. 4.29

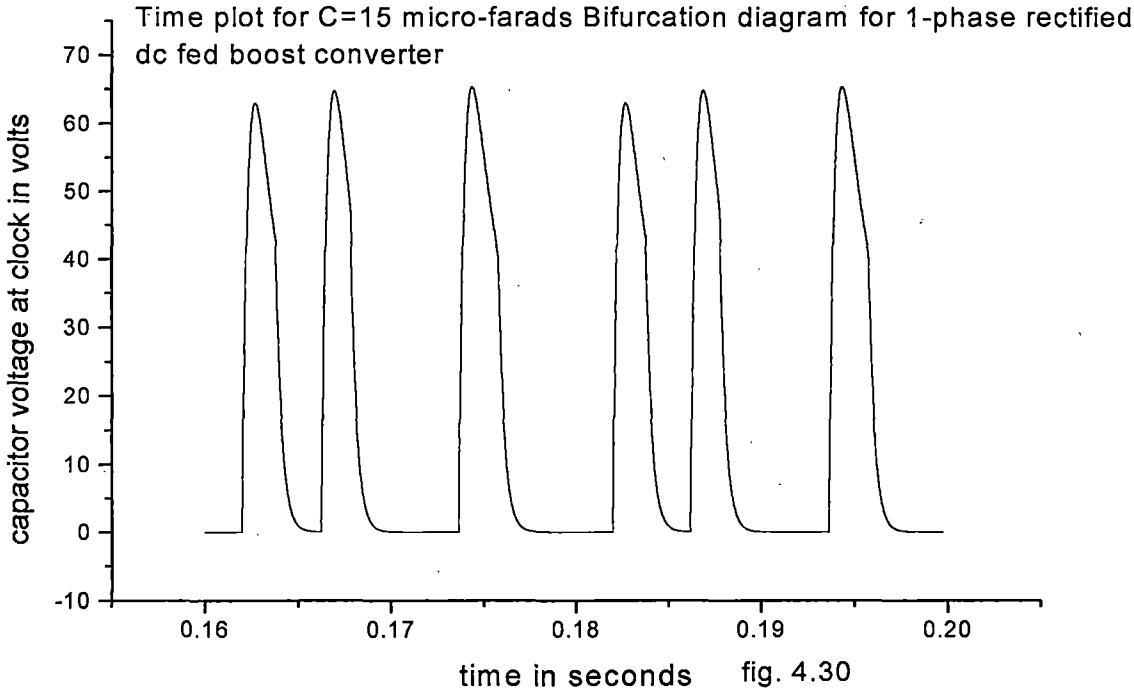

fig. 4.30

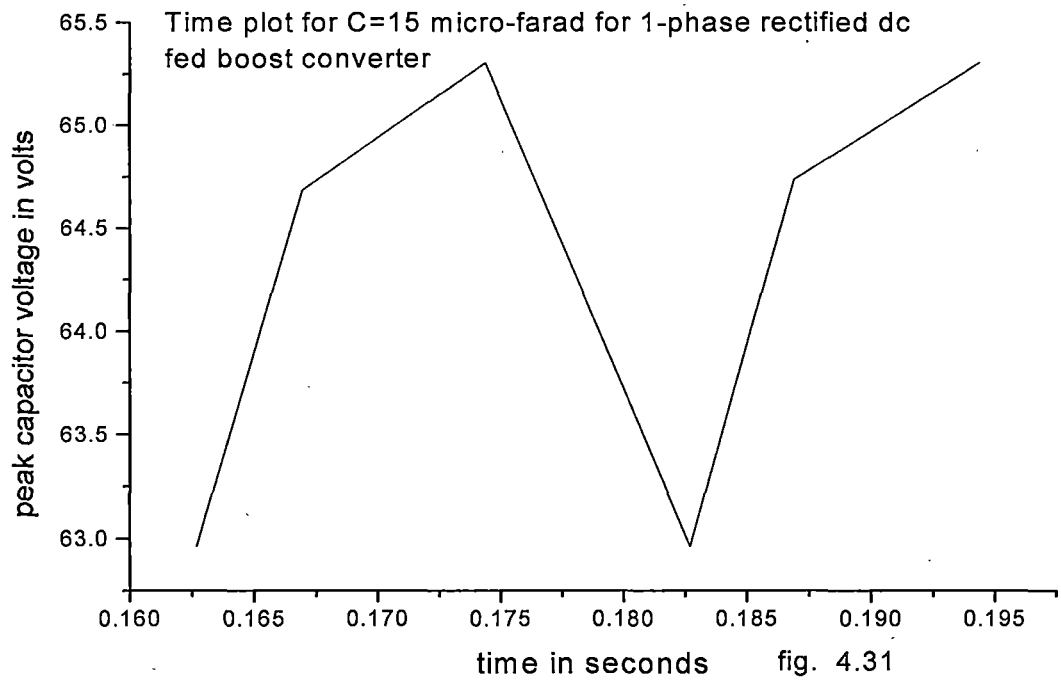

fig. 4.31

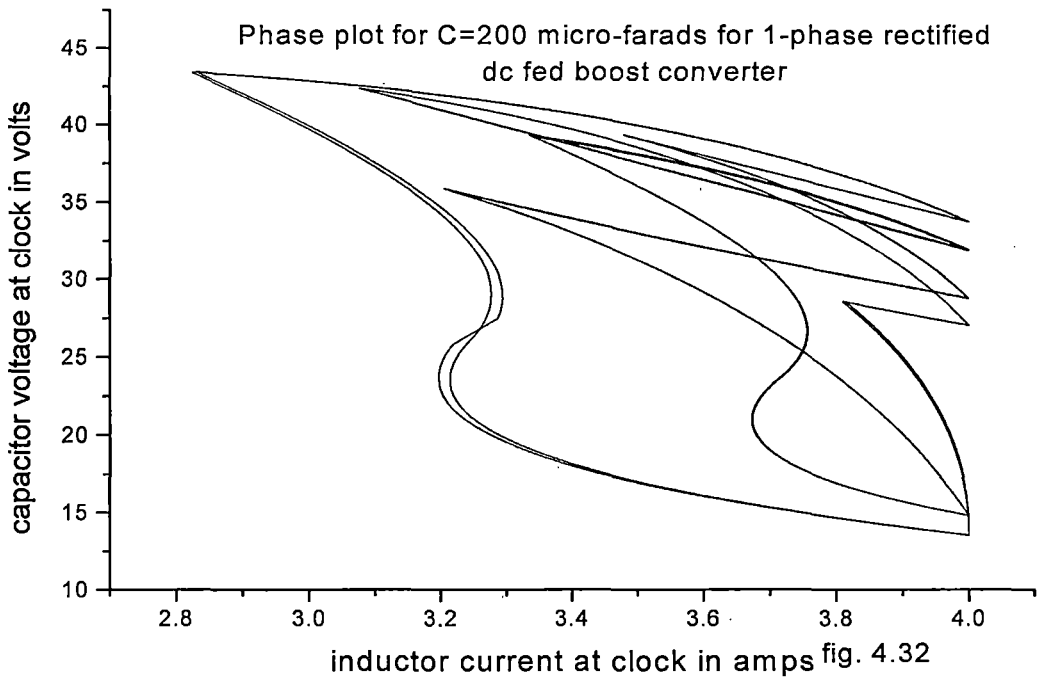

fig. 4.32

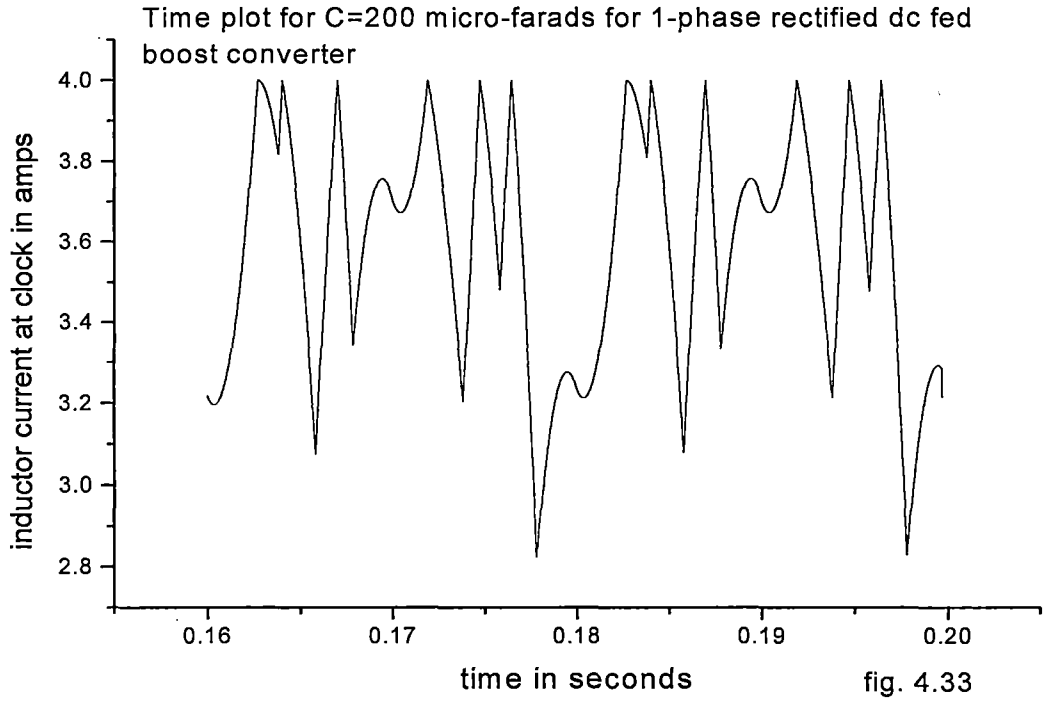

fig. 4.33

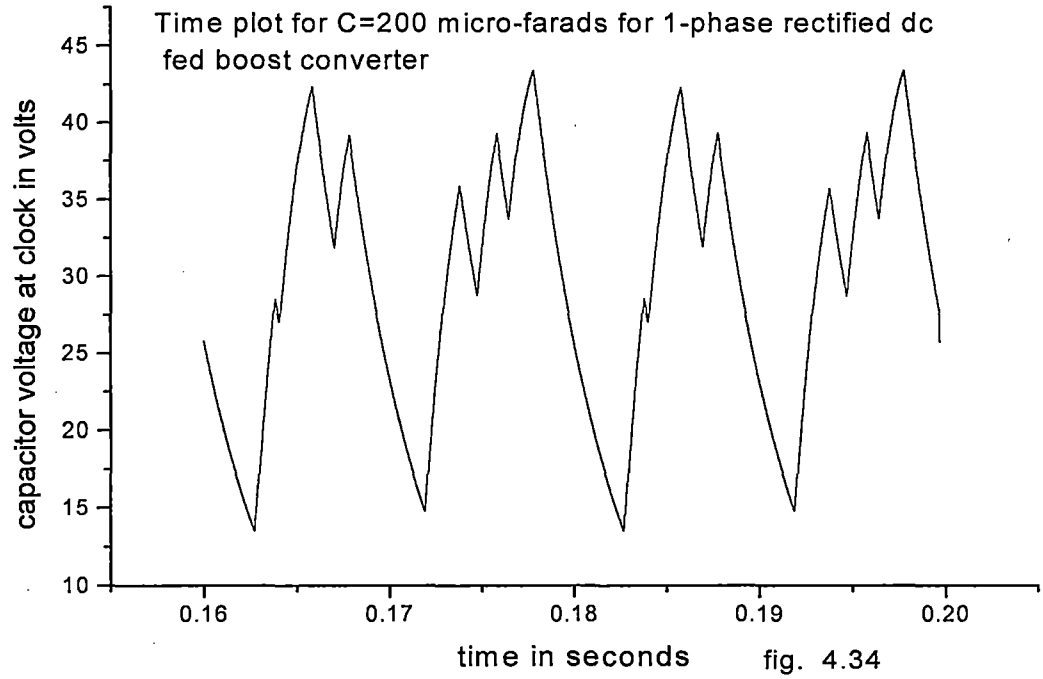

fig. 4.34

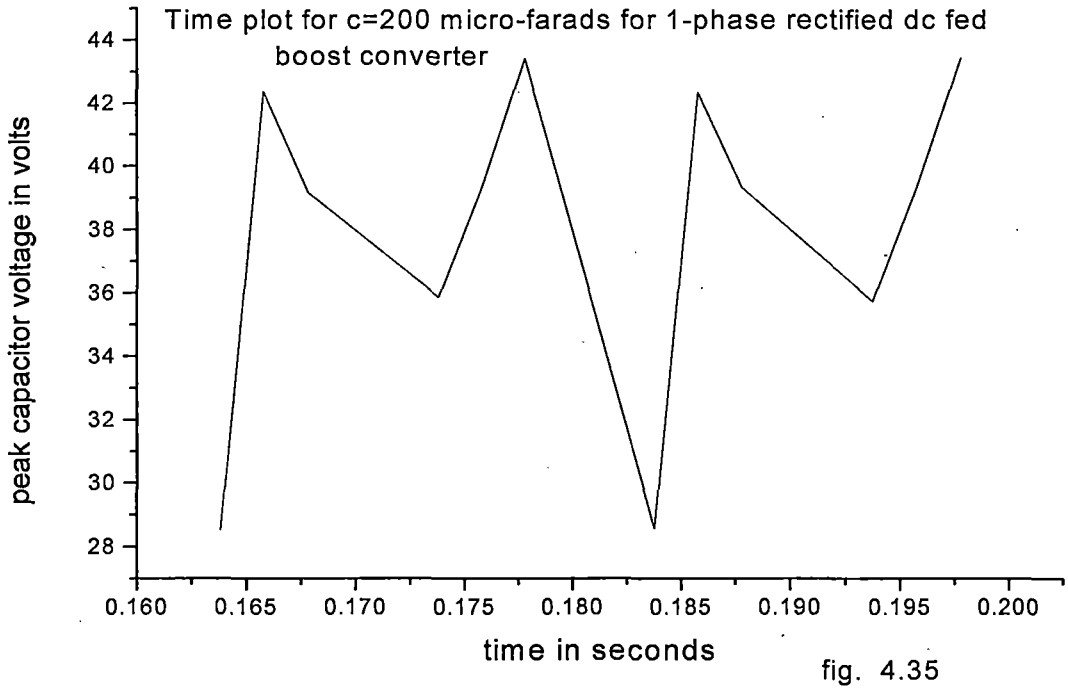

fig. 4.35

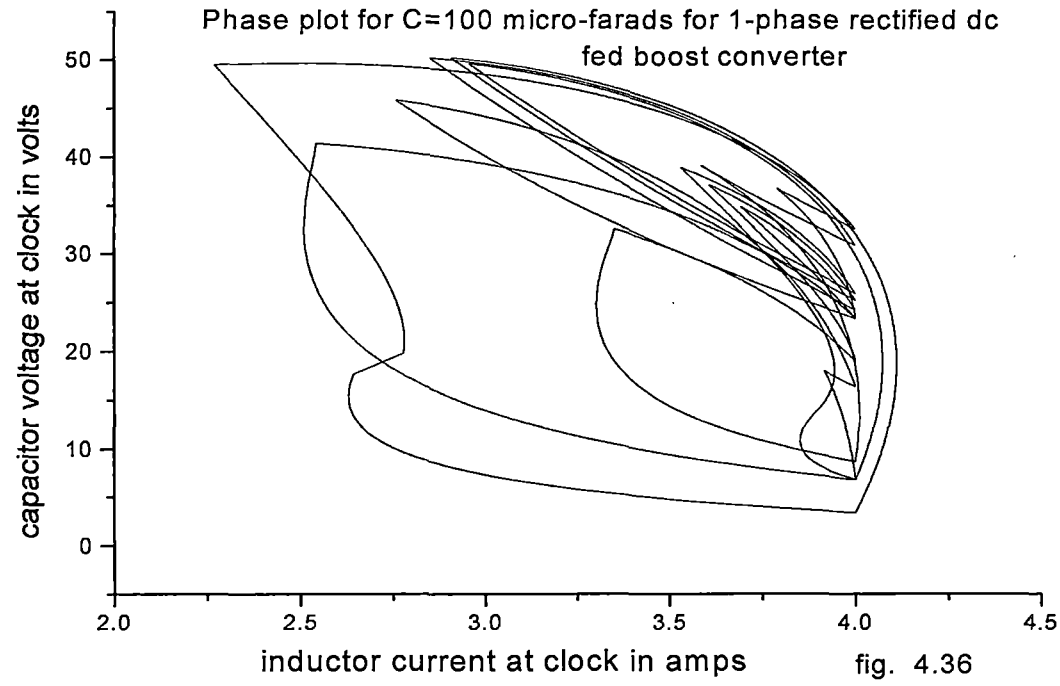

fig. 4.36

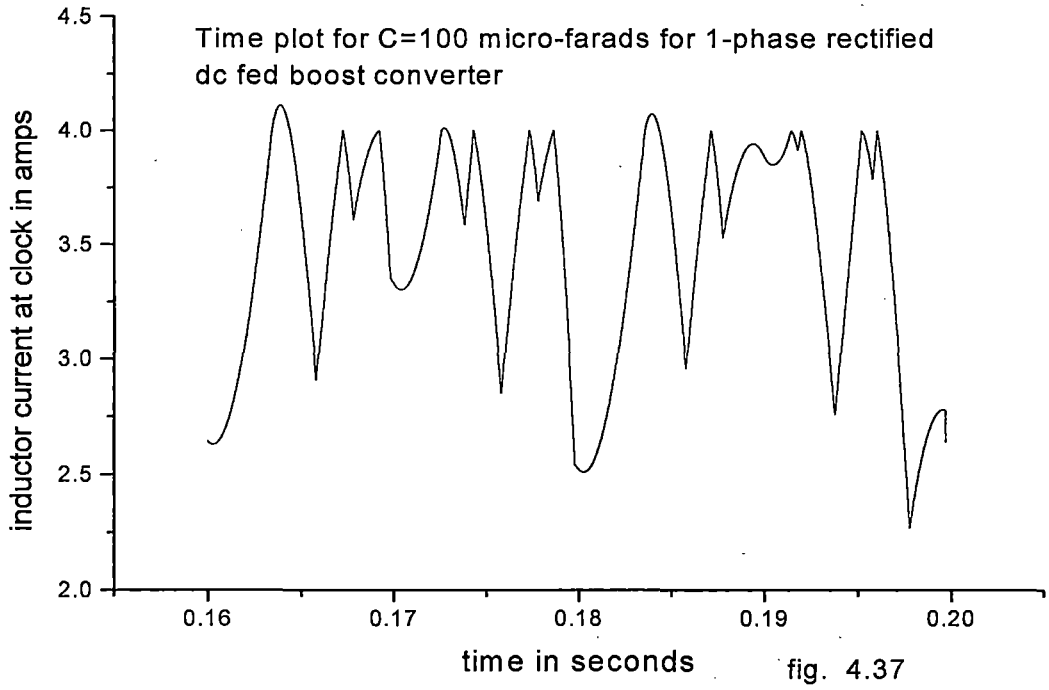

fig. 4.37

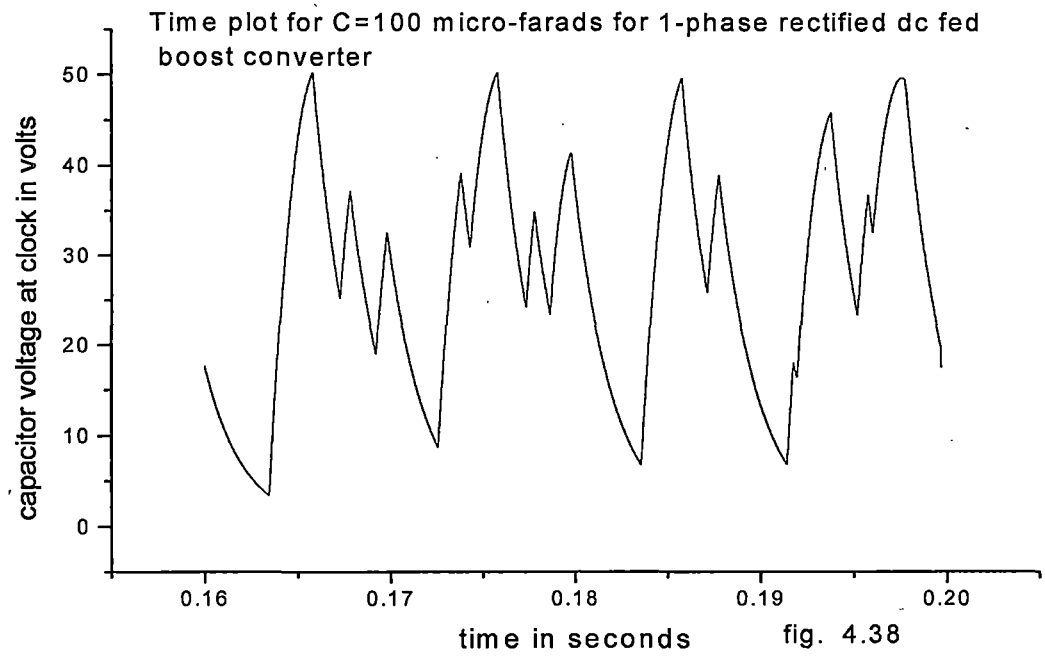

fig. 4.38

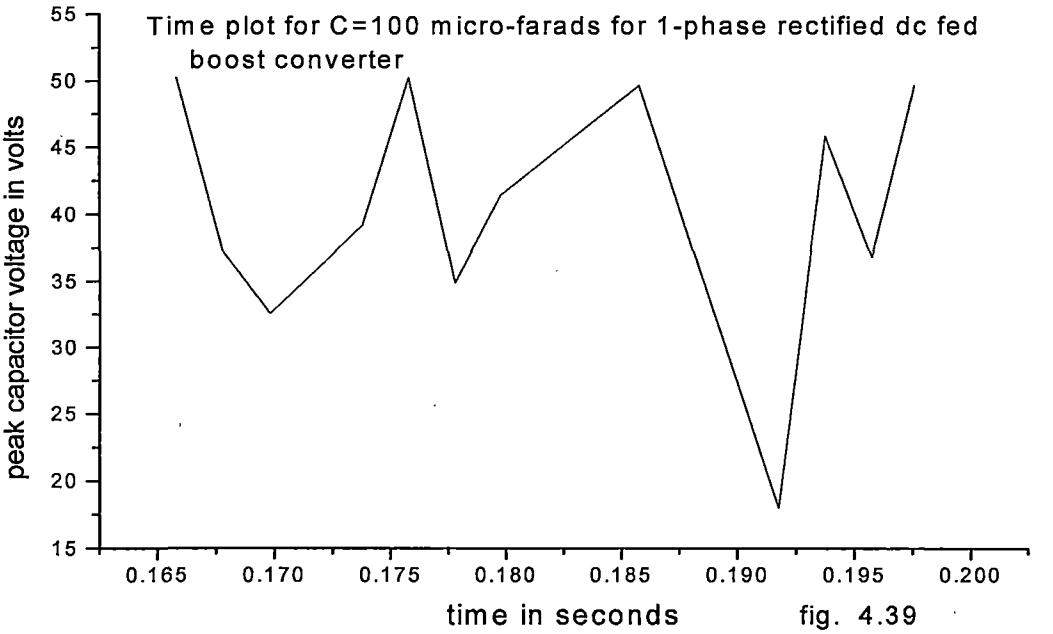

fig. 4.39

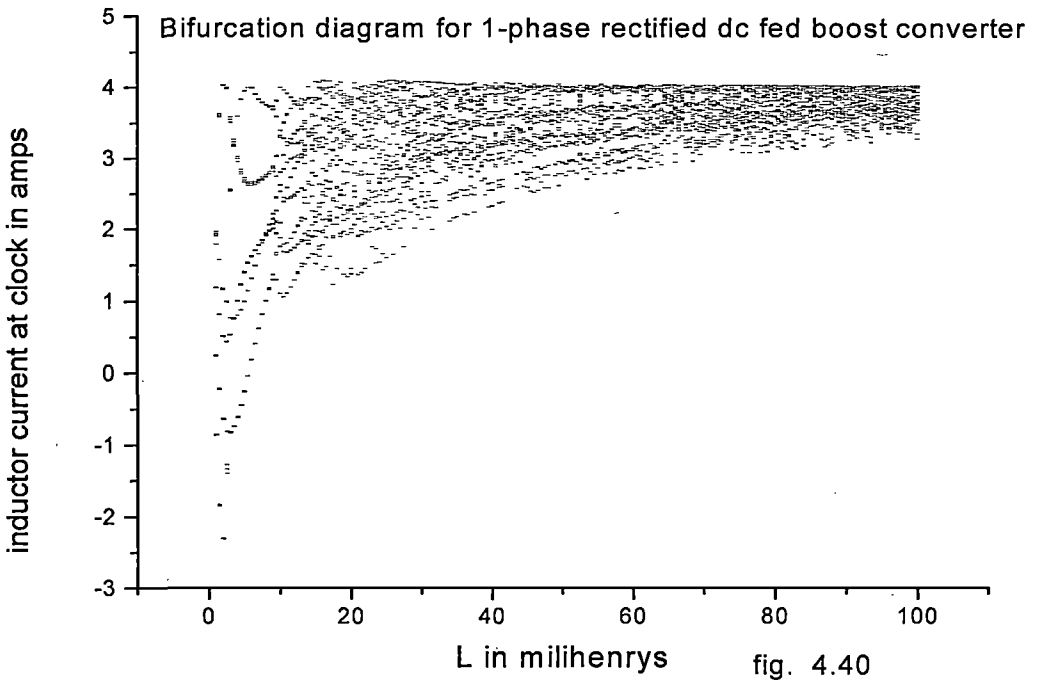

fig. 4.40

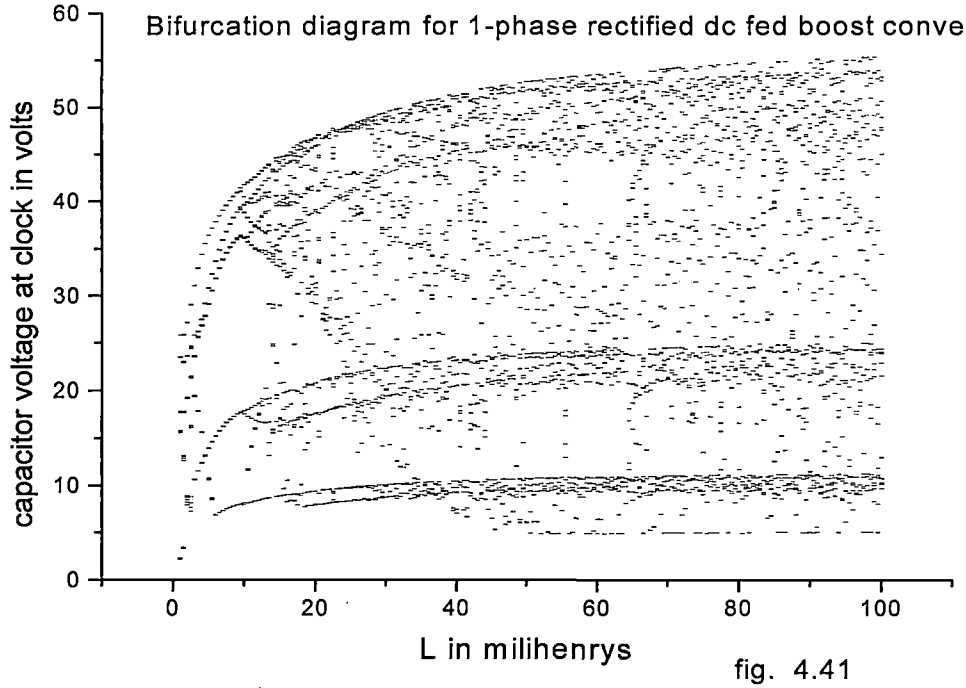

fig. 4.41

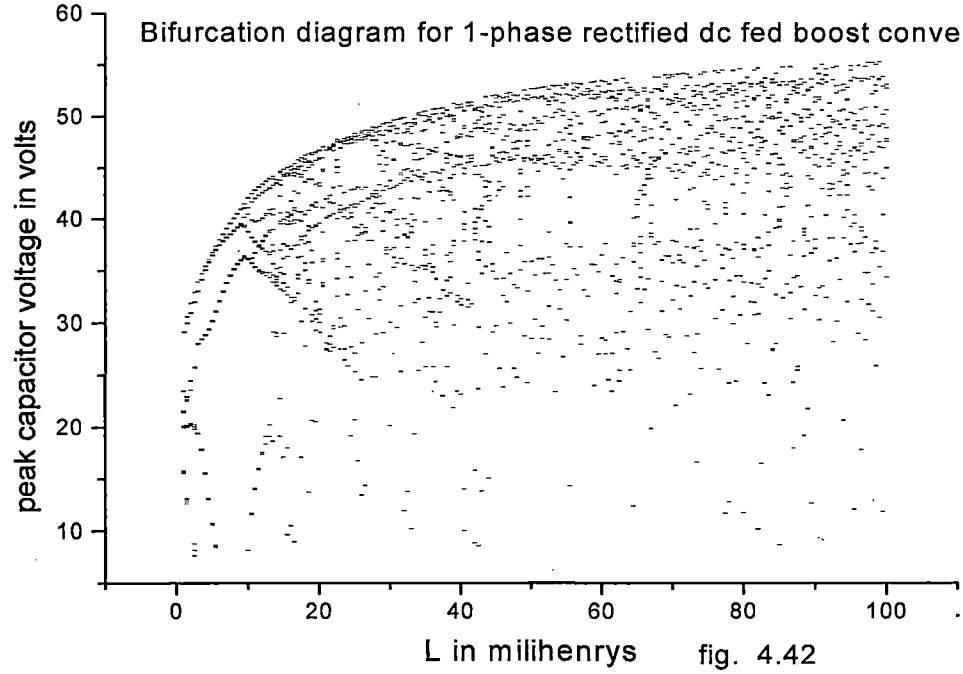

fig. 4.42

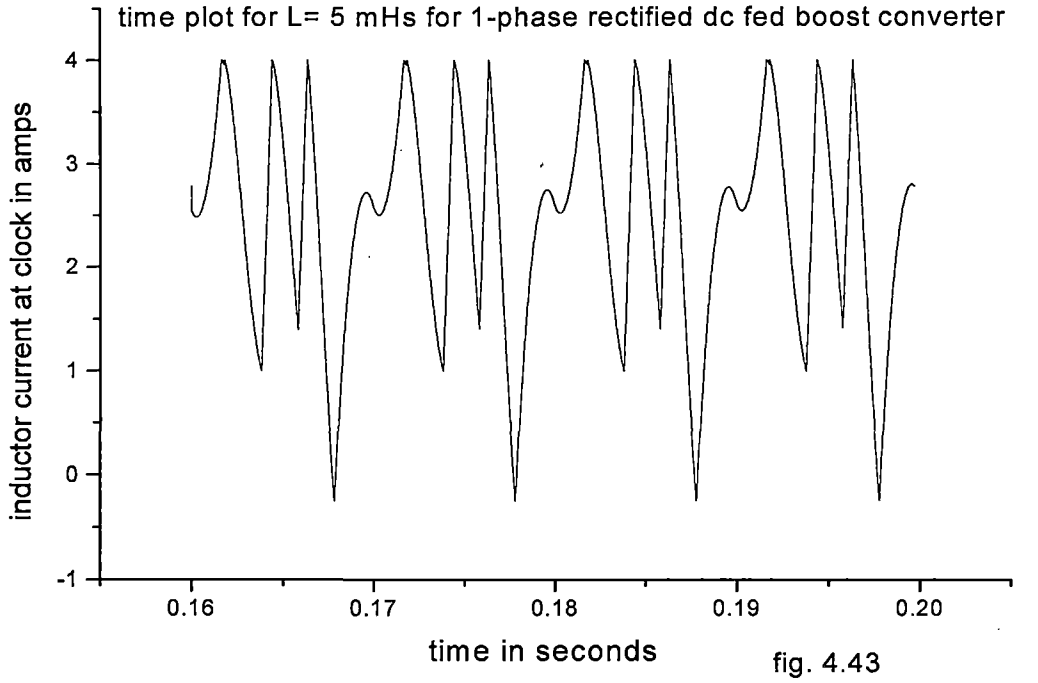

fig. 4.43

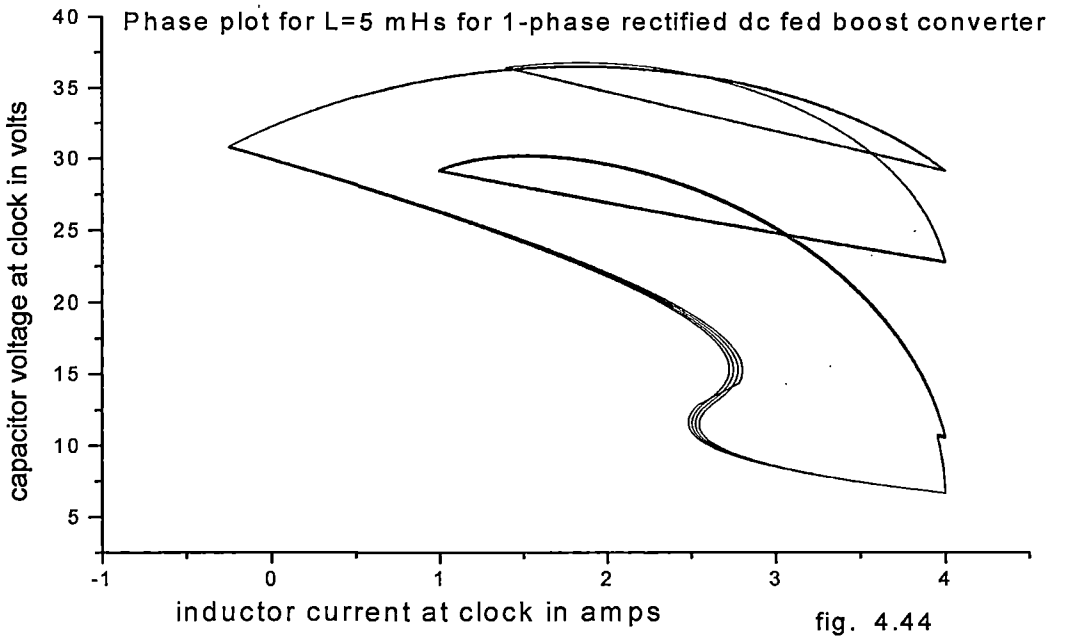

fig. 4.44

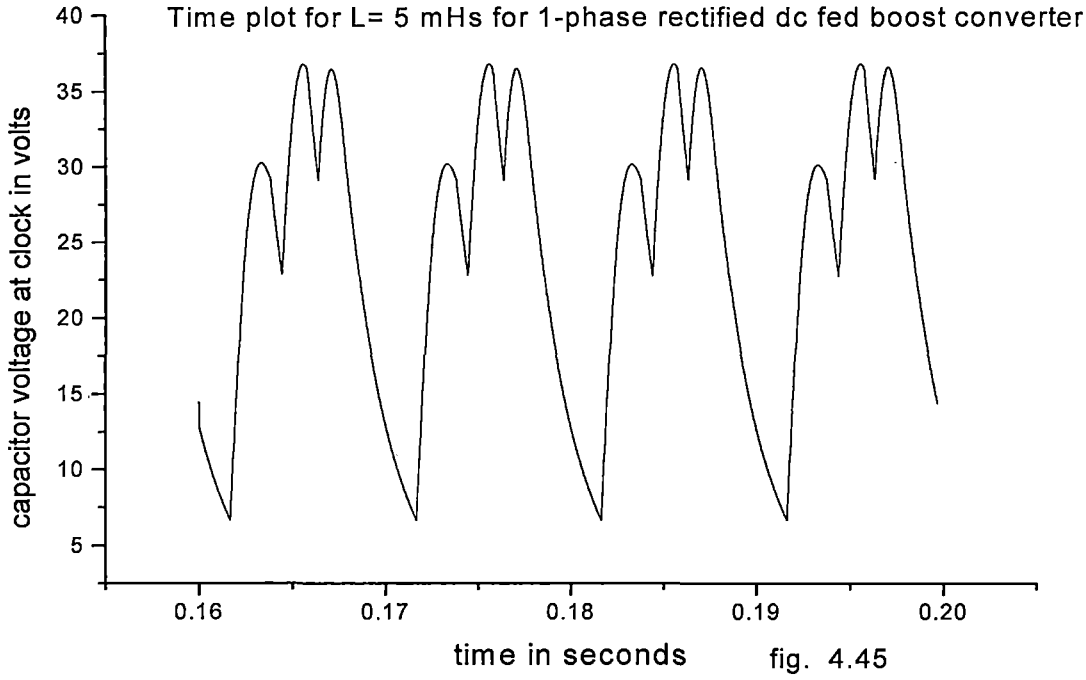

fig. 4.45

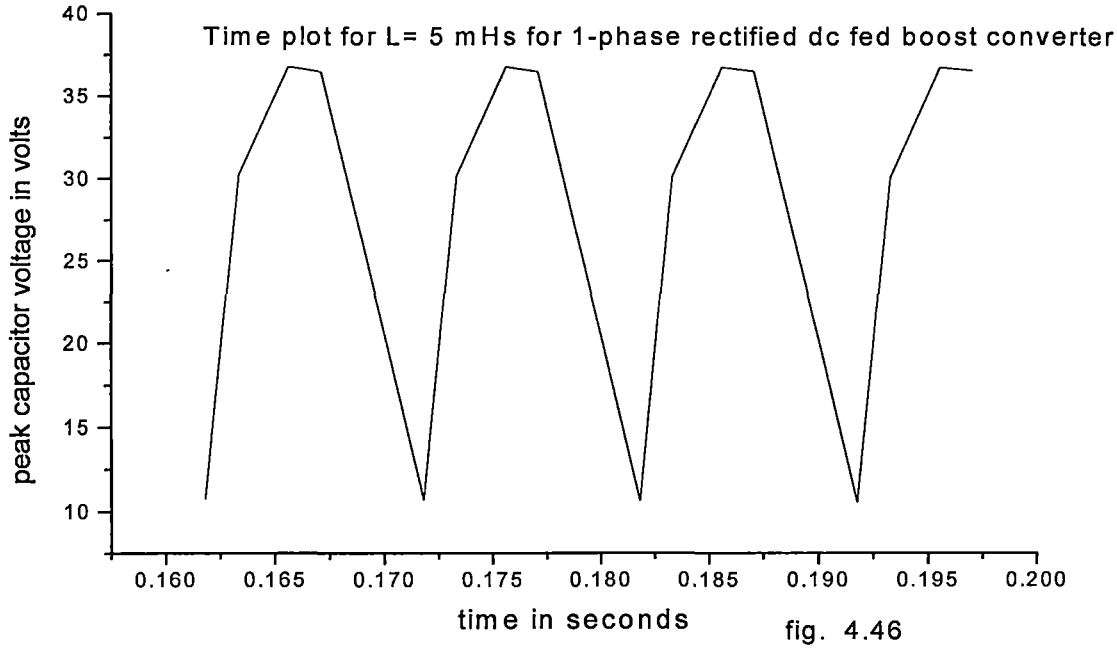

fig. 4.46

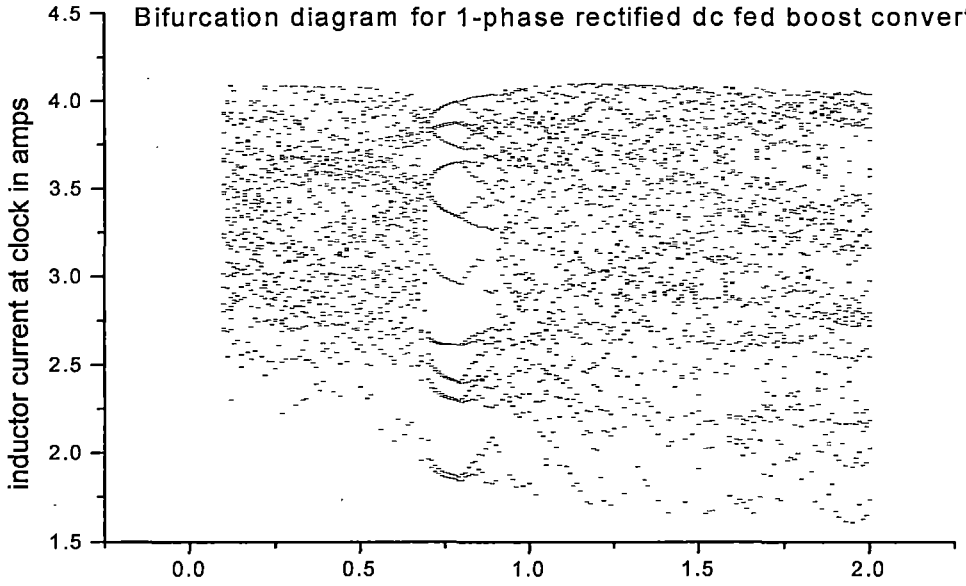

fig. 4.47

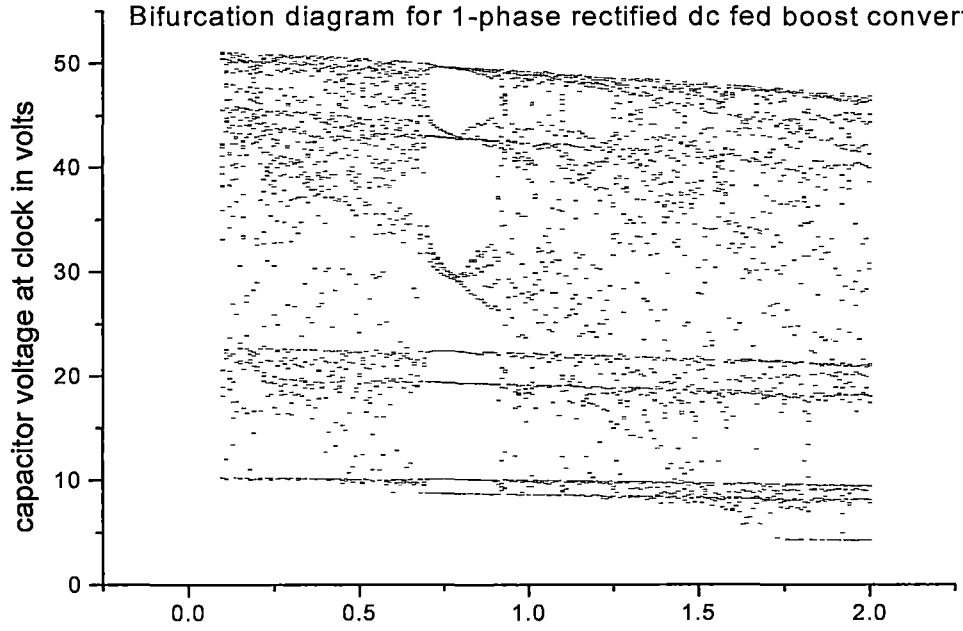

fig. 4.48

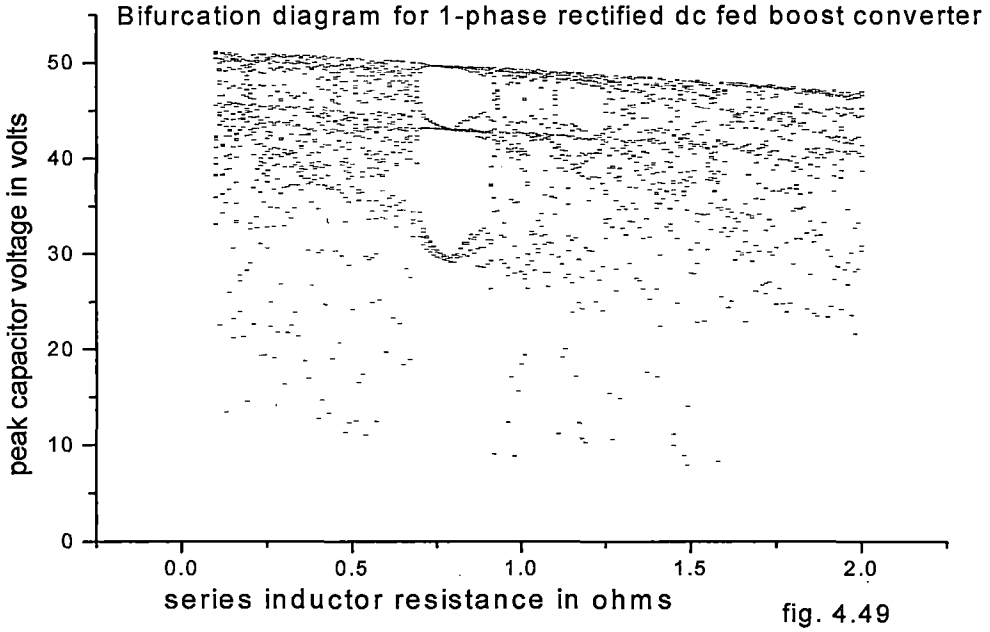

fig. 4.49

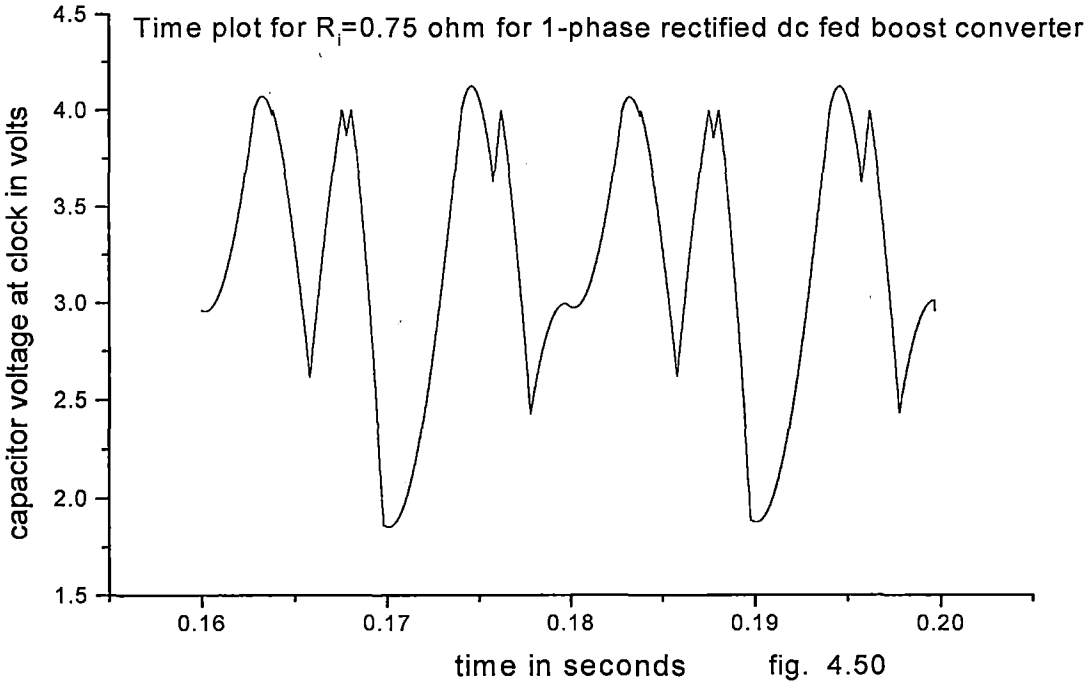

fig. 4.50

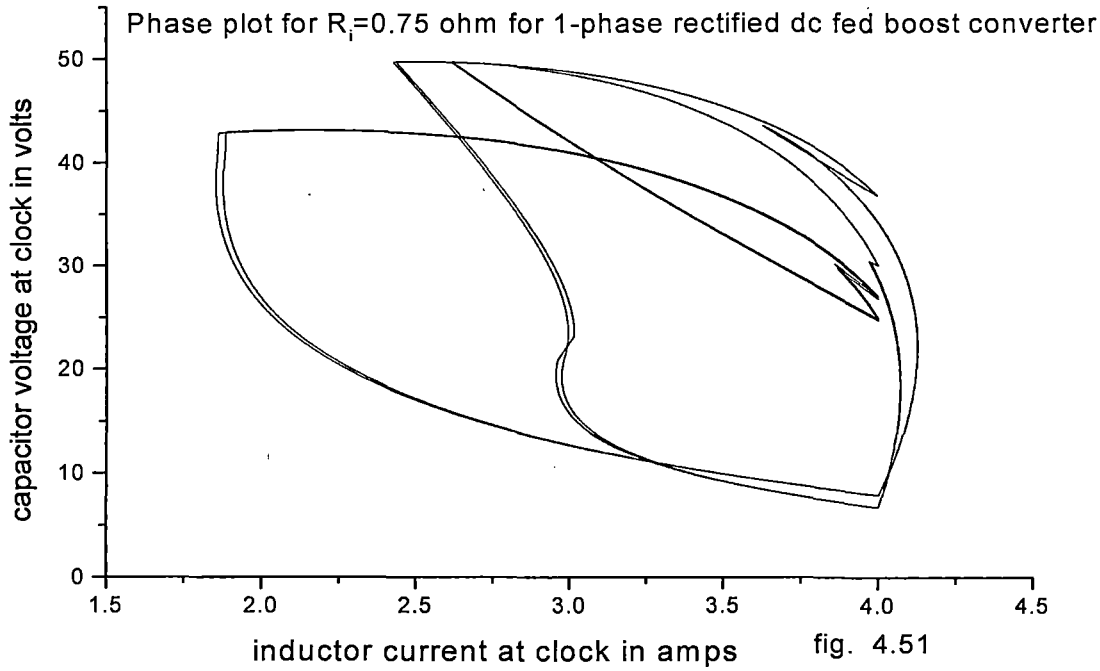

fig. 4.51

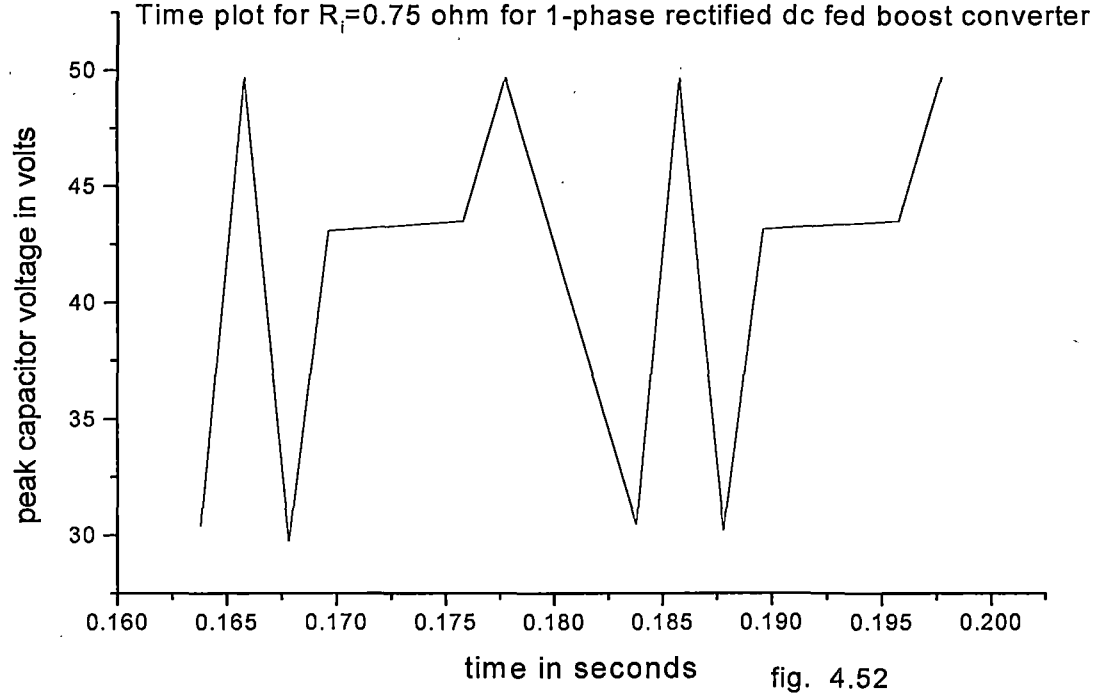

fig. 4.52

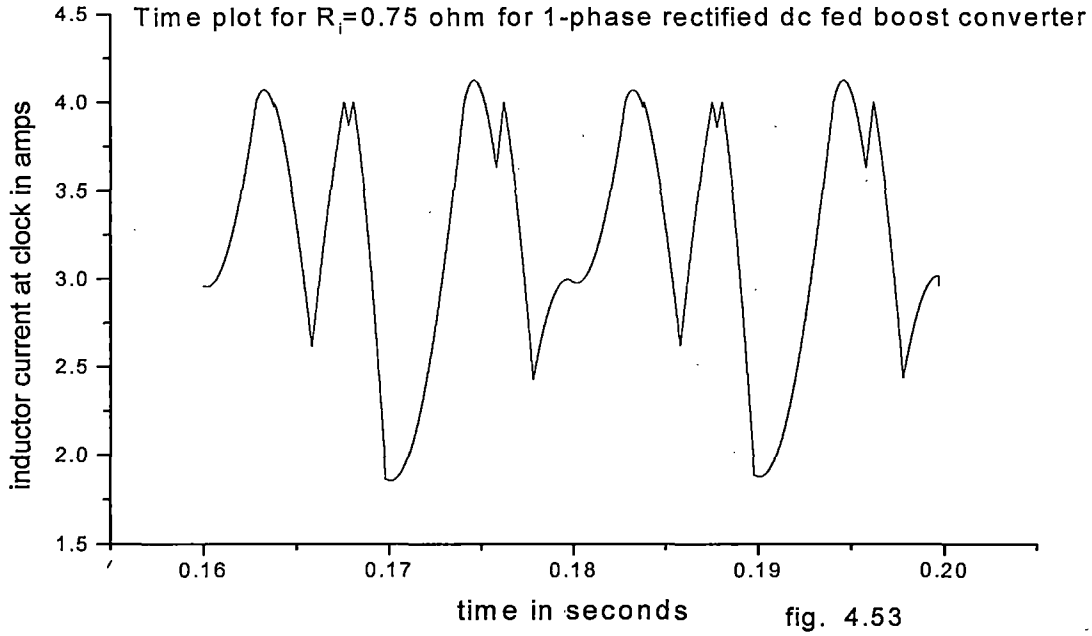

fig. 4.53

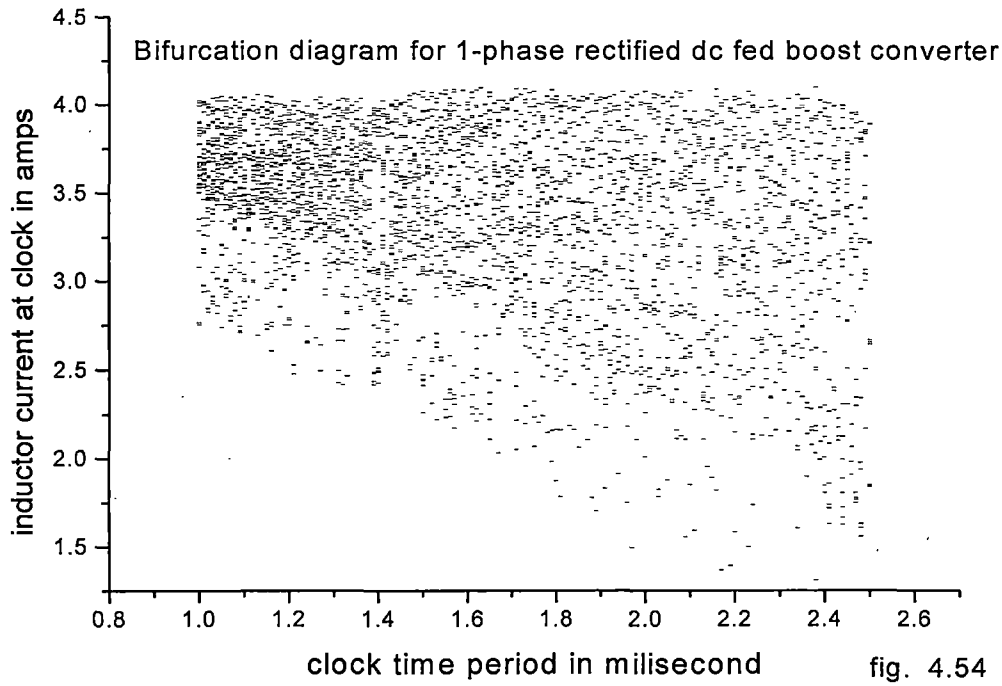

fig. 4.54

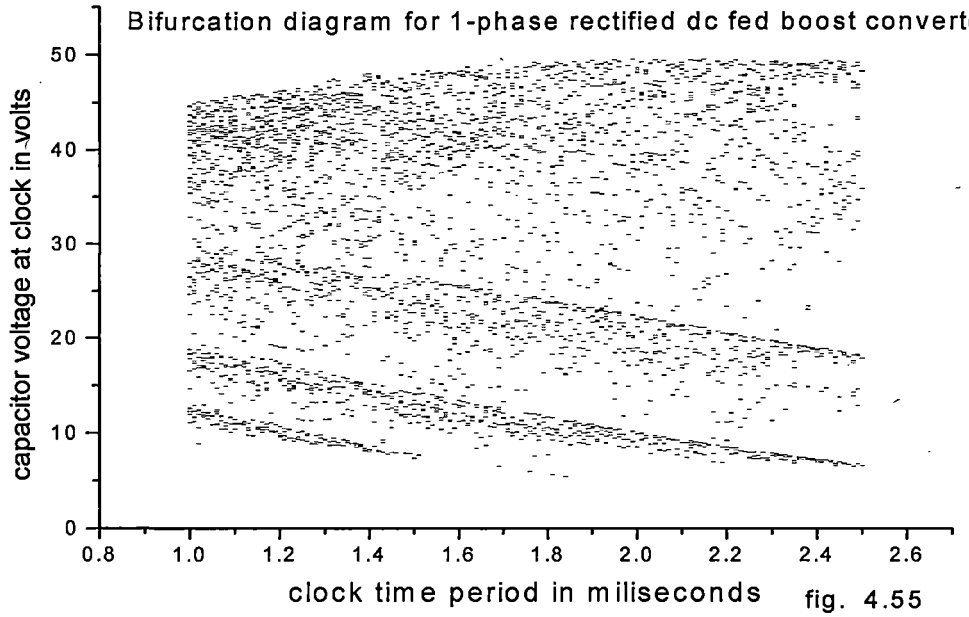

fig. 4.55

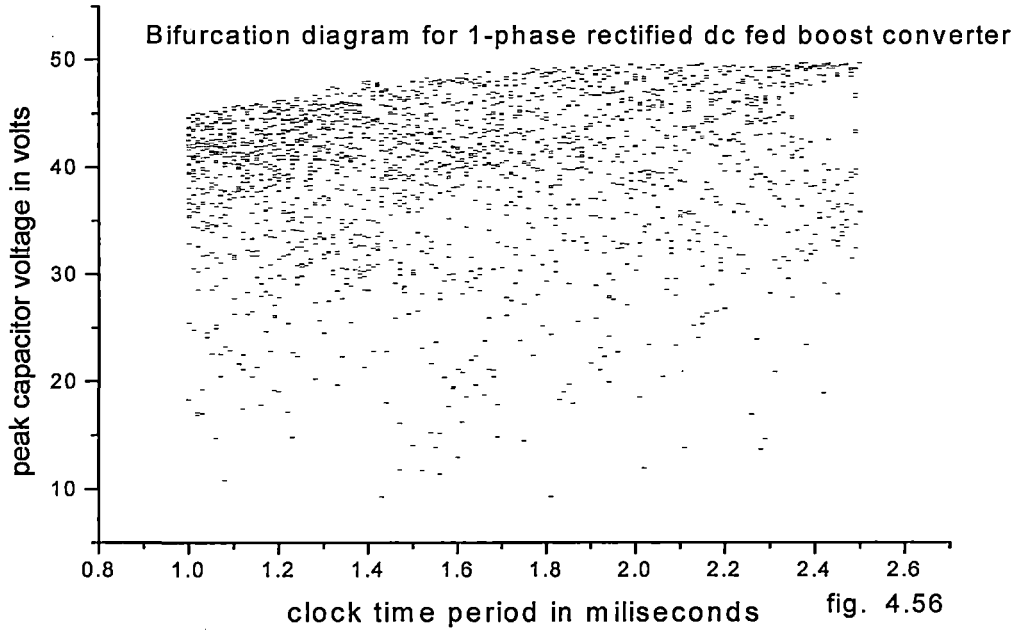

fig. 4.56

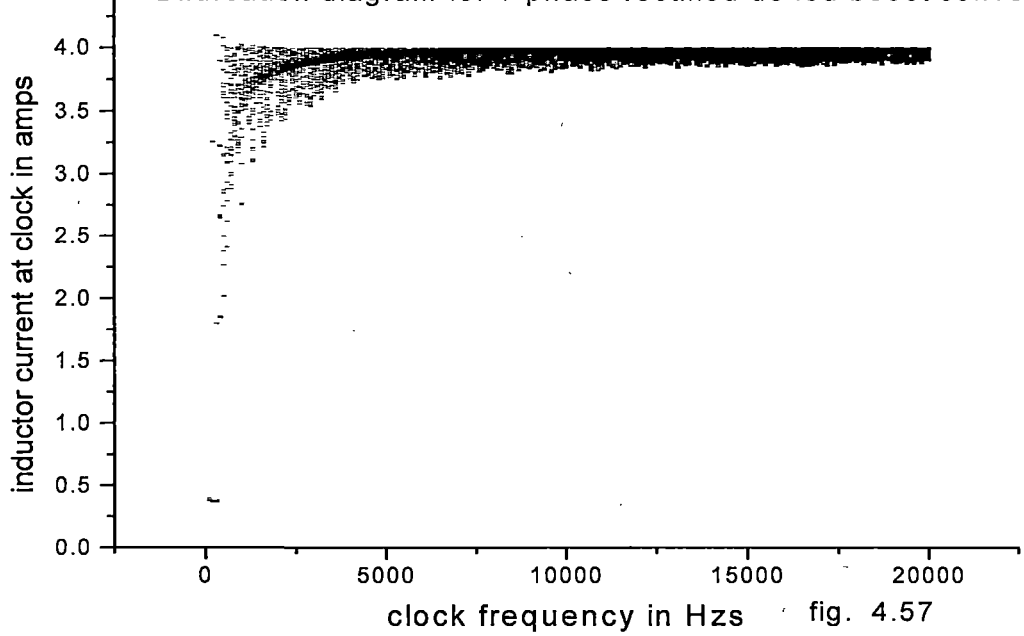

fig. 4.57

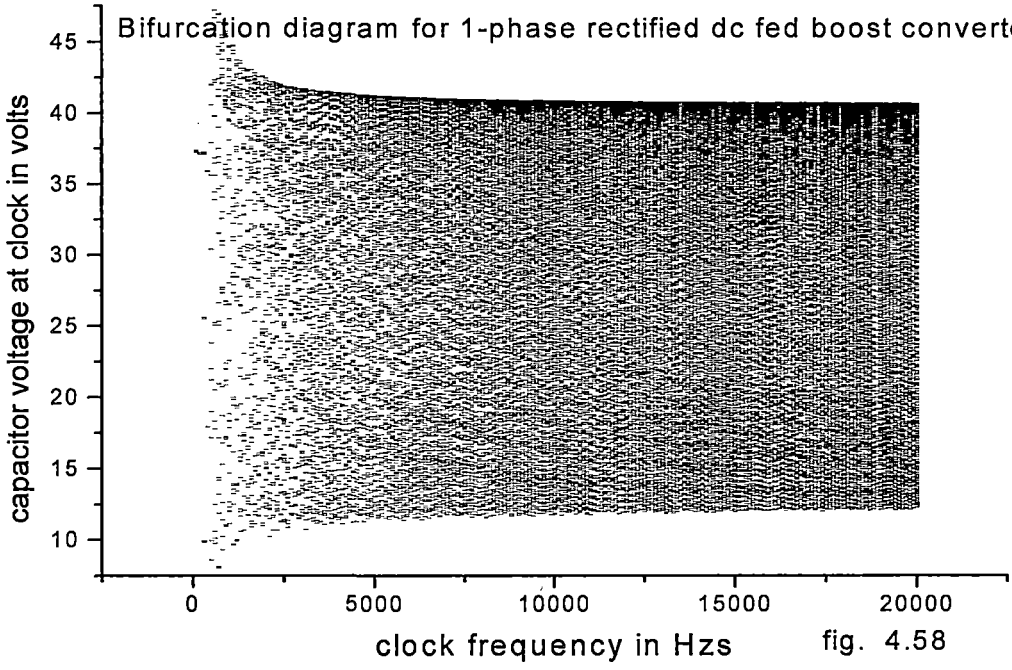

fig. 4.58

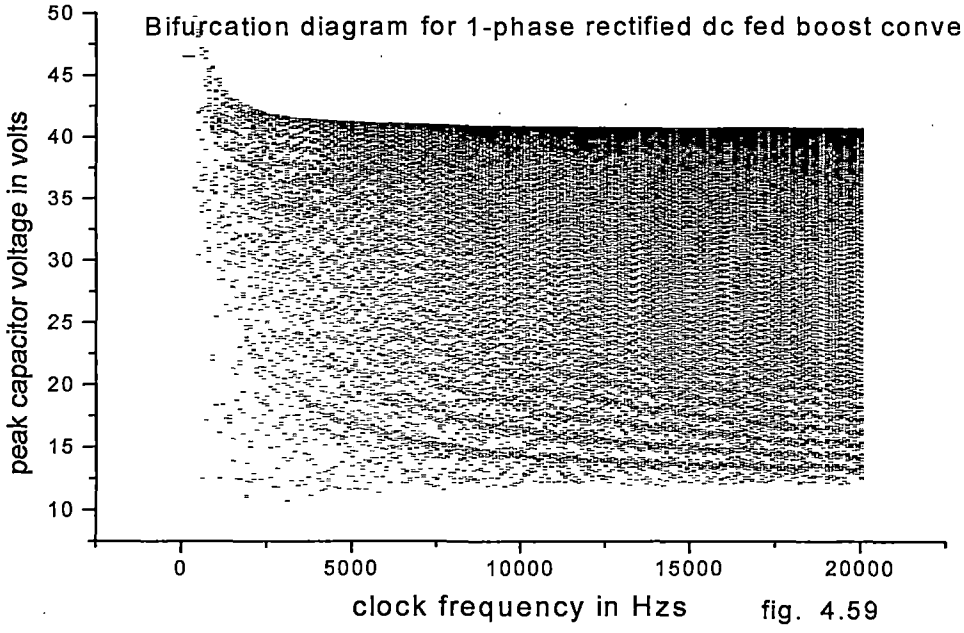

fig. 4.59

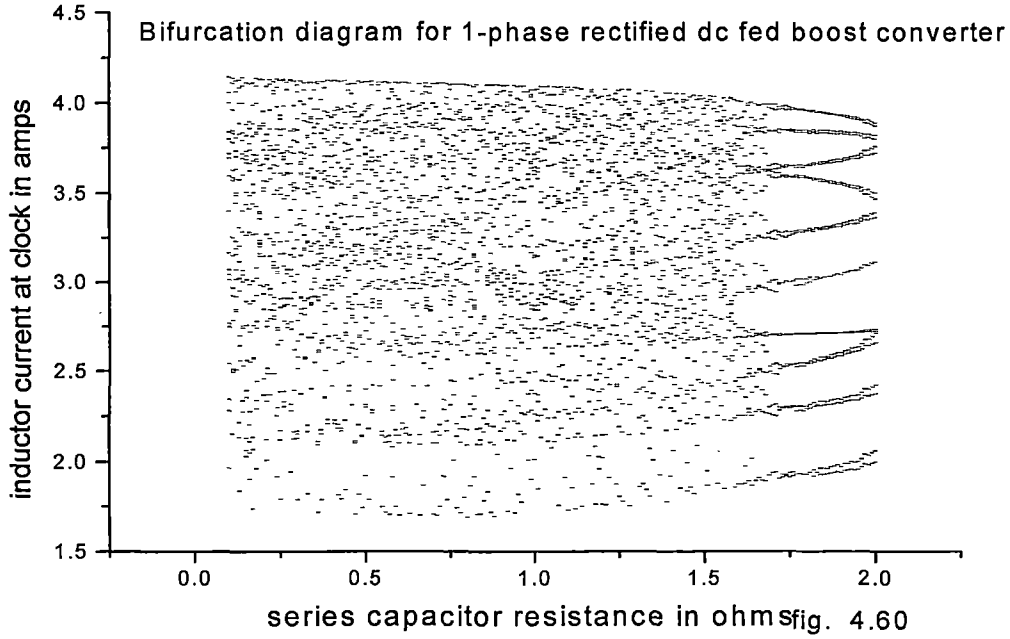

fig. 4.60

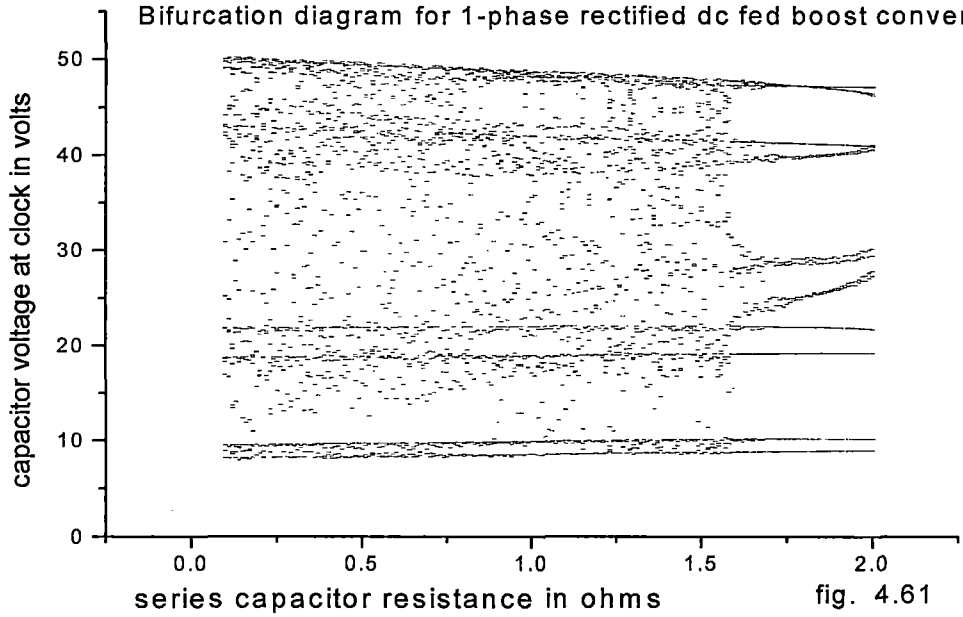

fig. 4.61

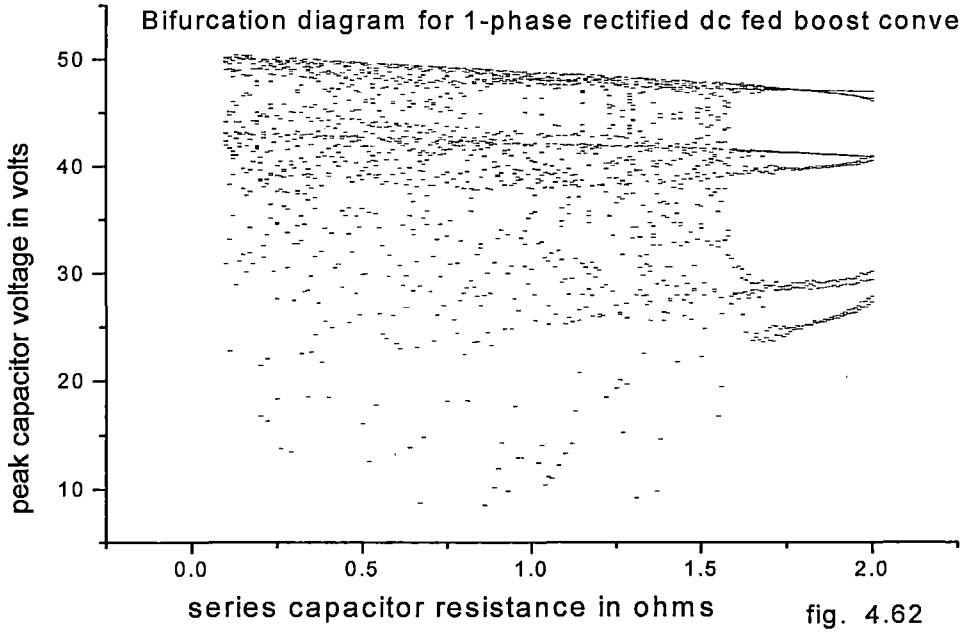

fig. 4.62

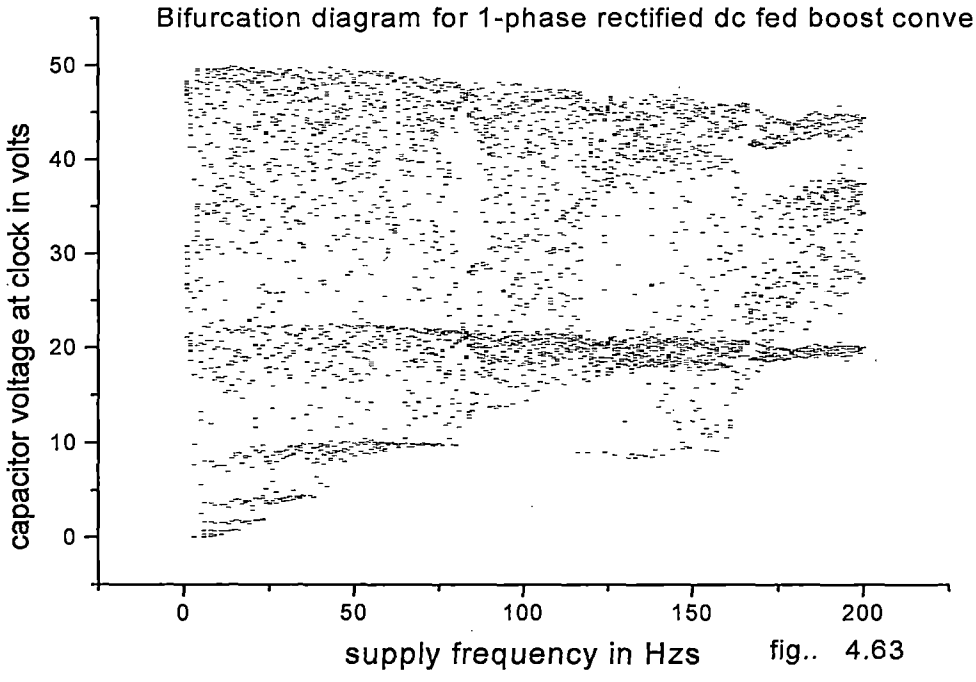

fig.. 4.63

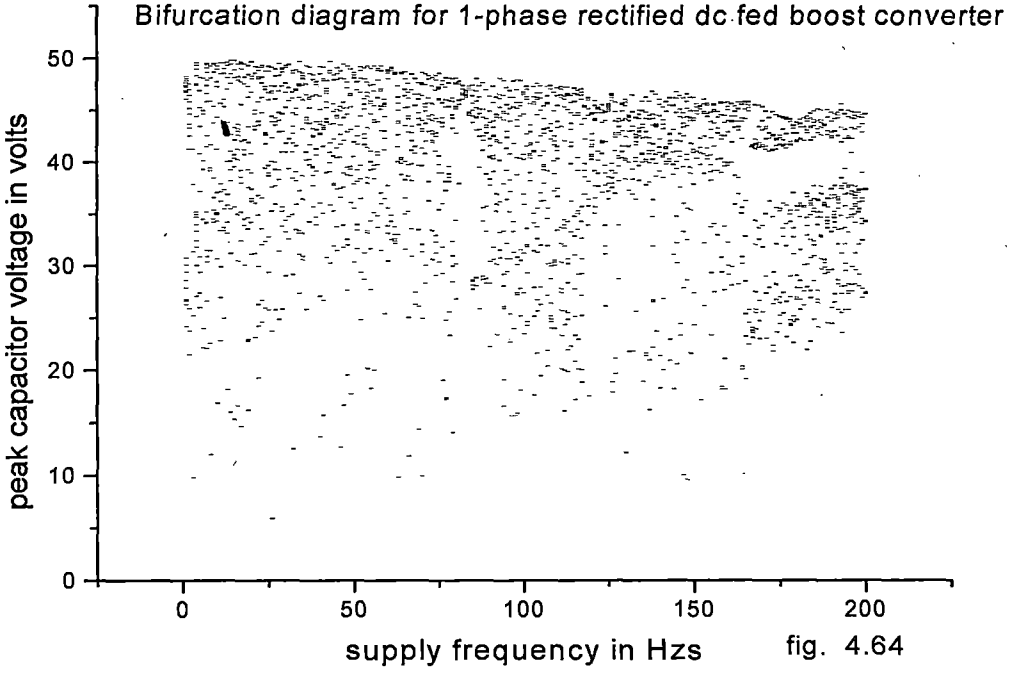

fig. 4.64

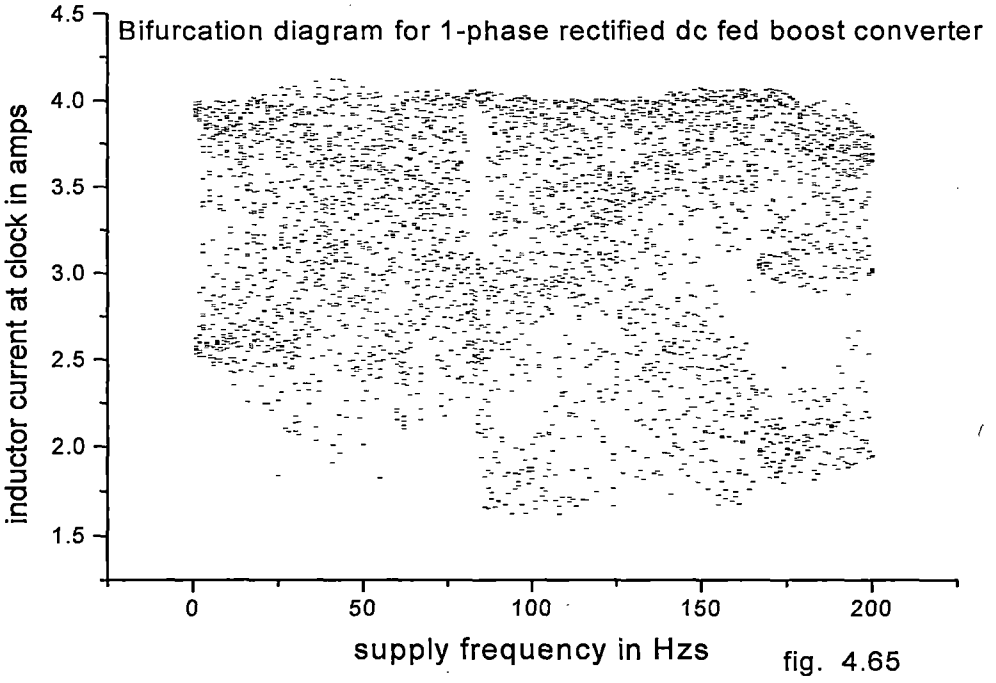

fig. 4.65

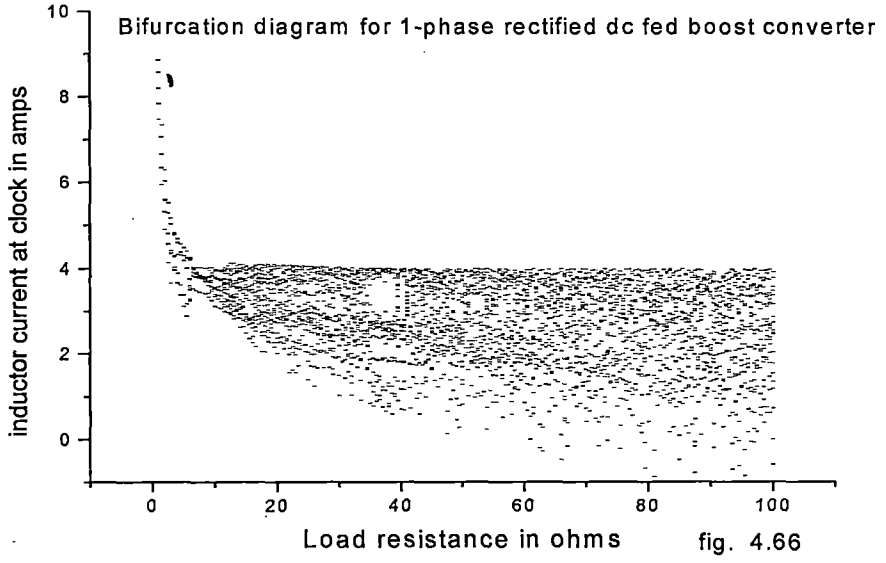

fig. 4.66

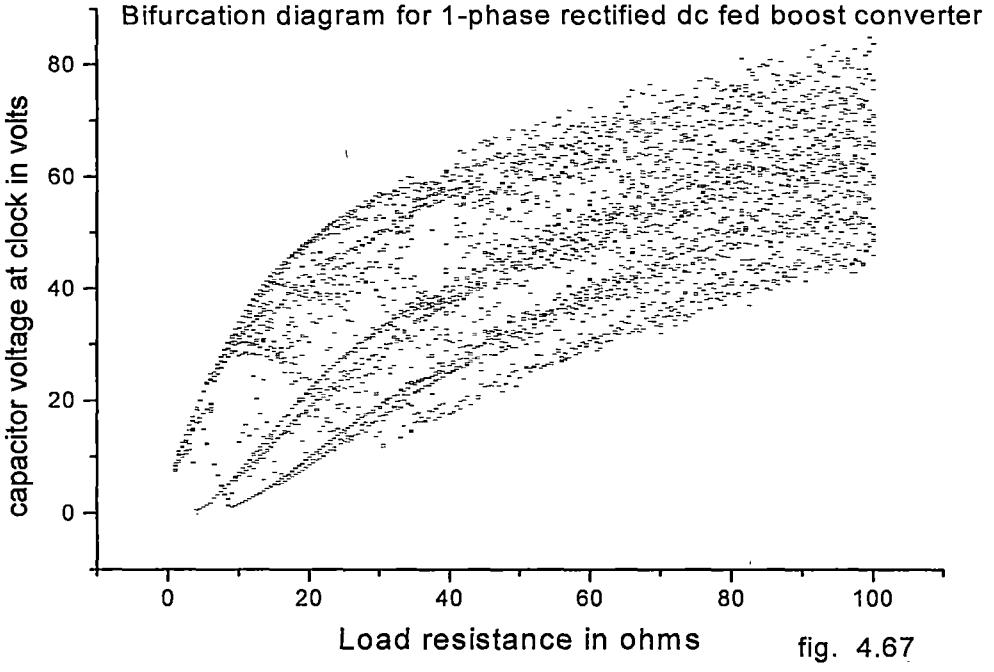

fig. 4.67

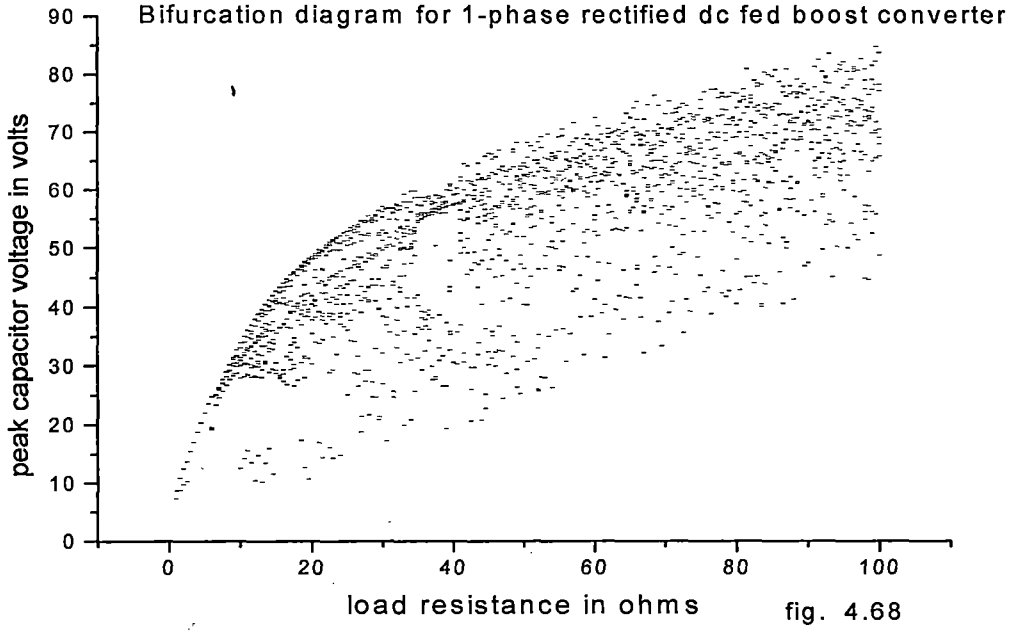

fig. 4.68

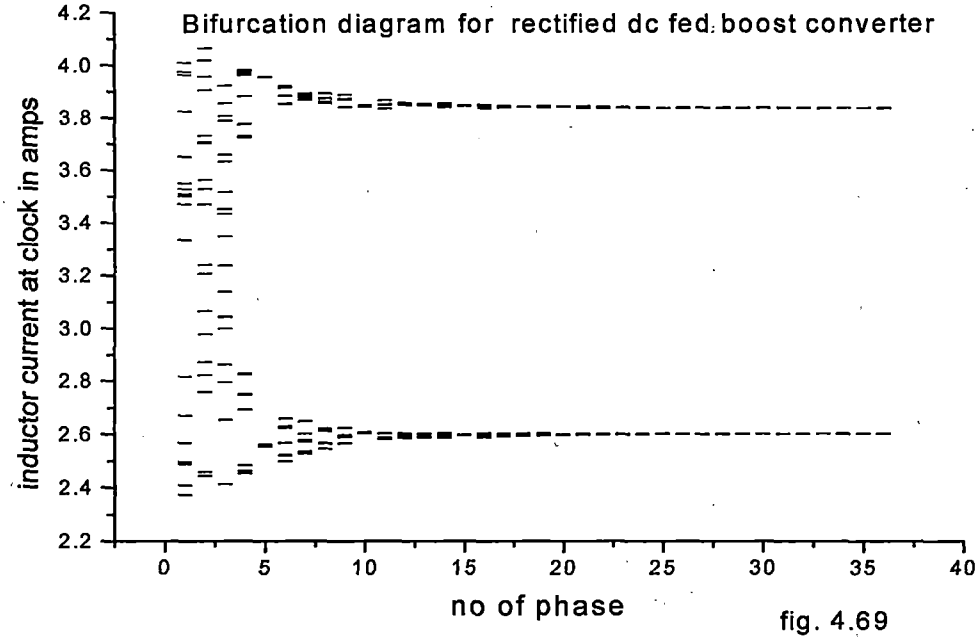

fig. 4.69

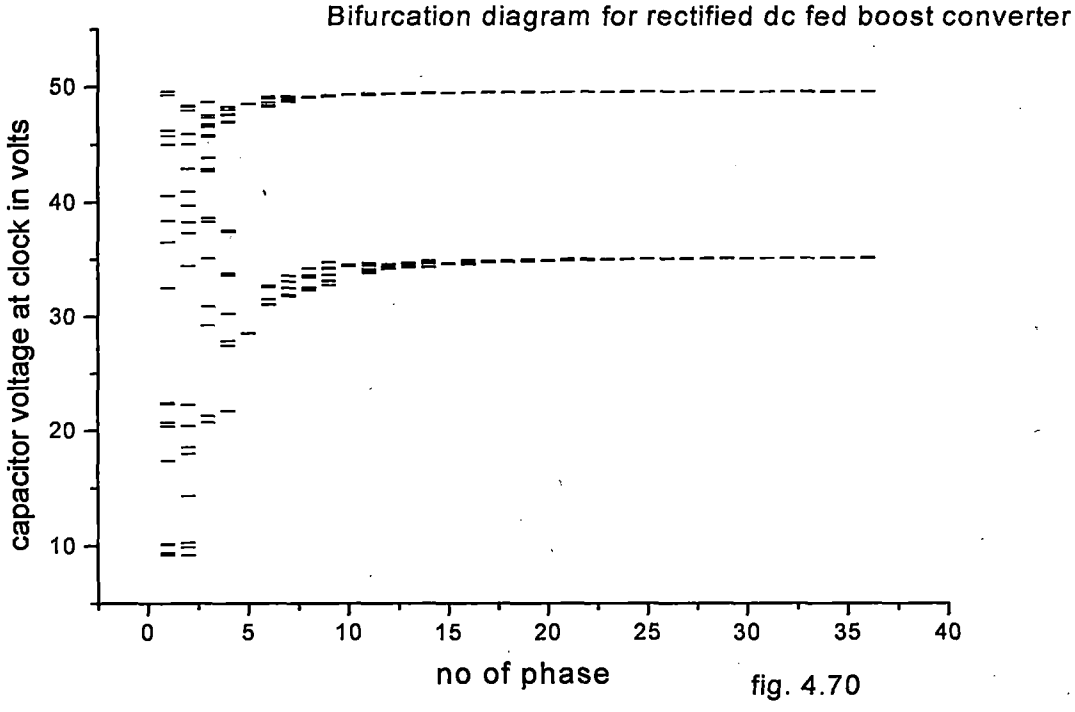

fig. 4.70

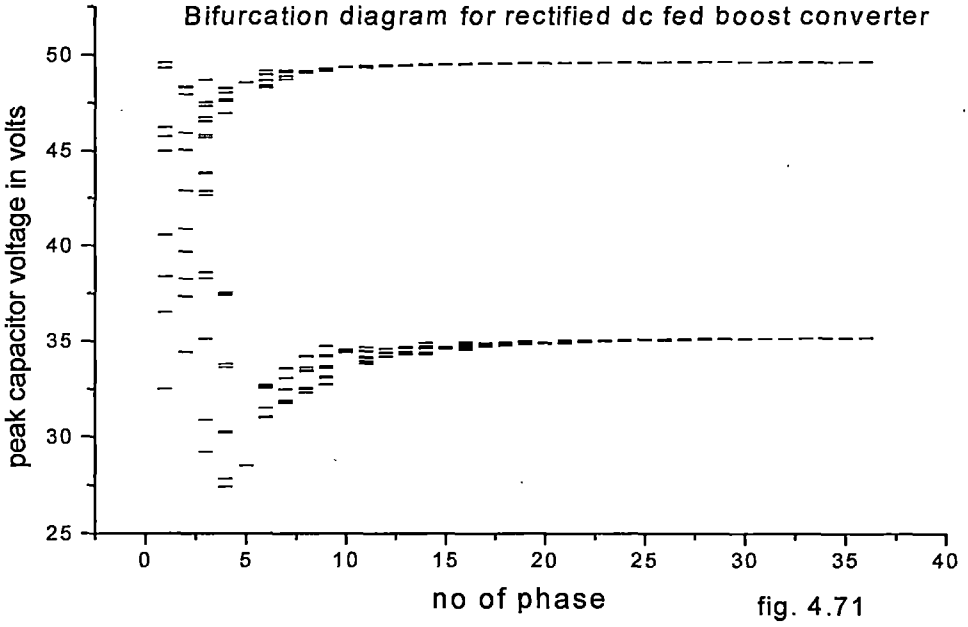

fig. 4.71

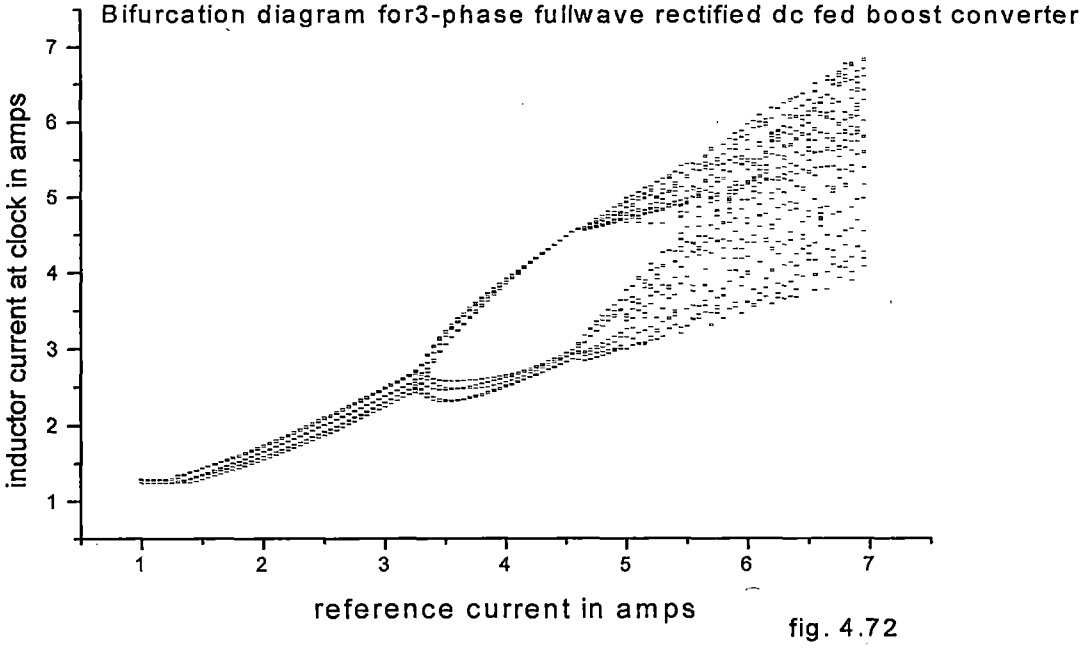

fig. 4.72

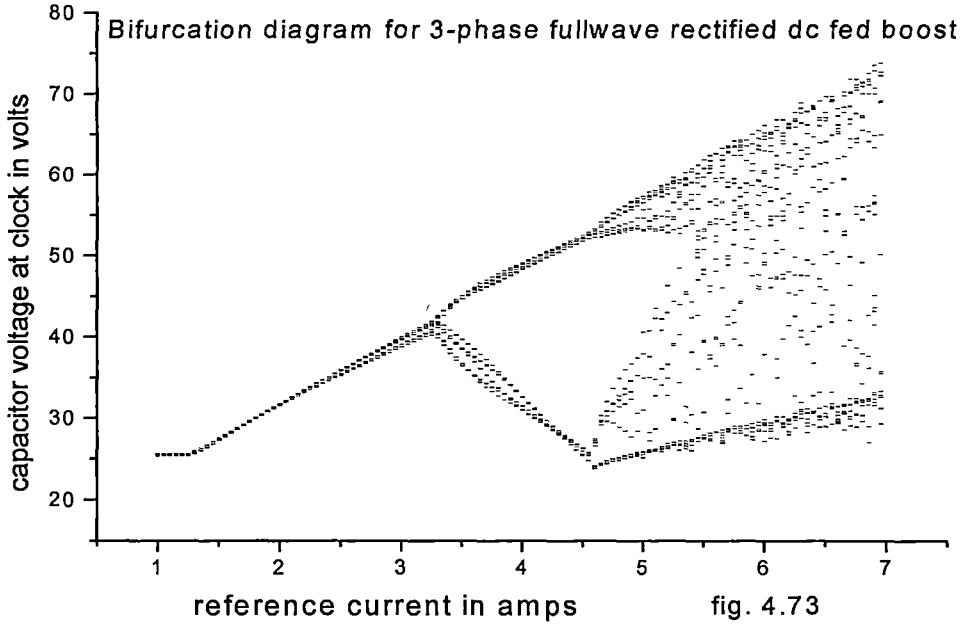

fig. 4.73

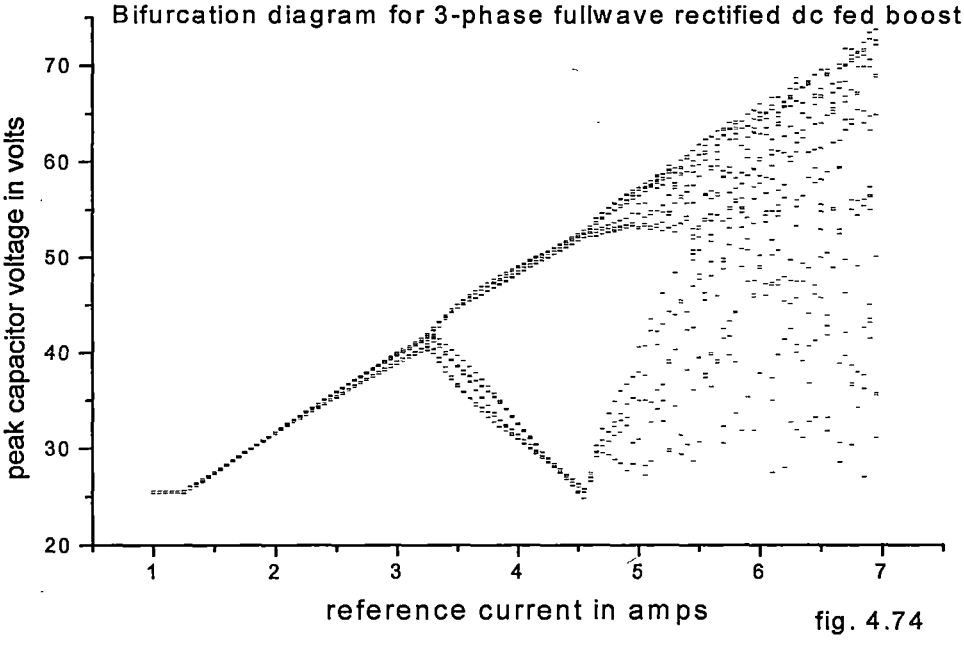

fig. 4.74

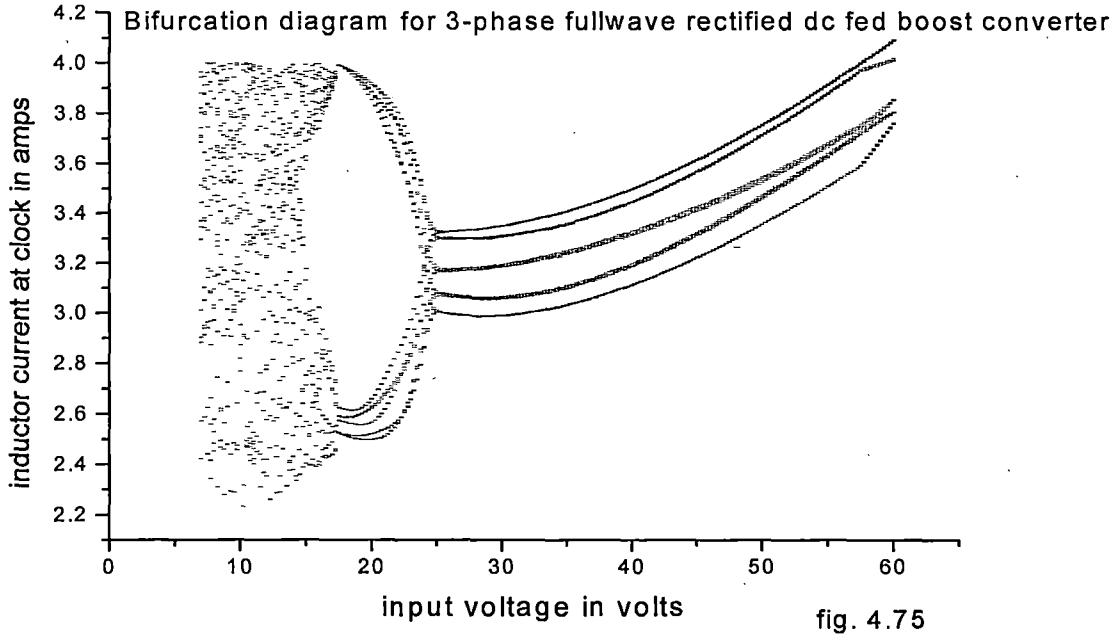

fig. 4.75

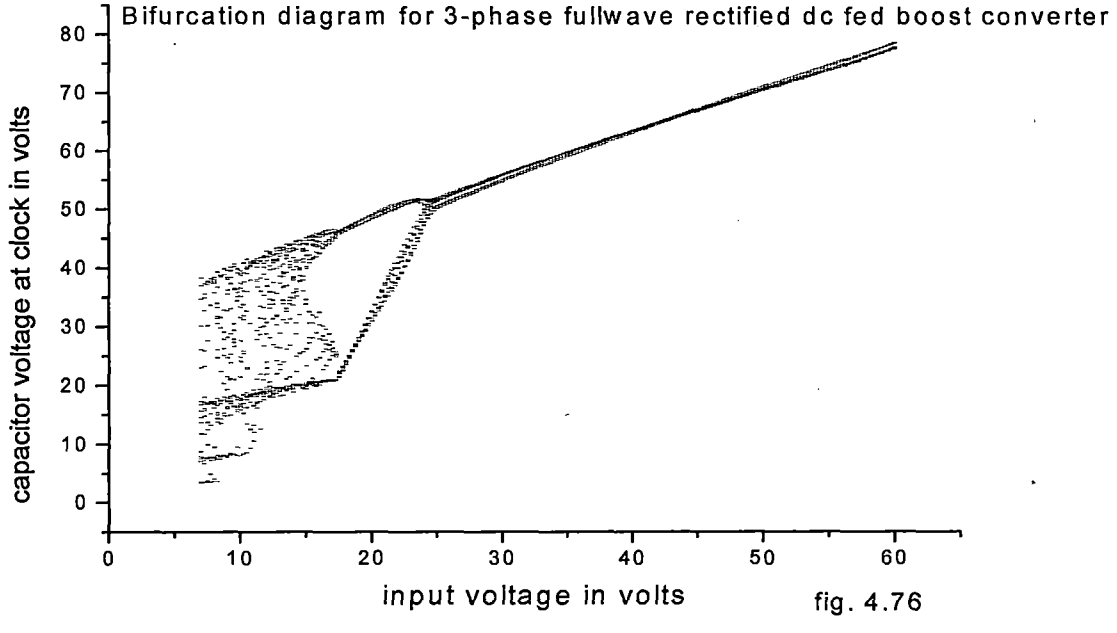

fig. 4.76

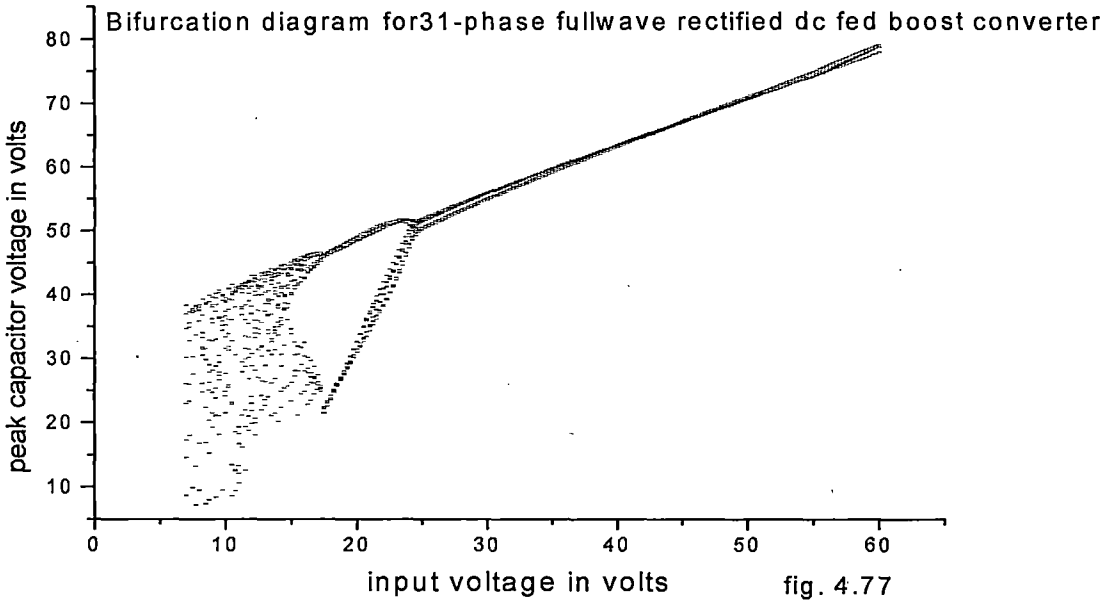

fig. 4.77

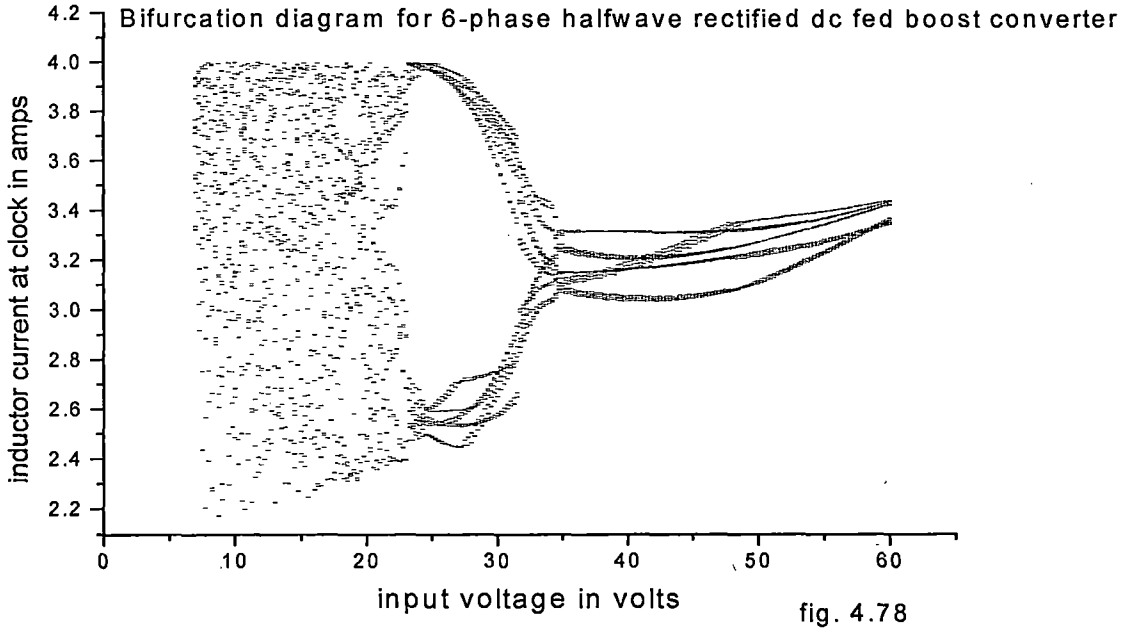

fig. 4.78

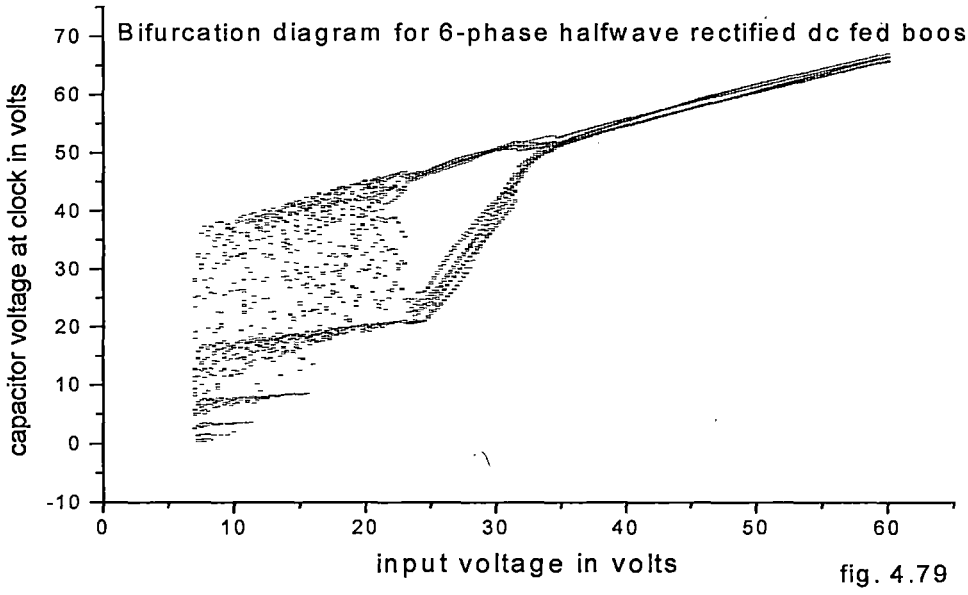

fig. 4.79

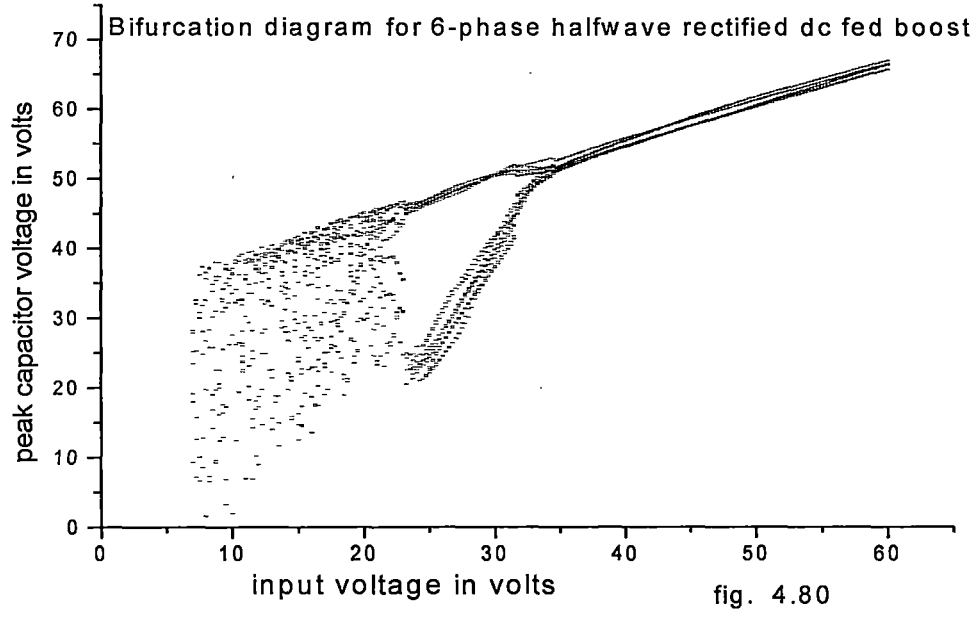

fig. 4.80

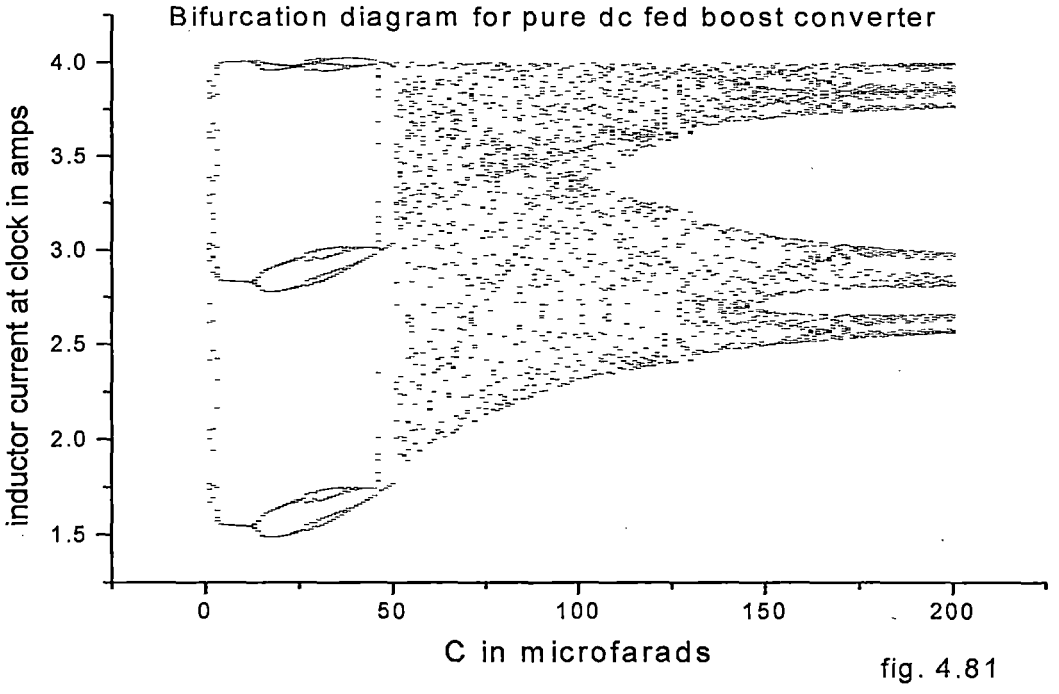

fig. 4.81

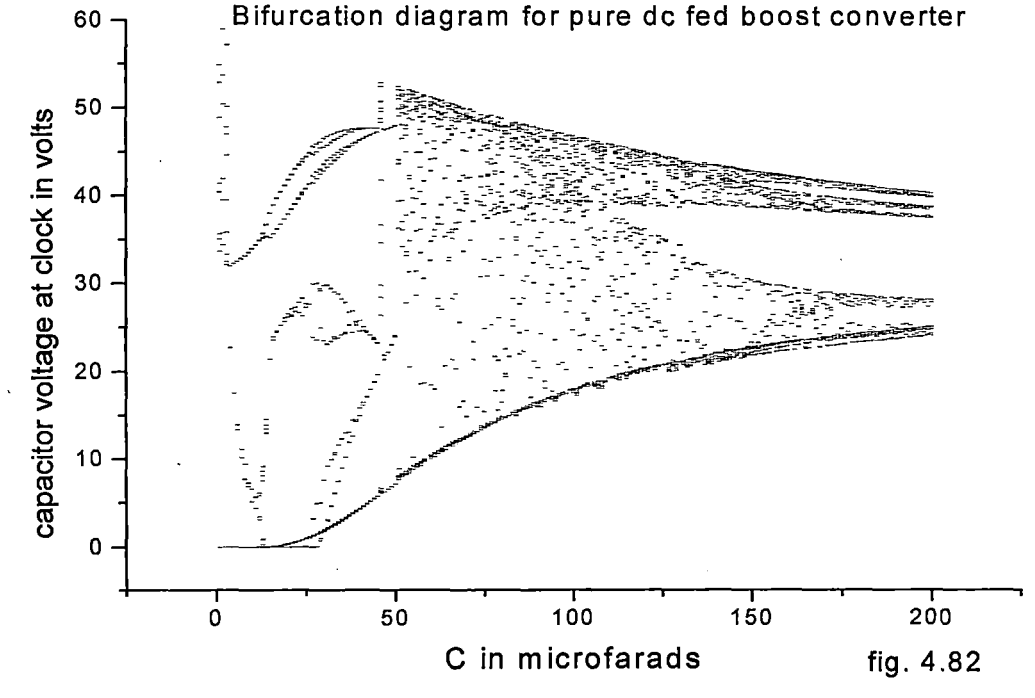

fig. 4.82

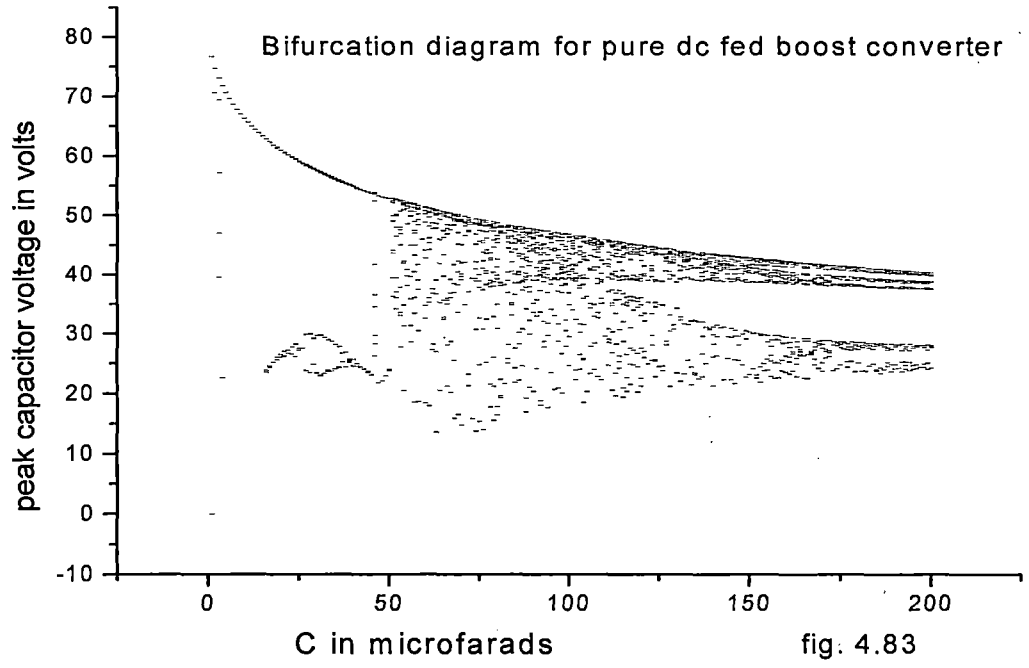

fig. 4.83

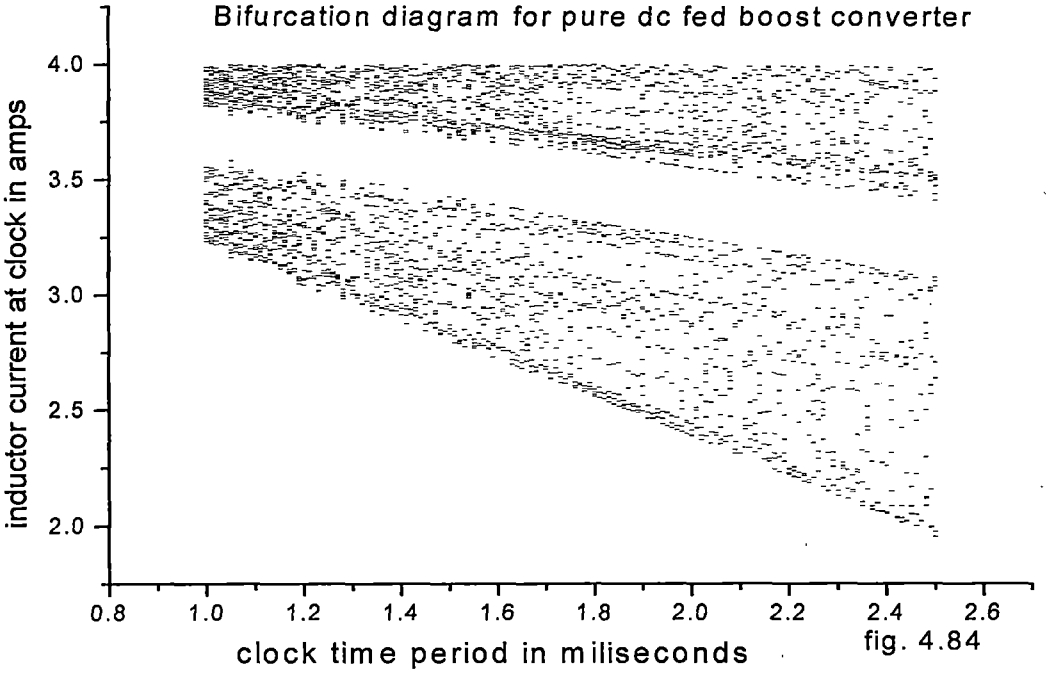

fig. 4.84

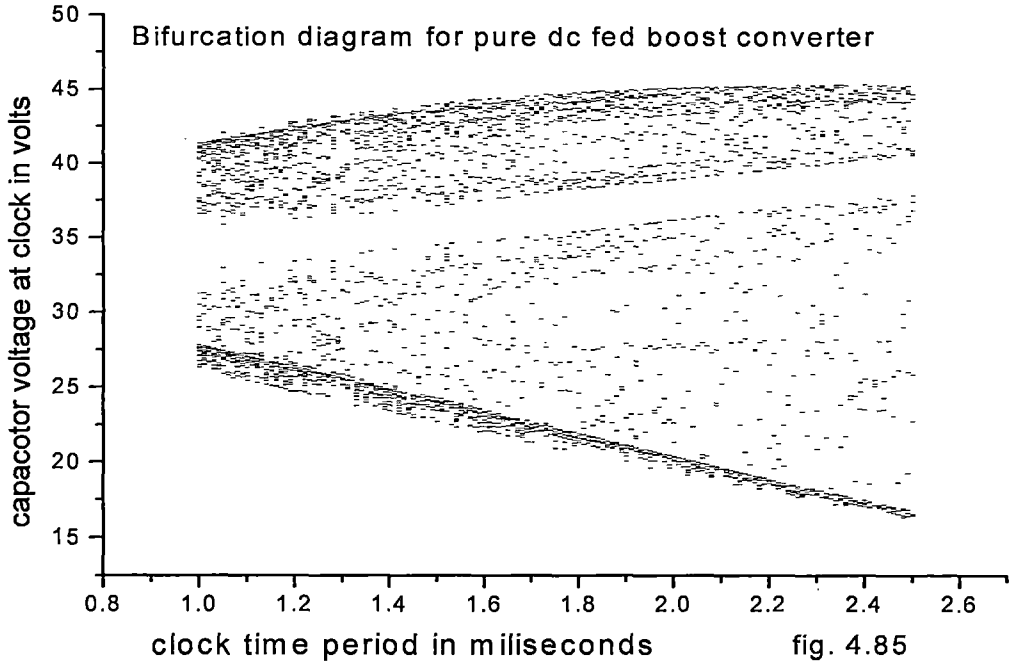

fig. 4.85

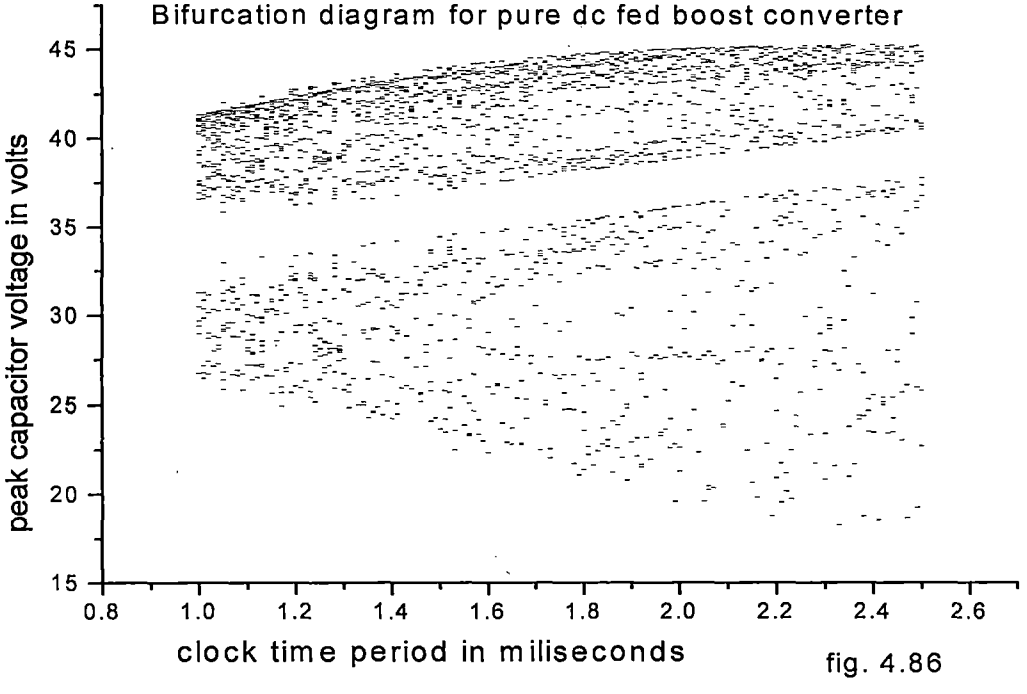

fig. 4.86

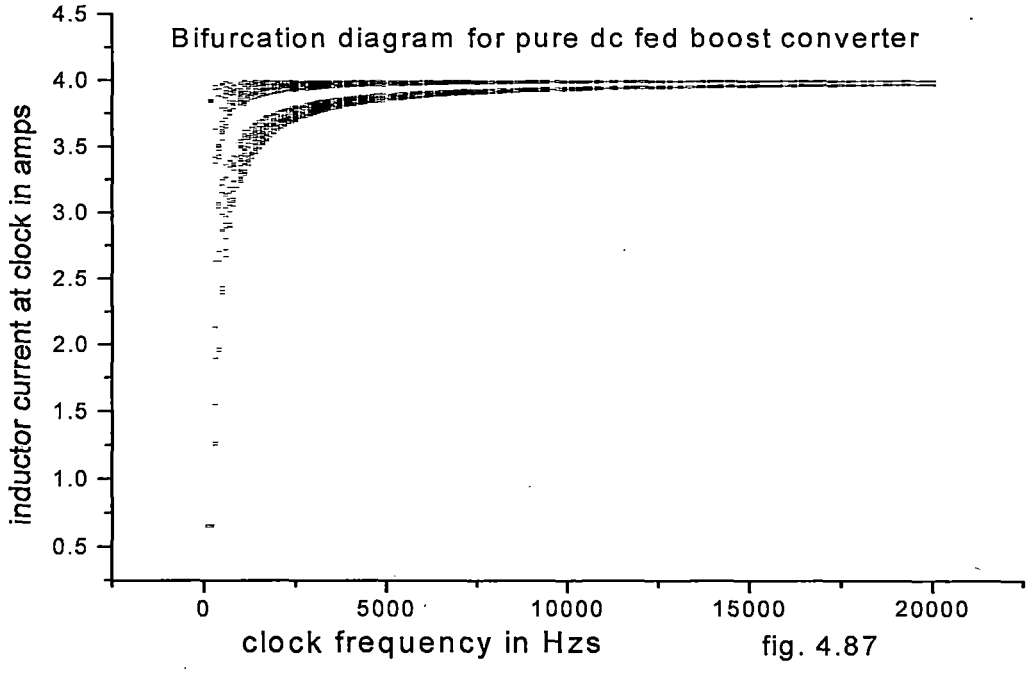

fig. 4.87

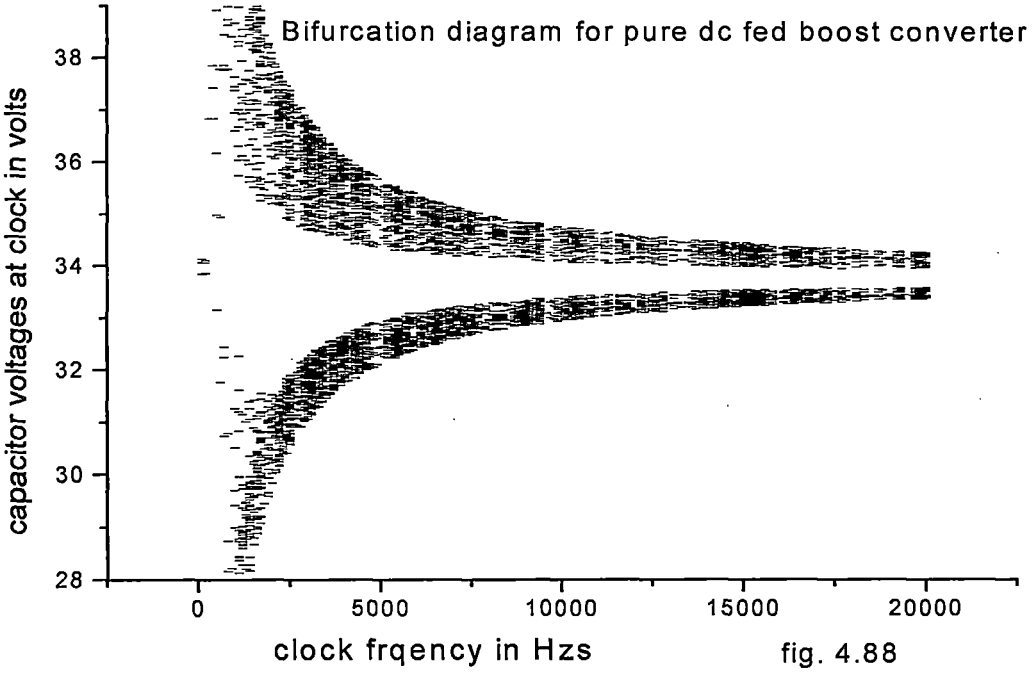

fig. 4.88

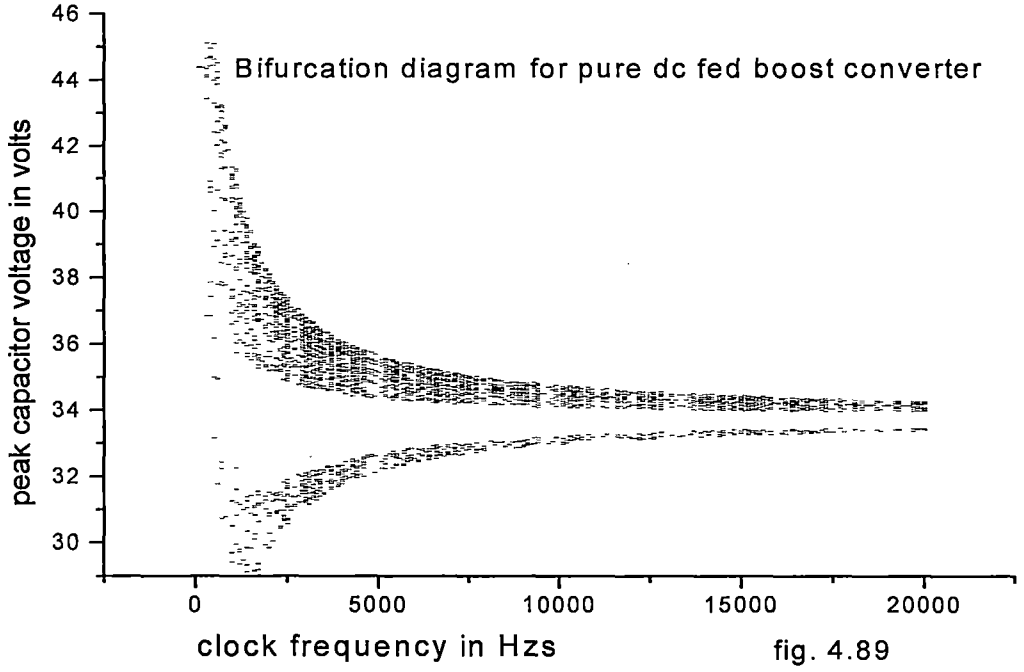

fig. 4.89

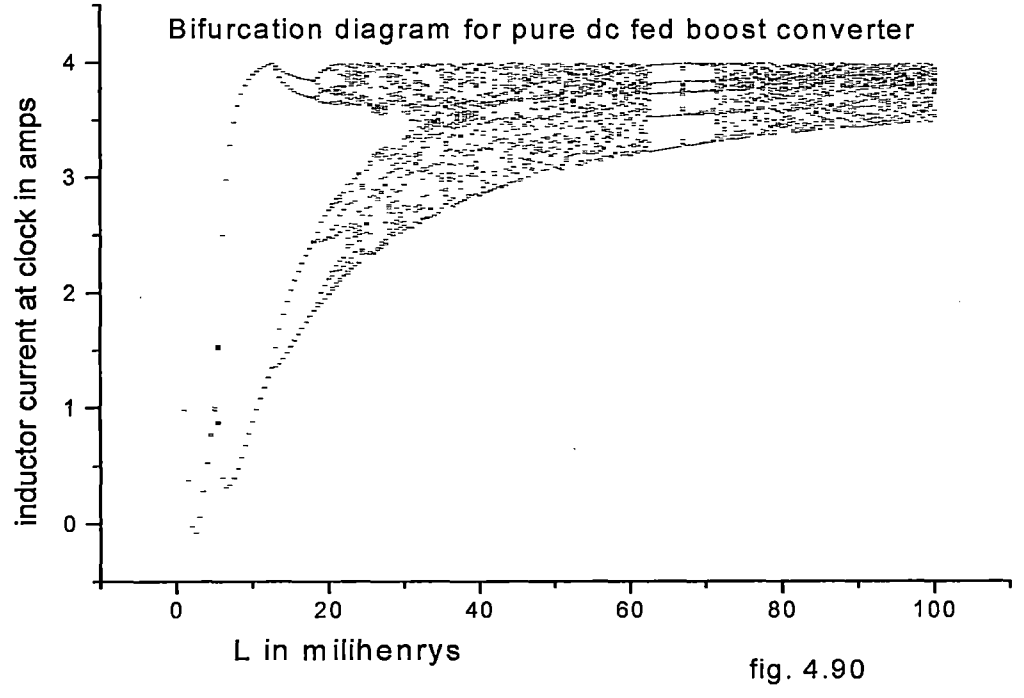

fig. 4.90

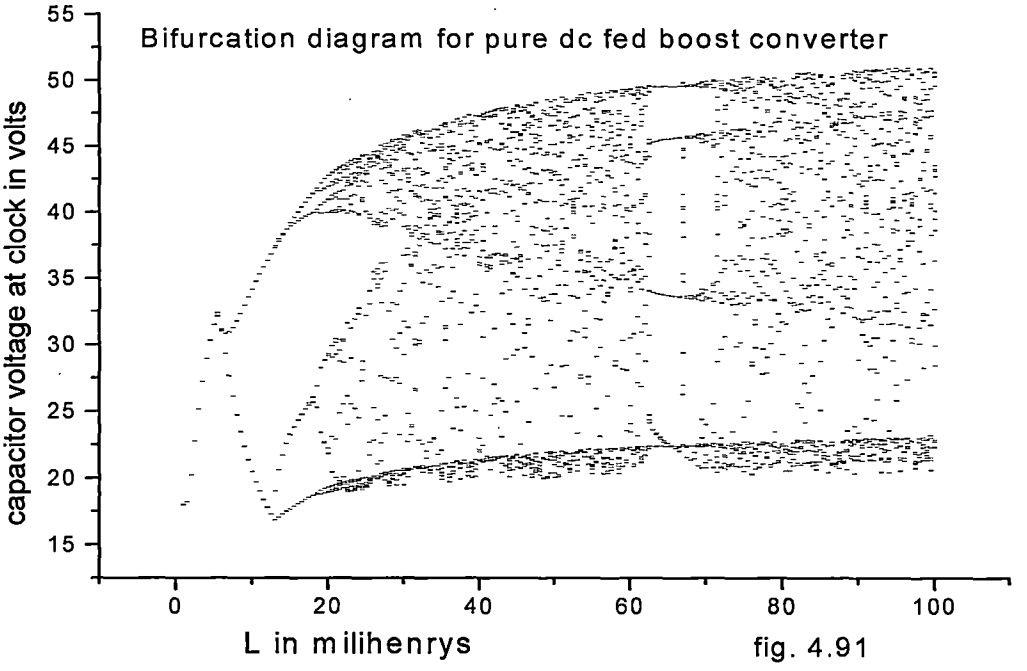

fig. 4.91

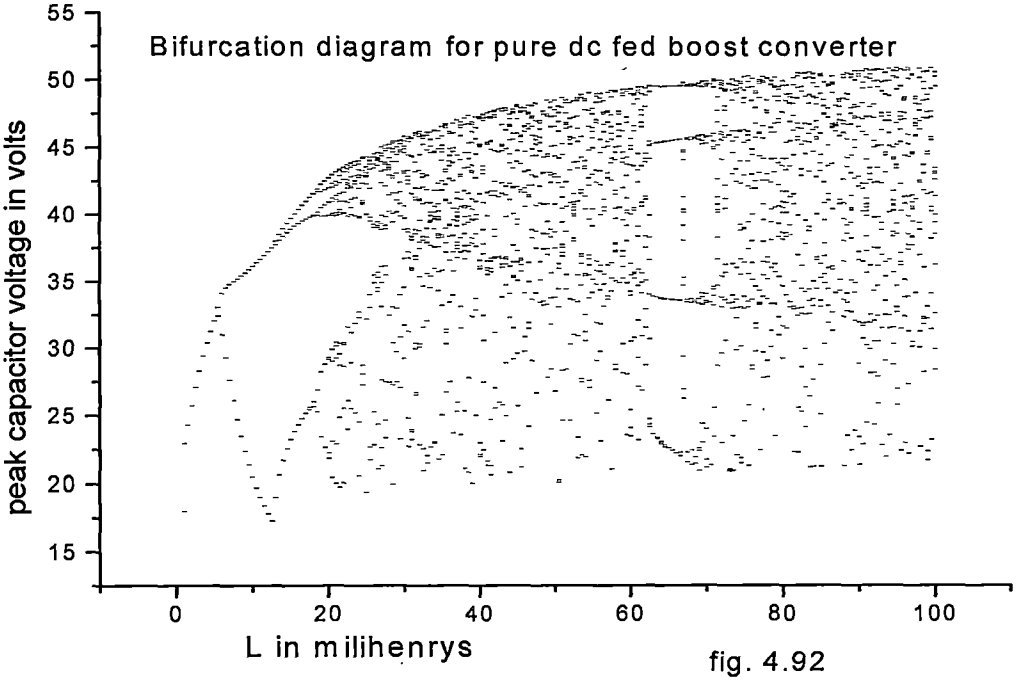

fig. 4.92

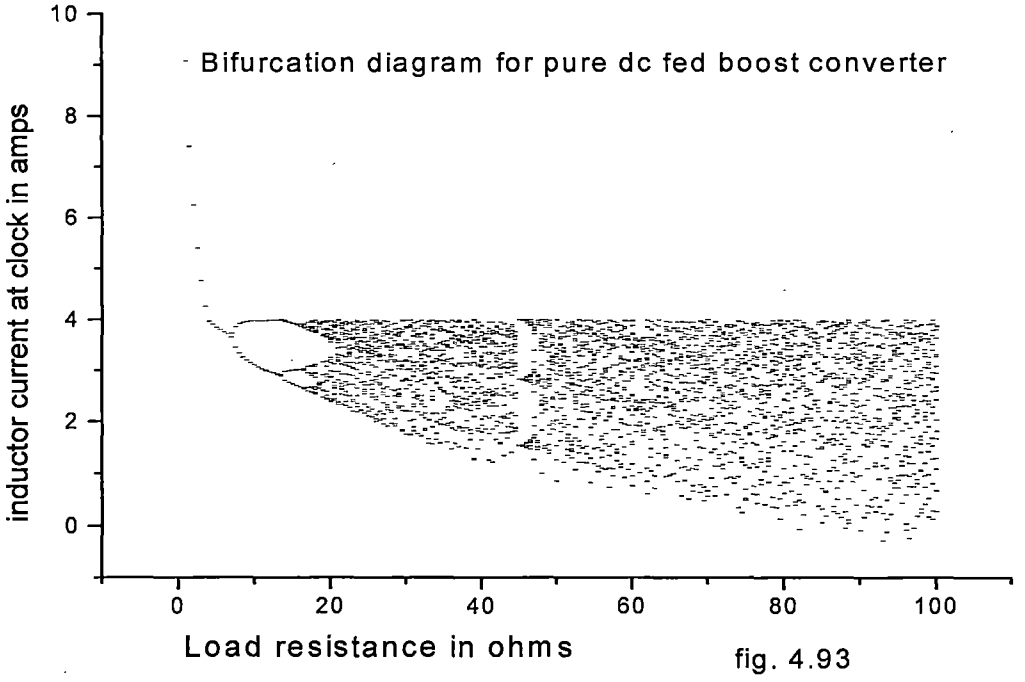

fig. 4.93

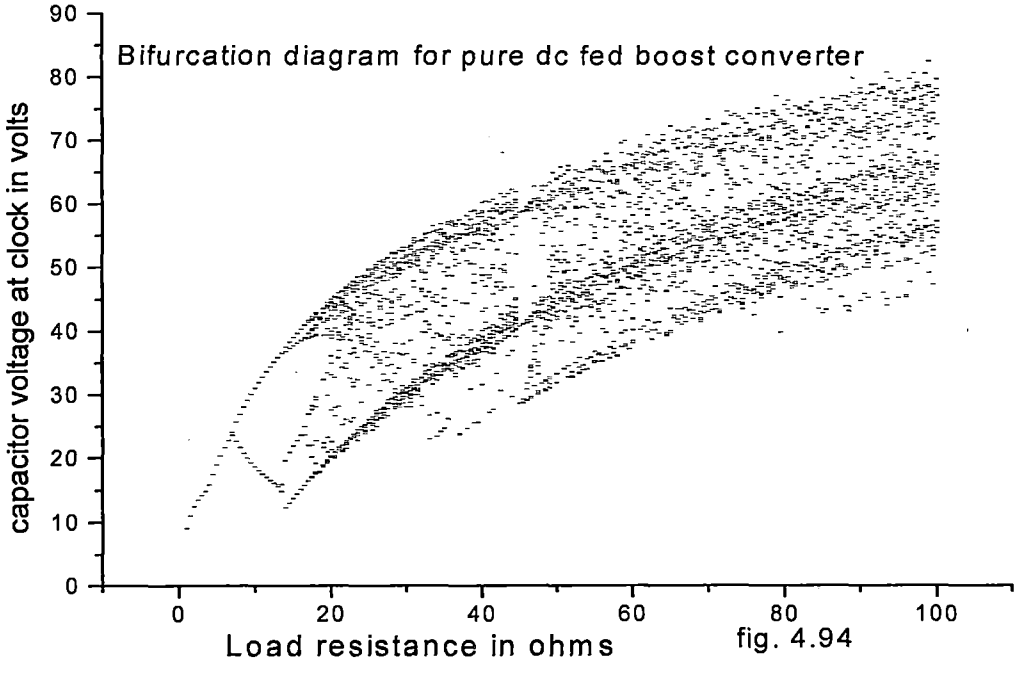

fig. 4.94

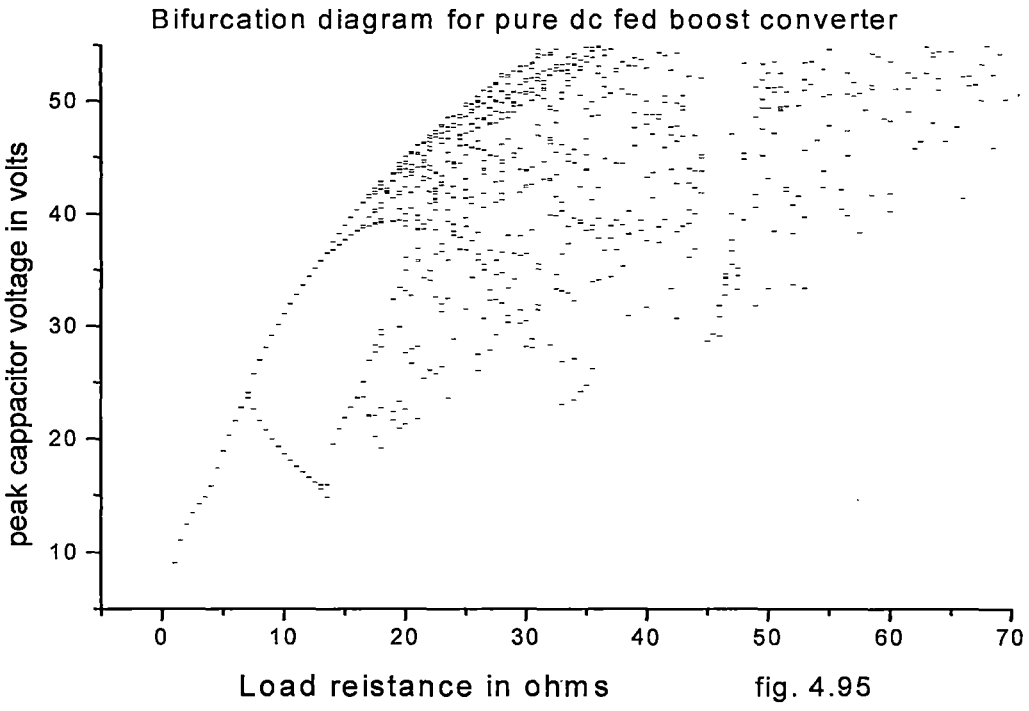

fig. 4.95

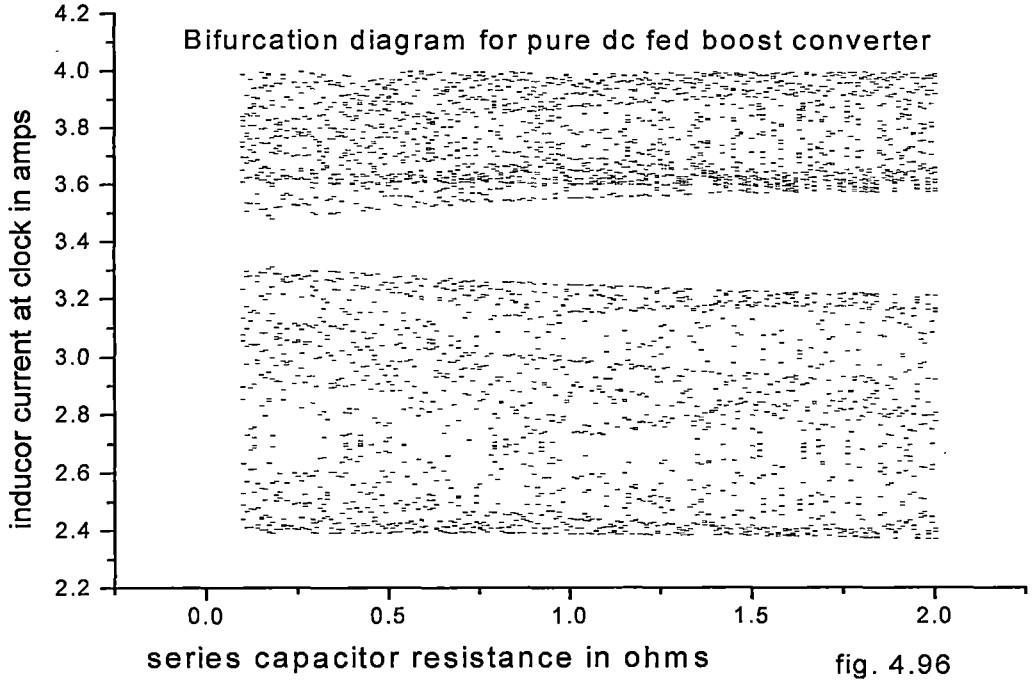

fig. 4.96

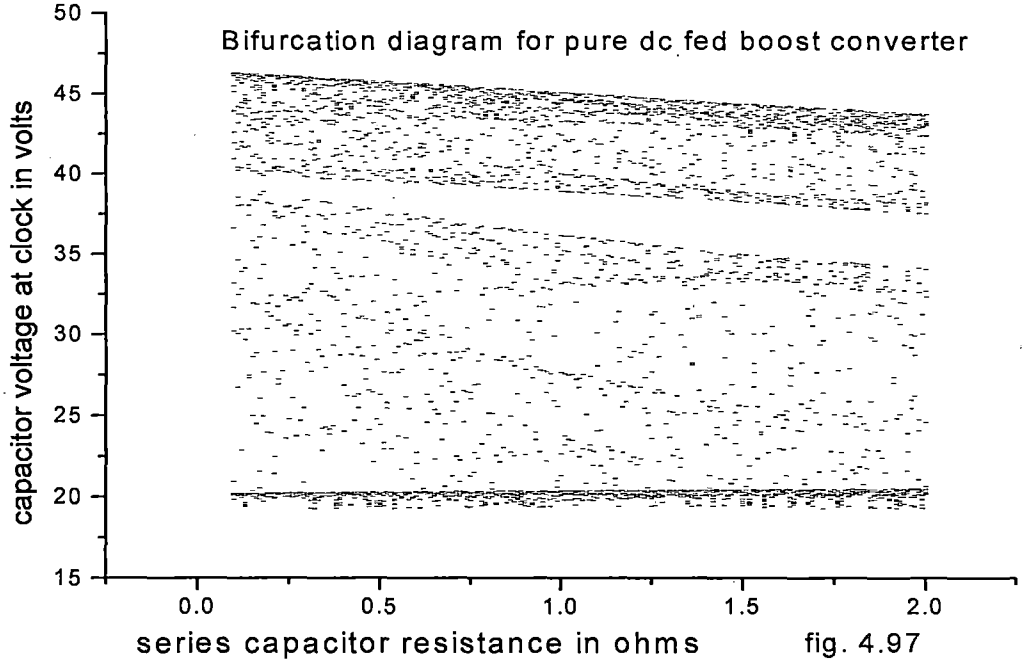

fig. 4.97

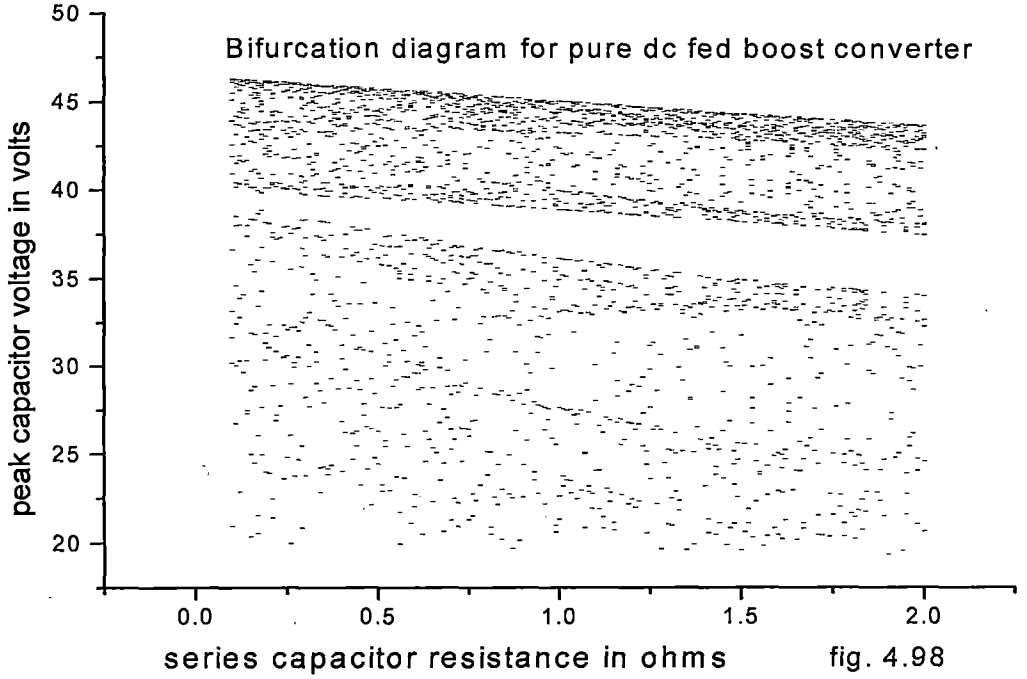

fig. 4.98

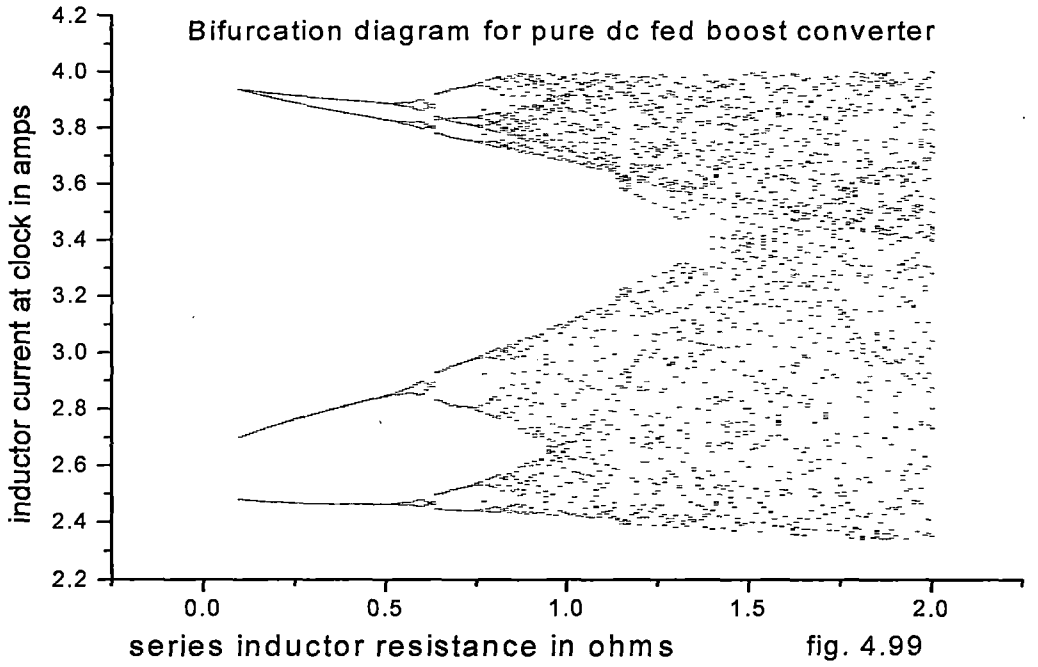

fig. 4.99

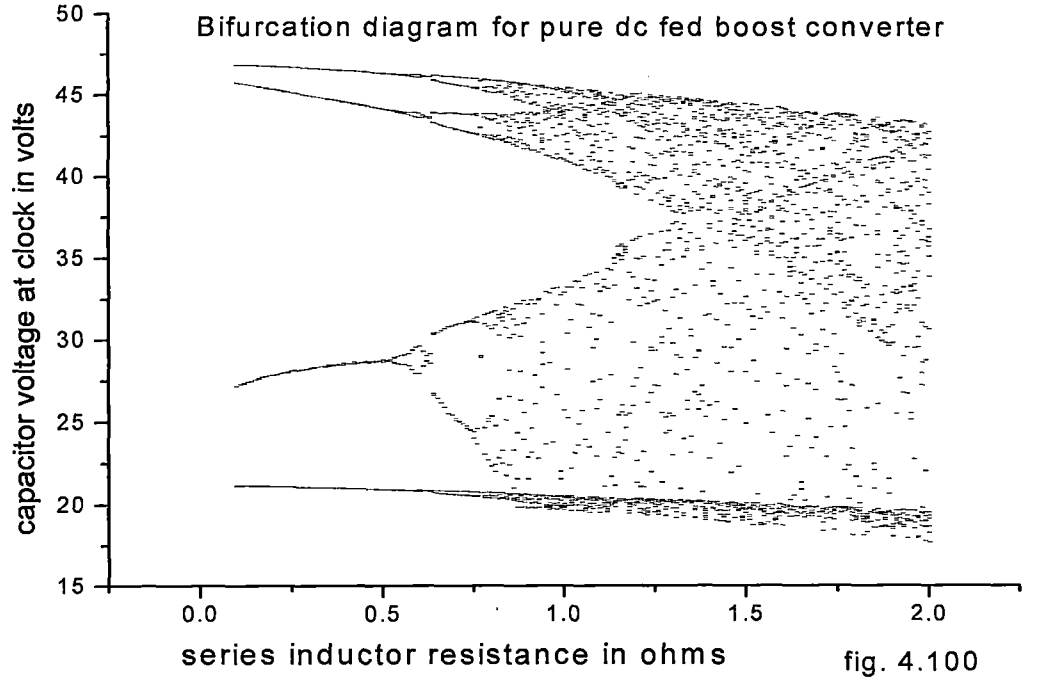

fig. 4.100

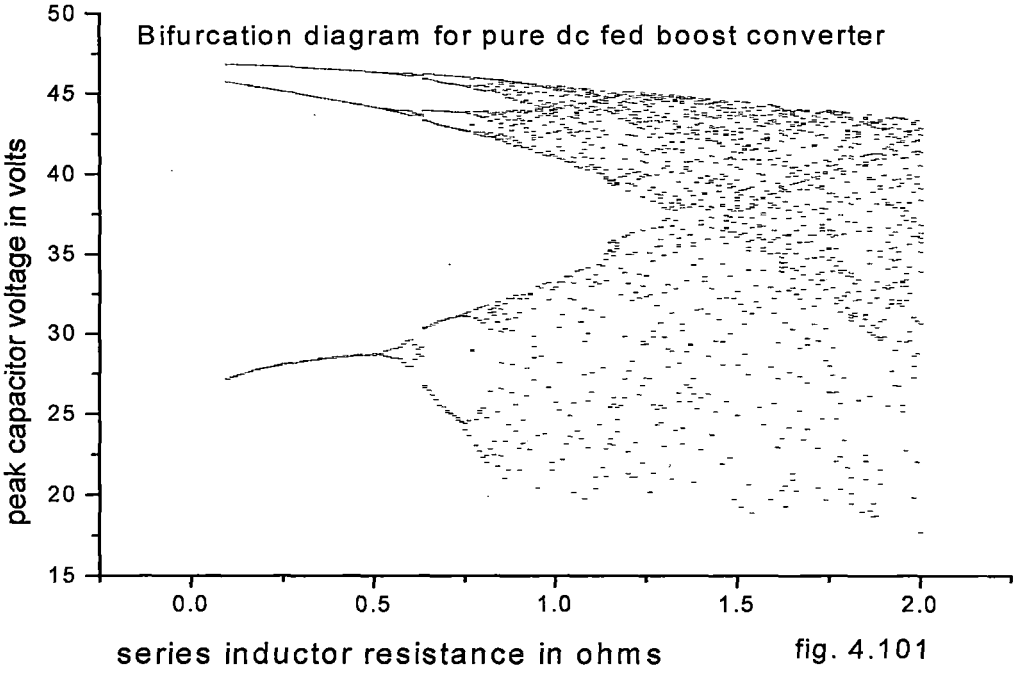

fig. 4.101

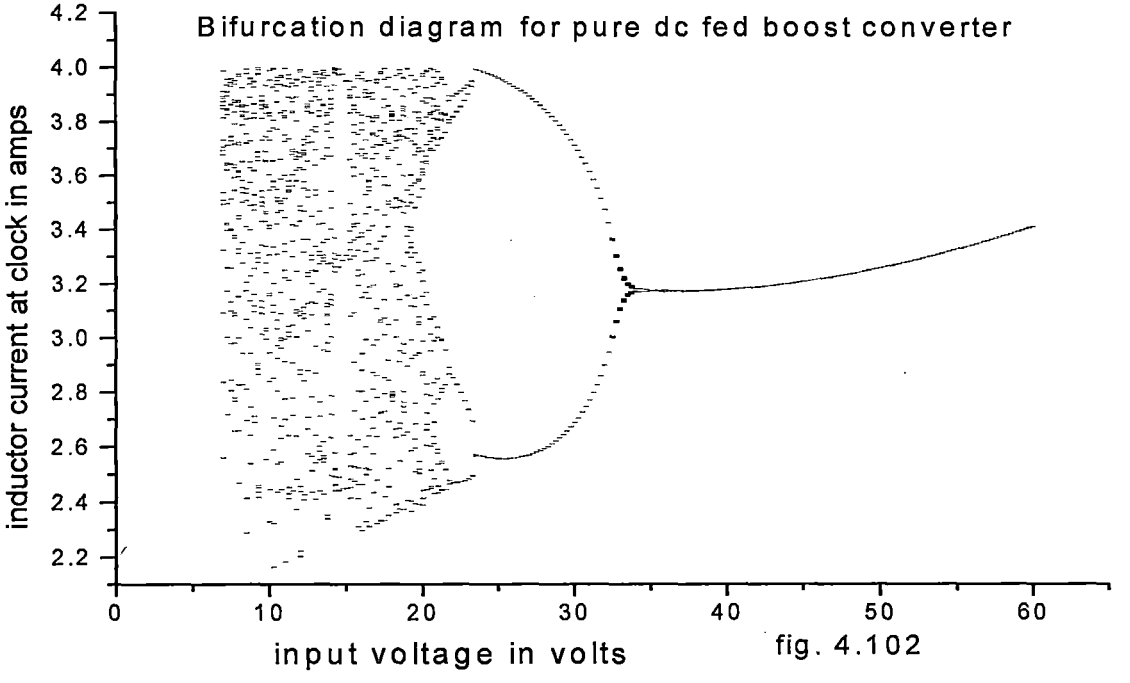

fig. 4.102

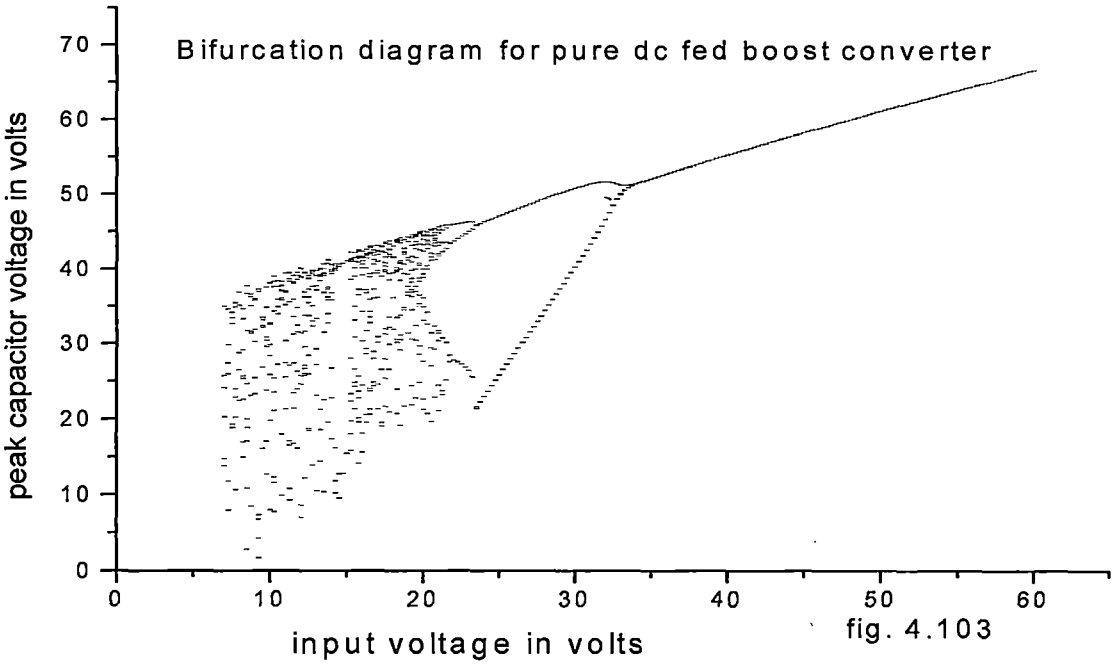

fig. 4.103

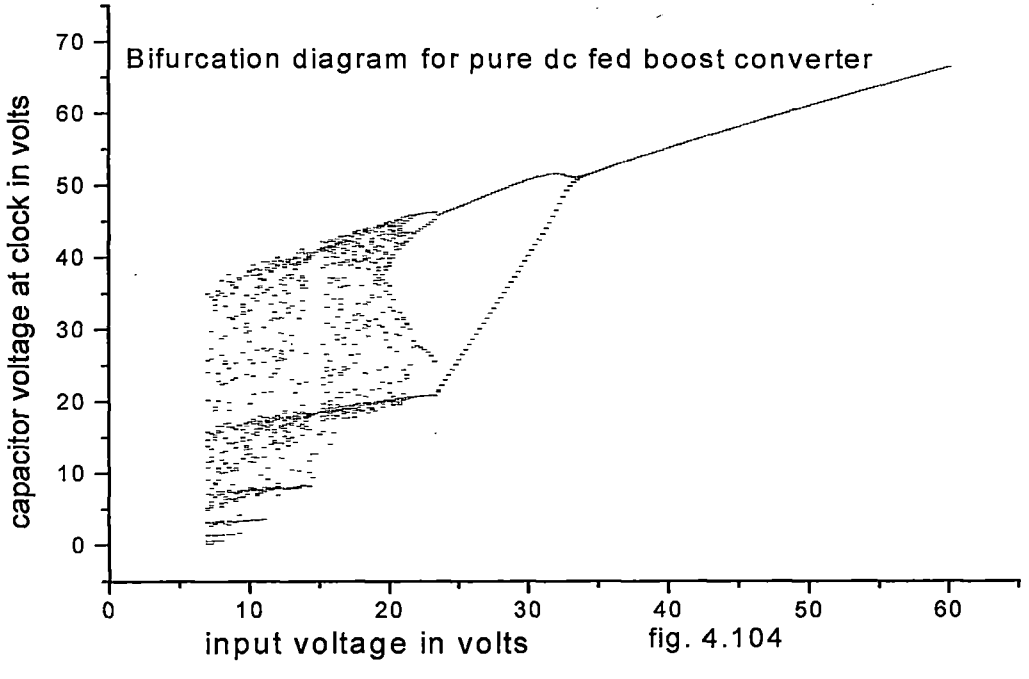

fig. 4.104

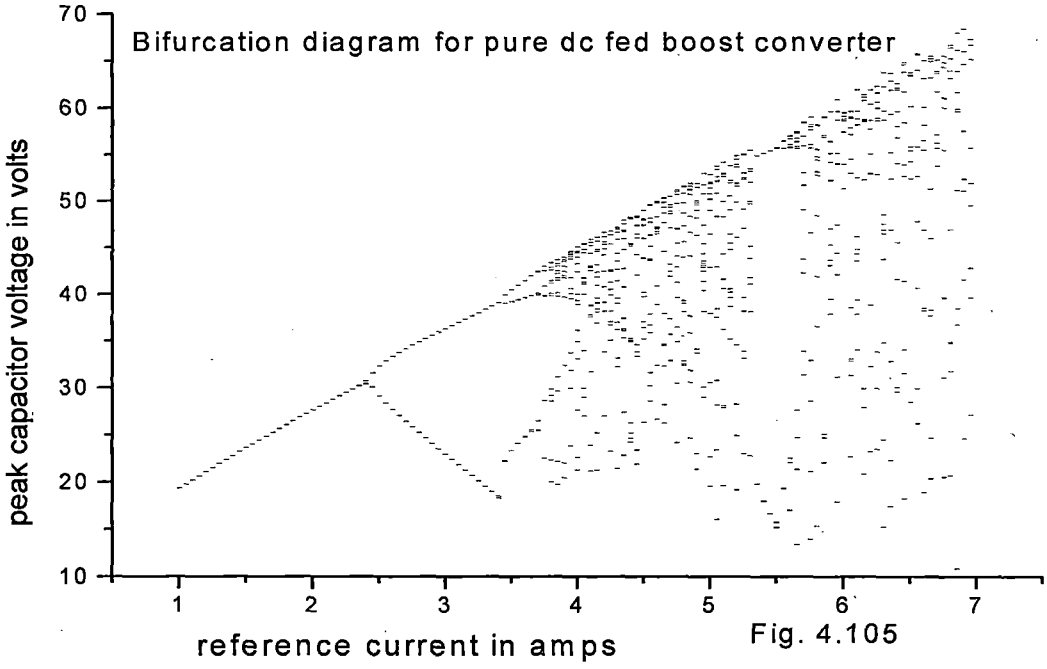

Fig. 4.105

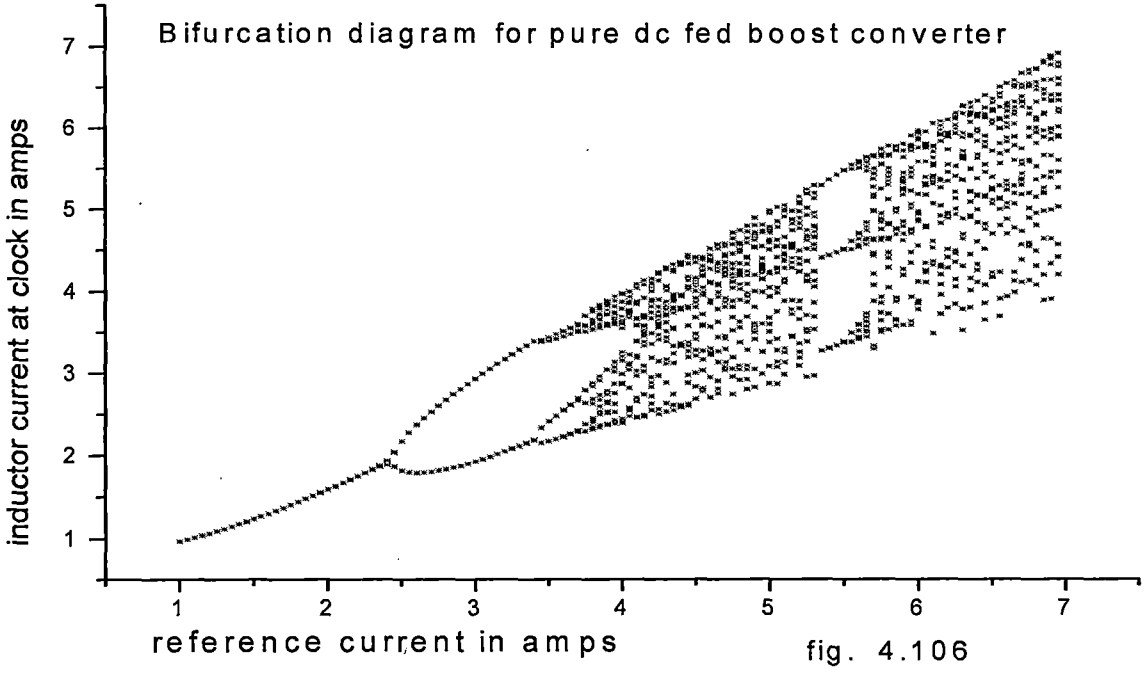

fig. 4.106

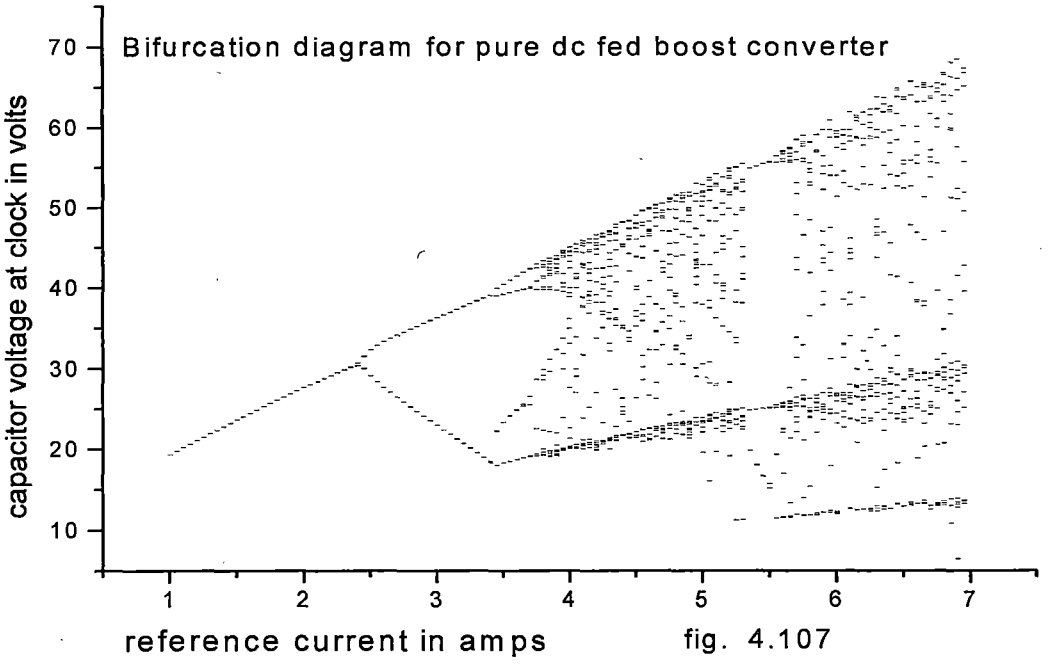
Bifurcation diagram for pure dc fed boost converter
capacitor voltage at clock in volts
70
60
50
40
30
20
10
1
2
3
4
5
6
7
reference current in amps

fig. 4.107

****

Chapter 5

BIFURCATIONS IN PRACTICAL ONE DIMENTIONAL BOOST CONVERTER

5.1 Introduction

It has been found that most feedback controlled switching circuits exhibit nonlinear phenomena and chaos over significant parts of the parameter space. It has also been revealed that in addition to saddle-node bifurcation and period-doubling cascade, the feedback controlled switching circuits exhibit many atypical bifurcation phenomena. Generally the nonlinear dynamics of physical systems are analyzed by obtaining discrete models popularly known as maps. Due to the existence of periodic clock pulses in the control logic, the Power electronic circuits like boost converters are suitable for such discrete domain modeling. We can observe the states in synchronism with the clock pulses and develop a function that maps the states from one clock instant to the next. A map is said to be smooth if it has a continuous derivative and monotonic if there is no change in the sign of the derivative. It has been found that the discrete domain modeling of most switching circuits i.e., maps are piecewise smooth and piecewise monotonic [1]. In the paper [14] the authors explored the dynamics of general piecewise smooth piecewise monotonic one dimensional (1-D) maps and apply the results in explaining the nonlinear phenomena in the boost converter without parasitic effect. The same type of analysis and application are presented in [2],[17] for two dimensional (2-D) maps. In this chapter, we explore the dynamics of piecewise smooth piecewise monotonic one dimensional (1-D) maps of Pure DC fed boost converter with parasitic effect and Rectified DC fed boost converter with parasitic effect.

5.2 Bifurcation in Piecewise smooth map:

a. The Piecewise Smooth Map

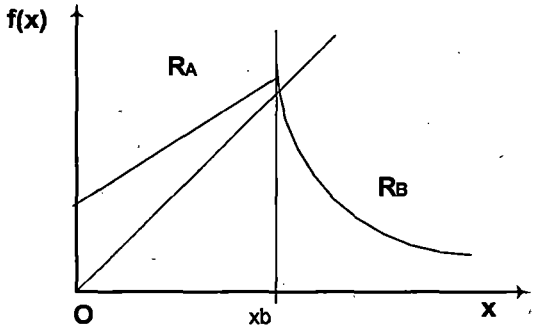

Fig. 5.1. 1-D piecewise smooth piecewise monotonic map f(x) with the border

A 1-D map f(x; μ) (fig.5.1) is considered which maps the real line R^1 to itself and depends smoothly on a parameter μ. A point x = $x_b(\mu)$ on the real line divides it into two areas R_A and R_B. The map f(x; μ) is piecewise smooth if 1) f(x; μ) is continuous in (x; μ) and 2) f(x; μ) is smooth in (x; μ) on each of the areas R_A and R_B but its derivative is discontinuous at x_b. The one-sided limits of the partial derivatives of f(x; μ) must exist at the border x_b. We require that $\frac{\delta f}{\delta x}$ can change sign only at the border x_b for piecewise monotonicity. Let the map be given by

$$f(x;\mu) = g(x;\mu), \text{ for } x \le X_b \text{ and } h(x;\mu), \text{ for } x \ge X_b \quad \ldots\ldots (5.1)$$

b. Bifurcations In The Smooth Regions

If a fixed point is in the regions either R_A or R_B, the bifurcations include the period doubling bifurcation and the saddle-node or tangent bifurcation. If $f(x;\mu_{1)=}x$ at $x_0 \neq x_b$ and $\frac{\partial}{\partial\mu} f(x;\mu) \neq 0$ and $\frac{\partial}{\partial x} f(x_0;\mu_1) = 1$ then there is a tangent bifurcation at $\mu = \mu_1$ In one side of

μ_1 there is no fixed point while in the other side of μ_1 there is one stable and one unstable fixed point. The fixed points originating in a tangent bifurcation can collide with the border with a further change of parameter. The results of such border collision bifurcation is outlined in the next sub-section. If $\frac{\partial}{\partial x} f(x_0;\mu_1) = -1$ then there is a period doubling bifurcation at $\mu = \mu_1$. In the case of piecewise monotonic maps, if a fixed point undergoes a period doubling bifurcation at μ_1 and the double-period orbit bifurcates at $\mu_2 \rangle \mu_1$ then the periodic orbit must collide with the border for some μ in $[\mu_1;\mu 2]$.

c. Border Collision Bifurcations

If the fixed point collides with the border and the parameters are changed , there is a discontinuous change in the derivative $\frac{\delta f}{\delta x}$ and the resulting phenomenon is called border collision bifurcation. Most of the bifurcations observed in power electronic circuits are of this type [1], [3],[98],[113],[114]. As the local structure of such bifurcations depends only on the local properties of the map in the neighborhood of the border, we study such bifurcations with the help of normal form: the piecewise affine approximation of f in the neighborhood of the border. The normal form is developed in the following way. We make a parameter-dependent change of coordinate by $\bar{x}$=x - x_b. The border is now given by $\bar{x} = 0$ and the map is given by $f(\bar{x} + x_b; \mu) = F(\bar{x}; \mu)$. The state space is now divided into two halves, L and R, where L = (-∞; 0] and R = [0; +∞). For simplicity, we write $F(\bar{x}; \mu)$ as F(x; μ). Suppose a fixed point of F(x; μ) is on the border when $\mu = \mu_0$, that is, F(0; μ_0) = 0. Without loss of generality, we define $\mu_0 = 0$. We expand F(x; μ) to the first order about x = μ = 0 and get

$$F(x;\mu) = ax + \mu v_A + o(x;\mu), \quad \text{for } x \le 0$$

$$F(x;\mu) = bx + \mu v_B + o(x;\mu), \quad \text{for } x \ge 0 \qquad \ldots\ldots\ldots (5.2)$$

where $$a = \lim_{x \to 0^-} \frac{\partial}{\partial x} F(x;0),$$

$$b = \lim_{x \to 0^+} \frac{\partial}{\partial x} F(x;0),$$

$$v_A = \lim_{x \to 0^-} \frac{\partial}{\partial \mu} F(x;0),$$

$$v_B = \lim_{x \to 0^+} \frac{\partial}{\partial \mu} F(x;0) \quad \ldots\ldots \qquad (5.3)$$

The continuity of the map F(x; μ) for all μ if $v_A = v_B$ and we assume this value is other than zero. v_A and v_B are eliminated from (5.2) by rescaling μ. For F(x; μ), we compute a and b, and obtain the 1-D normal form :

$$G_1(x;\mu) = ax + \mu, \quad \text{for} \quad x \le 0$$
$$= bx + \mu, \quad \text{for} \quad x \ge 0 \qquad \ldots\ldots..(5.4)$$

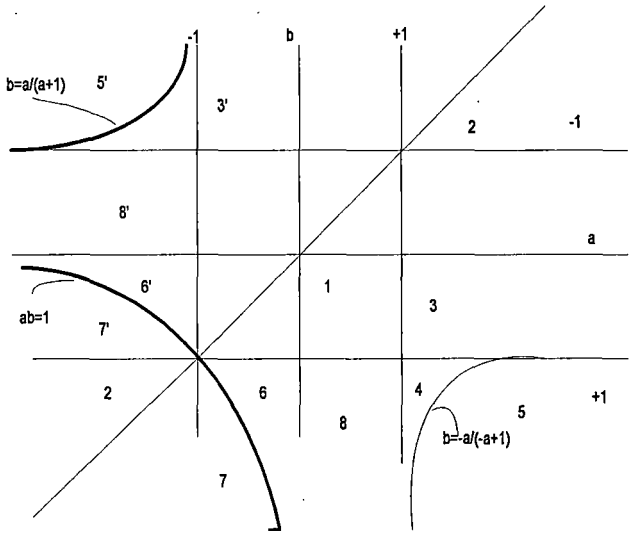

Fig. 5.2. Break up of the parameter space into regions with the same qualitative bifurcation phenomena. 1) Period-1 to Period-1; 2) No attractor to no attractor; 3) No fixed point to Period-1; 4) No fixed point to chaotic attractor; 5) No fixed point to unstable chaotic orbit (no attractor); 6) Period-1 to Period-2; 7) Period-1 to no attractor and 8) Period-1 to periodic or chaotic attractor. Primed numbers have the same bifurcation behavior as the unprimed ones when μ is varied in the reverse direction.

As μ is varied, the local bifurcation of the piecewise smooth map F(x; μ) is the same as that of the normal form G1. Various combinations of the values of a and b indicate different kinds of bifurcation behaviors as μ is varied. In Fig. 5.2, we break up the a-b parameter space into different regions with the same qualitative bifurcation phenomena.

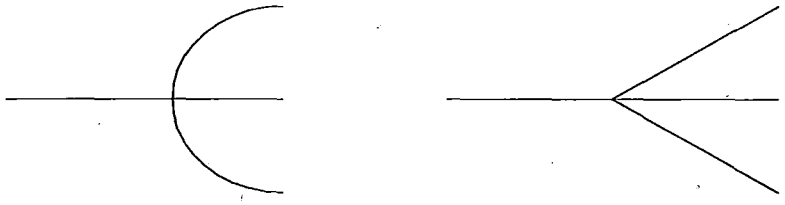

a. Standard period doubling of smooth map b. Border collision period doubling

Fig. 5.3. Bifurcation diagrams for a standard period doubling bifurcation of a smooth map and that of a border collision period doubling bifurcation of a piecewise smooth map. a. The Period-2 points diverge perpendicularly from the μ axis near the critical parameter value; b. in the second case, they may diverge at an angle that is less than 90 from the μ axis. The solid lines for attracting orbits and the dashed lines for unstable orbits.

For $\mu > 0$, all trajectories are bounded with existence of various periodic attractors and chaotic attractors. For $\mu > 0$ there can be a period adding cascade, with chaotic windows sandwiched between periodic windows, as the magnitudes of a,b are increased. It also be noted that for $\mu > 0$, the behavior is chaotic for the whole region of Case 4 and a significant portion of Case 8. The chaotic attractor of the 1-D normal form is robust in the contiguous region of the parameter space where no periodic windows exist[7]. Parameter regions are extensively studied in [4]-[6]. The current controlled boost converters are studied with respect to parameters. Regions in [8]-[10]

5.3 Boost converter with parasitic effect

a. Mathematical Modeling.

The practical boost converter (converter with parasitic effect) circuit is shown in Fig.5.4. Switching logic of the circuit is that when switch is closed the inductor current rises and

it continues till the inductor current reaches to Iref , ignoring any arriving clock pulse . As soon as the inductor current reaches to Iref , the switch is off and the inductor current falls. The switch closes again on the arrival of the next clock pulse. This is also explained by the fig.5.5.

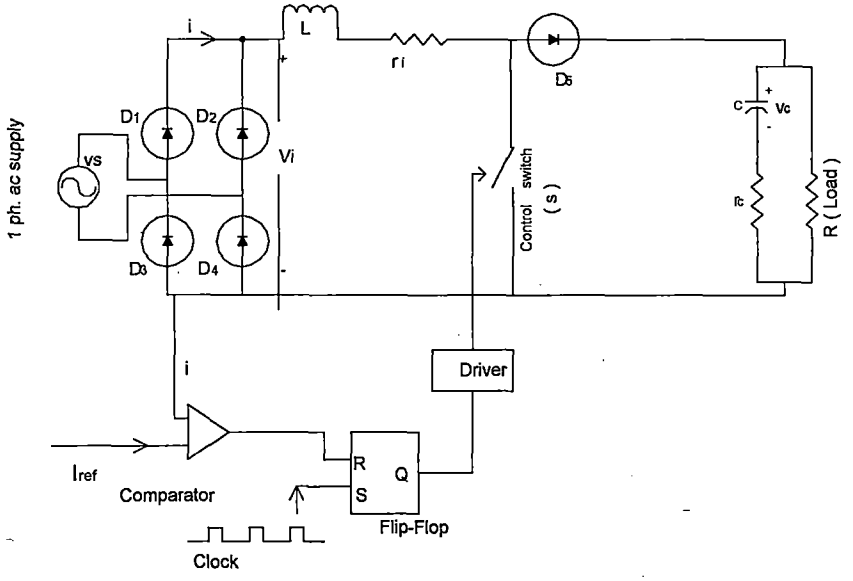

Fig. 5.4. The current mode controlled boost converter with parasitic effect and rectified DC input For pure DC input Vi is a pure DC voltage instead of a rectifier and ac input

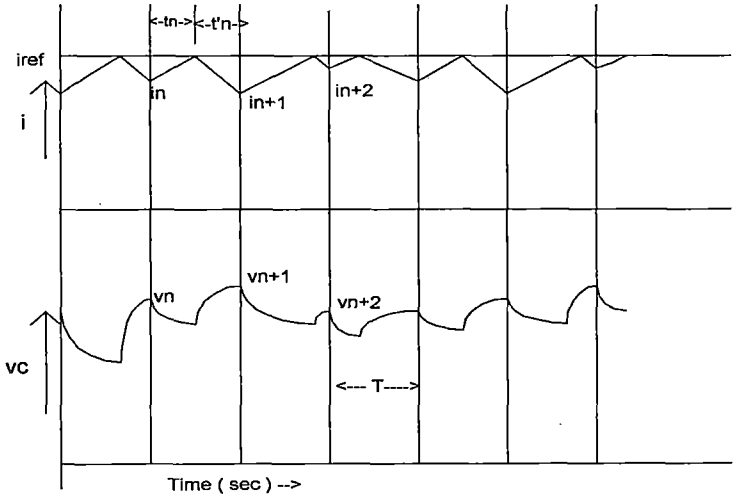

Fig. 5.5 Time plot of capacitor voltage and inductor current of the boost converter with clock pulses The circuit has two states depending on whether the control switch is opened or

closed. When switch is closed (on period) the state equations are

$$L\frac{di}{dt} = V_i - ir_i$$

$$C\frac{dv_c}{dt} = -\frac{v_c}{R + r_c} \qquad \ldots\ldots\ldots \quad (5.5)$$

and the states equations during off period (when switch is off) are

$$L\frac{di}{dt} = V_i - ir_i - i\frac{Rr_c}{R + r_c} - v_c\frac{R}{R + r_c}$$

$$C\frac{dv_c}{dt} = -\frac{v_c}{R + r_c} + i\frac{R}{R + r_c} \qquad \ldots\ldots\ldots \quad (5.6)$$

where Vi= constant for Pure DC and Vi = $|V_m Sin\omega t|$ for Rectified DC

We obtain the stroboscopic map under the following assumptions which have been adopted in a number of earlier studies [8], [9].

1) The capacitor connected in parallel with the load is large enough so that the fluctuation in the output voltage is insignificant.
2) The switching period (T) is short enough (i.e. T/RC << 1) for which he inductor current to be essentially linear during the on and off periods.

b. Bifurcations: In most practical converters the ripple amplitude is less than 1% of the output voltage and a high value of capacitance satisfies the second condition. This makes the above assumptions reasonable. Let m_1 and m_2 be the slopes of the inductor current waveform at a time during the on and off periods, respectively where L=inductance, Vo= output voltage & Vi= input voltage of the converter. The borderline between the two cases is given by the value of I_n for which the inductor current reaches I_{ref} exactly at the arrival of the next clock pulse. I_{n+1} is the next clock current value of I_n. The borderline in the state space is given by:

$$I_{border} = \left(\frac{V_i}{R}\right) + \left(I_{ref} - \left(\frac{V_i}{R}\right)\right) * e^{\frac{R}{L}T} \quad \ldots\ldots \quad (5.7)$$

The map is obtained from the equations (5.5), (5.6) and (5.7) as :

$$I_{n+1} = \left(\frac{V_i}{R}\right) + \left(I_n - \left(\frac{V_i}{R}\right)\right) * e^{-\frac{R}{L}T} \quad \text{if} \quad I_n \le I_{border} \quad \ldots\ldots \quad (5.8)$$

$$I_{n+1} = -\left(\frac{Vo}{R}\right)\left(1 - (V_i - I_n R)/(V_i - I_{ref} R)\right)e^{-\frac{R}{L}T} + \left(\frac{Vi}{R}\right) + \left(I_n - \left(\frac{V_i}{R}\right)\right)e^{-\frac{R}{L}T} \quad \text{if} \quad I_n \rangle I_{border}$$

$\ldots\ldots$ (5.9)

if $I_n > I_{border}$. The portion R_A (i.e., $i_n < I_{border}$) has slope unity, the break-point is located at (I_{border}, I_{ref}),and the portion R_B ($i_n > I_{border}$) has a slope $-m_2 / m_1$. The numerically obtained bifurcation diagram is shown in Fig. 5.6, 5.7 and 5. 8. The numerically obtained bifurcation diagram is found in [12] for pure DC fed current controlled boost converter. The parameter values are: Vi = 30 V, L = 0.1 H, T = 400 μs, Vo is varied and I_{ref} = 0.5 A. Among the diagram the fig. 5.6 already developed in [14]. fig. (5.7) is developed using the same method as in[12] with the parasitic effect To obtain fig. 5.8 input Vi is taken as rectified single phase voltage. We study the bifurcation in the system as a function of the parameter α = m2/m1. We find that there is a stable Period-1 orbit so long as α < 1. This condition of stability of the Period-1 solution (duty ratio <0:5) is well known in the theory of dc–dc converters. However, as α increases through unity, there is a period doubling bifurcation. Since R_B is linear, none of the points on R_B or their higher iterates can be stable. Therefore the fixed point moves discontinuously to the border. As the slope of R_A is unity, the resulting border collision bifurcation falls on the borderline between Cases 8 and 4. Notice that the behavior for both the regions of the parameter space is chaotic for μ > 0. Thus, there is a chaotic attractor after the border collision bifurcation. As expected, there is no periodic window for further change in the parameter. The chaotic orbit is robust. This is important from a practical point of view. It has been proposed to use chaos productively in spreading the spectrum of dc–dc converters [9], [13].

In such applications it would be necessary to ensure that the system does not come out of chaos into a periodic window due to small inadvertent change of parameters. The above observation gives a clue to designing converters with no periodic windows within the chaotic range of operation.

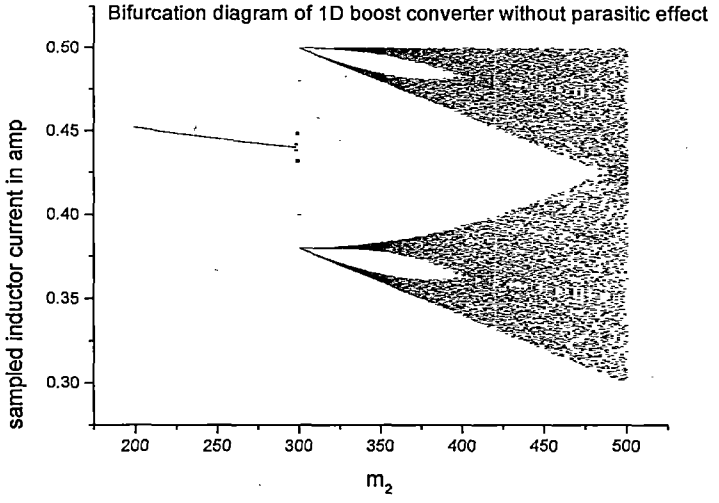

Fig.5.6. The bifurcation diagram of the current mode controlled pure DC fed boost converter without parasitic effect.

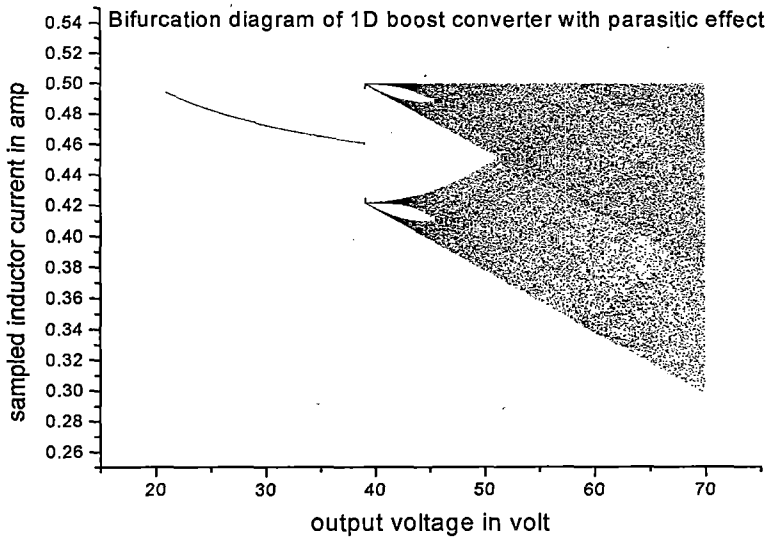

Fig.5.7. The bifurcation diagram of the current mode controlled pure DC fed boost converter with parasitic effect.

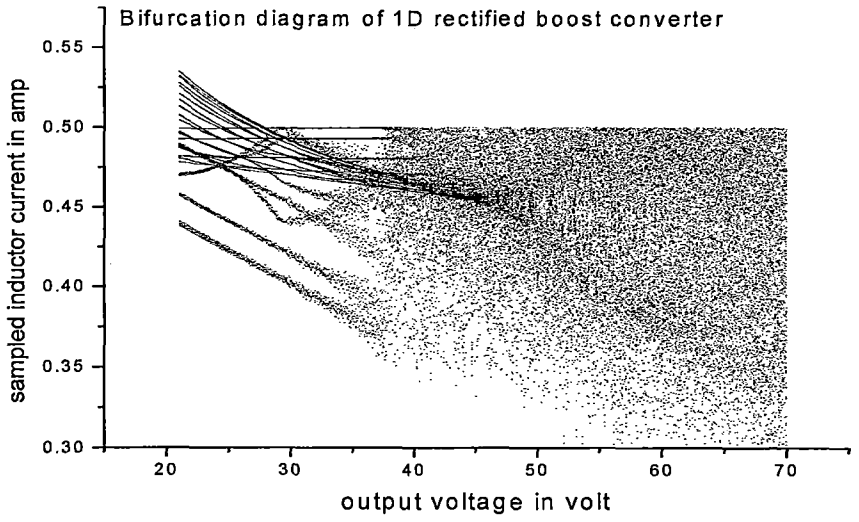

Fig.5.8. The bifurcation diagram of the current mode controlled rectified fed boost converter with parasitic effect.

5.4. Conclusions:

In this chapter we have applied the theory of bifurcations in 1-D piecewise smooth piecewise monotonic maps. We have shown that however complicated the map of a real system may be, the border collision bifurcations can be understood only in terms of its piecewise affine approximation at the border. We have developed the 1-D modeling of the boost converter with parasitic effect for two types of source voltage one for pure DC & another for Rectified DC. We presented the different Bifurcations diagram for the developed 1-D modeling which are useful in analyzing, identifying and describing the nonlinear phenomena in such circuits.

****

Chapter 6

BORDER COLLISION BIFURCATIONS IN ONE DIMENSIONAL DISCONTINUOUS MAPS OF PRACTICAL BOOST CONVERTER

6.1 Introduction

It has been found that most feedback controlled switching circuits exhibit nonlinear phenomena and chaos over significant parts of the parameter space. It has also been revealed that in addition to saddle-node bifurcation and period-doubling cascade, the feedback controlled switching circuits exhibit many atypical bifurcation phenomena. Generally the nonlinear dynamics of physical systems are analyzed by obtaining discrete models popularly known as maps. Due to the existence of periodic clock pulses in the control logic, the Power electronic circuits like boost converters are suitable for such discrete domain modeling. We can observe the states in synchronism with the clock pulses and develop a function that maps the states from one clock instant to the next. A map is said to be smooth if it has a continuous derivative and monotonic if there is no change in the sign of the derivative. It has been found that the discrete domain modeling of most switching circuits i.e., maps are piecewise smooth and piecewise monotonic [1]. In the paper[2], [14],[113],[114] the authors explored the dynamics of general piecewise smooth piecewise monotonic one dimensional (1-D) maps and apply the results in explaining the nonlinear phenomena in the boost converter without parasitic effect. In the paper [124] the authors explored the dynamics of general piecewise smooth piecewise monotonic one dimensional (1-D) discontinuous maps and apply the results in explaining the nonlinear phenomena in the boost converter without parasitic effect. Here we explore the dynamics of piecewise smooth piecewise monotonic one dimensional (1-D) discontinuous maps of Pure DC fed boost converter with parasitic effect and Rectified DC fed boost converter with parasitic effect.

The theory of border-collision bifurcations is developed for piecewise smooth maps in recent years by di Bernardo [2], Soumitra Banerjee [76] and others . They developed the form of the one dimensional maps is given below

$$f(x,y,\rho) = f_1(x,y\rho) \quad \text{for} \quad (x,y) \in R_1$$

$$f(x,y,\rho) = f_2(x,y\rho) \quad \text{for} \quad (x,y) \in R_2$$

$$f(x,y,\rho) = \text{----------} \qquad \text{----------(6.1)}$$

$$f(x,y,\rho) = \text{----------}$$

$$f(x,y,\rho) = f_n(x,y\rho) \quad \text{for} \quad (x,y) \in R_n$$

where R_1, R_2 are regions of the phase space with dividing borderlines and ρ is a parameter. It is assumed that the map is continuous but with a discontinuity across the borderlines. Investigation in this regard are reported in[3],[15],[46],[47],[72]-[75], [77]-[80]. A large class of practical systems in electrical engineering are modeled as piecewise smooth maps and border-collision bifurcations are common in them. A line of development shows that there are important classes of switching systems like thyristor circuits which yields discontinuous maps under discrete time modeling and nonstandard bifurcation phenomena can be there in such systems. The theory for understanding such bifurcation phenomena is developed by Parag Jain And Soumitra Banerjee [76]. In that paper they classified the border collision bifurcations that occur in one dimensional maps with discontinuity at the border. They also illustrated the application of the theory in practical example of a power electronic switching circuit with a delay in feedback loop(without parasitic effect).

6.2 The One-Dimensional Discontinuous Map

An 1-D map $f(x;\mu)$ that maps the real line R^1 to itself and depends on the parameter μ [122] . A point $x = x_b(\mu)$ divides on the real line it into two regions (fig. 6.1) R_A and R_B . The map $f(x;\mu)$ is piecewise continuous in the sense that it is continuous in (x ; μ) both the regions R_A and R_B , but is discontinuous at x_b . The one-sided limits of the partial derivatives of $f(x;\mu)$ exist at the border x_b. With all generality maps are considered whose partial

derivatives and the length of the discontinuity at the border are independent of the parameter μ. As we are concerned in the bifurcations that occur when a fixed point crosses the point of discontinuity x_b, we study these through the piecewise linear approximation in the neighborhood of the border:

$$x_{n+1} = ax_n + \mu \quad \text{for } x_n \langle 0$$

$$x_{n+1} = bx_n + \mu + l \quad \text{for } x_n \rangle 0 \quad \ldots\ldots \quad (6.2)$$

and the state space is divided into two halves L (left) and R (right) and l is the length of the discontinuity. A movement of the break-point is introduced towards the origin by transformation of coordinates. The fixed point in L is located at $x_L^* = \frac{\mu}{1-a}$ and that in R is located at $x_R^* = \frac{\mu + l}{1-b}$. The map intersects the 45^0 line for $\mu < 0$ and $\mu > -l$. It indicates that the fixed points collides with the border at $\mu = 0$ and $\mu = -l$. So two border collision events are expected as the parameter μ is varied.

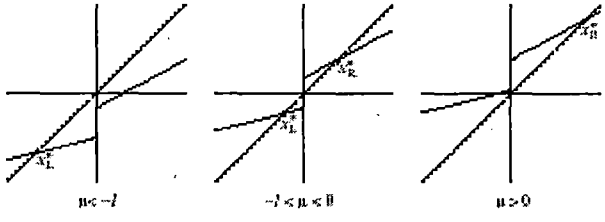

Fig. 6.1 Graphs of the map for $0\langle a\langle 1$, $0\langle b\langle 1$ and $l\rangle 0$

Different classification are made on the basis of different ranges of a and b.

Case 1: $0\langle a\langle 1$ and $0\langle b\langle 1$

Case 2: $0\langle a\langle 1$ and $b\rangle 1$

Case 3: $0\langle a\langle 1$ and $-1\langle b\langle 0$

Case 4: $0\langle a\langle 1$ and $b\langle -1$

Case 5: $a\rangle 1$ and $b\rangle 1$

Case 6: $a\rangle 1$ and $-1\langle b\langle 0$

Case 7: $a\rangle 1$ and $b\langle -1$

Case 8: $-1\langle a\langle 0$ and $-1\langle b\langle 0$

Case 9: $-1\langle a\langle 0$ and $b\langle -1$

Case 9: $a\langle -1$ and $b\langle -1$

Different types of Bifurcation diagrams are obtained for different cases of classification

6.3 Boost Converter with Parasitic Effect :

a. Mathematical Modeling.

The practical boost converter (converter with parasitic effect) circuit is shown in Fig.6.2. Switching logic of the circuit is that when switch is closed the inductor current rises and it continues till the inductor current reaches to Iref , ignoring any arriving clock pulse . As soon as the inductor current reaches to Iref , the switch is off and the inductor current falls. The switch closes again on the arrival of the next clock pulse, which is explained by the fig.5.5. A delay of δT is introduced in control logic to realize the industrial trend of higher and higher frequency as generated propagation delay in control circuit is significant for higher frequency. The circuit has two states depending on whether the control switch is opened or closed. When switch is closed (on period) the state equations are

$$L\frac{di}{dt} = V_i - ir_i$$

$$C\frac{dv_c}{dt} = -\frac{v_c}{R + r_c} \qquad \ldots\ldots\ldots \quad (6.3)$$

and the states equations during off period (when switch is off) are

$$L\frac{di}{dt} = V_i - ir_i - i\frac{Rr_c}{R + r_c} - v_c\frac{R}{R + r_c}$$

$$C\frac{dv_c}{dt} = -\frac{v_c}{R + r_c} + \mathrm{i}\frac{R}{R + r_c} \qquad \ldots\ldots\ldots \quad (6.4)$$

where Vi= constant for Pure DC and Vi = $|V_m Sin\omega t|$ for Rectified DC

We obtain the stroboscopic map under the following assumptions which have been adopted in a number of earlier studies [8], [9].

- The capacitor connected in parallel with the load is large enough so that the fluctuation in the output voltage is insignificant.
- The switching period (T) is short enough (i.e. T/RC << 1) for which the inductor current to be essentially linear during the on and off periods.

b. **Bifurcations:** In most practical converters the ripple amplitude is less than 1% of the output voltage and a high value of capacitance satisfies the second condition. This makes the above assumptions reasonable. If clock pulse period (T) is much smaller than the RC time constant the output voltage (Vo) is significantly constant. The slopes of the inductor current during on period and off period are Vi/L=m_1 and (Vo-Vi)/L=m_2 respectively where L=inductance, Vo= output voltage & Vi= input voltage of the converter. Vi= constant for Pure DC and Vi = $|V_m Sin\omega t|$ for Rectified DC . The borderline between the two cases is given by the value of I_n for which the inductor current reaches I_{ref} exactly at the arrival of the next clock pulse, i_{n+1} is the next clock current value of i_n.

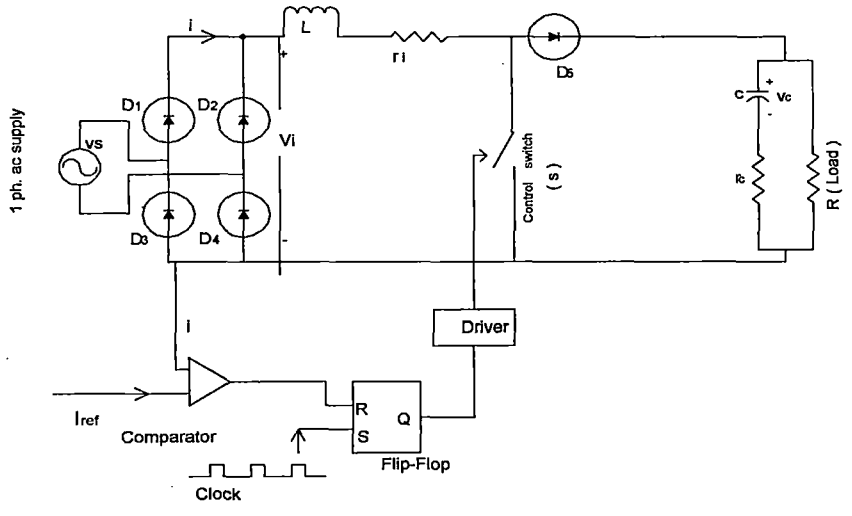

Fig. 6.2. The current mode controlled boost converter with parasitic effect and rectified DC input. For pure DC input Vi is a pure DC voltage instead of a rectifier and ac input.

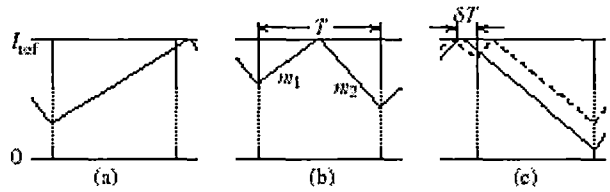

Fig. 6.3 Time plot of inductor current of the boost converter between two consecutive clock pulses the switch remains on (b) the switch remains both on and off (c) firm line indicates clock comes before δT delay of switch off and dashed line indicates clock comes after δT delay of switch off

Due to the delay of δT in the control logic, the inductor current has two borderlines I_{b1} and I_{b2} in the state space as follows:

$$I_{b1} = (V_i / R) + (I_{ref} - (V_i / R)) * e^{(R*T/L)} \quad \text{.....(6.5)}$$

$$I_{b2} = ((V_0 - V_i) / R) + (I_{ref} - ((V_0 - V_i) / R)) * e^{(R*\delta T/L)} \quad \text{.....(6.6)}$$

The map is obtained from the equations (6.3), (6.4), (6.5) and (6.6) as :

$$I_{n+1} = (V_i / R) - (I_n - (V_i / R)) * e^{(-R*T/L)} \quad \text{for } I_n \le I_{b1}$$

$$I_{n+1} = -(V_o / R) * (1 - (V_i - I_n * R)/(V_i - I_{ref} * R) * e^{(-R*T/L)}) + (V_i / R) + (I_n - (V_i / R)) * e^{(-R*T/L)}$$

$$\text{for } I_{b1} \le I_n < I_{b2}$$

$$I_{n+1} = ((V_0 - V_i) / R) - (I_n + ((V_0 - V_i) / R)) * e^{(R*T/L)} \quad \text{for } I_n > I_{b2} \quad \text{.....(6.5)}$$

where Vi= constant for Pure DC and Vi = $|V_m Sin\omega t|$ for Rectified DC

Here the map is continuous across the border I_{b1} but is discontinuous across the border I_{b2}

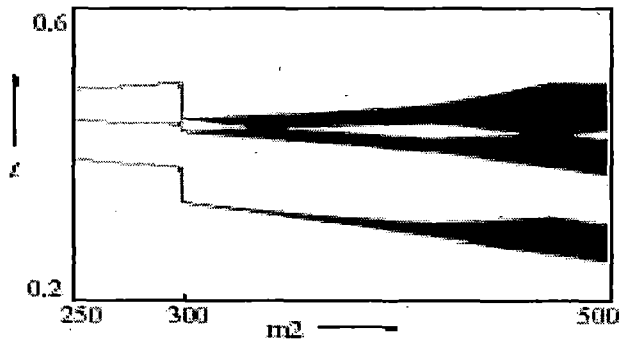

Fig. 6.4 Bifurcation diagram for the boost converter with delay in control loop for pure DC input

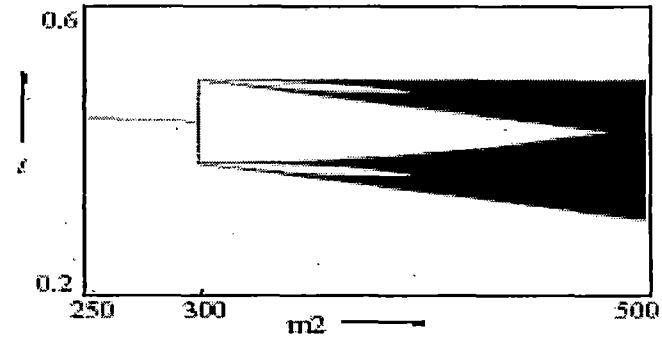

Fig. 6.5 Bifurcation diagram for the boost converter without delay in control loop for pure Dc input

The numerically obtained bifurcation diagram is shown in fig. (6.4) – (6.9). The parameter values are: Vi= 30 V, L = 0.1 H, T = 400 μ s, Vo is varied and I_{ref} = 0.5 A. Among the diagram fig. 6.4 and 6.5 are already developed in [14]. Fig. (6.6) - (6.9) are is developed using the same method as in [14] with the parasitic effect. To obtain fig. 6.6 and 6.8 input Vi is taken as pure dc voltage and fig. 6.7 and 6.9 input Vi is taken as rectified single phase voltage. We study the bifurcation in the system as a function of the parameter α = m2/m1. We find that there is a stable Period-1 orbit so long as $\alpha < 1$. This condition of stability of the Period-1 solution (duty ratio <0:5) is well known in the theory of dc–dc converters. However, as α increases through unity, there is a period doubling bifurcation. Since R_B is linear, none of the points on R_B or their higher iterates can be stable. Therefore the

fixed point moves discontinuously to the border. As the slope of R_A is unity, the resulting border collision bifurcation falls on the borderline between Cases 8 and 4. Notice that the behavior for both the regions of the parameter space is chaotic for $\mu > 0$. Thus, there is a chaotic attractor after the border collision bifurcation. As expected, there is no periodic window for further change in the parameter.The chaotic orbit is robust. This is important from a practical point of view. It has been proposed to use chaos productively in spreading the spectrum of dc–dc converters [9], [13]. In such applications it would be necessary to ensure that the system does not come out of chaos into a periodic window due to small inadvertent change of parameters. The above observation gives a clue to designing converters with no periodic windows within the chaotic range of operation.

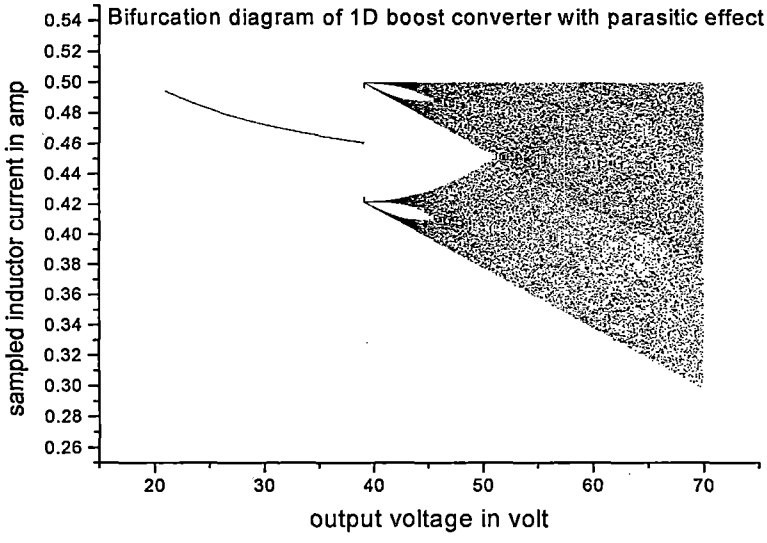

Fig.6.6. The bifurcation diagram of the current mode controlled pure DC fed boost converter with parasitic effect and without delay.

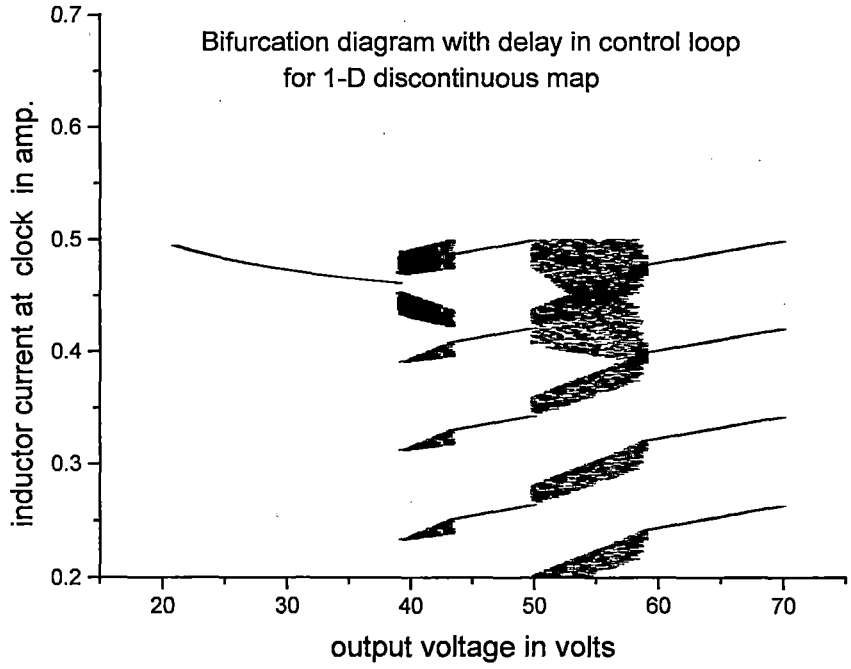

Fig.6.7. The bifurcation diagram of the current mode controlled pure DC fed boost converter with parasitic effect and with delay.

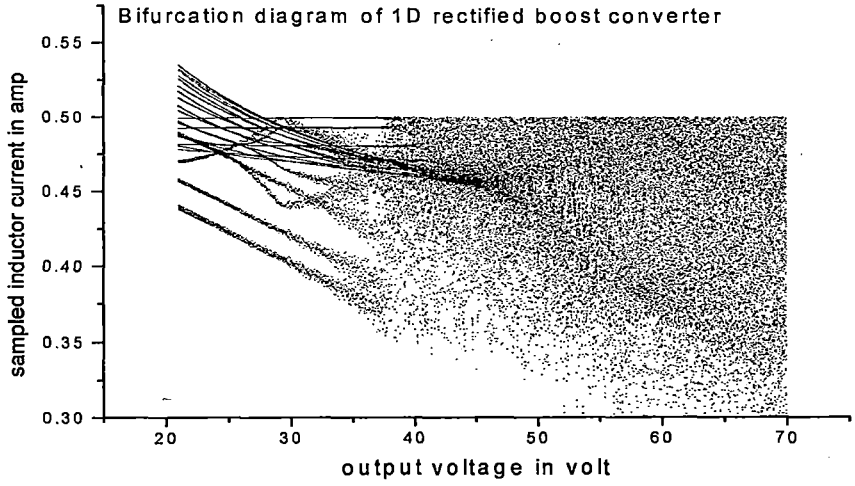

Fig.6.8. The bifurcation diagram of the current mode controlled Single phase rectified DC fed boost converter with parasitic effect and without delay.

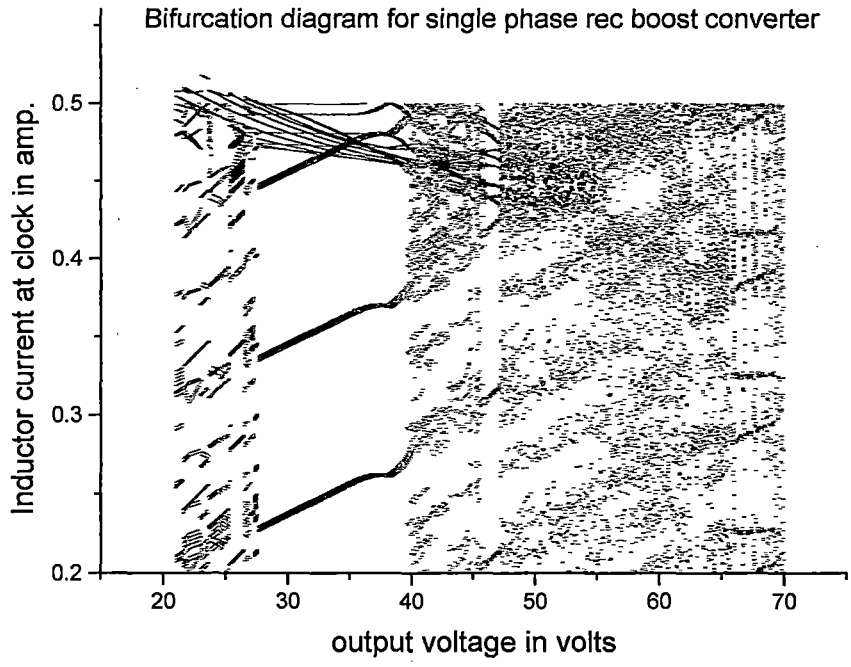

Fig.6.9. The bifurcation diagram of the current mode controlled
Single phase rectified DC fed boost converter with parasitic effect and with delay.

6.4. Conclusions:

Here we have applied the theory of bifurcations in 1-D discontinuous piecewise smooth piecewise monotonic maps. We have shown that however complicated the map of a real system may be, the border collision bifurcations can be understood only in terms of its piecewise affine approximation at the borders. We have developed the 1-D discontinuous modeling of the boost converter with parasitic effect for two types of source voltage one for pure DC & another for Rectified DC. We presented the different Bifurcations diagram for the developed 1-D discontinuous modeling which are useful in analyzing, identifying and describing the nonlinear phenomena in such circuits.

****

Chapter 7

BIFURCATION CONTROL IN PRACTICAL BOOST CONVERTER

7.1. Introduction

Bifurcation control deals with the design of a controller to alter the bifurcation properties of a nonlinear system for getting some desirable dynamical behaviors, specially sudden loss of stability i.e. sudden change in operating behaviors[38],[82],[123]. Sudden loss of stability or sudden change in operating behaviors is a common problem in current controlled dc-dc boost converter which results undesired subharmonic operation due to chosen improper parameters. All the subharmonic, quasi periodic and chaotic operations are considered as undesirable and should be avoided in this converter as it is harmful and unwanted in the converter. Effective design avoids the occurance of bifurcations in operating range with the variation of parameters. As the current controlled dc-dc boost converter bifurcates due to the parameter change, so the design should consider " Control of Bifurcation" and for that the bifucation analysis is required for proper design to stabilize it. Typical bifurcation control refers delaying the onset of an inherent bifurcation, introducing a new bifurcation at a desired parameter value , changing the parameter value of an existing bifurcation point , modifying the shape or type of a bifurcation chain , stabilizing a bifurcated solution or branch, monitoring the multiplicity, amplitude and/or frequency of some limit cycles emerging from bifurcation, optimizing the system performance near a bifurcation point or a combination of some of these objectives . Bifurcation control has been implemented successfully in experimental systems or tested by using numerical simulations. Bifurcation control suggests a viable and effective tools for chaos control as bifurcation and chaos are twins and in period-doubling bifurcation is a typical route to chaos in many nonlinear dynamical systems. Bifurcation properties of a system can be modified through various feedback control methods.

Once Bifurcation or chaos (as they are twins)is under control, it motivates the designer with a variety of properties, richness of flexibility and a cornucopia of new opportunities in various engineering applications as it has been felt that traditional engineering design suppresses irregular dynamical behaviors of a system by eliminating bifurcation, chaos and other complex behaviors.

7.2. **Various Bifurcation Control Methods:**

There are some bifurcation control approaches , which are implemented successfully in experimental systems or tested by using numerical simulations.

- Bifurcation control via state feedback and washout filter-aided dynamic
- feedback controllers
- Bifurcation control via normal forms and invariants
- Bifurcation control via harmonic balance approximations by
- Ramp compensation technique
- Variable ramp compensation technique

Among the above mentioned approaches ramp compensation technique is the most effective tool for bifurcation control for a pure dc fed current controlled dc-dc boost converter as it maintain fast response and sufficient clearance of bifurcation. But for rectified dc fed current controlled dc-dc boost converter it is variable ramp compensation technique. " Adaptive avoidance bifurcation" is realized by a variable ramp compensation technique.

7.3. **Bifurcation control in current controlled dc-dc boost converter.**

For the pure dc fed current controlled dc-dc boost converter (fig. 7.1) the control logic or switching logic of the circuit is that when switch is closed the inductor current rises and it continues till the inductor current reaches to Iref, ignoring any arriving clock pulse. As soon as the inductor current reaches to Iref , the inductor current falls. The switch closes again on the arrival of the next clock pulse. With the ramp compensation technique (fig. 7.3), the reference current is modified by subtracting a ramp voltage of slope -Mc as indicated in the fig. 7.3. The slope –Mc is varied to control the bifurcation characteristics.

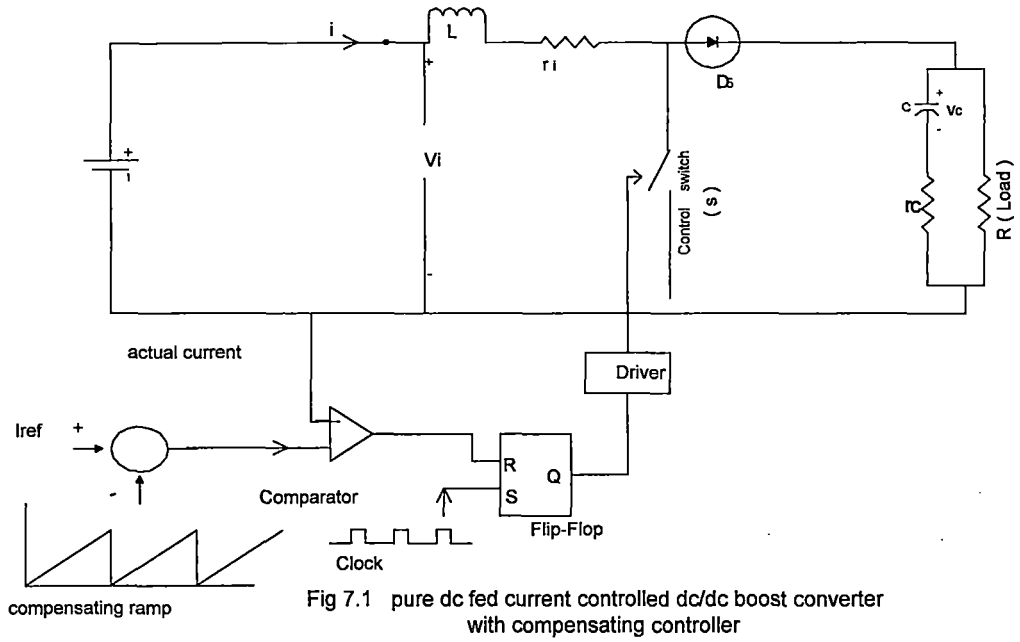

Fig 7.1 pure dc fed current controlled dc/dc boost converter with compensating controller

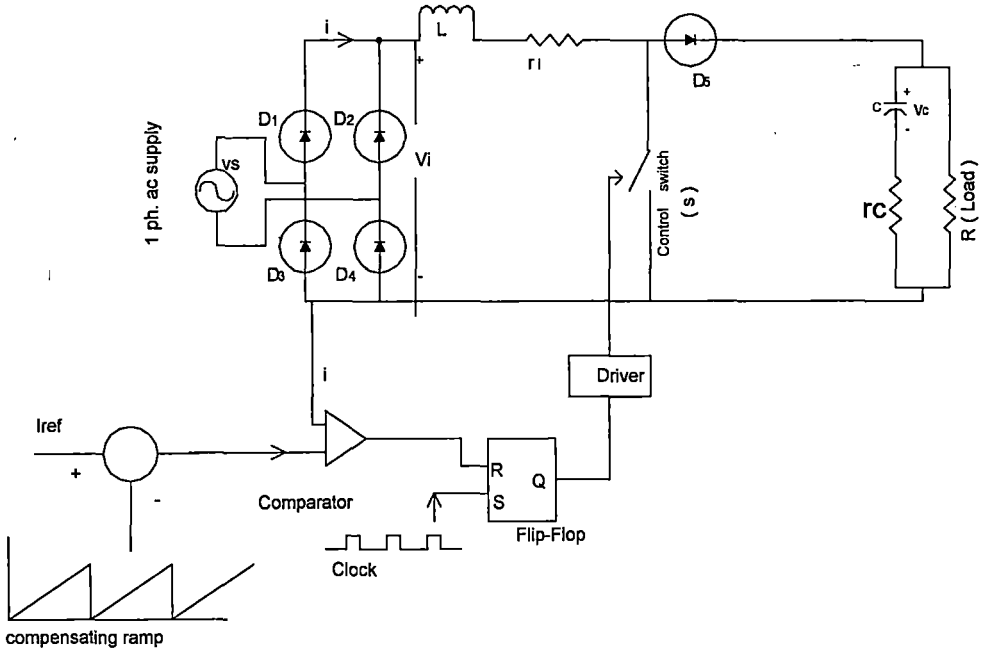

Fig. 7.2 Single phase rectified dc fed current controlled dc/dc boost converter with compensating controller

For the fullwave rectified dc fed current controlled dc-dc boost converter (fig. 7.2), to keep bifurcation away and maintaining fast response control (fig. 7.4) should have a

special function which dynamically adjusts the compensating ramp. For fixed load and output voltage, the compensating ramp needs only to be controlled according to

$$M_c(V_i) \geq \frac{v}{v_i} - 1 \quad \text{or} \quad m_c(V_i) \geq \frac{v - 2V_i}{2L} \qquad \ldots\ldots\ldots (7.1)$$

But with the time variable ramp compensation technique, the reference current is modified by subtracting a ramp voltage from a sinusoidal wave for rectified dc fed current controlled boost converter as indicated in the fig. 7.4. The input voltage of the converter is given by $v_i(t) = \hat{V}_i|\sin\omega_m t|$ where ω_m is the angular frequency. In terms of phase angle θ , it is $v_i(\theta) = \hat{V}_i|\sin\theta|$. For $0 \leq \theta < \pi/2$ the value of Iref increases and it can be said that a negative compensating ramp is applied to Iref (i.e. Mc<0). For $\pi/2 \leq \theta < \pi$ the value of Iref decreases and it can be said that a positive compensating ramp is applied to Iref (i.e. Mc>0). At π/2 no no ramp compensation is applied. The critical phase angle (θ_c) may be calculated at which period doubling occurs. As the duty ratio is equal to $1-{}^{v_i}\!/_{v}$ and Mc is $-(dI_{ref}/dt)L/\hat{V}_i|\sin\theta|$ so we have the value of θ_c is given by $|\sin\theta_c| = \dfrac{v + 2L\dfrac{dIref}{dt}}{2\hat{V}_i}$

. ..... (7.2)

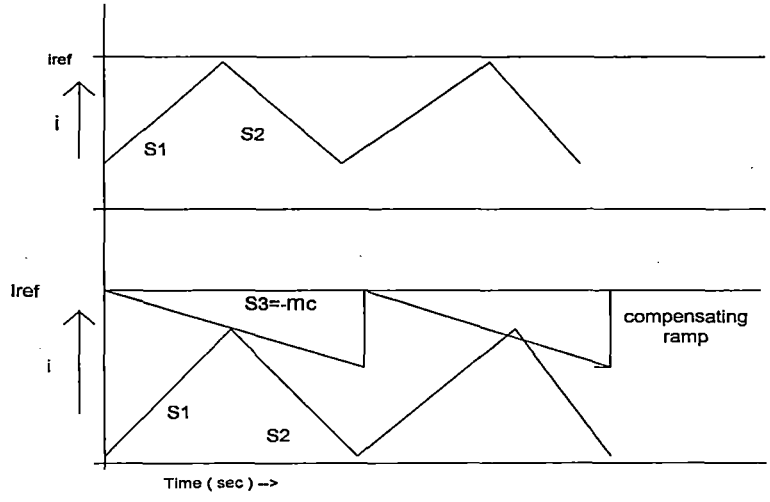

fig. 7.3 Time plot of inductor current of the boost converter without compensating ramp (upper one) and with compensating ramp (lower one).

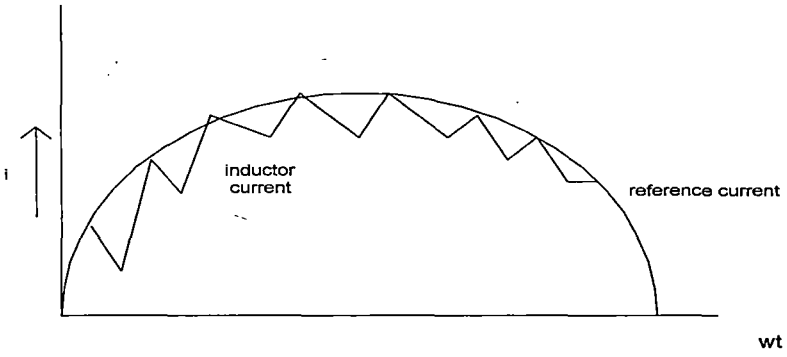

fig. 7.4 Time plot of inductor current of the boost converter without compensating ramp (upper one) and with variable compensating ramp along with sinusoidal reference current (lower one)

Taking $Iref \approx \hat{I}_i|\sin\theta|$ for $0 \le \theta < \pi$, we have $\frac{dI_{ref}}{dt} \approx \omega_m \hat{I}_i \cos\theta$ for $0 \le \theta < \pi$ .... (7.3)

$$\text{hence } \theta_c = 2\arctan\left(\frac{2\hat{V}_i \pm \sqrt{(4\hat{V}_i^2 - v^2 + +4\omega_m^2 \hat{I}_i^2 L^2)}}{v - 2\omega_m \hat{I}_{in} L}\right) \quad .....(7.4)$$

Considering power equality $\hat{V}_i \hat{I}_i / 2 = v^2 / R$, $r_v = \frac{v}{\hat{V}_i}$ and $\tau_L = L/R$

$$\theta_c = 2\arctan\left(\frac{2 \pm \sqrt{4 - r_v^2 + 16\omega_m^2 \tau_L^2 r_v^2}}{r_v - 4\omega_m \tau_L r_v^2}\right) \quad ..... (7.5)$$

The parameters for the converter, if not stated otherwise are : I_{ref} =4 amps, r_i=1.2 ohms, r_c=0.1 ohms(fs). R=20 ohms. Clock frequency(f_c)=500Hz. Input voltage(rms value)=20V, Input voltage frequency=50Hz, L=27 mH, C=120 μF. For these set values bifurcation diagrams of one state variables i.e. capacitor voltage with the variation of input voltage are reported in this chapter. Time plots of one state variable i.e. inductor current is reported also. Reading of the state values are taken at clock for non autonomous case and at their peak values for autonomous case.

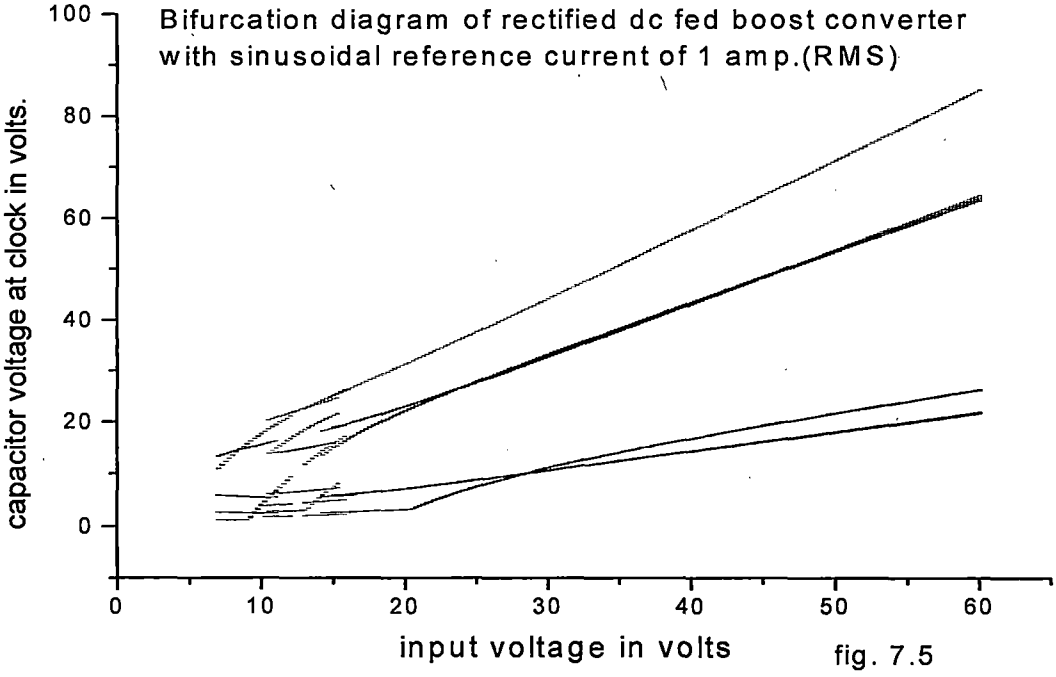
Bifurcation diagram of rectified dc fed boost converter
with sinusoidal reference current of 1 amp.(RMS)
capacitor voltage at clock in volts.
100
80
60
40
20
0
0
10
20
30
40
50
60
input voltage in volts

fig. 7.5

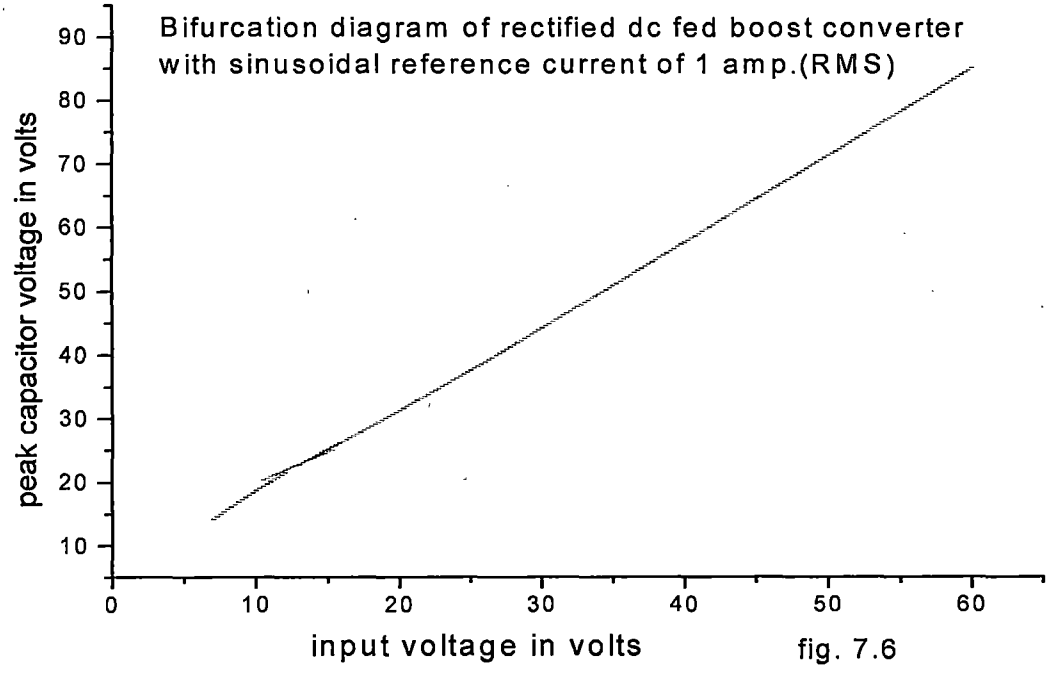
Bifurcation diagram of rectified dc fed boost converter
with sinusoidal reference current of 1 amp.(RMS)
peak capacitor voltage in volts
90
80
70
60
50
40
30
20
10
0
10
20
30
40
50
60
input voltage in volts

fig. 7.6

a. Input voltage (Vi) as bifurcation parameter: The bifurcation diagrams of the single phase full wave rectified dc fed boost converter with input voltage (Vi) as variable parameter are shown in figure 7.5, 7.6,7.7, 7.8, 7.9, 7.10, 7.11 and 7.12. Fig. 7.5, 7.7, 7.9, and 7.11 shows the bifurcation diagram for non autonomous system (capacitor voltage are sampled at clock) with the variable ramp compensation and sinusoidal rms reference current of 1 amp., 2 amps., 3 amps. And 4 amps. Fig. 7.6, 7.8, 7.10 and 7.12 shows the bifurcation diagram for autonomous system (i.e capacitor voltage are sampled at its peak values) with the variable ramp compensation and sinusoidal rms reference current of 1 amp., 2 amps., 3 amps. And 4 amps. Keeping other parameters at set values, the input voltage (Vi) is varied from 07 to 60 volts in step of 0.1 volt.

The autonomous (fig. 7.6, 7.8, 7.10 and 7.12) case of the converter shows period doubling bifurcation phenomenon but the point of bifurcation changes with the magnitude sinusoidal rms reference current. In non autonomous (fig. 7.5, 7.7, 7.9, and 7.11) case of the converter shows period doubling bifurcation phenomenon but the point of bifurcation changes with the magnitude sinusoidal rms reference current.

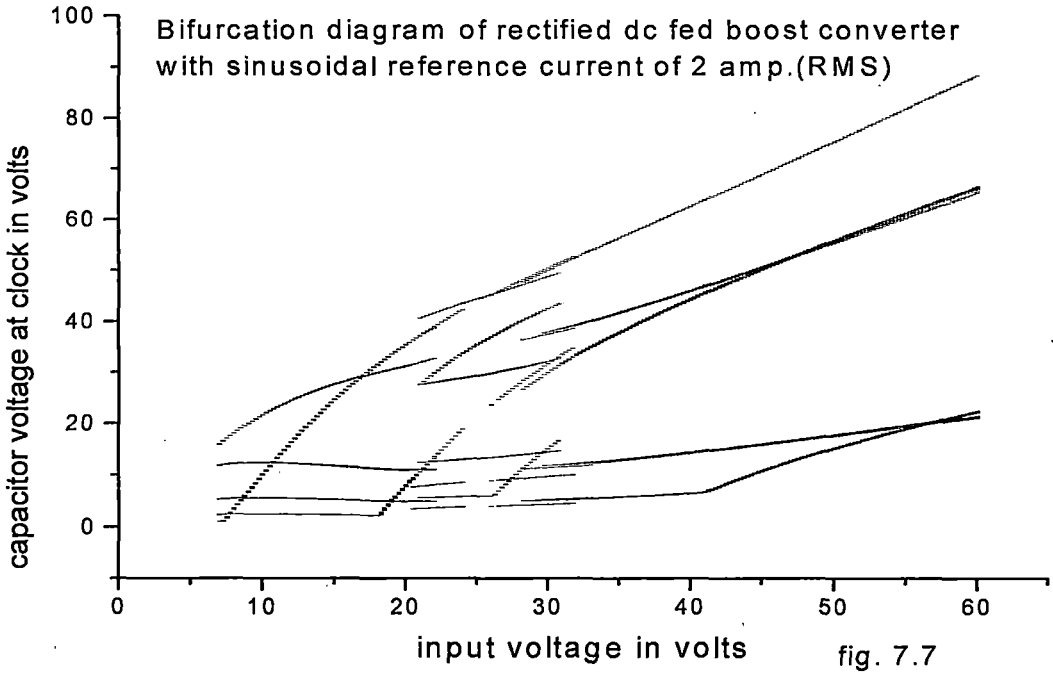
Bifurcation diagram of rectified dc fed boost converter
with sinusoidal reference current of 2 amp.(RMS)
capacitor voltage at clock in volts
100
80
60
40
20
0
0
10
20
30
40
50
60
input voltage in volts

fig. 7.7

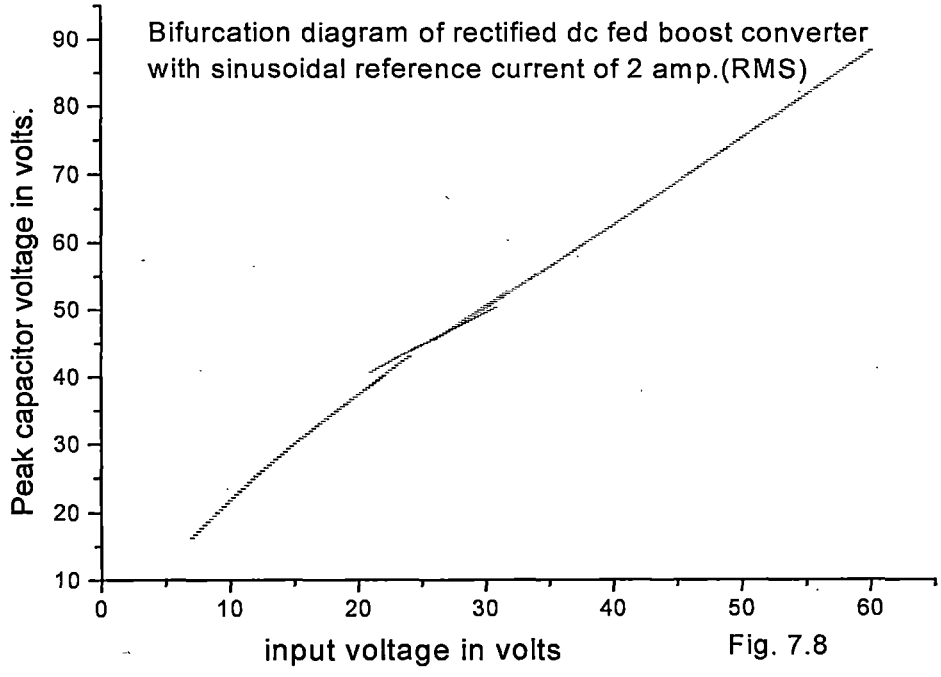
Bifurcation diagram of rectified dc fed boost converter
with sinusoidal reference current of 2 amp.(RMS)
Peak capacitor voltage in volts.
90
80
70
60
50
40
30
20
10
0
10
20
30
40
50
60
input voltage in volts

Fig. 7.8

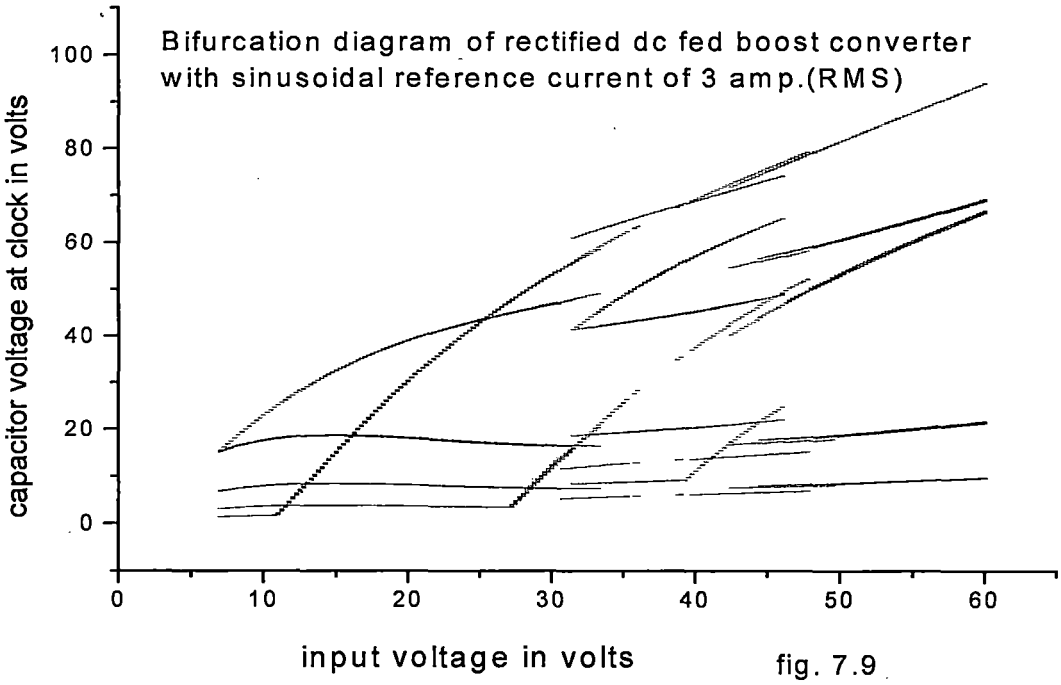

fig. 7.9

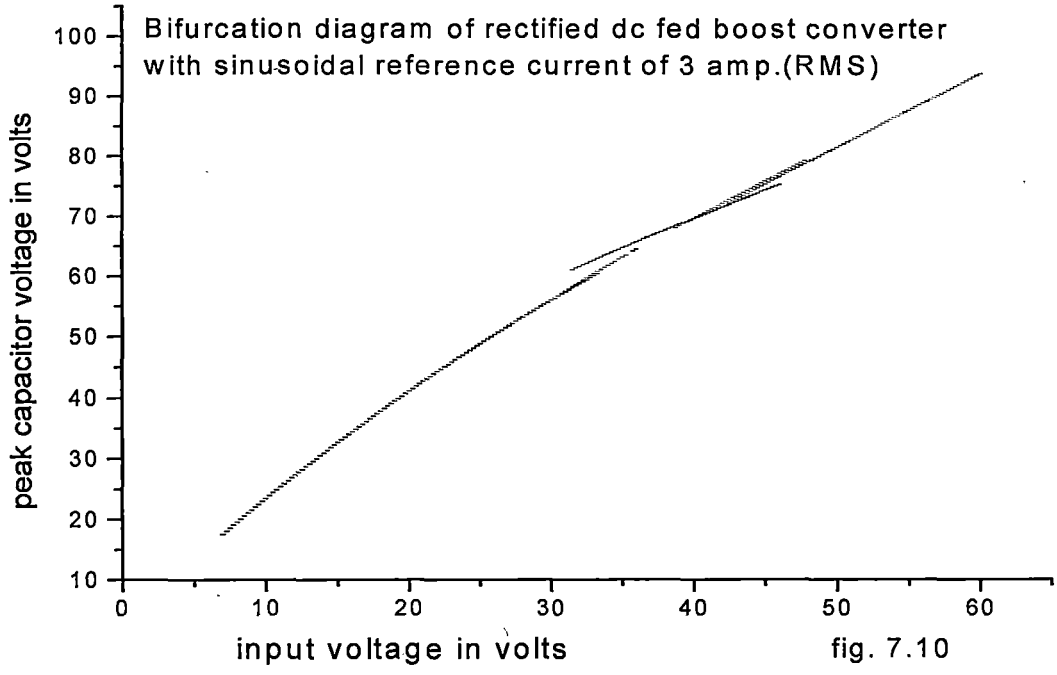

fig. 7.10

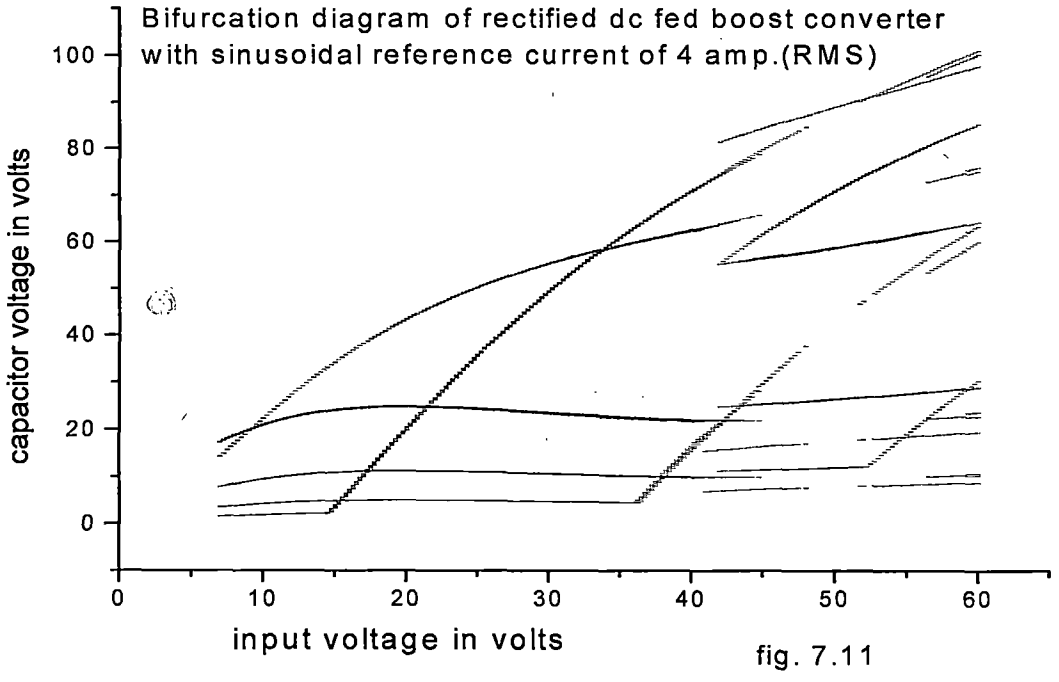

fig. 7.11

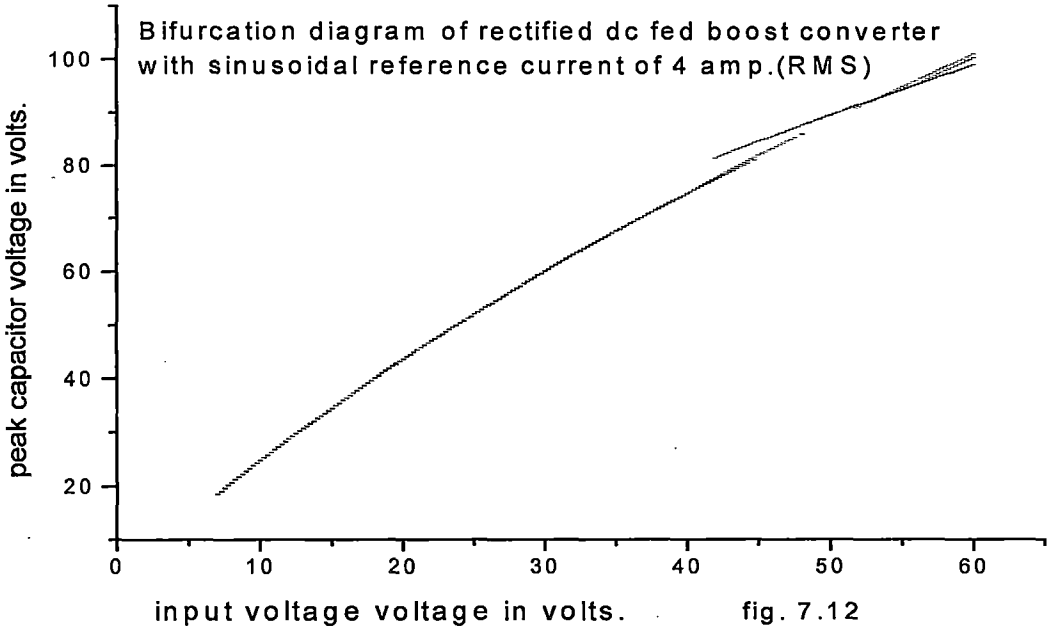

fig. 7.12

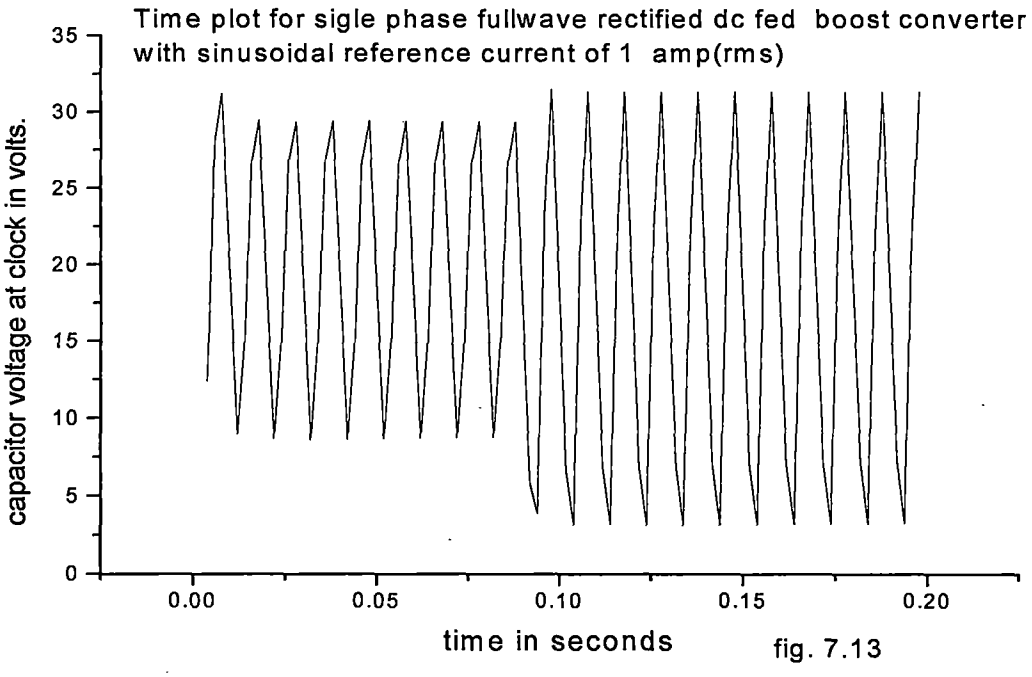

fig. 7.13

Fig. 7.13 shows the time plots of inductor current for a sinusoidal reference rms current of 1 amp.

So from the figures we can conclude that bifurcation or chaos (as they are twins)is under control. It helps the designer to eliminate or include or control bifurcation, chaos and other complex behaviors.

****

Chapter 8

CONCLUSIONS AND FUTURE EXPANSIONS

Some phenomena related to chaotic behavior of piecewise linear systems with switching nonlinearity are investigated for two power electronic circuits with all parasitic effect. The circuits are taken for our study are pure dc fed current controlled dc-dc boost converter and single phase full wave rectified dc fed current controlled dc-dc boost converter. In both systems the dynamics are governed by two sets of state variable equations. Each sets of equation corresponding to two switching status switching on and switching off. Map based models of the systems are formulated in the form of a mapping from one switching instant to another without any assumptions for simplification. This enables capturing and analysis of nonlinearity of the circuits. Earlier such type of modeling was done for pure dc fed current controlled dc-dc boost converter but all parasitic effect were not considered. The operation of our converters are studied from two points of view. Since the input clock has an periodicity that can be controlled externally, we identified the periodicity as the number of clock in a period of the output waveform which is termed as non autonomous system. Here the samplings are done at clock frequency and poincare section can be obtained. In the second method we are concerned only with the output states and we defined the periodicity as the repetitive behavior of the output waveform as seen in the phase plot of the state variables. This termed as autonomous system. Here the peaks of the output waveform of one of the state variables are identified and the periodicity is determined from the data.

In both the circuits, the period doubling cascade are the route to chaos which is established for others boost converter also. Like others boost converter the periodic windows are noted within the chaotic zone for both the circuits. In boost converter the capacitor voltage peak coincides with arrival of the clock pulse. For this reason, the bifurcation diagram obtained

from non autonomous system and autonomous system are identical for most parameter values. Differences between them occur when the on period have more than one clock pulses, which are identified from the bifurcation diagrams in terms of parameter region. A stair case like structure are also observed indicating more and more clock pulses in an output cycle.

The above phenomena are also observed for map based model of three phase full wave rectified dc fed current controlled dc-dc boost converter with all parasitic effect and six phase half wave rectified dc fed current controlled dc-dc boost converter with all parasitic effect. The bifurcation diagrams for different no of phase of input voltage of multi phase half wave rectified dc fed current controlled dc-dc boost converter with all parasitic are determined by which we can conclude that the operation is stable for higher number of phases.

We have applied the theory of bifurcations in 1-D piecewise smooth piecewise monotonic maps for both the pure dc fed current controlled dc-dc boost converter and single phase full wave rectified dc fed current controlled dc-dc boost converter. We have shown that however complicated the map of a real system may be, the border collision bifurcations can be understood in terms of its piecewise affine approximation at the border. We have developed the 1-D modeling for both the boost converter with parasitic effect. We presented the different Bifurcations diagram for the developed 1-D modeling which are useful in analyzing, identifying and describing the nonlinear phenomena in such circuits

We have also applied the theory of bifurcations in 1-D discontinuous piecewise smooth piecewise monotonic maps. We have developed the 1-D discontinuous modeling of the current controlled boost converter with parasitic effect for two types of source voltage one for pure DC & another for Rectified DC. We presented the different Bifurcations diagram for the developed 1-D discontinuous modeling which are useful in analyzing, identifying and describing the nonlinear phenomena in such circuits.

We have applied the theory of bifurcation control in the current controlled boost converter with parasitic effect for two types of source voltage one for pure DC & another for Rectified DC. We are able to present a successful method for controlling the bifurcation in the circuits. We presented the different Bifurcation diagrams and time diagram for the developed method, which are useful in identifying , analyzing and describing bifurcations and chaos due to the nonlinear phenomena in such circuits.

The results obtained in all the analysis and investigation may be compared experimentally . It can be said safely that our studies will be supported experimentally as the same is verified without parasitic effects.

Further studies and investigations may be done with different number of phases and with different types of filters for different types of load. The results obtained in all the cases may be verified experimentally and compared also with different software/simulation packages like MATLAB, PSPICE etc.

****

REFERENCES:

[1] S. Banerjee, E. Ott, J. A. Yorke, and G. H. Yuan, "Anomalous bifurcations in dc-dc converters: Borderline collisions in piecewise smooth maps," in *Proc. IEEE Power Electronics Specialists' Conf.*, 1997, pp. 1337–1344.

[2] S. Banerjee, P. Ranjan, and C. Grebogi, "Bifurcations in two-dimensional piecewise smooth maps—Theory and applications in switching circuits," *IEEE Trans.on Circuits and Syst-. I.* Vol.47, 2000,pp. 633-643

[3] G. H. Yuan, S. Banerjee, E. Ott, and J. A. Yorke, "Border collision bifurcations in the buck converter," *IEEE Trans. Circuits Syst. I*, vol. 45, pp. 707–716, July 1998.

[4] F. Takens, "Transition from periodic to strange attractors in constrained equations," in *Dynamical Systems and Bifurcation Theory*, Eds. New York, NY: Longman, 1987, vol. 160, pp. 399–421.

[5] H. E. Nusse and J. A.Yorke, "Border-collision bifurcations for piecewise smooth one dimensional maps," *Int. J. Bifurcat. Chaos*, vol. 5, no. 1, pp. 189–207, 1995.

[6] Y. L. Maistrenko, V. L. Maistrenko, and L. O. Chua, "Cycles of chaotic intervals in a time-delayed Chua's circuit," *Int. J. Bifurcat. Chaos*, vol. 3, pp. 1573–1579, 1993.

[7] S. Banerjee, J. A.Yorke, and C.Grebogi,"Robust chaos,"*Phys. Rev.Lett.*,vol.80, pp.3049–3052, 1998.

[8] J. H. B. Deane, "Chaos in a current-mode controlled boost dc-dc converter," *IEEE Trans. Circuits Syst. I*, vol. 39, pp. 680–683, Aug. 1992.

[9] J. L. R. Marrero, J. M. Font, and G. C. Verghese, "Analysis of the chaotic regime for dc-dc converters under current mode control," in *Proc. Power Electronics Specialists' Conf.*, 1996, pp. 1477–1483.

[10] S. Banerjee and K. Chakrabarty, "Nonlinear modeling and bifurcations in the boost converter," *IEEE Trans. Power Electron.*, vol. 13, pp. 252–260, 1998.

[11] D. M.Wolf, M. Varghese, and S. R. Sanders, "Bifurcation of power electronic circuits," *J. Franklin Inst.*, vol. 331B, no. 6, pp. 957–999, 1994.

[12] C. K. Tse and W. C. Y. Chan, "Experimental verification of bifurcations in current-programmed dc/dc boost converters," in *Proc. European Conf. Circuit Theory Design*, Budapest, Hungary, Sept. 1997, pp. 1274–1279.

[13] J. H. B. Deane and D. C. Hamill, "Improvement of power supply EMC by chaos," *Electron. Lett.*, vol. 32, no. 12, p. 1045, 1996.

[14] Soumitro Banerjee, M. S. Karthik, Guohui Yuan, and James A. Yorke,] " Bifurcations in One-

Dimensional Piecewise Smooth Maps—Theory and Applications in Switching Circuits" IEEE Transactions on Circuit and System -I: Fundamental Theory and Applications, vol.47, no. 3, March,2000, pp 389-394.

[15] Lorentz E.N, "Deterministic non periodic flow", Journal of the atmosphere in Sciences, 20(2), 1963,pp. 130-141.

[16] Wolf M, Swift J.B, Swinhey H.I and Vastano J.A," Determining Lyapunov exponents from time series"Physica D, 16(3)1985, pp. 285-317.

[17] Vastano J.A and Kostelich E.J,'Composition of algorithms for determining Lypunov exponents from experimental data"In G, Mayers Press, editor, Dimensions & Entropies in Chaotic system, Springer verlag,1986.

[18] B.K.Bose, Modern Power electr4onic: Evolution, Technology and applications, New York, IEEE press.1992.

[19] N.Mohan, T.M Undeland and W.P.Robbins, Power Electronic Converters, Applications and Design, John Wiley Third edition, 2004.

[20] R.E.Tartar, Solid Power Conversion Hand book, New York , Wiley inter science, 1993

[21] J.G.Kassakion, M.F.Schlecht and G.C.Verghese, Principles of Power Electronic, Addison – Wesley,Reading, MA,1991.

[22] M.H.Rashid, Power Electronic Circuits, Devices and Applications, Pearson Education, Third edition, 2004.

[23] R.M.May, "Simple mathematical models with very complicated dynamics", Nature, vol-261,June 1976, pp.459-467.

[24] M.J.Feigenbaum, " Universal behaviors in nonlinear systems. Vol-1,1980, Los Alamos Science.

[25] B. van der Pol and J.van der Mark, "Frequency demultiplication", Nature, vol-120,september 1927, pp.363-364.

[26] M.P.Kennedy and L.O.Chua, "Van der pol and chaos" IEEE Transactions on Circuits and Systems, 33, 974-980,October 1986.

[27] J.Baillieul, R.W.Brockett abd R.B.Washburn, " Chaotic motion in nonlinear feedback system". IEEE Transactions on Circuits and Systems, 27, 990-997. Nov 1980.

[28] P.S.Linsay, "Period doubling and chaotic behavior in driven anharmonic oscillator", Physical Review Letters, vol.27, pp.1349-1352,Novenber 1981.

[29] L.O.Chua, " The genesis of Chua's circuit", Archiv fur Elektronik and Ubertragungstechnik, vol.46,pp.250-257,1992.

[30] L.O.Chua, "Chua's circuit 10 years later", Int. J. circuit Theory and appl., vol.22,pp.279-

305,1994.

[31] R.W. Brockett and J.R.Wood, "Understanding power converter chaotic behavior in protective and abnormal modes",in Powercon II,1984.

[32] D.C.Hamill and D.J.Jefferies, " Subharmonics and Chaos in power electronic circuits ". IEEE Transactions on Circuits and Systems, 35,No.8, pp.1059-1061. 1988

[33] J.R.Wood, "Chaos: a real phenomenon in power electronics" in applied power electronics conference, (Baltimore MD, pp.115-124, March 1989.

[34] J.H.B.Deane and D.C.Hamill, " Analysis, simulation and experimental study of chaos in buck converter", in power electronics Specialists Conference, (San Antonio, TX, USA) , pp.491-498,1990 .

[35] J.H.B.Deane and D.C.Hamill, " Instability, subharmonics and chaos in power electronics circuits", IEEE transactions on power electronics, vol.5 , pp.260-268, July-1990

[36] J.H.B.Deane and D.C.Hamill, " Modeling of chaotic dc-dc converters by iterated nonlinear mapping", IEEE transactions on power electronics, vol.7 , pp.25-36, January-1992.

[37] J.H.B.Deane and D.C.Hamill, " Chaotic behavior in current mode controlled dc-dc converter", Electronics Letters, vol.27 , pp.1172-1173,June1991

[38] J.H.B.Deane and D.C.Hamill, "Chaos in a current mode controlled dc-dc converter", in IEEE transactions on Circuits and Systems - I, vol.39 , pp.680-683, August-1992.

[39] C.K.Tse, "Flip bifurcation and chaos in three state boost switching regulators", in IEEE transactions on Circuits and Systems - I, vol.CAS-41 , pp.16-23, January-1994

[40] I.Zafrany and S.Ben-Yaakov, "A chaos model of subharmonic oscillations in current mode pwm boost converters",in Power Electronics Specialists Conference, pp.1111-1117,1995.

[41] K. Chakrabarty, G.Poddar and S. Banerjee , " Bifurcation behavior in buck converter," *IEEE Trans. Power Electron.*, vol. 11, no.3,pp. 439-447, 1996.

[42] E.Fossas and G.Olivar, " Study of chaos in the buck converters", in IEEE transactions on Circuits and Systems - I, vol.43 , no.1,pp.13-25, 1996.

[43] M. di.Bernardo and F.Vasca, " On discrete time maps for the analysis of bifurcations and chaos dc/dc converters", in IEEE transactions on Circuits and Systems - I, 1999

[44] M. di.Bernardo, F.Garofalo, L. Glielmo and F.Vasca, " Quasi periodic behaviors in dc/dc converters", in Power Electronics Specialists Conference, pp.1376-11381,1996

[45] W.C.Y.Chan and C.K.Tse, "Study of bifurcations in current programmed dc/dc boost converters from quasiperiodicity to period doubling , in IEEE transactions on Circuits and Systems - I, vol.-44 , no.12,pp.1129-1142, 1997.

[46] Nusse, H. E., Ott, E. & Yorke, J. A. [1994], "Bordercollision bifurcations: An explanation for observed bifurcation phenomena," Physical Review E, 49, 1073–1076.

[47] Rajaraman, R., Dobson, I. & Jalali, S. [1996], "Nonlinear dynamics and switching time bifurcations of a thyristor controlled reactor circuit," IEEE Transactions on Circuits and Systems-I, 43, 1001–1006.

[48] S.Banerjee, " Coexisting attractors, chaotic saddles and fractal basins in a power electronic circuit" , IEEE transactions on Circuits and Systems - I, vol.-44 , no.9,pp.847-849, 1997.

[49] L.O.Chua, M.Hasler, J.Neirynnk and P.Verbugh, "Dynamics of a piecewise linear resonant circuit" , IEEE transactions on Circuits and Systems , vol.-29 ,pp.535-547, August-1982.

[50] C.Kiney, " Application of the bifurcation theory in studying and understanding the global behavior of a ferroresonant electric power circuit", IEEE transactions on Power delivery, vol.-6 , pp.866-872, April-1991.

[51] A.E.A.Araujo, A.C.Soudak and J.R.Marti, "Ferroresonance in power systems",IEE Proc. Part C, vol.140, pp.237-240, May 1993.

[52] J.H.B.Deane, "Modeling of a chaotic circuit containing a saturating/hysteretic inductor", Electronics Letters,vol.29, pp.957-958, May 1993.

[53] J.H.B.Deane, "Modeling the dynamics of nonlinear inductor circuits", IEEE transactions on Magnetics, vol.30 , pp.2795-2801, September 1994.

[54] H.G.Kwatny, A.K.Pasrija and L.H.Bahar, " Static bifurcations electric power network: loss of steady-state stability and voltage collapse" , IEEE transactions on Circuits and Systems, vol.-33 , pp.981-991, October-1986.

[55] H.D.Chiang, C.W.Liu, P.P.Varaiya, F.F.Wu and M.G.Lauby, " Chaos in simple power system", IEEE transactions on Power Systems, vol.-8 , pp.1407-1417, November-1993

[56] B.Lee and V.ajjarappu, "Period doubling route to chaos in an electrical power systems",IEE Proc. Part C, vol.140, no.6, pp.490-496, 1993.

[57] C.W.Liu, J.S.Thorpe, J.Lu, R.J.Thomas and H.D.Chiang, " Detection of transiently chaotic swings in power system using real time phasor measurements", IEEE transactions on Power Systems, vol.-9 , no.3, pp.1285-1292,1994

[58] H.O.Wang, E.Abed and A.M.A.Hamdan , " Bifurcations , chaos and crises in voltage collapse of a model power system" , IEEE transactions on Circuits and Systems, part-I, vol.-41 , no.9,pp.294-303, March-1994.

[59] Burns W.W and Wilson T.G, " Analytical derivation and evaluation of a state trajectory control law for dc-dc converters", in IEEE Power Electronics Specialists Conference Rec, pp.70-85.

[60] Sira- Ramirez H, "Sliding motion in bilinear switched networks", IEEE Tran s. Circuits and systems, 34(8):919-933, 1987.

[61] Sanders S.R, Verghese G.C and Cameron D.E, "Nonlinear control of switching power converters control",Theory and Advanced Technology, 10(3):302-3091995.

[62] Malesani L, Rossetto L, Spiazzi G and Tenti P, " Performance optimization of Cuk converters sliding mode control", IEEE transactions on power electronics, 10(3): 302-309, 1995

[63] Middlebrook R.D and Cuk S , " A general unified approach to modeling switching converter power stages", In IEEE Power Electronics Specialists Conference Rec, pp.18-34, 1976

[64] Sanders S.R and Verghese G.C , " Lyapunov based control for switched power converters", IEEE transactions on power electronics, 7(1): 17-24, 1992

[65] Sira- Ramirez H and Prada-Rizzo M.T,"Nonlinear feedback regulator design for the cuk converter", IEEE Trans. Automatic control, 37(8):1173-1180, 1990

[66] Kawasaki N, Nomura H and Mashuhiro M, " The new control of bilinear dc-dc converters developed by direct application of Lyapunov", IEEE transactions on power electronics, 10(3): 318-325, 1995

[67] Hsu S.P, Brown A, Rensik L and Middlebrook R.D , "Modeling and analysis of switching dc-to-dc converters in constant frequency current program mode", In IEEE Power Electronics Specialists Conference Rec, pp.284-301, 1979

[68] Sanders S.R, Noworolski J.M and Verghese G.C , " Generalized averaging method for power conversion circuits", IEEE transactions on power electronics, 6(2): 251-259, 1991

[69] Caliskan V.V, Verghese G.C and Stankovic A.M, " Multifrequency averaging of DC/DC converters", IEEE transactions on power electronics, 14(1): 124-133, 1999

[70] Stankovic A.M, Sanders S.R and Aydin T , " Analysis of unbalanced AC machines with dynamic phasors", Naval Symposium on Electric Machines, 219-224, 1998

[71] M.Oestreich, N. Hinrichs, K.Popp and C.J.Budd,"Analytical and experimental investigation of an impact oscillator", Proceedings of the ASME 16th Biennial Conf. On Mech. Vibrations and Noise, 1996.

[72] Banerjee, S. & Verghese, G. C., editors [2001] Nonlinear Phenomena in Power Electronics: Attractors,Bifurcation, Chaos, and Nonlinear Control. (IEEE Press).

[73] Budd, C. [1995] "Grazing in impact oscillators," in Real and Complex Dynamical Systems, eds. Branner, B. & Hjorth, P., (Kluwer Academic Publishers) pp. 47–64.

[74] Budd, C. & Dux, F. [1994] "Chattering and related behaviour in impacting oscillators," Phil. Trans Roy.Soc., 347, 365–389.

[75] Chin, W., Ott, E., Nusse, H. E., & Grebogi, C. [1995],"Universal behavior of impact oscillators near grazing incidence," Physics Letters A, 201, 197–204.

[76] Di Bernardo, M., Feigin, M. I., Hogan, S. J. & Homer, M. E. [1999], "Local analysis of – bifurcations in n-dimensional piecewise smooth dynamical systems,"Chaos, Solitons & Fractals, 10, 1881–1908.

[77] Dobson, I. [1995], "Stability of ideal thyristor and diode switching circuits," IEEE Transactions on Circuits and Systems-I, 42, 517–529.

[78] Jalali, S., Dobson, I., Lasseter, R. H. & Venkataraman,G. [1996], "Switching time bifurcations in a thyristor controlled reactor," IEEE Transactions on Circuits and Systems-I, 43, 209–218.

[79] Maggio, G. M., Di Bernardo, M. & Kennedy, M.P. [2000], "Nonsmooth bifurcations in a piecewise linear model of the Colpitts Oscillator," IEEE Trans. on Circuits and Systems-I, 47, 1160.

[80] Nusse, H. E. & Yorke, J. A. [1992], "Border-collision bifurcations including "period two to period three" for piecewise smooth maps," Physica D, 57, 39–57.

[81] P. R. Severns and G. E. Bloom, Modern DC-to-DC Switch mode Power Converter Circuits, Van Nostrand Reinhold, New York, 1985.

[82] P. T. Krein, Elements of Power Electronics, Oxford University Press, New York,1998.

[83] C.Hayashi, Nonlinear Oscillations in Physical Systems, Princeton University Press, 1964.

[84] R. Oruganti and F. C. Lee, "State-plane analysis of parallel resonant converter,"IEEE Power Electronics Specialists Conf. Rec., pp. 56-73, 1985.

[85] S. R. Sanders and G. C. Verghese,"Lyapunov-based control of switched Power Converters," IEEE Power Electronics Specialists Conf. Rec., pp. 51-58, 1990.

[86] R. Tymerski, "Volterra series modeling of power conversion systems," IEEE Power Electronics Specialists Conf. Rec., pp. 786-791, 1990.

[87] J. Foutz, "Chaos in power electronics," SMPS Technology Knowledge Base, http://www.smpstech.com/chaos000.htm, 1996.

[88] D. C. Hamill, "Power electronics: A .eld rich in nonlinear dynamics," *Proc. Int. Workshop on Nonlinear Electronics Systems,* pp. 165-178, Dublin Ireland, 1995.

[89] J. H. B. Deane and D. C. Hamill, "Instability, subharmonics and chaos in power electronics systems," *IEEE Power Electronics Specialists Conf. Rec.,* 1989.

[90] P. T. Krein and R. M. Bass, "Types of instabilities encountered in simple power electronics circuits: Unboundedness, chattering and chaos," *IEEE Applied Power Electronics Conf. and Exposition,* pp. 191-194, 1990.

[91] D. C. Hamill, J. B. Deane and D. J. Je.eries, "Modeling of chaotic DC/DC converters by iterated nonlinear mappings," *IEEE Trans. Power Electronics,* Vol. 7, No. 1, pp. 25-36, January 1992.

[92] D. C. Hamill, S. Banerjee and G. C. Verghese, "Chapter 1: Introduction," in *Nonlinear Phenomena in Power Electronics*, ed. by S.Banerjee and G.C. Verghese, IEEE Press, New York, 2001.

[93] M. di Bernardo and F. Vasca, "Discrete-time maps for the analysis of bifurcations and chaos in DC/DC converters," *IEEE Trans. Circ. Syst. I,* Vol. 47, No. 2, pp.130–143, February 2000.

[94] C. K. Tse, "Recent developments in the study of nonlinear phenomena in power electronics," *IEEE Circ. Systems Society Newsletter,* Vol. 11, No. 1, pp. 14–48, March 2000.

[95] C. K. Tse, "Chaos from a buck switching regulator operating in discontinuous mode," *Int. J. Circuit Theory Appl.,* Vol. 22, No. 4, pp. 263–278, July–August,1994.

[96] W. C. Y. Chan and C. K. Tse, "On the form of control function that can lead to chaos in discontinuous-mode DC/DC converters," *IEEE Power Electronics Specialists Conf. Rec.,* pp. 1317–1322, 1997.

[97] C. K. Tse and W. C. Y. Chan, "Chaos from a current-programmed 'Cuk converter," *Int. J. Circuit Theory Appl.,* Vol. 23, No. 3, pp. 217–225, 1995.

[98] S. Banerjee, E. Ott, J. A. Yorke and G. H. Yuan, "Anomalous bifurcation in DC/DC converters: borderline collisions in piecewise smooth maps," *IEEE Power Electronics Specialists Conf. Rec.,* pp. 1337–1344, 1997.

[99] M. di Bernardo, F. Garofalo, L. Glielmo and F. Vasca, "Switchings, bifurcations and chaos in DC/DC converters," *IEEE Trans. Circ. Syst. I,* Vol. 45, No. 2, pp. 133–141, February 1998.

[100] A. B. Nordmark, "Non-periodic motion caused by grazing incidence in an impact oscillator," *J. Sound and Vibration,* Vol. 2, pp. 279–297, 1991.

[101] M. di Bernardo, C. J. Budd and A. R. Champneys, "Grazing, skipping and sliding: analysis of the non-smooth dynamics of the DC/DC buck converter,"*Nonlinearity*, Vol. 11, No. 4, pp. 858-890, 1998.

[102] C. K. Tse, Y. M. Lai and H. H. C. Iu, "Hopf bifurcation and chaos in a freerunning current-controlled 'Cuk switching regulator," *IEEE Trans. Circ. Syst. I,* Vol. 47, No. 4, pp. 448–457, April 2000.

[103] Y. Kuroe and S. Hayashi, "Analysis of bifurcation in power electronic induction motor drive system," *IEEE Power Electronics Specialists Conf. Rec.,* pp. 923–930, 1989.

[104] Z. S¨uto, I. Nagy and E. Masada, "Avoiding chaotic processes in current control of AC drive," *IEEE Power Electronics Specialists Conf. Rec.,* pp. 255–261, 1998.

[105] H. H. C. Iu and C. K. Tse, "Instability and bifurcation in parallel-connected buck converters under a master-slave current-sharing scheme," *IEEE Power Electronics Specialists Conf. Rec.,* pp. 708–713, 2000.

[106] S. Wiggins, *Introduction to Applied Nonlinear Dynamical Systems and Chaos,* Springer-Verlag, New York, 1990.

[107] T. Tsubone and T. Saito, "Hyperchaos from a 4-D manifold piecewise-linear system," *IEEE Trans. Circ. Syst. I,* Vol. 45, No. 9, pp. 889–894, September.1998.

[108] T. Suzuki and T. Saito, "On fundamental bifurcations from a hysteresis hyperchaos generator," *IEEE Trans. Circ. Syst. I,* Vol. 41, No. 12, pp. 876–884,December 1994.

[109] M. Ohnishi and N. Inaba, "A singular bifurcation into instant chaos in a piecewise- linear circuit," *IEEE Trans. Circ. Syst. I,* Vol. 41, No. 6. pp. 433–442,June 1994.

[110] A.B. Nordmark, "Non-periodic motion caused by grazing incidence in impact oscillators, "*J. Sound and Vibration,* Vol. 2, pp. 279–297, 1991.

[111] M. I. Feigin,"Doubling of the oscillation period with C-bifurcations in piecewise continuous systems," *PMM,* Vol. 34, pp. 861–869, 1970.

[112] M. I. Feigin, "On the generation of sets of subharmonic modes in a piecewise continuous system," *PMM,* Vol. 38, pp. 810–818, 1974.

[113] M. I. Feigin, "On the structure of C-bifurcation boundaries of piecewise continuous systems," *PMM,* Vol. 2, pp. 820–829, 1978.

[114] M. di Bernardo, C. J. Budd and A. R. Champneys, "Corner collision implies border collision " *Physica D,* Vol. 154, pp. 171–194, 2001.

[115] M. di Bernardo, C. J. Budd and A. R. Champneys, "Grazing and border-collision in piecewise-smooth systems: a uni.ed analytical framework," *Physical Review Letters,* Vol. 86, pp. 2553–2556, 2001.

[116] M. I. Feigin, "The increasingly complex structure of the bifurcation tree of a piecewise-smooth system," *J. Appl. Math. Mech.,* Vol. 59, pp. 853–863, 1995.

[117] S. Banerjee and C. Grebogi, "Border collision bifurcations in two-dimensional piecewise smooth maps," *Physical Review E,* Vol. 59, pp. 4052–4061, 1999.

[118] M. di Bernardo, K.H. Johansson and F. Vasca, "Self-oscillations in relay feedback systems: symmetry and bifurcations," *Int. J. Bifur. Chaos,* Vol. 11, April 2001.

[119] T. Kousaka, T. Ueta and H. Kawakami, "Bifurcation in switched nonlinear dynamical

systems," *IEEE Trans. Circ. Syst. II,* Vol. 46, No. 7, pp. 878–885, July 1999.

[120] M. di Bernardo, "The complex behaviour of switching devices," *IEEE CAS Newsletter,* Vol. 10, No. 4, pp. 1–13, December 1999.

[121] F. Ueno, I. Oota and I. Harada, "A low-noise control circuit using Chua's circuit for a switching regulator," *Proc. European Conf. Circuit Theory and Design,* pp. 1149–1152, 1995.

[122] P. J. Aston, J. H. B. Deane and D. C. Hamill, "Targeting in systems with discontinuities, with applications to power electronics," *IEEE Trans. Circ. Syst.I,* Vol. 44, No. 10, pp. 1034–1039, October 1997.

[123] C. Batlle, E. Fossas and G. Olivar, "Stabilization of periodic orbits of the buck converter by time-delayed feedback," *Int. J. Circuit Theory Appl.,* Vol. 27,pp. 617–631, 1999.

[124] Jain, Parag., and Banerjee, s., "Border collision bifurcations in one dimensional discontinuous map",

Relevant paper published for this thesis:

[1] P K Saha and G K Panda," Nonliner Phenomenon in DC- DC Boost Converter with Nonsmooth (Single Phase Full wave rectified) DC Supply," Proceedings of National Conference on Applicable Mathematics in Wave Mechanics and Vibrations, 2003, pp10-15.

[2] P K Saha and G K Panda ,"Nonlinear Dynamic System- It's Mathematical Modelling and Study of Chaos," Proceedings of National Conference on Applicable Mathematics in Wave Mechanics and Vibrations, 2003, pp12-17.